THE UNIVERSITY of ADELAIDE

Metabolic disruptions in oocytes and embryos modifies DNA and histone methylation and alters embryonic development

Alexander Penn

School of Medicine

University of Adelaide

July 2021

Thesis submitted in fulfilment of the requirements for the admission to the Degree of Doctor of Philosophy in Medicine

Table of Contents

Thesis Abstract

Maternal obesity results in poorer offspring outcomes that may be caused by programming changes induced by metabolic and mitochondrial functional imbalance during oocyte maturation and early embryo development. Metabolic function may influence epigenetic changes during oocyte/embryo development, in particular DNA methylation (5mC-5caC) and histone 3 lysine 4 (H3K4) methylation, which are removed via the Ten-Eleven Translocase (TET) and lysine demethylase 5 (KDM5) protein families. Whilst it is understood that impaired metabolism alters the embryonic epigenetic profile, the mechanism remains unclear. The TCA cycle intermediary α-ketoglutarate is utilised as a substrate by TET1-3 and KDM5A-C in the oocyte and embryo, thus TCA cycle alterations may impact α-ketoglutarate supply, modulating 5mC-5caC and H3K4me3-1. The aim of this thesis was to establish if changes to metabolism and α-ketoglutarate availability in the oocyte and early embryo directly alters DNA and H3K4 methylation and its influence on developmental outcomes.

Female mice were fed a control diet (CD, 6% fat) or a high fat diet (HFD, 21% fat) for 6 weeks. Maternal HFD increased oxidation of mitochondrial pyruvate and decreased global 5hmC in 2-cell embryos, while increasing 5fC.

Embryos from female mice were cultured to blastocyst stage in 0, 1.4, 3.5, or 14.0 mM α-ketoglutarate, or with 0 or 20 mM of the TET inhibitor 2-hydroxyglutarate (2HG). Culture with 1.4 mM and 14.0mM α-ketoglutarate decreased 5mC in 2-cell embryos. 2HG culture increased 5mC in 2-cells, decreasing the 5fC:5mC and 5caC:5mC ratios. 14.0 mM α-ketoglutarate blocked development beyond the 2-cell and 20mM 2HG reduced development past the 4-cell stage and reduced total cell and inner cell mass cell counts in blastocysts.

Immature oocytes were collected from female mice and underwent *in vitro* maturation (IVM) with either 0 or 20 mM 2HG. IVM±2HG decreased cumulus expansion and increased whole oocyte KDM5A compared to ovulated oocytes. In addition, IVM increased global H3K4me3 and H3K4me2 in the oocyte relative to ovulated MII. In 2-cells H3K4me3 was increased in *in vitro* fertilised (IVF) derived embryos compared to *in vivo* flushed embryos and was further

increased after IVM and IVM+2HG. H3K4me2 and H3K4me1was increased in IVM and IVM+2HG 2-cells relative to both IVF and *in vivo* flushed 2-cells. With culture to blastocyst, IVM+2HG delayed day-3 embryo development (more 4-6 cell embryos and fewer 8-cell/compacting embryos) and yielded fewer day 5 hatching blastocysts and decreased inner cell mass and total cell count relative to IVF derived blastocysts.

In human follicular (cumulus and granulosa) cells, *TET1-3* expression was assessed from biobanked cDNA. Elevated maternal body mass index (BMI>25 kg/m^2) did not alter expression of *TET1-3* in cumulus or granulosa cells but reduced the number of oocytes collected. Regression analysis demonstrated decreased granulosa cell *TET1* expression associated with increased fertilisation and decreased granulosa cell *TET2* expression was associated with an increased proportion of grade 4 (the lowest quality) embryos on day 3.

Overall, these findings demonstrate that alterations to the metabolic environment including α-ketoglutarate availability during oocyte maturation and preimplantation embryo development can directly alter DNA and H3K4 methylation which may have lifelong health consequences.

Declaration

I certify that this work contains no material which has been accepted for the award of any other degree or diploma in my name, in any university or other tertiary institution and, to the best of my knowledge and belief, contains no material previously published or written by another person, except where due reference has been made in the text. In addition, I certify that no part of this work will, in the future, be used in a submission in my name, for any other degree or diploma in any university or other tertiary institution without the prior approval of the University of Adelaide and where applicable, any partner institution responsible for the joint-award of this degree.

I acknowledge that copyright of published works contained within this thesis resides with the copyright holder(s) of those works.

I also give permission for the digital version of my thesis to be made available on the web, via the University's digital research repository, the Library Search and also through web search engines, unless permission has been granted by the University to restrict access for a period of time.

I acknowledge the support I have received for my research through the provision of an Australian Government Research Training Program Scholarship.

Alexander Penn

20 July 2021

Acknowledgements

First, I would like to thank my supervisors, Associate Professor Deirdre Zander-Fox, Dr Tod Fullston and Dr Nicole McPherson for their guidance and assistance throughout my PhD.

A huge thank you to my formerly Co-supervisor, now Primary supervisor Deirdre Zander-Fox, who stepped into the role despite just moving to Victoria. While I was busy delving deeply into the minutiae, Deirdre was there to remind me of the "bigger picture" of my research.

Thanks to Tod Fullston for all his helpful advice, for his endless quest for grammatical perfection in all of my chapters, and for continuing to be a supervisor despite taking a full time job as a Genetics Coordinator.

Thanks to Nicole McPherson for her years of unofficial supervision, and for not hesitating to become an official supervisor in my time of need. Nicole taught me how to work hard and be more efficient through a work day, so you can guilt-free have a better work/life balance.

I would also like to thank all past and present members of the Gamete and Embryo Biology group, in particular Helana Shehadeh and Lauren Sandeman for all their help, as well as keeping me sane in the office on long days of data analysis, and thanks to the Honours students for making it feel like a big research family (in no particular order) Cassandra, Dania, Kristina, Bridget, Lauren V, Victoria and Casidhe. Also, thanks to the staff at Repromed, in particular Leanne Pacella-Ince and Victoria Nikitaras for their assistance in helping collection of clinical data.

A huge thank you to my family for their support and understanding over the many years of this project. Throughout all the setbacks over the years, and the whooshing noise the deadlines made as they went by, they patiently supported my efforts, with minimal pestering over the time it was taking.

Finally, thanks to the late Professor Michelle Lane for all her assistance and mentorship. Michelle tragically passed away in February 2020 after battling illness. Her enthusiasm for science, along with constantly driving me has turned me into the scientist I am today. Michelle showed me the importance of research and how it can directly lead to helping people in the clinic. I will be forever grateful for the opportunity Michelle gave me to learn the wonders of the embryo, she will be sorely missed.

I acknowledge the funding I received during my PhD candidature: My Research Training Program scholarship and an NHMRC Project Grant awarded to Professor Michelle Lane.

"Your assumptions are your windows to the world. Scrub them off every once in a while, or the light won't come in." ***Alan Alda***

Abstracts arising from this thesis

2017 The Annual Scientific Meeting of the Endocrinology Society of Australia and the Society for Reproductive Biology (ESA-SRB) 2017

Maternal obesity alters the levels of Ten-Eleven Translocase (TET) proteins reducing 5-methylcytosine and 5-hydroxymethylcytosine in the early embryo

Finalist for the Oozoa Award for best student oral presentation

List of Tables

List of Figures

Chapter 1 Literature review

1.1 Introduction

The concept that early life exposures influence adult health was first proposed by Barker and colleagues (Barker and Osmond, 1986), who determined that maternal diseases linked to low socioeconomic status influenced the risk of adult disease. This subsequently resulted in the understanding that maternal health and diet during pregnancy can affect the disease risk of the resulting child, becoming broadly known as the Barker Hypothesis of developmental origins of health and disease. Over the last decade there has been increasing awareness that this also applies to a smaller window of time surrounding peri-conception that may also influence the health of the resultant children, highlighting the peri-conception period as an important window for intervention for preventing disease in the next generation (Kwong et al., 2000).

Currently, one of the most prevalent human health risk factors in reproductive aged women is obesity, with 56.2% of women being classified as overweight or obese and being responsible for 9% of the disease burden in Australia (ABS, 2011-2012). Maternal obesity has been linked to increased foetal birth weight, increased risk of obesity, metabolic syndrome and insulin resistance in resultant children (Boney et al., 2005).

Although it is accepted that the maternal milieu can affect growth and metabolic health of the offspring, the mechanism responsible of this programming particularly for peri-conception exposures that can endure into adulthood is not well understood. It is thought that epigenetic programming, or changes that occur to DNA “above genetics” (i.e. not altering the nucleotide sequences within the DNA) is responsible for the programming of preconception events. This review will focus on epigenetic mechanisms, in particular DNA methylation, and how this may be changed in oocytes and early embryos, due to the surrounding metabolic environment, to elicit perturbed offspring health.

1.1.1 Programming of adult health by paternal pregnancy exposure

The Barker Hypothesis (Barker and Osmond, 1986) was formed from the results of a population study in England and Wales that highlighted that there was a correlation with infant mortality rates due to low birth weight and adult mortality from coronary heart disease. This led to the hypothesis that individuals from lower socioeconomic regions, where their mother had reduced nutrition before and during pregnancy, may be at risk of other health complications later in life due to this exposure of gestational stress. The original population study focused on mortality rates from both children and parents; however, newer data demonstrated a relationship also existed between low birth weight and diabetes, glucose tolerance and metabolic syndrome and hypertension in later life (Huxley et al., 2000, Phipps et al., 1993).

These early studies used historical medical records that were typically limited to the recording of only birth weight, allowing for only narrow conclusions on the mechanisms of the origins of adult health programming. Over the last 20 years, clinicians have collected more information at birth, including placental weight, gestation time, head circumference and foetal length at birth (Phipps et al., 1993), thus our understanding of the impact maternal physiology has on offspring health has also increased. We now understand that elements of maternal health such as nutrition, insulin sensitivity and obesity all impact reproductive function, metabolic health, cardiovascular health and risk of diabetes in children (Barker and Osmond, 1986, Catalano and Ehrenberg, 2006, Phipps et al., 1993).

1.1.2 Programming of adult health by maternal peri-conception exposures

The majority of the earliest insight that the peri-conception period might also be involved in the programming of offspring phenotypes came from studies in rodent models.

In mouses model of protein insufficiency, where a reduced protein diet (9% protein as compared to a standard 18%) was fed to the mother prior to conception or for the 4 days prior to embryo implantation, resulted in female offspring being heavier at birth and remaining heavier throughout their life, compared to offspring from mothers fed normal amount of protein (18%

protein) (Watkins et al., 2008a, Watkins et al., 2008b). As adults, male and female offspring from protein restricted mothers also had increased systolic blood pressure, altered postnatal behaviour, and decreased fear and/or stress response (Watkins et al., 2008b).

Subsequently, several studies assessed rodents fed a high fat diet (HFD) during the peri-conception developmental window and then transferring these HFD blastocysts to a normal weight surrogate mother, which still resulted in reduced embryo length, smaller placental diameter, and abnormal brain development (Luzzo et al., 2012, Wyman et al., 2008), demonstrating the importance of the peri-conception window on determining pregnancy and offspring developmental trajectories.

One paradigm used to dissect out the impact of peri-conception maternal environments from the impacts of gestation is to follow the birth outcomes of donor oocyte and recipient cycles from clinical IVF treatments. In this scenario, the BMI of the pre-conception environment, as represented by the oocyte donor can be separated from the post-implantation gestational period, as represented by the oocyte recipient. In this scenario, it is possible to assess clinical outcomes where the oocyte is only exposed to maternal obesity through the oocyte developmental period in the donor and after that is transferred into a normal BMI uterine environment.

With increased oocyte donor BMI, the number of eggs retrieved, fertilisation rate and cleavage rate were not significantly different to patients of lower BMI (Cardozo et al., 2016). However, oocytes from overweight and obese donors resulted in lower biochemical and clinical pregnancy rates after transfer to a normal weight recipient, thereby modelling an ovarian exposure to obesity and an in utero exposure at a normal body weight (Cardozo et al., 2016). Interestingly, birthweight and live birth weights of the babies born were not significantly different, however they were consistently reduced compared to oocytes received from normal weight donors, suggesting that the preconception exposure to obesity has a demonstrable effect after fertilisation that cannot be fully mitigated from *in vitro* embryo culture and transfer to a non-obese uterus.

Together these studies suggest that the preconception period is a key time for embryonic programming, where stresses applied during this critical developmental window can have lasting impacts on the health and disease burden in offspring.

1.2 Oocyte and preimplantation embryo development

1.2.1 Oocyte

During the third trimester of pregnancy within the ovary of the developing foetus, primordial gem cells (PGCs) differentiate first into oogonia, which divide using mitosis to form a pool of primordial follicles, containing primary oocytes arrested at prophase I of meiosis 1 surrounded by a single layer of granulosa cells (Peters et al., 1975). The primordial follicles remain at this stage until puberty (with exact timing dependent on species) (van den Hurk and Zhao, 2005), within humans new primordial follicles are stimulated daily throughout the reproductive lifespan of the woman. This is believed to occur independent of follicle stimulating hormone (FSH) as human primordial follicles lack FSH receptors and rodents have inactive FSH receptor genes (van den Hurk and Zhao, 2005). After two layers of granulosa cells have formed, now termed a secondary follicle, the oocyte increases RNA and protein synthesis, increases biogenesis of mitochondria, and produces glycoproteins to form the zona pellucida (van den Hurk and Zhao, 2005). Oocyte maturation from the secondary stage is better understood, with growth through to the antral follicle to immediately before ovulation controlled by FSH and luteinizing hormone (LH) (van den Hurk and Zhao, 2005).

Meiosis is resumed in the arrested germinal vesicle (GV) oocyte (arrested at prophase I after primordial follicle activation) and occurs from a preovulatory surge of LH, which signals the cumulus cells to disrupt the gap junctions to the oocyte, triggering a signal cascade to the oocyte to trigger nuclear maturation, resuming meiosis, breaking down the germinal vesicle, with meiosis I ending with the formation of the first polar body. The cell cycle continues until metaphase II, where the metaphase plate forms in a subplasmalemmal location (i.e. near the zona pellucida) before arresting before ovulation.

1.2.2 Fertilisation

Fertilisation of the transcriptionally silent ovulated MII oocyte occurs in the ampulla, a region of the oviduct nearest the ovary after the fimbria. The sperm fuses with the ovum after burrowing through the zona pellucida by binding to the plasma membrane (Talbot, 1985). The sperm's genetic material is then de-condensed, where the majority of the male protamines are replaced with maternal histones, ultimately forming the paternal pronucleus, termed PN0 (Figure 1.1a) (Morgan et al., 2005).

At the same time, metaphase II of meiosis II is resumed, initiating anaphase and telophase, and then forming the second polar body and the maternal pronuclei. At this stage, the embryo contains the maternal and paternal pronuclei that become co-located by traveling along microtubules, with the varying stages being classified as PN1-5 based on progress towards the centre of the oocyte and the relative size of the pronuclei (Figure 1.1a) (Austin, 1962). The later pronuclear stages (PN2-5, Figure 1.1a) are a common stage for the assessment of fertilisation in the laboratory as the pronuclei in many species are visible through the translucent cytoplasm using an inverted microscope, including mouse (Adenot et al., 1997), pig (Kubisch et al., 1995), and human (Scott and Smith, 1998).

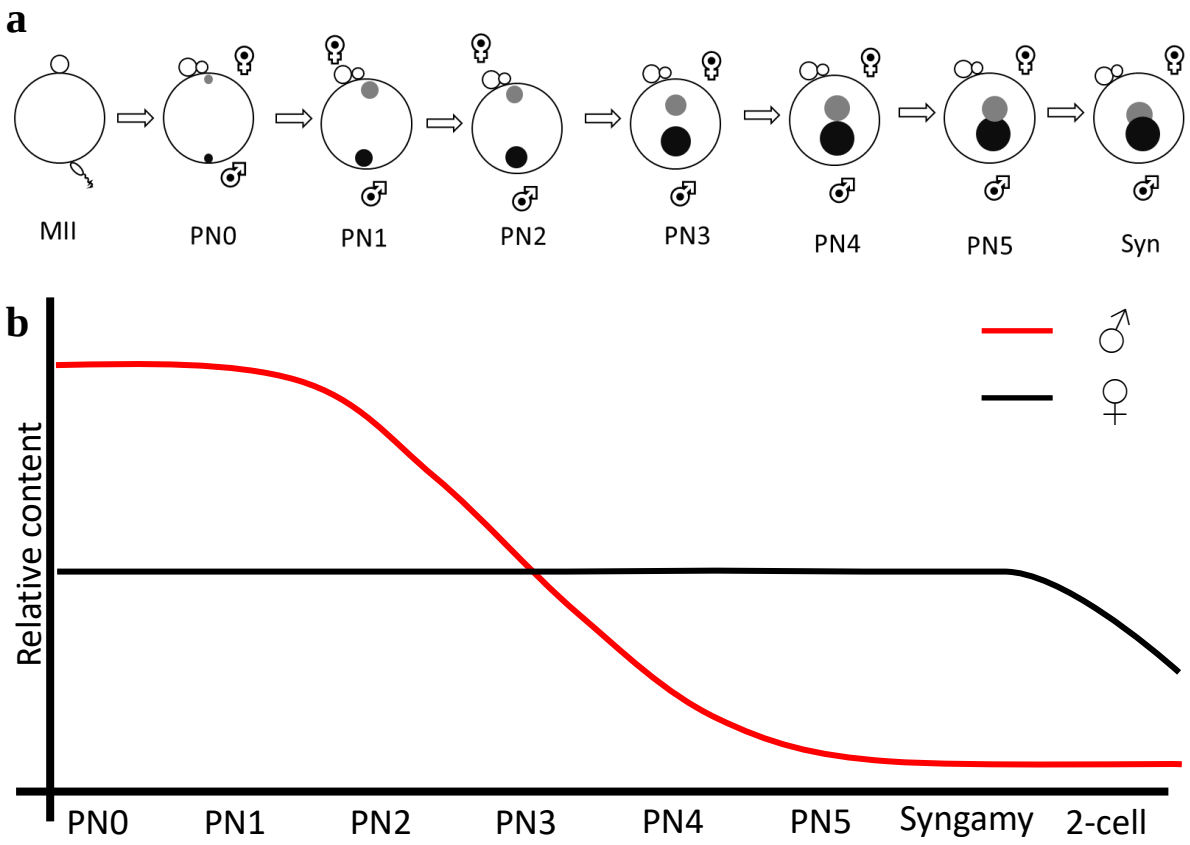

Figure 1.1 a Schematic representation of pronuclear stages in the mouse embryo from MII oocyte through to syngamy, with maternal pronucleus in grey and paternal pronucleus in black. Adapted from Adenot et al., (1997) and **b** Maternal/paternal DNA methylation levels throughout pronuclear development. Adapted from (Santos et al., 2002, Shen et al., 2014b)

Prior to the joining of the maternal and paternal pronuclei to form a single diploid nucleus, a process termed syngamy, the paternal genome is actively stripped of its methylation marks (Santos et al., 2002). Demethylation of DNA by dioxygenase enzymes (see section 1.7 *Tet* history and discovery) relies on the conversion of α-ketoglutarate to succinate, where metabolism through the tricarboxylic acid (TCA) cycle would produce NADH and GTP (Krebs and Johnson, 1937). With NADH being equivalent to 2.5 ATP molecules, global demethylation is an energy demanding process, therefore increases or decreases in metabolism could lead to a concomitant increase or decrease the demethylation from physiologically normal levels.

After removal of paternal protamines and methylation marks, syngamy can occur, where the nuclear envelopes of the maternal and paternal pronuclei dissociate, and the maternal and paternal genomes pair together (Zamboni et al., 1972). Once paired, anaphase and telophase occur, and the first round of diploid mitosis follows. Post syngamy the embryo is often termed the zygote, rather than fertilised oocyte or pronuclear stage embryo.

Immediately after fertilisation, maternal proteins begin to be degraded (Tsukamoto et al., 2008b) and new proteins begin to be synthesised from amino acids (Gao et al., 2017). This process is initiated via autophagy protein 5 (ATG5), an E3 ubiquitin ligase, which degrades oocyte specific proteins through activation of microtubule-associated protein light chain 3 (LC3) (Tsukamoto et al., 2008a). Without this proteasomal degradation of maternal proteins, fertilised zygotes arrest at the four to eight cell stage (Tsukamoto et al., 2008a), and similarly maternally derived transcripts begin degradation post sperm entry and continues through to post cleavage (Schultz, 1993).

1.2.2.1 DNA methylation during pre- and peri-conception development

Studies have focussed on *in vitro* fertilisation (IVF) in order to construct a regimented timeline for pronuclear formation, detection and syngamy in order to assess the methylation status of the separate maternal and paternal pronuclei, where the time after insemination can be accurately recorded as compared to *in vivo* mating and collection of putative zygotes (Santos et al., 2002). In a mouse model, the formation of the paternal pronucleus and replacement of protamines with maternally sourced histones on the paternal genome was shown approximately 60 min after placing the sperm with the egg (Santos et al., 2002). Approximately 5 h after insemination, these nascent histones begin to become methylated at histone 3 lysine 4 (H3K4me1), which increases through the 1-cell stage to H3K4me2 and H3K4me3 (Lepikhov and Walter, 2004).

With regards to DNA methylation, PN3 is the final stage where methylation could be observed in the paternal pronucleus using immunocytochemical methods, with no measurable methylation seen in later stages of paternal pronuclear expansion (PN4-5) and migration to the centre of the zygote (Santos et al., 2002). By contrast, the maternal DNA maintains a relatively consistent level of methylation through the pronuclear zygote until syngamy (Figure 1.1b) (Santos et al., 2002). Lamins from the cytoplasm of the oocyte were shown to associate with the paternal pronucleus, allowing the movement of proteins from the cytoplasm into the pronucleus to decondense and demethylate the pronucleus (Santos et al., 2002), requiring one molecule of α-ketoglutarate to be converted to succinate per base demethylated.

After syngamy, the maternal and paternal chromosomes can be broadly identified by their respective hypermethylation and hypomethylation, with weak methylation seen in the paternal chromosomes, likely to control the transcription of tightly regulated key developmental genes (Amouroux et al., 2016, Santos et al., 2002). This pattern of methylation remains consistent until compaction where the chromosomes duplicate, re-condense to form the chromatid structure, align on the metaphase plate, then break apart at the centromeres at anaphase, separating into two new nuclei through telophase. The 2-cell nucleus has now formed. This process is reductive mitosis where there is no replication of cellular machinery, rather the

organelles are separated into two separate cells, compared to identical copies of all contents as seen in regular mitosis.

1.2.3 Embryonic genome activation

Genome activation, or the beginning of transcription and translation from the embryonic DNA/RNA, is first seen in the paternal pronucleus, much earlier than the more well-known major zygotic genome activation. Only a basal level of transcription occurs at this stage; however the pool of paternal pronucleus sourced transcripts increases through syngamy to the 2-cell stage (Hamatani et al., 2004).

Studies performing gene expression arrays at each stage of preimplantation development (zygote, 2- cell, 4-cell, 8-cell, morula, and blast) have identified that there are three distinct clusters of gene expression in preimplantation development, with different groups of genes expressed in each phase (Hamatani et al., 2004). The first cluster is at major embryonic genome activation triggering the maternal to embryonic transition, the second at mid-preimplantation activation for genes expressed for compaction and blastocyst development, and the third group of genes that are basally transcribed, which happen at specific developmental stages when required (Eckersley-Maslin et al., 2018, Hamatani et al., 2004, Ko, 2006).

Gene expression prior to the major embryonic genome activation consists of genes associated for ribosome biogenesis which are required for the major embryonic genome activation (EGA) to occur (Hamatani et al., 2004). For these genes, there are two distinct groupings: those genes that are further transcribed in the major EGA, and those transcribed in the 1-cell minor genome activation (Abe et al., 2018). Noteworthy genes that are expressed in the zygote but not at major embryonic genome activation include genes required for metabolism and energy production such as pyruvate dehydrogenase kinase *Pdk3* (Abe et al., 2018), the enzyme that catalyses pyruvate to Acetyl-CoA for pyruvate to be added to the TCA cycle (Figure 1.2a), and acyl-CoA dehydrogenase, required for ß-oxidation of fatty acids (Abe et al., 2018). Genes expressed first in the 1-cell but additionally at major EGA include transcripts for DNA and histone

demethylation, *Tet2* for active DNA demethylation (see Section 1.7 and 1.8), *Kdm4a-d* lysine demethylases for H3K9me3, and *Kdm5b*-d, lysine demethylases specific for H3K4me3 (See Section 1.10.4 for further information on KDM5) (Abe et al., 2018). It has been demonstrated that inhibiting transcription in 1-cell embryos does not permit progress past the 2-cell stage (Abe et al., 2018), indicating that expression of these genes is critical for major EGA to be carried out for normal embryonic formation.

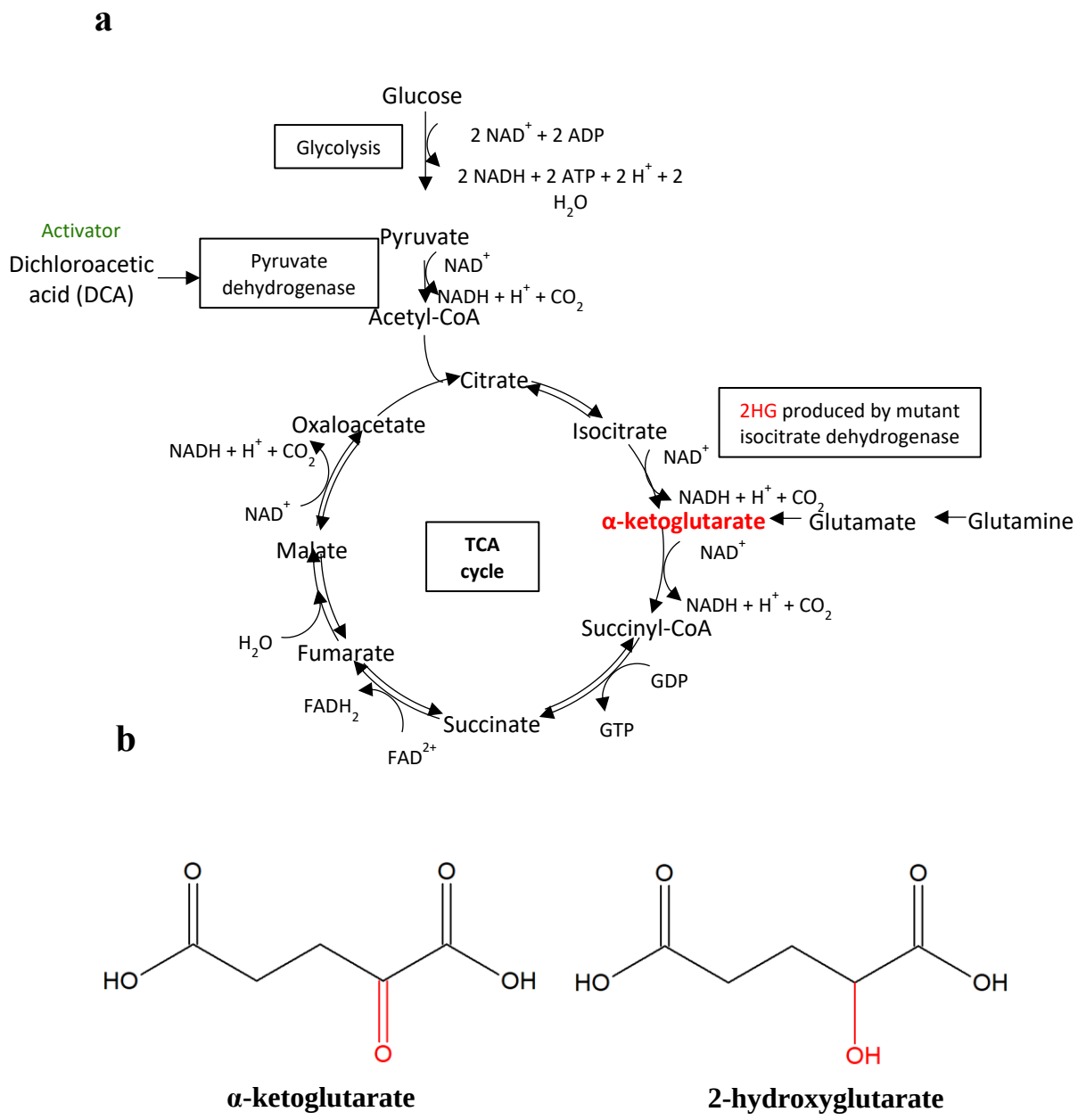

Figure 1.2 a Tricarboxylic acid (TCA) cycle, with mechanism of dichloroacetic acid (DCA) activation of the TCA cycle, and production of 2HG, and **b** Chemical structure of α-ketoglutarate and 2-hydroxyglutarate, with differing bonds highlighted in red

In the major embryonic genome activation, the activated genes predominantly encode for cellular machinery, principally ribosomes, ribonucleoproteins, ion transporters and proteasomal complexes. The activation of these gene networks show that EGA primes the preimplantation embryo with the machinery needed for subsequent blastocyst development (Hamatani et al., 2004). Major embryonic genome activation occurs at different stages for different species. For example the human major EGA occurs at the 4-cell stage (Braude et al., 1988), at the 2-cell stage in mice (see below), and 8-cell stage in bovine (Meirelles et al., 2004). During these cleavage stages up to compaction, the individual cells, termed blastomeres, remain totipotent, whereby each blastomere can differentiate into any other cell type within the organism.

It is at the 2-cell stage that the major activation of the embryonic genome occurs in mice (Hamatani et al., 2004, Telford et al., 1990, Whittingham, 1975). The few genes that were activated in the zygote stage are now being transcribed, producing the required machinery such as ribosomes and proteins used for ion transport and the proteasome complex (Hamatani et al., 2004). Without the production of these components, the embryos will arrest at the stage where major embryonic genomic activation occurs as the necessary proteins could not be produced for compaction to occur (Whittingham, 1975). After the major embryonic genome activation in the 2-cell in the mouse, another round of division occurs in each of the two blastomeres, forming a 4-cell embryo, followed by another round of mitosis, creating an 8-cell embryo. It is at the 8-cell stage in the mouse that the preimplantation embryo produces the required proteins and factors to allow for compaction to occur.

Mid-preimplantation genome activation occurs at the 4-cell to 8-cell stage in mouse (Hamatani et al., 2004), with over 4000 uniquely upregulated genes, many more than the earlier EGA at the zygote to four cell stage. Key genes transcribed at this activation include methyltransferases, endopeptidase inhibitors and genes required for gap junction and tight junction formation (Hamatani et al., 2004).

The transcript abundance of these mid-preimplantation activated genes is reduced immediately prior to compaction, indicating that they are required for compaction and cavitation; however, they are not required for continued production after the morula is formed. Methyltransferases, including the DNA methyltransferases DNMT1, DNMT3A, and DNMT3B are required after compaction in order to methylate certain genes after the global demethylation event described above (Hamatani et al., 2004, Robertson et al., 1999).

1.2.4 Compaction

Compaction is a process where there are major structural changes that occur in the preimplantation embryo. In the mouse and human this begins at the 8-cell stage, while bovine embryos begin compaction at the 16-32 cell stage (Van Soom et al., 1997). The individual blastomeres begin to adhere to each other through the expression of the cell adhesion protein E-cadherin to form tight junctions between the blastomeres (Riethmacher et al., 1995, Gumbiner et al., 1988). Gap junctions form between the blastomeres to allow the movement of the various molecules and other signals between each other in a controlled manner (Fléchon et al., 2004). The formation of these tight junctions assists in changing the morphology of the blastomeres, polarising them so the nuclei are centrally located in the preimplantation embryo, with actin-containing microvilli toward the outside of the embryo (Ziomek et al., 1982). Compaction occurs at the approximate time where the preimplantation embryo moves from the oviduct into the uterus *in vivo* (Li et al., 2010).

1.2.5 Morula

Morulae, due to the tight junctions between blastomeres, do not have defined cellular borders when viewed under light microscopy as compared to earlier multicellular preimplantation embryo stages. Morulae usually have between 16-32 cells, where the blastomeres on the outside of the preimplantation embryo maintain polarization, with tight junctions between cells, while the new internal cells are apolar, or show no change in morphology (Ziomek et al., 1982). *In vitro* studies have determined that at this stage both the polar and apolar cells maintain totipotency. In mice, this stage is reached on day 3 (Gardner et al., 2004), day 5 in cows (Van Soom et al., 1997) and human on day 4 (Nikas et al., 1996).

1.2.6 Blastocyst

Cellular differentiation begins at the late morula stages, where the inner and outer cell layers begin to differentiate to become the blastocyst. The polarised outer cells of the embryo differentiate into trophectoderm (TE) cells, which maintain both the tight junctions and gap junctions seen in the morula stage embryo (Bavister, 1995, Riethmacher et al., 1995). The apolar internalised cells lose their tight junctions and appear larger than the TE cells (due to their slower cleavage rate compared to TE cells) but maintain gap junctions. At this stage, the TE cells are no longer totipotent, and are now committed to becoming extra-embryonic tissues after implantation. The internal cells, now termed the inner cell mass (ICM), retain their totipotency, and will later become the foetus (Bavister, 1995, Gardner and Lane, 1997). During this process the TE cells transport ions from the outside milieu into the embryo using aquaporins, creating a fluid filled cavity termed the blastocoel (Watson and Barcroft, 2001), which allows the transport of glucose and select proteins from the trophectoderm after uptake from the surrounding medium. The activation of these aquaporins and sodium/potassium/ATPase antiporters require one ATP molecule for three sodium ions and two potassium ions and thus requires a large proportion of the energy produced up to, and including at this stage, to be used for this process alone. The Na^+/K^+/ATPases increase in abundance

dramatically post compaction, with very little Na^+/K^+-ATPase via immunofluorescent immunocytochemical staining in cleavage stage embryos in a murine model (Watson and Kidder, 1988). TE cells use glucose as their primary source of fuel producing pyruvate through oxidative glucose metabolism (Bavister, 1995). In contrast, ICM cells use anaerobic glycolysis (Hewitson and Leese, 1993). It is believed that the trophectoderm functions to provide the substrates for the anaerobic glycolysis (explained further in Section 1.3.4).

1.3 Role of mitochondria in the development of preimplantation embryos

The metabolism of the oocyte and preimplantation embryo is known to reflect its subsequent viability, with perturbations in metabolism and more specifically mitochondrial function commonly reported after environmental exposures to suboptimal conditions (Bavister, 1995, Lane et al., 2014a, Lane et al., 2014b, McPherson et al., 2015). This is important for the oocyte and cleavage stage embryo as, unlike somatic cells, these cell types are completely reliant on mitochondria for ATP production (Chi et al., 1988, Dumollard et al., 2007, Gu et al., 2015, Houghton et al., 1996). Pathways such as glycolysis cannot generate ATP until the blastocyst stage, even though the cellular machinery, including hexokinase (phosphorylates glucose to glcose-6-phosphate for the first irreversible step in glycolysis), are present at the earlier stages of development (Bavister, 1995, Chi et al., 1988, Gardner and Leese, 1988, Houghton et al., 1996, Lane and Gardner, 2005, Leese, 2012, Leese and Barton, 1984), leaving pyruvate and carboxylic acid metabolism through the TCA cycle as the key energy generating pathway for the cleavage stage embryo.

1.3.1 Oocyte mitochondria

All of the mitochondria in the embryo originate from the oocyte (Babayev and Seli, 2015). After this initial replication phase during oogenesis, the mitochondria within the oocyte of mature follicles cannot undergo biogenesis. As a result, the mature oocyte contains a large number of mitochondria, approximately 125,000 as measured by mtDNA copy number, assuming two copies of mtDNA per mitochondrion (Wiesner et al., 1992), where these mitochondria are then allocated into each cell through each subsequent division (Luzzo et al., 2012). The mitochondria in the oocyte do not have the same morphology of mitochondria from a somatic cell, rather they typically have a spherical structure, with very few of the cristae, or folds in the outer membrane, typically seen in mature mitochondria (Sathananthan and Trounson, 2000). As a result, oocyte mitochondria are relatively quiescent with low ATP output and oxygen consumption (QO_2) similar to that of bone (Babayev and Seli, 2015, Conaghan et al., 1998, Leese, 2012, Wilding et al., 2001). This is thought to be an evolutionary strategy to ensure a reduction in oxidative stress to minimise production of mtDNA mutations during the long phase of the oocyte being dormant in the ovary until ovulation.

In the human, the mitochondria have a polarised distribution throughout the oocyte, with a diffuse pattern towards the centre of the metaphase II arrested oocyte, but more granular, aggregated mitochondria seen closer to the plasma membrane (Wilding et al., 2001). This polarisation appears to be critical, with aged or vitrified MII oocytes presenting with a diffuse, homogenous pattern throughout the oocyte and no granularity near the zona pellucida that may not be optimal (Figure 1.3) (Wilding et al., 2001, Zander-Fox et al., 2013). A similar pattern in healthy mouse oocytes is seen, however the mitochondria appear to be much less abundant toward the zona pellucida (Figure 1.3) (Van Blerkom et al., 2000, Zander-Fox et al., 2013).

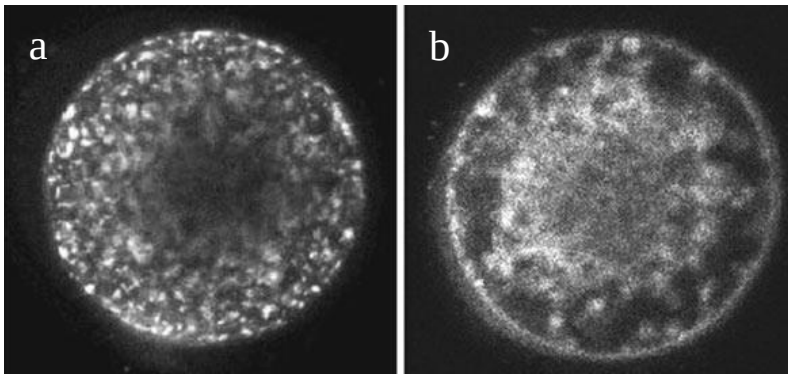

Figure 1.3 Mitochondrial distribution and membrane potential of ovulated oocytes at metaphase II (MII) stained using mitochondrial membrane potential dye 5,5′6,6′-tetrachloro-1,1,3,3′-tetraethylbenzimidazolycarbocyanineiodide (JC-1), where **a** high quality, and **b** vitrified, and low quality. Note the peripheral and intermediary staining of the fresh, high quality oocyte and the vitrified oocyte displaying increased intermediary staining with decreased peripheral staining. Images from (Zander-Fox et al., 2013)

Mitochondrial membrane potential as measured by 5,5′,6,6′-tetrachloro-1,1′,3,3′-tetraethylbenzimidazolylcarbocyanine iodide (JC-1) shows the ability of the mitochondrial membranes to produce a gradient of hydrogen ions, effectively showing the metabolic potential of mitochondria (Wilding et al., 2001). The mitochondrial membrane potential of mouse GV stage oocytes appears uniform regardless of where the mitochondria are located (Salehnia et al., 2013) however in human GV oocytes, the membrane potential appears highest in the subplasmalemmal region (i.e. the region close to the zona pellucida), continuing through to the MII stage after *in vitro* maturation (Ou et al., 2012).

1.3.2 Mitochondria at fertilisation

Mitochondrial distribution changes post fertilisation, with the mitochondria moving to surround the pronuclei (Sathananthan and Trounson, 2000). Before fertilisation, rodent embryos begin with a diffuse mitochondrial localisation with increased membrane potential in the subplasmalemmal region (Ou et al., 2012), which post-fertilisation changes to a perinuclear region, diffusing to a lower concentration in the subplasmalemmal region (Bavister and Squirrell, 2000). The clustering of mitochondria changes after fertilisation, with the mitochondria distributed more evenly throughout the cytoplasm (Bavister and Squirrell, 2000). The mitochondria themselves also begin to form a more typical ovoid shape, with many more cristae in the membrane to dramatically increase inner membrane surface area. The increased surface area allows for increased pyruvate metabolism through the TCA cycle in the PN stage embryo and zygote compared to the unfertilised oocyte (Reynier et al., 2001, Bavister and Squirrell, 2000, Babayev and Seli, 2015).

Fertilisation also changes the mitochondrial membrane potential in human oocytes, whereby metaphase II oocytes showed similar membrane potential for both subplasmalemmal and perinuclear mitochondria regions, whereas post-fertilisation heterogeneity was shown between regions within the fertilised oocyte. The higher potential mitochondria present in a peri-pronuclear distribution (Babayev and Seli, 2015, Van Blerkom et al., 2000), whilst lower

potential was seen in the subplasmalemmal regions (Babayev and Seli, 2015, Van Blerkom et al., 2000). In mouse pronuclear stage embryos, the same heterogeneity in mitochondrial activity was seen, however the gradient of heterogeneity is less pronounced (Van Blerkom et al., 2002).

1.3.3 Two-cell to 8-cell stage mitochondria

After the first division to the 2-cell embryo, both lactate and phosphoenolpyruvate (PEP) can be utilised as energy sources in addition to pyruvate (Whittingham, 1969). Lactate is converted to pyruvate using lactate dehydrogenase (LDH) and metabolised through the TCA cycle. The malate-aspartate shuttle allows lactate metabolism by shuttling the NAD^+ required by lactate dehydrogenase in the cytoplasm. (Lane and Gardner, 2005), although sufficient aspartate is required (Lane and Gardner, 2005).

The use of lactate is crucial as it facilitates the uptake of pyruvate based on the embryo developmental stage, with the highest rates of metabolism being observed when both substrates are provided (Biggers and Stern, 1973). From the 4-cell stage, facilitated glucose pore proteins are expressed, including *Glut1*, *Glut2*, *Glut3* and *Glut9*, which form pores in the nuclear and outer membranes of the embryo to facilitate transport of glucose with a Na^+ ion (Carayannopoulos et al., 2004, Pantaleon et al., 2001, Purcell and Moley, 2009).

The expression of glucose transporters, including GLUT5, increases in bovine embryos from the 8-cell stage as shown from electrophoresis of RT-PCR amplicons (Augustin et al., 2001). This increase is in preparation for glycolysis, with increased glucose and pyruvate uptake being seen (Gardner and Leese, 1988). It has been shown that the 8-cell mouse embryo will develop on glucose alone *in vitro* (Brinster and Thomson, 1966, Gardner and Leese, 1988), likely from expression from mid-preimplantation genome activation mentioned in Section 1.2.3, with the 8-cell embryo in a transition stage prior to compaction. The process of glucose metabolism produces pyruvate from aerobic glycolysis, which then carries through the TCA cycle as used for energy production in earlier stages.

By the two cell stage in mice, the mitochondrial distribution differs substantially between species, with mice showing minor clustering around the nuclei (Bavister and Squirrell, 2000), while human embryos show a more diffuse gradient from the nuclei to the outer membrane (Noto et al., 1993). In non-viable human embryos, random aggregations of mitochondria are seen throughout the cytoplasm (Noto et al., 1993). At this 2-cell stage, both elongated and immature mitochondria exist at approximately a 1:1 ratio as concluded from mouse embryo ultrastructural studies (Calarco and Brown, 1969).

By the 8-cell stage mitochondria all have matured, with a diameter of 600-1000 microns (Calarco and Brown, 1969), and large cristae that allow for increased metabolism in both the TCA cycle and oxidative phosphorylation.

1.3.4 Morula/blastocyst mitochondria

Oxygen consumption remains consistent from the zygote stage through to the morula stage, before increasing dramatically throughout the remainder of preimplantation development, culminating in the blastocyst consuming approximately three times the amount of oxygen as earlier stages based on embryo dry weight (Houghton et al., 1996). Using ultramicrofluorimetric analyses of glucose uptake and lactate production, glucose uptake was increased 4-fold between the 8-cell and the blastocyst stage, with a concomitant increase in lactate production of the same magnitude (Gardner and Leese, 1988).

Localisation of GLUT1 transporters to basolateral membranes begins to occur at this stage, not bound to the nuclear membrane or diffuse in the cytoplasm (Pantaleon et al., 2001), allowing for the GLUT transporters to perform their function of transporting glucose and other energy substrates into the cells of the morula. Post compaction, the matured mitochondria appear to become less dense, increasing the size of the mitochondrial matrix (Sathananthan and Trounson, 2000).

The trophectoderm in cavitated blastocysts functions to mediate the transport of glucose into the blastocoel in a highly controlled fashion, because the blastocoel cannot contain high concentrations of glucose at any given time as it can cause hyperglycaemic damage to ICM cells (Hewitson and Leese, 1993). The ICM utilises as much as three times the glucose compared to the TE on a per cell basis whilst anaerobically producing lactate (Houghton, 2006), suggesting that the primary function of the TE is to provide the ICM with the required nutrients, which continues post implantation where the cytotrophoblast cells differentiate into the placenta after implantation to provide nutrients during foetal development (Niakan et al., 2012). Oxidative metabolism throughout the TCA cycle continues to occur in the TE so the inner cell mass is still in total ATP production energetically quiescent in comparison.

In tandem with the differences of nutrient uptake; measurements of oxygen consumption of whole blastocysts and whole inner cell mass cells were generated using a mouse model, it was deduced that the TE oxygen consumption made up the difference between the two measurements (Houghton, 2006). This showed that oxygen consumption of the inner cell mass was ~33% lower than the oxygen consumption of the TE (Houghton, 2006), and that the majority of oxidative phosphorylation occurs in the TE, the region in the blastocyst where the majority of the mitochondria are localised.

1.4 Impact of environmental exposures on preimplantation embryo metabolism and viability

As stated above, genome activation, compaction/cavitation, and differentiation require large amounts of energy to occur. It has been hypothesised that nutritional and metabolic imbalances are associated with poor oocyte and embryo viability (Leese, 2002). For example, embryos that are less metabolically efficient (i.e. require more than the average amount of oxygen to produce the same amount of energy in the form of ATP than "normal" embryos) produce more reactive oxygen species, such as superoxide and hydrogen peroxide (Chason et al., 2011, Leese, 2012). While these are essential signalling molecules at basal levels, increased concentrations can cause significant damage to the cell, including damage to the mitochondrial membrane, reducing the production of energy, as well as damaging the structure of proteins and thus altering their function. Therefore, metabolic activity of the oocyte and embryo must be maintained at an intermediate level, where either an increased or decreased uptake or use of metabolites is associated with poor viability.

1.4.1 *In vitro* effects on embryo metabolism

The concept that *in vitro* conditions impact on the regulation of the metabolism of the early embryo was first reported in 1970's where Menke and McLaren (1970) demonstrated in a mouse model that culturing embryos *in vitro* reduced oxygen consumption compared to uterine collected blastocysts (Menke and Mclaren, 1970). This has been followed by several studies, primarily in rodent embryos, that demonstrated that modifications to the carbohydrate content of the culture media can modify embryo metabolism compared to blastocysts allowed to develop *in vivo*. These alterations in embryo metabolism, which were almost exclusively a redirection away from mitochondrial oxidative metabolism to the less energetically efficient glycolytic conversion to lactate, was reflected in reductions in embryo development and viability. This was frequently accompanied by an increase in glucose uptake by blastocysts, however utilised less effective pathways for ATP production, results in up to 50% decline in

ATP and therefore available energy in the embryo (Gardner and Sakkas, 1993, Gardner and Leese, 1990, Lane and Gardner, 2000).

It has further been demonstrated that this reduction in viability and impairment in mitochondrial metabolism and reduction in ATP output occurs after just 6 h in sub-optimal culture system (Lane and Gardner, 1998).

In vitro maturation (IVM) of oocytes from the GV stage through to MII oocytes is routinely carried out in domestic animal research, particularly bovine, pig and also rodent (Barnes et al., 1989). Human maturation of oocytes is most common where immature oocytes are collected for fertility preservation of prepubertal girls undergoing cancer treatment, as these girls will not respond to routine hormonal stimulation. IVM may also be used for women with polycystic ovarian syndrome (PCOS) where standard controlled ovarian stimulation regimes may carry a high risk of ovarian hyperstimulation syndrome (OHSS) or those with oestrogen responsive cancers (Shirasawa and Terada, 2017).

In vitro maturation carries implications for perturbed mitochondria and metabolism in the mature oocyte and throughout embryo development. Compared to oocytes from naturally cycling mice, IVM mouse oocytes show significantly lower mtDNA copy number, lower mitochondrial membrane potential via JC-1 and lower ATP content, with increased ROS production (Ge et al., 2012a). Indicating that the mitochondria have been somewhat compromised from IVM compared to *in vivo* conditions. As a consequence, IVM embryos exhibit lower fertilisation rates, reduced day 5 blastocyst formation rates, and reduced total blastocyst cell number compared to *in vivo* matured oocytes (Sanfins et al., 2015). This reduced fertilisation rate may be due to a greater rate of meiotic chromosome alignment abnormalities (Li et al., 2006), which may fertilise at a lower rate compared to normal alignment. Studies have also demonstrated that mouse oocytes that are matured *in vitro* compared to *in vivo* have a greater proportion of blastocysts with cells positive for DNA damage (Banwell et al., 2007) and reduced placental weight after transfer (Banwell et al., 2007). Furthermore, *in vitro* matured porcine oocytes produce blastocysts with decreased developmental rates and decreased total

cell number (Stokes et al., 2005). This indicates that the period of oocyte development after re-activation of the cell cycle is particularly sensitive to external stressors and may not yet be optimised for this period of oocyte maturation.

These effects extend into adult offspring generated from these embryos, leading to reduced cardiac output and decreased pulse rate (Eppig et al., 2009). Together, these results indicate that *in vitro* maturation of mouse oocytes can lead to reduced mitochondrial effectiveness in the oocyte, resulting in reduced embryo development and adverse health outcomes in adult offspring.

1.5 Effect of pharmacological inhibition of mitochondria on oocyte, embryo and viability and offspring

As outlined in Section 1.4 many different *in vitro* stressors, including culture with poor media, perturb the early embryo ultimately resulting in a loss in viability. One of the first detectable changes in the preimplantation embryo is a significant reduction in mitochondrial metabolism, linking mitochondrial metabolism with embryo viability (Igosheva et al., 2010, Lane and Gardner, 1992, Lane and Gardner, 1998, Wu et al., 2015b). Several studies have demonstrated a direct link of mitochondria function with early embryo development and viability by means of chemical inhibitors.

1.5.1 Inhibitors of oxidative phosphorylation

In the oocyte/preimplantation embryo, early studies examined the effects of cyanide, a cytochrome C inhibitor which inhibits oxidative phosphorylation, to determine to what extent the electron transport chain was used for energy production by cavitating blastocysts (Brison and Leese, 1994). In the presence of 1.0 mM cyanide, rat blastocysts appeared to not utilise the TCA cycle for energy production, as blastocoel formation was still possible in the absence of the electron transport chain (Brison and Leese, 1994). In contrast, in the mouse, 1.0 mM cyanide inhibited blastocyst formation, demonstrating that oxidative phosphorylation is essential for murine blastocyst cavitation (Trimarchi et al., 2000). It is thought that the rat embryo can carry out this switch in substrate utilisation due to its increased capacity for glucose uptake and lactate production compared to mouse embryos, allowing for glycolysis to produce sufficient ATP for cavitation, where the mouse embryo cannot (Brison and Leese, 1991).

1.5.2 Inhibitors of mitochondrial shuttles

Another important function for mitochondria metabolism is the transport of NADH across the inner mitochondrial membrane for use in the mitochondrial electron transport chain (ETC) to produce ATP. At the same time NAD^+ is regenerated in the cytoplasm, which is important for glucose and lactate metabolism. This co-relocation of redox substrates occurs by the shuttling of oxidised substrates from the matrix of the mitochondria into the cytoplasm, where they are reduced by dehydrogenase enzymes, converting NADH to NAD^+ in the cytoplasm. The reduced substrate is then returned to the matrix through an antiporter and oxidised in the matrix to "shuttle" the NADH across the inner mitochondrial membrane. The most studied system that carries out this process the malate aspartate shuttle (MAS) (Figure 1.4).

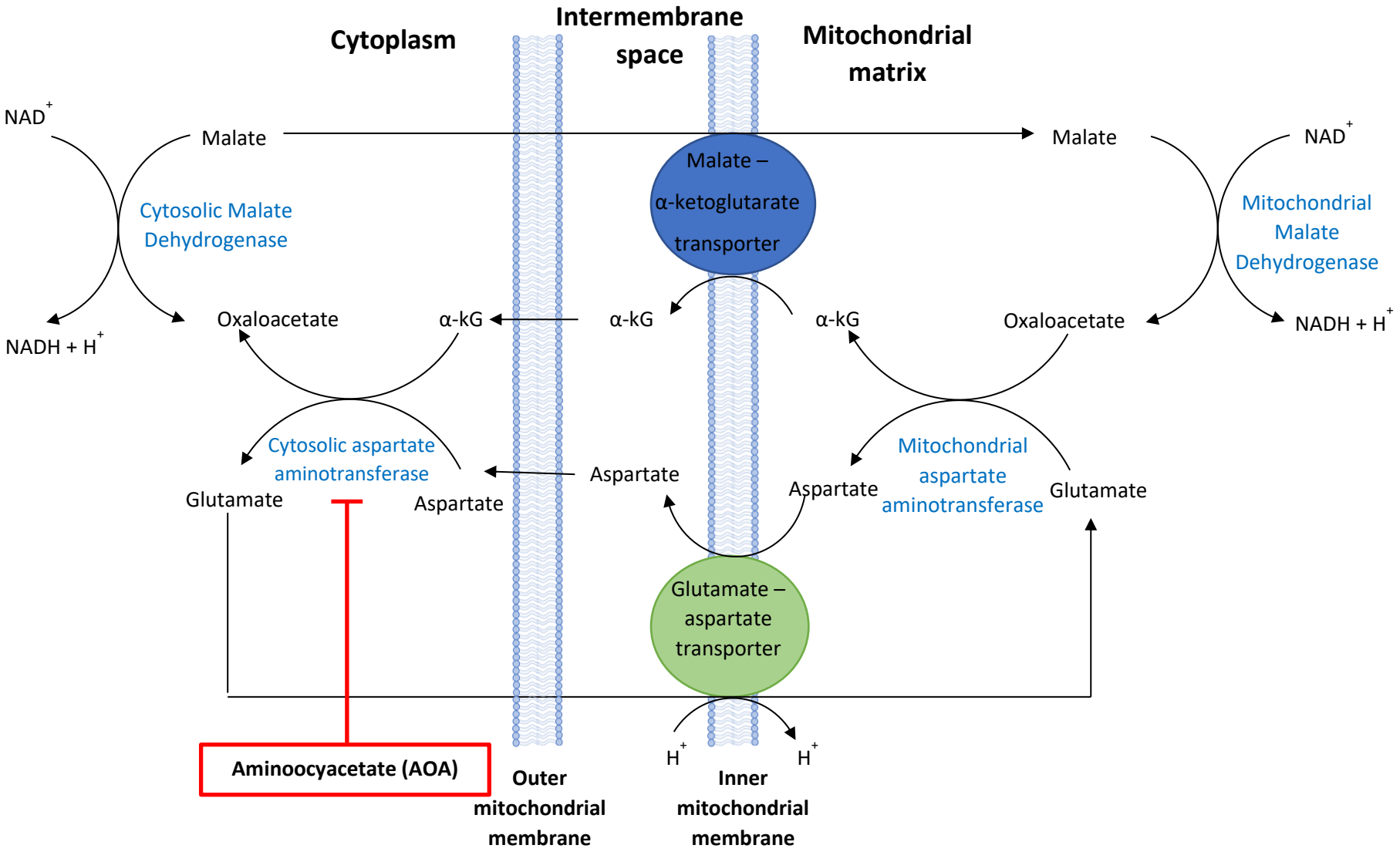

Figure 1.4 Malate-aspartate shuttle (MAS) with target site of aminooxyacetate (AOA), where α-kG = α-ketoglutarate

Several studies have inhibited the MAS using aminooxyacetate (AOA), an inhibitor of cytoplasmic aspartate aminotransferase (Kauppinen et al., 1987), a critical component of the MAS which catalyses the interconversion of aspartate and α-ketoglutarate to oxaloacetate and glutamate (Hewitson et al., 1996, Lane and Gardner, 2005) (Figure 1.4). Supplementation with increasing concentrations of AOA inhibited metabolism and inhibited development to the blastocyst stage (Lane and Gardner, 2005).

At concentrations of AOA that reduce ATP output by mouse blastocysts by approximately 60% (Wakefield et al., 2011), embryos were still able to develop to the blastocyst stage , however with reduced implantation rates and numbers of viable offspring compared to controls (Mitchell et al., 2009, Wakefield et al., 2011). Interestingly, this reduction in mitochondrial metabolism also reduced foetal size and altered the transcriptome in the resultant foetal mouse brain, with transcripts pertaining to carbohydrate metabolism, neurological development, cellular proliferation, DNA replication and repair, and methylation and acetylation all altered (Fullston et al., 2011). This indicates that reduced mitochondrial shuttle activity in the preimplantation embryo can have lasting impacts on foetal development involved in methylation and acetylation of histones and DNA, programming future embryo and offspring development.

1.5.3 Uncouplers of oxidative phosphorylation and the TCA cycle

Other inhibitors act as ionophores, rather than targeting specific enzymes, transporting ions across the inner mitochondrial membrane for oxidative phosphorylation, such as 2,4-dinitrophenol (DNP), and carbonyl cyanide–*p*-trifluoromethoxyphenylhydrazone (FCCP). After addition of these ionophores, the proton gradient that is essential for ATP synthase is lost, effectively uncoupling aerobic respiration with the TCA cycle in the treated cells. The two ionophores DNP and FCCP have both separately been added to the culture media for oocytes and preimplantation embryos to establish the impact on development and viability.

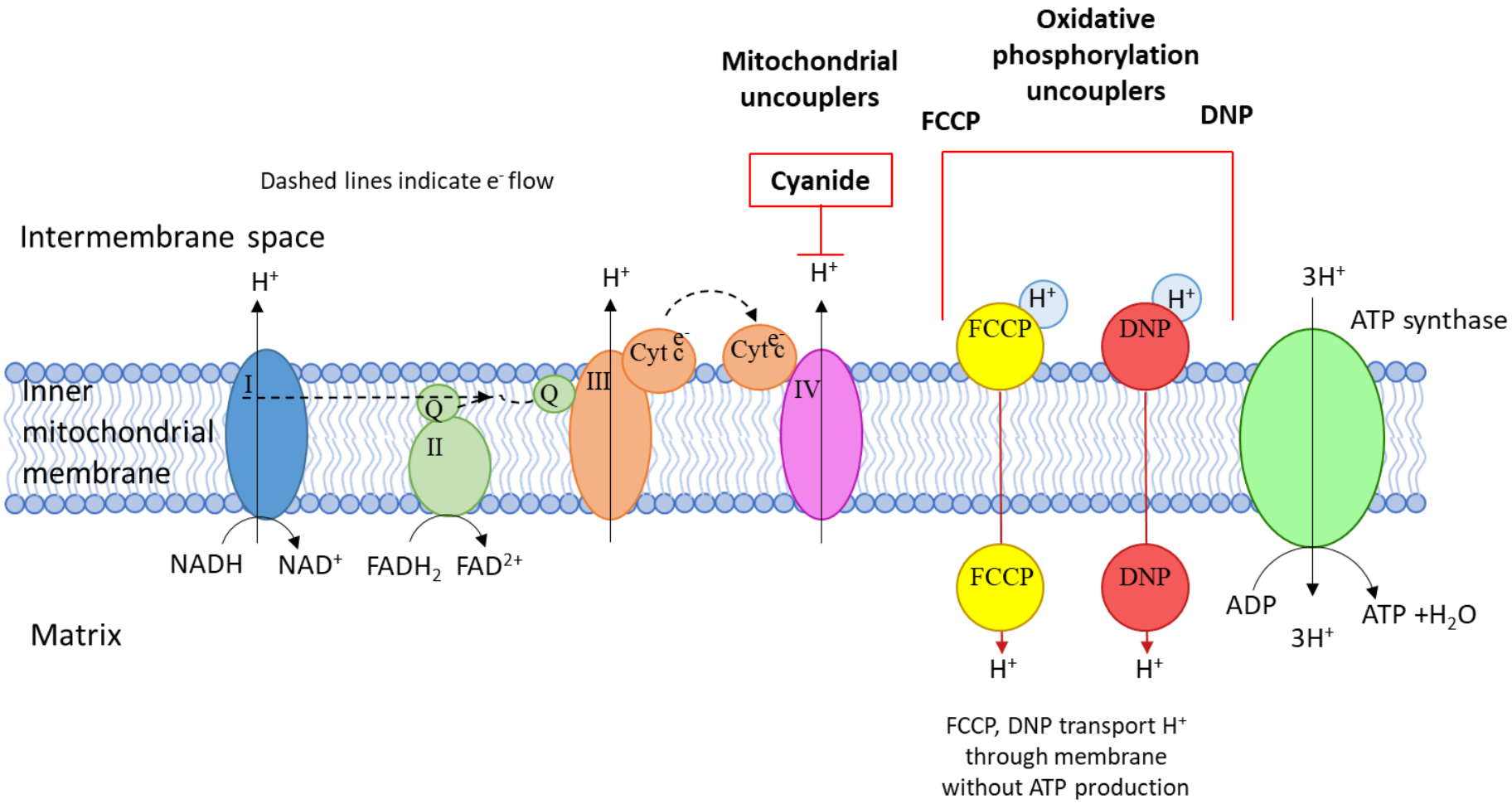

Figure 1.5 Mitochondrial electron transport chain (ETC), with targets for the mitochondrial uncouplers carbonyl cyanide–p-trifluoromethoxyphenylhydrazone (FCCP), 2,4-dinitrophenol (DNP) and the oxidative phosphorylation inhibitor cyanide

DNP has been utilised to generate much of our current knowledge base about the differing energy sources and requirements in sheep and bovine preimplantation embryos across different developmental stages (Harvey et al., 2004, Rieger et al., 2002, Thompson et al., 1991). In an ovine model, 50 µM DNP, a dose where development to the blastocyst stage was unaffected, did not produce a significant difference in glucose uptake if pyruvate was present in the medium; however if pyruvate was omitted the glucose uptake was 4-fold higher (Thompson et al., 1991). This suggests that sheep embryos were able to adapt to the inability to produce energy through oxidative phosphorylation by increasing pyruvate-based metabolism, whilst anaerobic glycolysis was required if no pyruvate was available. Although the TCA cycle can provide additional NADH, a much larger increase in nutrient uptake was required compared to anaerobic glycolysis.

Bovine morulae cultured in media containing 100 µM DNP- had decreased total blastocyst development by 45%, suggesting that there may be a threshold of mitochondrial metabolism after which the embryo cannot compensate by increasing other pathways (Green et al., 2016). Interestingly, of those that reached the blastocyst stage, a significant portion were male (Green et al., 2016), which may be due to female blastocysts taking up increased glucose (Gardner et al., 2011). This resulted in a negative selective pressure for female embryos, evidenced by fewer female embryos that reached the blastocyst stage (Green et al., 2016).

In contrast to domestic animals, this result was exacerbated in rodent models, with DNP increasing glucose uptake and lactate production even in medium containing pyruvate (100 µM DNP) (Brison and Leese, 1994). This occurred with increased *Glut1* transcription (10 µM DNP) (Harvey et al., 2004), further highlighting the importance of mitochondria in maintaining ATP balance in the early embryo. When combined with the data from oxidative inhibition using cyanide in rats, where glucose uptake was increased, it is clear that reduced oxidative phosphorylation can alter gene expression to maintain energy production in rats.

In mouse GV oocytes, supplementing *in vitro* maturation medium with 1 mM DNP showed a reduction in ATP content to 3% of initial ATP levels after a 90 min incubation (Van Blerkom et al., 1995). For exposures over 90 min, resumption of meiosis did not occur, yet if the oocyte was returned to control medium the ATP levels began to trend towards normal levels (Van Blerkom et al., 1995). This suggests that maintenance of the balance between oxidative phosphorylation and the TCA cycle can resume after an acute stress, where the milieu returns to a "normal' state, but a chronic uncoupling can reduce the ATP:ADP ratio to a point where the embryo cannot recover.

FCCP also acts as an ionophore to transport hydrogen ions across the mitochondrial membrane, uncoupling ATP synthesis from the mitochondrial electron transport chain (Figure 1.5). In a mouse model, FCCP has been shown to decrease mitochondrial membrane potential (Acton et al., 2004). Similarly to DNP, the effect was reversible when embryos were returned to control medium (Acton et al., 2004), again indicating that once there is no supply of the ionophore, the potential across the inner mitochondrial membrane can be restored. Exposure to FCCP during IVM also reduced polar body formation, with spindle and chromosome misalignment (Ge et al., 2012b), as is seen in oocytes of low mitochondrial membrane potential or incorrect mitochondrial distribution in other models described above. Using 62.5 nM of FCCP, a dose that results in a partial uncoupling, and a net reduction of ATP by 18% (Zander-Fox et al., 2015), mouse embryos cultured for 48 h from zygote to the 8-cell had a decreased total cell numbers in the mouse blastocyst, but not the ICM:TE ratio, compared to cultured blastocysts in absence of FCCP (Zander-Fox et al., 2015). These blastocysts cultured in FCCP were able to implant when transferred to pseudopregnant normal weight mothers, with similar pregnancy rates (Zander-Fox et al., 2015). However, offspring birth weights were reduced and there were alterations in the metabolic health of the offspring, specifically reduced plasma glucose and high density lipoprotein (HDL), and intolerance to glucose bolus (Zander-Fox et al., 2015). Interestingly, the changes to offspring were sex specific, where female offspring gained a greater percentage of fat mass after 14 weeks, with a 3.9% increase from week 4 to week 14

compared to control female offspring where the embryo was not exposed to FCCP (Zander-Fox et al., 2015). Male offspring showed 1.5% decreased fat mass ($P<0.05$) at 4 weeks of age, but no differences later in life (Zander-Fox et al., 2015). Combined with the data from DNP treated embryos, it appears that male embryos can potentially withstand mitochondrial uncoupling to a greater extent than female embryos, where female embryos may be more susceptible to metabolic cues.

Taken together, these findings have shown that direct inhibition of mitochondrial function either through disruptions to the TCA cycle, or by membrane transport via shuttles or oxidative phosphorylation, inhibits growth in the embryo to the blastocyst stage and impairs the health of resulting offspring, providing the first evidence that control of mitochondrial metabolism is linked to offspring health in later life.

1.5.4 Stimulation of mitochondrial activity in oocytes and early embryos

To further assess how mitochondrial function influences the development of the oocyte and early embryo, adding mitochondrial stimulants to embryo culture media may improve developmental capabilities. One such *in vitro* supplement which has been investigated is dichloroacetic acid (DCA), which stimulates pyruvate dehydrogenase, increasing the rate of conversion of pyruvate to Acetyl-CoA, in turn providing additional substrate directly into the TCA cycle (Figure 1.2a). Due to the reliance of the cleavage stage embryo on pyruvate-based metabolism, DCA supplementation could assist with energy production where mitochondria may be impaired. One study showed a small increase in the number of 4-cell mouse embryos that developed after 24 h in culture with DCA compared to control, with no differences in subsequent blastocyst developmental rate (Penzias et al., 1993).

A subsequent study investigated the impact of DCA using embryos from aged mice where mitochondrial membrane potential and metabolism is decreased, and oxidative stress increased (McPherson et al., 2014). Treatment of embryos from the zygote to the blastocyst stage with 1.0 mM DCA increased pyruvate oxidation, ATP content and mitochondrial membrane

potential at the blastocyst stage (McPherson et al., 2014), whilst reducing intracellular ROS (McPherson et al., 2014).

While this DCA supplementation did not change implantation rates or placental mass after transfer, foetal weight and crown to rump length was increased to be more similar to *in vivo* derived embryos (McPherson et al., 2014). While information on offspring health would be the next logical stage of this research, these findings indicate that the murine cleavage stage embryo is very sensitive to changes in developmental milieu, and that improvement of metabolism in embryos with mitochondria compromised by ageing, obesity or otherwise may be possible.

During oocyte maturation the compound resveratrol, which acts as an activator for *Sirt1*, has also been studied (Borra et al., 2005). SIRT1 plays a critical role in the regulation of oxidative stress during oocyte maturation (Di Emidio et al., 2014). In an aged mouse model (48-52 weeks) IVM media was supplemented with 1 μM resveratrol, resulting in increased oocyte maturation rates and increased blastocyst development rates compared to control (Liu et al., 2018). The resultant mature oocytes also showed elevated fluorescence through Mitotracker Green, indicating elevated mitochondrial mass (Liu et al., 2018). Resveratrol is believed to also act as an antioxidant, scavenging and reducing mitochondrial ROS (Liang et al., 2018), and may also prevent lipid peroxidation (Liu et al., 2013). These results show that improvement of the oocyte maturation environment through stimulation of mitochondria can improve oocyte and embryo development.

1.6 The effects of obesity on oocyte and embryo mitochondria and metabolism

In addition to sub-optimal culture conditions affecting oocyte and embryo metabolism, maternal obesity has been shown to alter oocyte mitochondrial health. Embryo culture experiments that investigate embryos from obese animals implicate the pre-conception period as a main time point that these oocytes are exposed to obesity-related stress. Using murine models of pre-conception obesity, many invasive procedures can be carried out on oocytes and embryos to assess metabolic function that is not ethically possible on human embryos.

In obese female mice (fed 10% simple sugars, 20% saturated fat supplemented with sweetened condensed milk), the ratio of active mitochondria to total mitochondria was measured using tetramethyl rhodamime methyl ester (TMRM), which is sequestered only by active mitochondria. In this model a 3-fold increase in TMRM intensity was observed in obese mice compared to oocytes from mice fed a control diet (3% fat, 7% simple sugars), which is indicative of more active mitochondria (Igosheva et al., 2010). In addition, the distribution of active mitochondria was heavily distorted in oocytes from obese females, with the diffuse pattern seen in control oocytes being replaced with subplasmalemmal and central intensity, with large regions showing no active mitochondria (Igosheva et al., 2010). As discussed previously, mitochondrial distribution in oocytes is associated with normal meiosis and polar body formation, and therefore it is also not surprising that mouse oocytes exposed to preconception obesity also demonstrate severe spindle defects and variable meiotic progression (Reynolds et al., 2015). Mitochondrial DNA copy number is also increased in the obese mouse oocyte (Luzzo et al., 2012), indicating that there has been a stimulation in mitochondrial biogenesis during oocyte maturation due to the obesogenic environment.

In another model of physiological perturbation, the oocytes from obese mice that also have dietary induced hyperinsulinemic conditions, take up increased levels of fatty acids and triglycerides (Boudoures et al., 2016). These can react with intracellular ROS, forming lipid peroxidases, which damage the plasma membranes of organelles, particularly mitochondria and the endoplasmic reticulum (ER). Germinal vesicle stage oocytes had reduced mitochondrial

membrane potential, particularly in mitochondria in the pericortial region, which have high membrane potential when sourced from a normal weight mother in contrast to the obese hyperinsulinemic model (Wu et al., 2010). Increased apoptosis co-presented with reduced mitochondrial membrane potential was also seen in granulosa and cumulus cells in this study (Wu et al., 2010). The reduced mitochondrial membrane potential is likely reducing the efficiency of energy production, with hydrogen ions leaking though the membrane instead of through ATP synthase, reducing the energy produced from the same substrate input. Damage to the ER plasma membrane may also occur from lipid peroxidase and ROS damage, allowing proteins to exit the ER before higher order structures can be formed. These unfolded proteins affect the oocyte and early embryo by diverting energy that would otherwise be used for essential cellular function and cleavage, toward the removal/degradation of these non-functional proteins.

In a human model, the calcium ion level in follicular fluid increases as maternal BMI increases (Wu et al., 2010), where Ca^{2+} levels are positively associated with ER stress. Invasive viability assessment are difficult to make on human oocytes and embryos given the ethical considerations, however the above study used a mouse model of obesity to show a decrease in mitochondrial membrane potential in oocytes in this setting (Wu et al., 2010). Combined, these suggest that the lipotoxicity seen in hyperinsulinemic obesity correlates to ER and membrane stress, reducing the available energy and energy production potential in the mitochondria to be used for necessary functions.

An alternative theory to lipotoxicity induced mitochondrial activity includes imbalanced substrates altering the reduction/oxidation balance in the oocyte, or a “leak” of ROS from the mitochondrial electron transport chain (Seidler and Moley, 2015). Due to the preconceptional inheritance of mitochondria into oocytes, maternal obesity may cause damage to the mitochondria in the oocyte before fertilisation.

Post fertilisation, the mouse zygote from an obese mother has also been shown to have an increased mitochondrial membrane potential (Reynolds et al., 2015). Furthermore, the pattern

of staining in the obese oocyte or embryo was highly aggregated and non-specific compared to those obtained from normal weight controls, indicating perturbations in mitochondria distribution (Reynolds et al., 2015). These changes correlate with reduced developmental potential as demonstrated with greater time required to reach the blastocyst stage and lower number of cells present at the blastocyst stage (Leary et al., 2015).

A leptin double knockout mouse model (ob/ob) is often used as a model for obesity, as this removal of the satiety trigger results in mice overfeeding and become obese whilst being fed a control chow (Hou et al., 2016). Leptin knock out females have reduced ovarian function as shown by the collection of half the number of GV oocytes compared to wild type females (Hou et al., 2016). Metaphase II arrested oocytes collected from ob/ob mice indicated 4-fold increased rates of abnormal spindle morphology; with an approximate 30-fold increase in intracellular ROS (Hou et al., 2016). This indicates that preconception obesity increases oxidative stress in the GV stage oocyte, likely with an elevated chance of aneuploidy due to disruptions in spindle morphology.

In a diet-induced obese mouse model (HFD = 35.7% fat, CD = 6.3% fat), voluntary exercise from an exercise wheel reduced the number of lipid droplets in GV stage oocytes to the same abundance as control diet fed females, but damage to spindles was not restored suggesting that this damage was already present and could not be repaired (Boudoures et al., 2016). In this study, the exposure to a high fat diet occurred during the phase of oocyte growth and development that includes the development of the GV oocyte. Therefore, implying that perturbations to these stages of meiosis may not be reversed with exercise. Further evidence in obese and hyperinsulinemic mice has shown that one quarter of the global mitochondrial membrane potential in GV oocytes was impaired (Wu et al., 2015a). This was then mitigated by salubrinal, an agent that alleviates stress in the endoplasmic reticulum (ER) (Wu et al., 2015a). In this model development after *in vitro* fertilisation was delayed with obesity, with reduced cleavage rates and blastocyst development that was improved by salubrinal (Wu et al., 2015a). These data suggest that preconception obesity coupled with hyperinsulinemia triggers

ER stress in the oocyte, but recovery is possible. ER stress is likely caused by ROS damage to the membrane, which is most likely originating from the mitochondria.

1.7 Mechanisms for embryo programming

The sections above demonstrate that perturbations in the metabolism of the oocyte and embryo impacts viability, affecting implantation and pregnancy rates as well as impacting offspring health. However, the mechanism by which this information is transmitted from the embryo and into the offspring is currently unknown.

It has been suggested that epigenetic regulation could be the mechanism behind the transmission of the perturbed offspring metabolic phenotype dictated by environmental cues to the embryo, where the information could be encoded via DNA methylation, histone acetylation or methylation, and non-coding RNAs, among others. The most well characterised epigenetic mark is DNA methylation, and has been shown to be a mechanism of transmission from the paternal genome to preimplantation embryos and offspring (Lane et al., 2014b) and is the focus of this review. We will also discuss histone methylation at histone 3 lysine 4 (H3K4) as these have also been studied and appear to be affected by changes to metabolism. For our purposes, we will focus on only DNA methylation at 5C and on histone 3 lysine 4 methylation, as these are the most studied DNA and histone modifications respectively, and both are demethylated by enzymes that utilise α-ketoglutarate as a metabolic cofactor.

1.7.1 DNA methylation

DNA methylation is defined as the addition of methyl groups directly to any of the four bases of DNA. The first paper that demonstrated methylated cytosine marks in tuberculosis bacterial DNA was published in 1925 (Johnson and Coghill, 1925). While new epigenetic modifications are constantly being discovered and analysed, the most common modification seen and studied in genomic DNA is 5-methylcytosine (5mC), where the methyl group is attached to the 5th carbon molecule of the cytosine ring structure. The modified cytosine bases are commonly found next to a guanine residue, termed CpG sites to differentiate from cytosine to guanine base pairing (Jabbari and Bernardi, 2004). CpG residues are most often exist in islands, and generally occur upstream of genes in the control regions (Deaton and Bird, 2011, Jeziorska et al., 2017), including at transcription factor binding sites, where the methylated bases interact with DNA binding proteins differently than un-methylated cytosine (Deaton and Bird, 2011). 5mC can also exist outside of CpG residues and islands, however approximately 70% of all 5mC residues are situated at CpG sites (Jia et al., 2018).

There are four characterised DNA methyl-cytosine variants: 5mC (5-methylcytosine), 5-hydroxymethylcytosine (5hmC), 5-formylcytosine (5fC), and 5-carboxycytosine (5caC), which all originate as 5mC but are further modified to the following forms (Figure 1.6). 5hmC is created when the methyl group on 5mC is hydroxylated to 5hmC, allowing for hydrogen bonding to occur, altering the protein binding characteristics. 5fC is produced by the oxidation of the hydroxyl group of 5hmC to an aldehyde and 5caC is further oxidation of the aldehyde group of 5fC to a carboxylic acid. These final two bases have a much shorter life compared to the first two variants; occurring at much lower proportions in the genome than the former two bases (Zhu et al., 2017). These two modifications are thought to de-stabilise the deoxyribose backbone, signalling their removal from the genome. Removal of the bases can occur through two different pathways: thymine DNA glycosylase (TDG) or the base excision repair pathway (BER).

TDG has been shown to have very high affinity for both 5fC and 5caC compared to 5mC and 5hmC (Maiti and Drohat, 2011). TDG removes the cytosine residue leaving an abasic site, which is restored via DNA polymerases as part of the base excision repair pathway (BER) (Schomacher et al., 2016). TDG has been shown to be specific for the final two bases, but not 5mC or 5hmC (Maiti and Drohat, 2011). 5fC and 5caC are also known to mutate to thymidine from exposure to oxidizing agents such as ultraviolet light, where the less reactive 5mC and 5hmC react to a lesser extent (Privat and Sowers, 1996).

Whilst 5fC and 5caC may be considered as transitional "demethylation" bases as they can be actively excised from the genome, both can also exist as stable modifications in the genome (Bachman et al., 2015, Neri et al., 2016, Neri et al., 2015). These stable form of 5fC and 5caC are most commonly found at transcription start sites and at enhancer regions, particularly sites where the present histones for those regions are trimethylated for histone 3 lysine 4 (H3K4me3), a histone modification associated with transcriptionally active regions (Neri et al., 2015). This stable form of 5fC or 5caC in the genome indicates that their presence may not just signal for demethylation of said bases, rather may impart a functional change in transcription, and are likely associated with broader transcriptional activity.

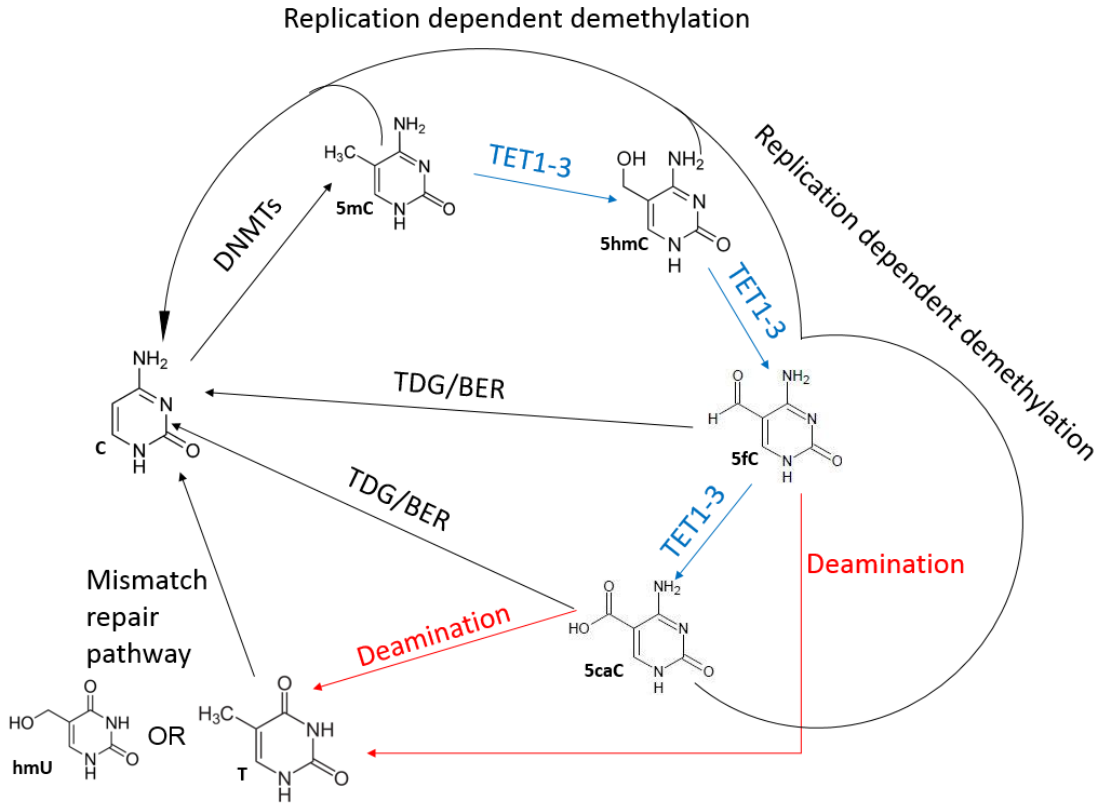

Figure 1.6 Schematic of the methylation and demethylation of cytosine, where BER = base excision repair, TDG = Thymine DNA glycosylase

1.7.2 Significance of 5C methylation variants

5mC cannot affect the activation or repression of genes in itself, rather it allows for the binding of methyl-CpG binding proteins (MBD's) (Du et al., 2015). These proteins bind specifically to methylated CpG (mCpG) islands, interacting with histones to change the chromatin structure, allowing the genes of interest to be more or less available to transcriptional machinery (Du et al., 2015). Each of the different MBD's have different binding specificities, with some binding 5hmC with the same affinity as 5mC, whilst others cannot bind 5hmC (Du et al., 2015). The importance of these proteins in the transcriptional regulation of silenced genes can be seen in the diseases caused from mutations in them, such as cancer (Patra et al., 2003) and neurological disorders, such as Rett syndrome (Amir et al., 1999), where the genes normally silenced by them are upregulated at the protein level to bind the hypermethylated sties in order to effect the transcription in both diseases.

Initial studies into the MBD binding of 5fC demonstrate that 5fC appears to bind developmentally important proteins, including FOXP1 (Iurlaro et al., 2013). The binding of FOXP1 in embryonic stem cells promotes expression of *Oct4* and *Nanog* (Gabut et al., 2011), which are critical for maintaining pluripotency of these cells. 5fC has also been shown to bind MBD3, along with histone deacetylases HDAC1 and HDAC2 (Iurlaro et al., 2013), suggesting it is required to alter chromatin formation through the deacetylation of histone marks. Together this suggests that the presence of appropriate amounts of 5fCand 5caC is important to the embryonic genome, and alterations to the normal physiological balance of these bases could have lasting effects on embryonic growth.

1.7.3 TET history and discovery

Ten-Eleven Translocase (TET) proteins were named as such due to the observed translocation of *Tet1* from chromosome 10 into the mixed lineage leukaemia (*MLL*) gene on chromosome 11, where this translocation triggers the aforementioned cancer (Pastor et al., 2013). Two other isoforms, *Tet2* and *Tet3* are believed to have been generated from a gene triplication event seen with the first common ancestor of jawed vertebrates (Pastor et al., 2013).

All three TET proteins contain two structural domains: a cysteine rich region (Cys-rich); which facilitates binding of the protein to DNA, and a double stranded beta helix (DSBH), which contains the active site. The remainder of the structure common to all three genes is much less conserved by protein sequence as it forms the globular structure away from the active site (Hu et al., 2013). TET1 and TET3 also contain a CXXC zinc finger domain (Iyer et al., 2011), which appears to increase specificity of the Cys-rich region to methylated CpG regions, evidenced by the TET2 Cys-rich region alone (which does not contain this domain) appears to bind methylated and un-methylated cytosine with similar affinity (Hu et al., 2013). It is thought that the DNA coding for the CXXC zinc finger domain was removed from *Tet2* due to an inversion event, with the removed portion of *Tet2* produced as the protein IDAX (Iyer et al., 2011). From studies that knocked out the CXXC domain of DNMT1, it appears that the Cys-rich domain is sufficient to bind CpG regions (Frauer et al., 2011), indicating that the CXXC region may provide some redundancy for binding or for greater sequence specificity.

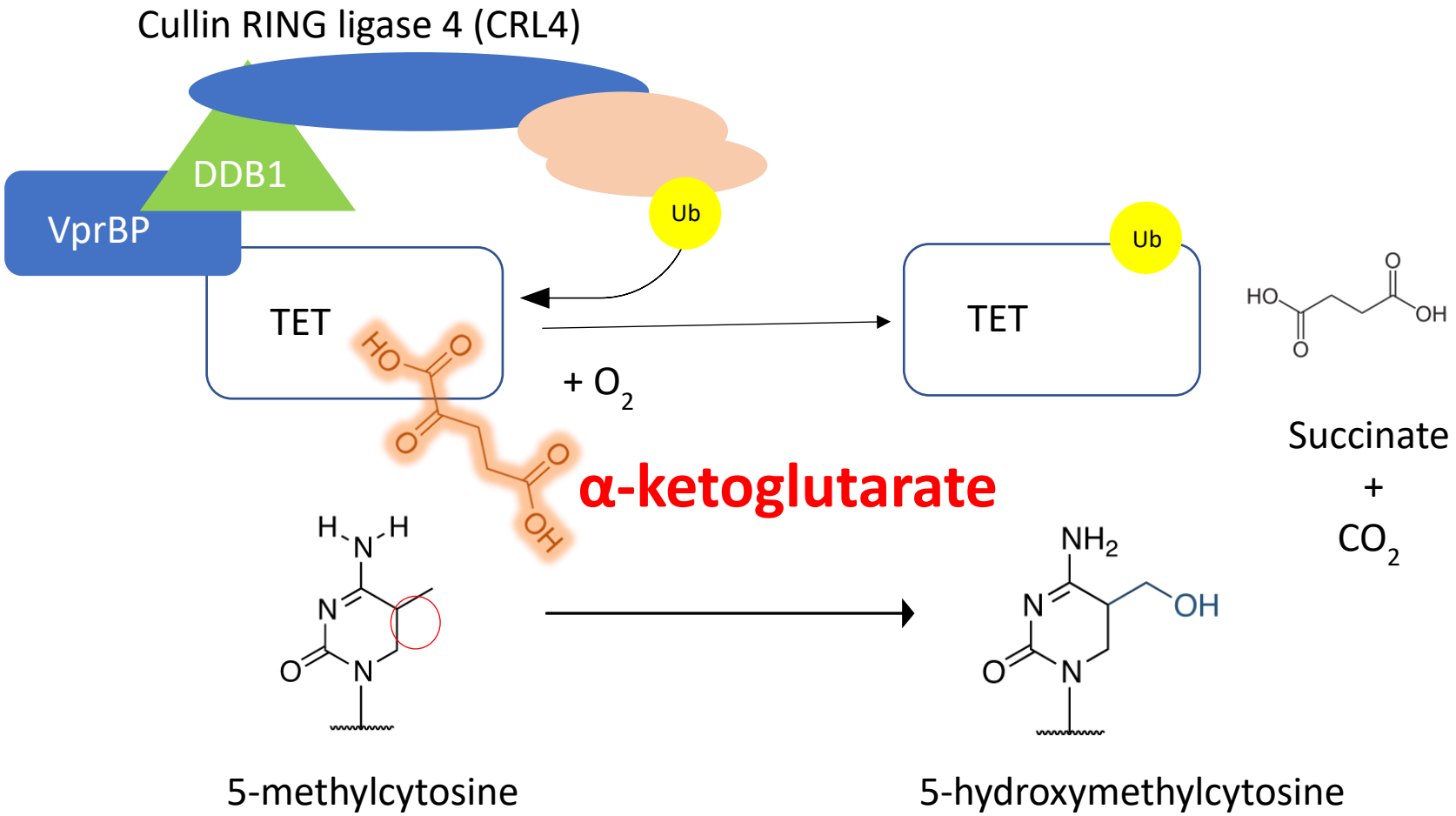

Figure 1.7 Involvement of alpha ketoglutarate (α-ketoglutarate) and the cullin RING ligase 4 (CRL4) complex on the hydroxymethylation of 5-methylcytosine (5mC)

1.7.4 TET-mediated demethylation: mechanism of function

TET proteins are the members of Fe(II)/α-ketoglutarate-dependent dioxygenases, which require Fe(II) as a metal cofactor and α-ketoglutarate as a co-substrate. The methyl group on the cytosine is orientated between the iron atoms and the molecule of α-ketoglutarate (if present) (Hu et al., 2013). With oxygen present, the ketone group from α-ketoglutarate is removed, while the electrons from the ketone group and molecular oxygen transferred to the iron atoms, temporarily forming Fe^{4+} ions (Hu et al., 2013). The second carbon from α-ketoglutarate is removed along with the ketone group, forming CO_2 along with oxidising α-ketoglutarate to succinate. The oxygen from this reaction oxidises the methyl group to a hydroxymethyl group (see Figure 1.7).

TETs have several critical cofactors required for their function, including the cullin RING ligase 4 (CRL4) complex. There are many different CRL complexes which have the similar function of ubiquitination of proteins, which targets these proteins for proteasomal degradation. Cullin RING ligase 4 is present in embryos (Yu et al., 2013), with one known function – to ubiquitinate TET to change its conformation, as shown experimentally in mouse embryos (Yu et al., 2013). CRL4 binds to TET using the adaptor protein viral protein R binding protein (VprBP), with the ROC and E2 proteins adding the ubiquitin unit to the TET. This creates a conformational change, allowing for greater binding affinity to DNA, with the CXXC domain of ubiquitinated TET able to preferentially bind methylated cytosine compared to other CXXC domain containing proteins (Nakagawa et al., 2015).

3D crystallography revealed that the DSBH core sits above the strand of DNA, where the methylated cytosine base is rotated out in relation to the sugar backbone of DNA and inserted into the catalytic core of TET. Loops from the Cys-rich region either side of the DSBH core interacts with the DNA, with zinc cations from the zinc fingers between the Cys rich and DSBH domains to stabilise the DNA and protein to maintain the correct conformation for catalysis to occur (Hu et al., 2013). TET can also function to further oxidise these bases. The action of TET

uses the energy of another α -kG molecule to catalyse the hydroxyl group to an aldehyde group, forming 5fC.

1.7.5 TET Proteins act as metabolic sensor

The requirement of the presence of alpha ketoglutarate for TET protein activity generates a paradigm by which changes to metabolism could alter DNA methylation marks. Alpha ketoglutarate (α-ketoglutarate), a small molecule, can pass freely from the cytoplasm into the nucleus, so the nuclear membrane is not believed to be the main block for nuclear availability of α-ketoglutarate. Rather, the mitochondrial activity, which is responsible for the production of this TCA intermediate, would likely affect its nuclear availability. Additionally, α-ketoglutarate cannot cross the inner mitochondrial membrane unless using a shuttle, such as the malate-aspartate shuttle, so activity of this shuttle will also affect the availability of α-ketoglutarate (See Section 1.5) (Monné et al., 2012).

A direct link between metabolism and DNA methylation has been shown in liver cells where an intraperitoneal glucose injection into a mouse altered liver tissue 5hmC levels, as measured by methylated DNA immunoprecipitation sequencing (MeDIP-seq). The greatest changes were seen at 30mins post injection, where blood glucose levels reached their peak concentration (Yang et al., 2014). Additionally, DNA hydroxymethylation was reduced 60 min post injection, indicating that the DNA was further modified to 5fC and 5caC or returned to cytosine (Yang et al., 2014). Intraperitoneal injections of glutamine and glutamate were also able to increase liver α-ketoglutarate and the global 5hmC levels at both 30 min and 60 min post injection, in contrast to glucose that did not after 60 min (Yang et al., 2014). As glutamine and glutamate are readily converted to α-ketoglutarate in cells, this indicates that a supply of α-ketoglutarate substrate may be able alter the DNA methylation profile of the mouse liver.

A recent study on embryonic stem cells have shown a direct relationship between the cellular α-ketoglutarate levels and DNA methylation status (Carey et al., 2015). In a normal situation, embryonic stem cells take up glutamate from the culture medium which is converted to α-

ketoglutarate via glutamate dehydrogenase. Addition of α-ketoglutarate to the culture medium resulted in a change in the pattern of histone methylation associated with the maintenance of pluripotency (Carey et al., 2015), indicating a direct link between the availability of α-ketoglutarate and DNA methylation which impacted on cellular development/differentiation.

Isocitrate dehydrogenase (IDH) is an enzyme immediately upstream of α-ketoglutarate dehydrogenase, which under normal physiological conditions in the TCA cycle oxidises isocitrate to α-ketoglutarate whilst reducing NAD^+ to NADH and producing carbon dioxide. A common mutation in gliomal cancers and acute myeloid leukaemia (AML), occurs where arginine residue 132 of IDH is mutated to histidine (termed ^{R132H}IDH) (Dang et al., 2009), replacing an aliphatic amino acid with an aromatic acid, reconfigures the shape of the active site. This mutant ^{R132H}IDH is still able to form a protein and bind and react with substrate, however it oxidises isocitrate to 2-hydroxyglutarate rather than α-ketoglutarate (Dang et al., 2009). α-ketoglutarate contains a hydroxyl group on the second carbon of the ketone group and whilst very similar in terms of overall structure to isocitrate, this hydroxyl group can form a hydrogen bond where a ketone group alone could not from this secondary bond, ultimately altering the conformation of the molecule in the active site of enzymes that requires α-ketoglutarate as a substrate (Figure 1.2b). The D-isomer of 2-HG which is produced by ^{R132H}IDH has shown to be bound to TETs, however due to the changed orientation of the hydroxyl group; D-2HG cannot be cleaved to oxidise methylcytosines (Evans et al., 2015), so the hydroxylation of 5mC to 5hmC cannot be carried out. This reduces TET activity, creating the hypermethylation pattern seen in these cancers where little 5hmC or further oxidation states are present (Dang et al., 2009).

1.8 Regulation of methylation in oocytes/embryos

1.8.1 DNA methylation marks in oocytes and embryos and how they change during development

There is no detectable amount of either 5mC or 5hmC in primary arrested oocytes in neonatal mice (Sakashita et al., 2014). Using immunocytochemical techniques the presence of 5mC becomes apparent in growing primary oocytes at neonatal day 15, with weak nuclear global staining of 5hmC (Sakashita et al., 2014). Global (i.e. non-sequence specific) 5mC detected using antibody based immunocytochemistry protocols, showed nuclear staining matching the nuclear reference dye in growing oocytes from 20 day old mice, remaining constant throughout oocyte maturation to the GV stage as collected from 4 week old mice (Sakashita et al., 2014). In contrast, 5hmC staining only shows weak nuclear localisation in growing oocytes, however at a lower intensity of staining than 5mC (Sakashita et al., 2014). This indicates that the regulatory proteins for the hydroxymethylation and eventual demethylation are not present in oocytes until the later stages. Furthermore, this has been confirmed with quantitative reverse transcription PCR (qPCR) for *Tet3*, where no expression was detected before day 10 (Sakashita et al., 2014), suggesting there is a very narrow window in which regulation of TET proteins can occur in the growing oocyte. Unfortunately, these studies do not perform assessment of the localisation or abundance via protein densitometry (Iqbal et al., 2011, Sakashita et al., 2014). *Tet1* and *Tet2* transcript levels were not measured, although these have already been shown not to be expressed in the oocyte at the MII stage via quantitation of transcript levels (Iqbal et al., 2011). To date, there have been no studies that show the dynamics of TET3 from the GV stage to the arrested MII stage prior to fertilisation in mice. However, in a porcine model TET3 appears diffuse throughout the cytoplasm, and become co-localised with the genetic material at MII (Page-Lariviere and Sirard, 2014).

Many studies from different research groups have assessed the DNA methylation of the maternal genome in early pronuclear mouse embryos, immediately after the paternal pronucleus is formed in the newly fertilised embryo. There are differing views on the DNA methylation patterns in pronuclear stage embryos (Li and O'Neill, 2012, Sakashita et al., 2014, Santos et al., 2002). The discord is focussed on the binding of methyl-CpG binding proteins (MBD's), which as their name suggests, bind methylated CpG regions (Li and O'Neill, 2012). There is a consensus that 5mC in the maternal pronucleus remains consistent from PN0 (See Figure 1.1a for description of pronuclear staging in Section 1.2.2) through to syngamy using global immunocytochemical assays (Li and O'Neill, 2013, Li and O'Neill, 2012, Santos et al., 2002, Iqbal et al., 2011). The paternal pronucleus however remains a point of contention, with some reports in the mouse showing a reduction of global 5mC through to syngamy (Sakashita et al., 2014, Santos et al., 2002). This is in contrast to studies from another group, which utilizing tryptic digestion to remove the MBD's, showed 5mC to be shown consistently in the paternal pronucleus from PN1 through to syngamy and into the 8-cell stage (Li and O'Neill, 2013, Li and O'Neill, 2012). This result would seemingly be dependent on whether the paternal genome contains more MBD's bound to the DNA compared to the maternal genome, of which no evidence has been provided by their own immunocytochemical analysis (Li and O'Neill, 2012). Additionally, porcine studies have shown that 5hmC content via immunocytochemistry is increased in the late pronuclear stages as compared to earlier pronuclear embryos in both maternal and paternal pronuclei (Lee et al., 2014). Rabbit embryos show a loss of 5mC as well, with a putative increase in 5hmC (Reis Silva et al., 2011). Based on this inference, it is likely that 5mC is actively demethylated in the paternal pronucleus of mammalian embryos.

It must be noted that there were differences in DNA methylation staining via immunocytochemistry in mouse embryos between those produced via IVF through zygote culture from PN1 and from fresh PN5 zygotes. However, the overall trend showed greater 5mC staining in the maternal pronucleus than the paternal pronucleus (Li and O'Neill, 2012), indicating that *in vitro* fertilisation can change the DNA methylation status of the pronuclear stage embryo relative to natural mating.

In the mouse, global 5mC measurement via immunocytochemistry past the pronuclear stage indicates a gradual DNA demethylation after cleavage up to compaction (Figure 1.8) (Iqbal et al., 2011, Santos et al., 2002), with the morula showing polarization between the inner and outer blastomeres and the inner apolar cells showing higher 5mC levels (Santos et al., 2002). This is believed to occur through a dilution of the methylated marks, with the newly synthesised DNA strands formed without the methylated cytosine bases that were present on the previous reverse strand.

Less is known about 5fC and 5caC marks in embryos. In the mouse pronuclear embryo 5fC doubles from PN4 onwards in the paternal pronucleus relative to earlier PN stages (Inoue et al., 2011). 5caC follows a similar trend, however with an 8-fold increase at PN4 in the paternal pronucleus, with no global increases in 5fC or 5caC in the maternal pronuclei throughout pronuclear development (Inoue et al., 2011).

These results have been confirmed using single cell, single base 5fC sequencing (Zhu et al., 2017), where the maternal and paternal pronuclei were shown to have a similar number of 5fC sites. However the majority of the sites were newly generated, i.e. new bases that were not previously measured as being 5fC modified in oocytes or embryos in the maternal and paternal pronuclei respectively (Zhu et al., 2017). 5fC was at its greatest abundance in the zygote, consistent with the active demethylation known to be present at this stage. This further indicates that 5mC is removed from the paternal pronucleus actively as illustrated by the increased oxidation state of each of these bases.

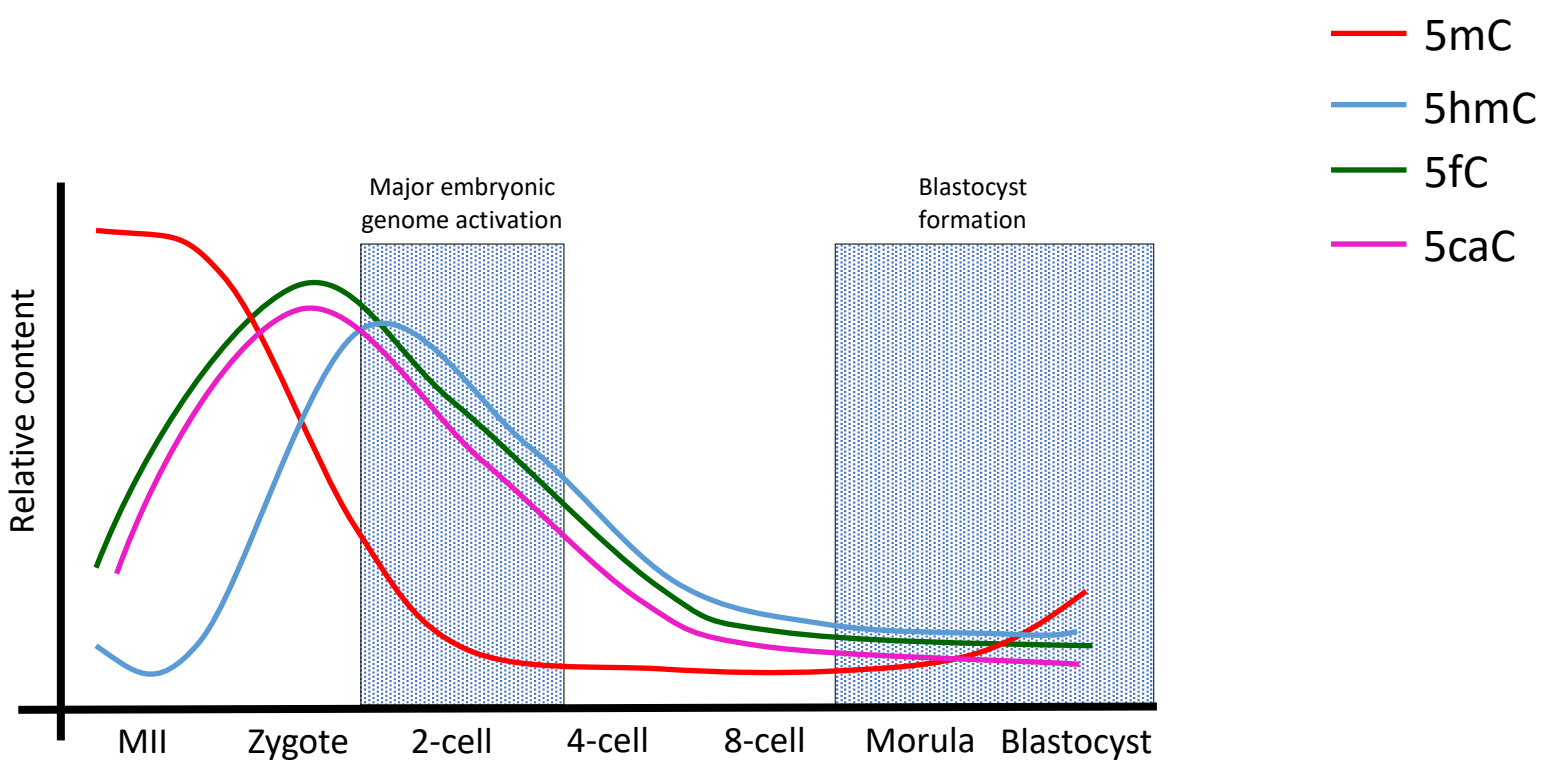

Figure 1.8 DNA methylation dynamics throughout mouse preimplantation development. Adapted from (Inoue et al., 2011, Inoue and Zhang, 2011, Shen et al., 2014a, Shen et al., 2014b, Zhu et al., 2017). Y axis not to scale for base content in the genome.

Using synthetic small interfering RNAs (siRNAs), which halted TET3 translation by binding to its mRNA's 3'UTR, porcine zygotic 5hmC was reduced significantly compared to controls (Lee et al., 2014). The substantial reduction in 5hmC levels indicated that TET3 is the most abundant dioxygenase enzyme capable of DNA hydroxymethylation at this stage of embryo development, however it must be noted that a minimal amount of 5hmC persisted. This was confirmed via qPCR analyses for *TET3* transcript in porcine zygotes in the same study, although *TET1* and *TET2* mRNA were also present in low abundance (Lee et al., 2014) which may be responsible for the low levels of 5hmC that persisted.

Furthermore in the mouse, the presence of the three *Tet* gene transcripts in the embryo has to date only been reported in a single paper (Yu et al., 2013). In this paper, *Tet1* was expressed from the GV stage, with expression increasing from the MII stage to the zygote, with peak transcription at the 4 cell stage, which is then decreased post-compaction. *Tet2* increases from the zygote through to blastocyst, while *Tet3* was found to be expressed only in GV/MII oocytes, with a reduction after fertilisation (Yu et al., 2013). This study is interesting in that there are reported increases in expression of *Tet1-3* where these early embryos are thought to be transcriptionally quiet (Hamatani et al., 2004). This may be the result of the choice of the endogenous control gene, *Gapdh,* which although commonly used in studies of somatic cells, it is known to have alterations to transcript abundance throughout preimplantation embryo development (Robert et al., 2002). Further analyses of TET1-3 proteins for all preimplantation stages would confirm this phenomenon, as presence of mRNA is not confirmation of an increase or decrease at the protein level, especially considering the unique translational dynamics in the preimplantation embryo. Whilst the levels of TET proteins may alter throughout development (albeit this is unclear in the mouse), the levels of the key co-factors CRL4 proteins VPRBP and DDB1 were shown to be highly abundant and localised to DNA from mouse GV stage oocytes through to 2-cell embryos (Wu and Zhang, 2011). However, whether gene and protein expression continue after this stage in the preimplantation embryo is unknown.

Analysis of porcine data has shown that after the pronuclear stage, TET1 protein begins to be expressed in the 2-cell embryo at a very low level, which is then increased in the 4-cell stage (i.e. porcine major embryonic genome activation), with high expression in the blastocyst in both the TE and ICM cells (Lee et al., 2014). This pattern is confirmed in the blastocyst, where the inner cell mass shows global 5mC staining co-localised to the nuclear reference stain, with the TE cells presenting partial nuclear staining relative to the nuclear reference co-stain (Lee et al., 2014). Gene expression has also confirmed increased *TET3* expression in the zygote and 2-cell relative to the GV oocyte (Lee et al., 2014), with reduction in all three *TETs* at the 4-cell stage (porcine embryonic genome activation). This appears similar to mouse *Tet* dynamics, with the peak of *Tet3/TET3* transcript in the embryo occurring at the stage before embryonic genome activation (Figure 1.8).

1.8.2 DNA methylation regulation in response to environmental factors

As a mechanism for the transmission of information across generations, DNA methylation is a cardinal candidate as it acts to repress genes so that they are not expressed, or when transmitted to the next generation can act to change the expression of key genes.

There have been numerous studies in the preimplantation embryo that have shown changes in the expression of imprinted genes due to *in vitro* stress. These changes have been linked to alterations to the methylation status of the regulatory elements that regulate the expression of these genes. An *in vitro* model of heat stress, where murine embryos were exposed to 40ºC as opposed to 37ºC for 1 h before culture to blastocyst stage, showed a modified methylation pattern of *H19* and *IGF-2r* and an overall doubling of hypermethylation in these sequences (Zhu et al., 2007). This heat stress was also linked to the observed reduction in blastocysts, implying that the differential methylation may be attempting to block cell differentiation through *H19*, and ultimately reduce the ability of the embryo to form a viable pregnancy (Matsuzuka et al., 2005).

Furthermore, preimplantation development in some of the earlier developed and less-complex culture media used for preimplantation embryo culture have shown to alter the methylation of both maternal and paternal genomes in the blastocyst (Doherty et al., 2000, Mann et al., 2004). Using a model to differentiate the maternal or paternal expression of *H19*, two cell embryos cultured in Whittens medium (a simple media known to be lacking critical nutrients such as amino acids) to the blastocyst stage showed expression of paternal *H19*, where embryos cultured in KSOM with additional amino acids (KSOM + aa) and *in vivo* derived blastocysts showed only expression from the maternal copy (Doherty et al., 2000). This was confirmed to be epigenetically regulated via radiometric assessment of DNA methyltransferase incorporation into the genomes, with a decrease in methyltransferase activity in cultured blastocysts (Doherty et al., 2000). Interestingly; these changes were only apparent in the trophectoderm, with confirmation in further studies that this pattern persists into placental tissue after implantation of cultured embryos, as shown by differential methylation in the *H19* promoter region (Mann et al., 2004). While culture in KSOM + aa abrogated many changes; differential methylation and expression was still apparent, suggesting that improved culture media cannot fully replicate the *in vivo* milieu (Mann et al., 2004).

Gamete and embryo cryopreservation is also known to impact on DNA methylation. Vitrification of oocytes has been shown to reduce the developmental rate of the resulting embryos, resulting in reduced cleavage and blastocyst rates (Cao et al., 2019). Unlike the results observed by Han and colleagues with HFD fed mice (Han et al., 2018), the resulting vitrified embryos did not show altered 5mC nor 5hmC levels in the 1-cell embryo throughout pronuclear development, and no significant difference in 5mC throughout preimplantation development (Cao et al., 2019). 5hmC however was reduced from the 8-cell stage, with 5hmC remaining reduced through to expanded blastocyst stage, with 5fC reduced from the morula onwards (Cao et al., 2019). These timings do not indicate that vitrification is affecting TET3-mediated oxidation of 5mC, where TET3 is present in the oocyte and pronuclear embryo. Rather, this timing correlates to the expression of *Tet1*, which is transcribed from the 4-cell stage in mouse

embryos (Cao et al., 2019, Yu et al., 2013), where in these vitrified oocytes the resulting embryos showed reduced *Tet1* expression (Cao et al., 2019). When 8-cell mouse embryos were vitrified, resultant foetuses on E9.5 (6 days after transfer) produced foetuses that showed reduced *Tet2* and *Tet3* expression, and a concomitant increase in 5mC relative to cultured, but not frozen embryos (Ma et al., 2019).

These changes in the preimplantation environment due to *in vitro* culture and other stressors have been shown to alter DNA methylation not only in the embryo itself; but creating epigenetic changes that persist after implantation and into the resultant foetus. These changes due to the preimplantation culture are believed to be due to changes in embryonic metabolism, as evidenced by the differences between all media used for embryos (handling media, culture media, and vitrification media) with all other factors consistent.

1.9 Relationship between metabolic changes and epigenetic mechanisms

While many reviews have speculated on the links between metabolism and epigenetic regulation (Brown et al., 2015, Donohoe and Bultman, 2012, Hanover et al., 2012, Kaelin Jr and McKnight, 2013, Sassone-Corsi, 2013), there are few studies that directly confirm metabolic alteration as the mechanism that triggers a change to DNA methylation. Considering that α-ketoglutarate is a direct substrate necessary for the oxidation of 5mC by the TET proteins, changes to metabolic processes may alter the levels of cytoplasmic α-ketoglutarate, which in turn could then alter DNA methylation.

Interestingly, in patients with schizophrenia (SZ), where second-generation antipsychotics have been likened to metabolic syndrome (Paredes et al., 2014) it has been shown that peripheral blood lymphocytes from SZ patients contained higher amounts of mRNA for both *TET1* and *DNMT1* (Auta et al., 2013). This links the metabolic disorder with alterations to gene expression that appear to be mediated by DNA methylation status.

Through cell culture, immortalised bronchial epithelial cells treated with 150 μM H_2O_2 (to induce a mild oxidative stress to mimic what occurs in chronic obesity) showed that TET activity was halved (Niu et al., 2015) with a concomitant increase in 5mC (Niu et al., 2015). This study indicates that ROS can also directly reduce the activity of TETs.

As highlighted earlier, $IDH1^{R132H}$ mutations produce 2HG instead of α-ketoglutarate, contributing to a 50% decrease in α-ketoglutarate in mutant cells (Zhao et al., 2009). This drop in normal IDH function and α-ketoglutarate concentration contributed to a decrease in 5hmC in grade 4 malignancies (Liu et al., 2012). Many cancer researchers have hypothesised that this alteration to α-ketoglutarate can be tied to the Warburg effect (Warburg, 1956), whereby cancer cells exhibit preference for anaerobic respiration using glycolysis, with very little reliance on the TCA cycle and oxidative phosphorylation. This is of significance as the Warburg effect is also apparent in the inner cell mass of blastocysts, which are the cells that ultimately produce the foetus, raising the possibility that a similar mechanism may be functional in the blastocyst.

There has been some suggestion that caloric restriction can alter the methylome (Michan, 2013, Kim et al., 2016, Kopeina et al., 2017). In a rat model, aged rats (25 months) were fed 60% of the food they usually consumed, methyl-DNA immunoprecipitation (meDIP) from the kidney was assessed and compared with both aged rats (25 months) and young rats (6 months). Of note, DNA methylation of LINE retrotransposon elements was decreased in caloric restricted aged rats relative to aged mice (eating normal diet) and young mice (Michan, 2013, Kim et al., 2016, Kopeina et al., 2017) and DNA methylation in introns and promoter regions of genes was equivalent to that of young rats (Kim et al., 2016). Combined with rodent studies linking caloric restriction with extended lifespan (Speakman et al., 2016, Patel et al., 2016), the amelioration of DNA methylation in this model appears to be an explanation for this phenotype. While the mechanism for the DNA methylation was not assessed, it is possible that the restriction of the diet (which contained 58.64% total carbohydrate) depleted the Acetyl-CoA levels, which in a short-term intervention would alter homeostasis of DNA methylation by α-ketoglutarate dependent dioxygenases such as TETs.

Further, when rats were fed a high fat diet, urinary TCA intermediates were significantly decreased compared to control diet fed rats, with α-ketoglutarate decreased by 20-40% (An et al., 2013), as would be expected with increased beta oxidation to provide acyl-CoA instead of glycolysis to fuel the TCA cycle. This decrease in urinary α-ketoglutarate suggests an increase in TCA cycle activity and oxidative phosphorylation in these obese rats as intermediaries are retained. Further, in human studies, serum from obese patients showed decreased TCA cycle intermediaries compared to normal weight patients (Mardinoglu et al., 2014), suggesting that α-ketoglutarate levels are altered which may affect protein families such as the TETs. Whether these TCA intermediates are similarly altered in the oocyte and embryos of obese females is unclear, or whether α-ketoglutarate availability can impact DNA methylation in oocytes and embryos is also unknown.

Maternal obesity itself has also been shown to alter 5mC and 5hmC in the early embryo. Where mice were fed a HFD (60% calories from fat) and compared with mice fed a control diet for 16 weeks, 5mC was reduced in the maternal pronuclei at PN5 stage (Figure 1.1a-b) with an increase seen in 5hmC, however was not changed in the paternal pronucleus (Han et al., 2018). This differential result between maternal/paternal pronuclei is believed to be a result of the already current active demethylation of the paternal genome at this stage of embryo development (See Section 1.8.1), so there would not be any possible increase in the rate to demethylation potential (Santos et al., 2002). When *Tet3* was silenced using siRNA, this resulted in increases in 5mC and reduction in 5hmC on both maternal and paternal pronuclei, proving that the alterations to methylation are directly attributed to TET3 in both the maternal and paternal pronuclei (Han et al., 2018). These embryos silenced for TET3 were still able to reach the blastocyst stage, and interestingly blastocyst rates were increased in HFD fed silenced embryos (Han et al., 2018), showing that the increase to DNA methylation is modulating developmental rate, likely through mechanisms such as ROS production (See Section 1.8.2 for details on maternal diet alterations to embryonic growth).

While these changes in TET levels and activity partially explain the results, the altered metabolism through the TCA cycle may also play a role in the increased 5hmC seen in this model. As α-ketoglutarate is an essential cofactor for TET-mediated demethylation, it may explain how silencing of TET3 did not fully ameliorate the HFD embryo 5hmC to the same levels at that shown in the CD (Han et al., 2018). With addition of 150 μM α-ketoglutarate to embryo culture media, both 5mC and 5hmC were increased at the blastocyst stage relative to control cultured embryos, although was still reduced compared to in-vivo flushed blastocysts (Zhang et al., 2019). In addition the TET activity of these *in vivo* blastocysts was also increased 3-fold compared to the cultured blastocysts with no alterations to the relative expression of *Tet1* or *Tet2* (Zhang et al., 2019). This shows that the mechanism for the observed changes to DNA methylation dynamics does not need to be related to TET protein levels in the oocytes and embryos, rather the rate of reaction of the present TETs may be increased by the greater availability of the substrate α-ketoglutarate, which may be the rate limiting factor in this scenario. Resulting pups born from embryo culture supplementation with 150 μM α-ketoglutarate showed increased birthweight and weaning weights (Zhang et al., 2019), indicating that mild increases in α-ketoglutarate concentrations may be beneficial to the embryo. This study however did culture embryos in atmospheric oxygen concentrations rather than at 5% oxygen, so these results may be indicative of this exact culture system only, especially as metabolism in the embryo is also affected by increased O_2 levels (See section 1.3) (Houghton et al., 1996, Trimarchi et al., 2000, Kelley and Gardner, 2019).

1.10 Histone methylation

This review has so far discussed the effects of DNA methylation through the α-ketoglutarate dependent TET family in detail, however other important pathways also exist that contribute to the epigenetic regulation, including histone methylation. This next section will focus on one such pathway that also involves metabolic intermediates, namely demethylation of histone 3 lysine 4 methylation (H3K4) carried out by the KDM5 family, which similarly to TETs, uses α-ketoglutarate as an energy source and carbon donor for active demethylation.

1.10.1 Introduction to histone methylation

In addition to DNA methylation, methylation of the histones that package DNA can also impact on gene transcription, can be heritable (Cano-Rodriguez et al., 2016, McPherson et al., 2015, Stewart et al., 2015), and is often present at sites of elevated 5hmC and 5fC in the genome. For the purposes of this review, we will focus on H3K4 methylation in the form of mono-methylation (H3K4me1), di-methylation (H3K4me2) and tri-methylation (H3K4me3) as it is demethylated by the lysine demethylase 5 family (KDM5A-D), which use α-ketoglutarate as a substrate. This pathway is similar to TET protein DNA methylation modifications, and as such have the ability to be altered due to changes to the metabolic environment as seen in a maternal HFD model.

1.10.2 Histone 3 lysine 4 methylation and how it is formed

H3K4 methylation is facilitated by histone methyltransferase enzymes (HMTs), including SET1A, KMT2A (also known as MLL1) and KMT2D (MLL2) (Yu et al., 2017). These are the chromatin binding subunit proteins, part of the Complex Proteins Associated with SET1 (COMPASS) complex. The HMT enzyme binds the lysine to be methylated and adds the methyl group using S-asenosyl methionine (also known as SAM or AdoMet) as a carbon donor. This results in H3K4 becoming methylated to H3K4me1, and can occur via histone methyltransferases to form H3K4me2 and H3K4me3, by serial addition of methyl groups (Figure 1.9).

When KMT2D is knocked out in primordial germ cells, correct establishment of H3K4me3 cannot be carried out at loci required for specification into endoderm and ectoderm cell lineage (Hu et al., 2017), indicating that correct management of H3K4me3 at developmentally sensitive periods can significantly affect transcription and cell fate.

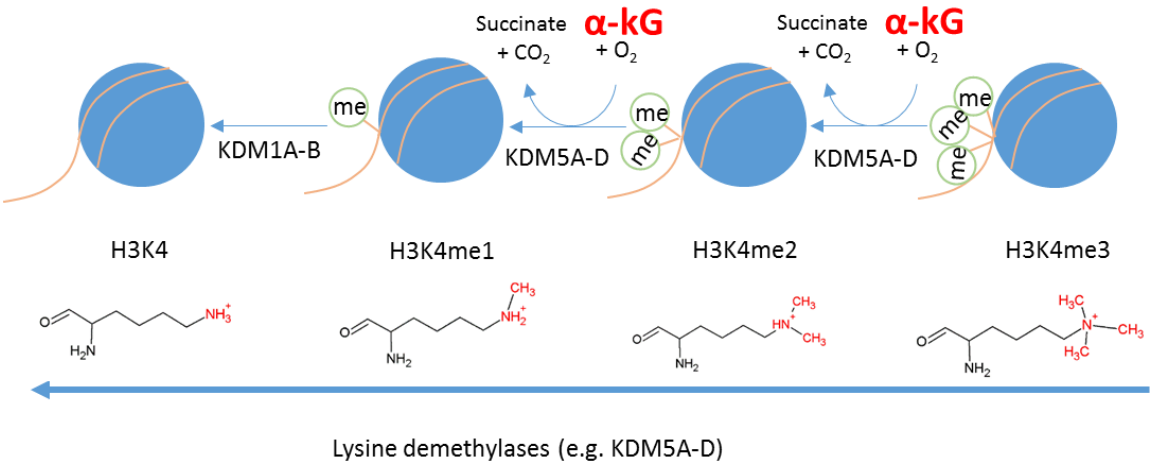

Figure 1.9 Removal of histone 3 lysine 4 methylation via lysine demethylases KDM5A-D and KDM1A-B

1.10.3 Significance of H3K4 methylation variants

Most of the literature surrounding mammalian H3K4me3 focusses on the correct programming throughout early development. There are two mechanisms in which it is believed that histone methylation alters transcription on cells: (i) direct alteration to chromatin structure, and (ii) binding of proteins to promote transcription. Addition of methylation to histone marks alters the hydrogen bonding, which may alter the binding of histones to the DNA itself, altering the formation of the chromatin architecture (Shogren-Knaak et al., 2006). Lysine modifications also alter the recruitment of transcription factors and chromatin binding proteins, which will themselves also alter the chromatin structure. This will then change the availability of the DNA itself for transcription depending on the abundance of histone modification at that region (See Table 1.1 for summary of effects on gene expression of H3K4me3-1). H3K4me3 specifically can bind proteins associated with DNA repair, including ING1 (Peña et al., 2008). It can also be directly associated with increased transcription via recruiting histone acetyltransferases to acetylate H3K4 at activated gene promoters immediately upstream of H3K4me3, including some overlapping regions where methylation and acetylation exist on the same histones (Guillemette et al., 2011). Demethylation of H3K4me3 to H3K4me2 also appears to limit accumulation of H3K4ac (Guillemette et al., 2011).

Unlike H3K4me3, H3K4me2 is not a clearly associated with activation or repression of the chromatin, where it can bind similar proteins to H3K4me3, though at a reduced rate (Peña et al., 2008). When viewed on the genome, it appears more present in the body of the gene, rather than at transcription start sites (Guillemette et al., 2011). Other reports suggest that it is also present in promoter regions, with ChIP-seq for H3K4me2 in human $CD4^+$ T-cells suggesting a much more allele specific function than H3K4me3 (Pekowska et al., 2010). It did appear that H3K4me2 presence in the gene body were associated with increased transcription, particularly in neuronal genes (Pekowska et al., 2010), suggesting both allele and tissue specific effects modulate the function of H3K4me2, indicating more complex outcomes compared with to confirm than H3K4me3. H3k4me1 when present at transcription start sites is a repressor or gene transcription and appears more strongly associated with gene repression (Cheng et al., 2014).

Table 1.1 Directional effects of H3K4me3, H3K4me2 and H3K4me1 on global gene transcription

Mark	Effect on transcription	Cell type (reference)
H3K4me3	Increases	2-cell mouse embryo (Huang et al., 2019)
H3K4me2	Differential	Human $CD4^+$ T-lymphocytes(Pekowska et al., 2010)
H3K4me1	Differential/repression	Mouse skeletal muscle myoblast C2C12 cell line (Cheng et al., 2014)

1.10.4 Lysine demethylase proteins KDM5

While establishment of histone methylation is important, methylation removal also plays a critical cellular role. H3K4 methylation is removed via lysine demethylases (KDMs). KDMs can be broadly grouped by either their carbon and energy cofactor required for methylation; or by their target methylation mark. For example, the KDM6 family use α-ketoglutarate as a substrate to demethylate H3K27me3, while KDM1A and KDM1B are able to demethylate H3K4me2 to H3K4me1, and H3K4me1 to remove methylation entirely, using $FADH_2$ as a substrate. The KDM5 family, the subject of this section, consist of proteins KDM5A, KDM5B, KDM5C and KDM5D, and use α-ketoglutarate as a substrate, along with O_2 to demethylate H3K4me3 to H3K4me2, and H3K4me2 to H3K4me1, producing succinate and CO_2 in the process (Gu and Lee, 2013) (Figure 1.9). The level of activity of each of these lysine demethylases is not fully understood along with their exact targets; though similar to the TET1-3 proteins, they have different sites that they target, and are expressed and translated at different stages of development.

Due to their requirement of α-ketoglutarate to function, it is believed that alterations to the levels of nuclear α-ketoglutarate are able to regulate the activity of these proteins.

1.10.4.1 Competitive inhibition of KDM5 proteins by 2-hydroxyglutarate (2HG)

As touched upon in Section 1.9, the oncometabolite 2HG also acts as a competitive inhibitor of KDM5C and KDM5D, similar to its competitive inhibition of TETs (See section 1.7.5) (Joberty et al., 2016). In a cell free system, α-ketoglutarate or 2HG were tethered to beads to then bound to KDM5s. This showed that 2HG was bound to KDM5C and KSM5D, although at a weaker affinity than α-ketoglutarate (Joberty et al., 2016), thus it does not fully attenuate the function of KDM5C-D (Xu et al., 2011). These studies suggest that 2HG can competitively inhibit α-ketoglutarate binding in KDM5 proteins, which will allow 2HG to be supplemented into media to show the effects of reduced α-ketoglutarate presence in model systems.

1.11 Alterations to histone methylation dynamics in the oocyte and preimplantation embryo

1.11.1 Histone methylation through oocyte maturation

During mouse oocyte maturation from the primordial follicle stage; histone methyltransferase KMT2D (MLL2) increases histone methylation from h3k4me1 to me2 and me3 throughout oogenesis (Andreu-Vieyra et al., 2010), using S-adenosylmethionine as a substrate similar to KMT2A. With knockout of KMT2D, the growing oocytes are not able to develop to the GV stage and fail to ovulate (Andreu-Vieyra et al., 2010).

After the induction of maturation at the GV stage to resume meiosis, H3K4me3 begins to be globally demethylated down by 96% once oocytes had reached MII as measured by Western blot (Xu et al., 2017) (Figure 1.10), indicating that histone methylation is being globally removed in the oocyte prior to fertilisation.

During the period of oocyte maturation; the only known lysine demethylase shown to be present at the protein level in mice is KDM1A (Andreu-Vieyra et al., 2010). As discussed in Section 1.10.2, KDM1A uses $FADH_2$, not α-ketoglutarate as a substrate and also is not able to remove H3K4me3 to H3K4me2 but can remove H3K4me1 to unmethylated H3K4 (Figure 1.9). While transcription of KDM5B (Xu et al., 2017) is present in GV oocytes, there has been no evidence of the presence of the protein to date. One study did show a decrease in H3K4me3 with overexpression on KDM5B via microinjection of mRNA into GV oocytes (Zhang et al., 2016), indicating that translation of KDM5B must be occurring at this stage to show this effect.

1.11.2 Histone methylation through embryo development

In the early embryo H3k4me3 is generally regarded to be an activating mark at promoter regions (Dahl et al., 2016) and is required for maintaining pluripotency within preimplantation embryos (Wang et al., 2010). In the mouse, H3k4me3 can be found in 80% of genes before mouse embryonic genome activation (EGA) at the 2-cell stage (Figure 1.10). After EGA however, in the 4-cell the global levels are reduced to 1/3rd of that observed in the 2-cell (Wang et al., 2010) (Figure 1.10). H3K4me3 increases again in late cleavage stages and after compaction (Wang et al., 2010). These fluctuations of H3K4me3 approximately align with times where active transcription of the genome is occurring within the embryo (See Section 1.2), suggesting chromatin conformational changes due to H3K4me3 allows for increased transcription at these stages. There is less known about H3K4me2 and H3K4me1 in the embryo. One other study has shown that levels of H3K4me2 levels are approximately double that of H3K4me3 at the 2-cell stage, then follows a similar trend to H3K4me3 throughout the remainder of embryogenesis, though at a lower level (Shao et al., 2014) (Figure 1.10). H3K4me1 shows a different trend, where levels of H3K4me1 do not increase at late cleavage stages (i.e. 4-cell until compaction), and with compaction as H3K4me3 does (Shao et al., 2014) (Figure 1.10). Paired with an increase in KDM1A, which is able to remove H3K4me1 (Shao et al., 2014), this indicates that H3K4me1 methylation may be fully removed at these loci, as compared to the more gradual reductions observed with DNA demethylation. This may indicate multiple demethylation events at the same loci may be occurring during a single round of DNA replication, or histone demethylation may even operate independently of DNA replication, whereas 5mC can only be demethylated at the S phase.

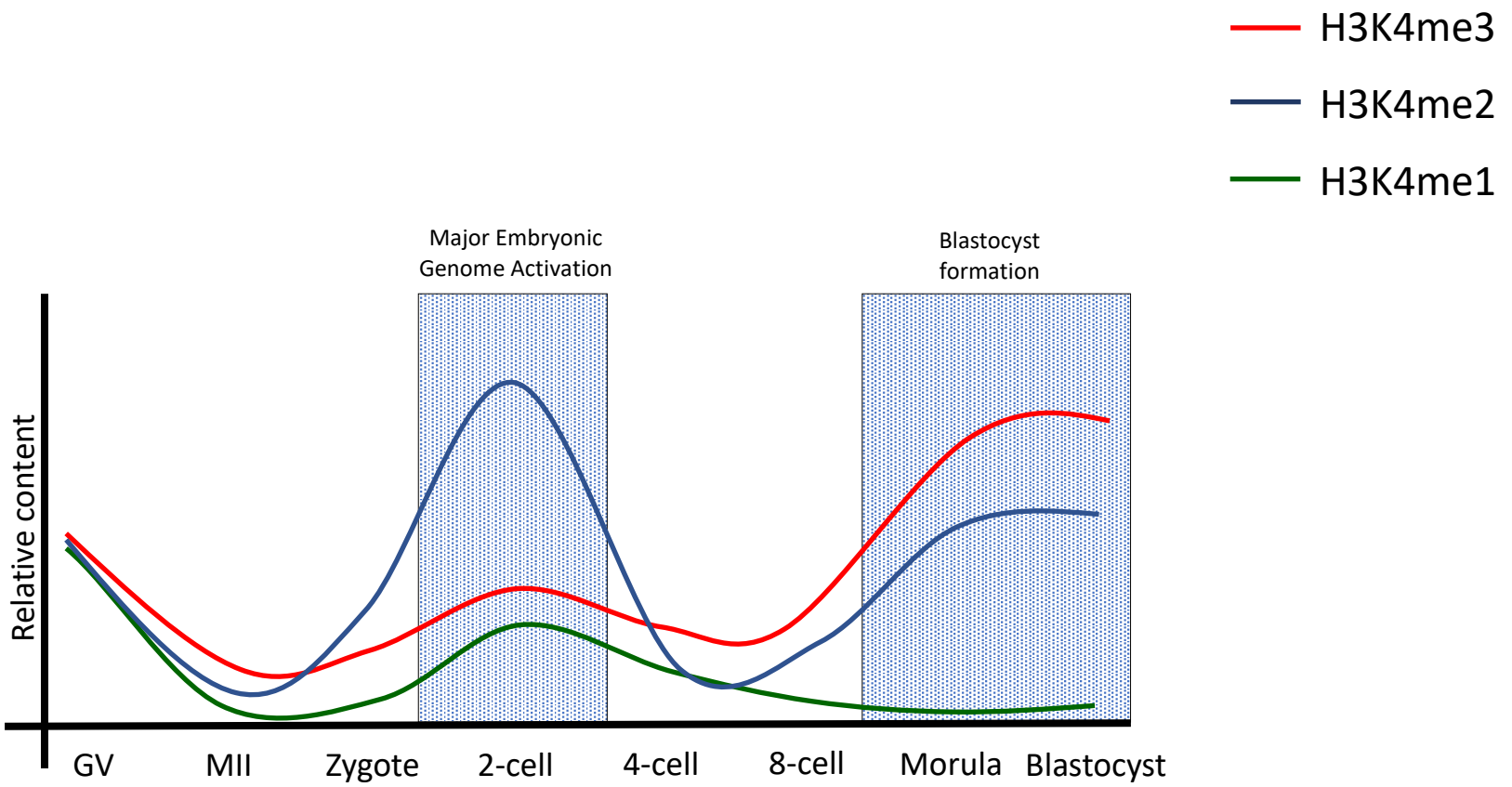

Figure 1.10 Histone 3 lysine 4 methylation throughout mouse oogenesis and preimplantation development. Adapted from (Sha et al., 2018, Shao et al., 2014, Shao et al., 2015)

1.11.3 Changes to H3K4 methylation as a result of environmental impacts in embryos

Much the same as DNA methylation through TETs, the ability of KDM5s to remove H3K4 methylation have been demonstrated to be modulated by the same metabolic stressors in culture systems and maternal environment due the requirement of α-ketoglutarate as a substrate.

One study examined the effects of *in vitro* fertilisation in a mouse model, where oocytes were collected and fertilised *in vitro* and cultured and compared to embryos cultured after being collected after natural mating (Wu and Zhang, 2012). The embryos produced via *in vitro* fertilisation showed reduced global H3K4me3 at all stages of embryo growth measured, except at the 4-cell stage (1-cell, 2-cell, 8-16-cell morula, and blastocyst) where it appears that H3K4me3 is removed to basal levels, and as such were not able to be decreased any further. Interestingly, addition of trichostatin A, a histone deacetylation inhibitor was shown to increase blastocyst formation in pigs ameliorating the decreased H3K4me3 methylation caused by the *in vitro* fertilisation at all stages, but did not fully return H3K4me3 observed in *in vivo* fertilised embryos (Wu and Zhang, 2012). This may relate to the previously discussed links between H3K4 acetylation and establishment of H3K4me3, whereby retention of H3K4ac may be protective and not allow erasure of H3K4me3 by KDM5 proteins (See Section 1.10.1).

As described in Section 1.8.1, oxygen concentration alters embryonic growth and glucose use in the blastocyst and subsequently alter offspring health (Kelley and Gardner, 2019). While there is no specific information for H3K4 methylation in response to oxygen tension in a mouse model, a bovine model testing 5% and 20% oxygen during embryo culture to the blastocyst stage showed global increases in H3K4me2 in blastocysts cultured at atmospheric oxygen (20%) as compared to physiological oxygen (5%) with no alterations to KDM5A transcription (Gaspar et al., 2015). This indicates an increase in KDM5 activity throughout preimplantation development likely due to the fact that KDM5 uses oxygen as a cofactor alongside α-ketoglutarate.

H3K4 methylation dynamics are also known to be altered by maternal ageing. In a mouse model, oocytes from aged mice (from 42-44 weeks old compared to 6-8 week old mice) were shown to contain reduced H3K4me2 in GV oocytes, and increased H3K4me2 and H3K4me3 in aged MII oocytes (Shao et al., 2015). While KDM5 proteins were not measured in this cohort, this model demonstrated that alterations to the maternal environment can alter H3K4 methylation before fertilisation and implantation. This may then alter the growth trajectory of these embryos as it may change the profile of maternally produced proteins used by the early embryo at the time of embryonic genome activation.

1.11.4 Changes to H3K4 methylation as a result of maternal phenotype

Unlike DNA methylation, the effect of parental obesity on H3K4me3 methylation has been studied in greater detail. Parental obesity has been demonstrated to affect H3K4me3 levels in the embryo. One such study assessed both maternal HFD (6 weeks HFD feeding) and paternal HFD (10 weeks HFD feeding) or a combination of both on H3K4me3 in the resulting 2-cell embryo compared with mice a fed a control diet (McPherson et al., 2015). In this model H3K4me3 was not significantly increased under a maternal HFD, however it was increased approximately doubled with paternal HFD feeding (McPherson et al., 2015). Taken alongside the altered H3K4 methylation seen with *in vitro* fertilisation, this indicates that the paternal constitution at the time of spermatogenesis and the environment that sperm are subjected to, can also contribute to alterations in H3K4me3 observed after fertilisation and appear to have a lasting impact the embryo and subsequent offspring.

Another study in rats assessed the effect of a maternal HFD from four weeks before conception until delivery coupled with streptozotocin given one week before delivery to simulate gestational diabetes (Upadhyaya et al., 2017). H3K4me3 was measured via ChIP-seq on material derived from neonatal hearts to determine any maternal effects. The maternal HFD in the absence of

streptozotocin showed increased H3K4me3in many genes involved in metabolic processes compared to controls, including ATP synthase and heat shock proteins in the cardiac tissue (Upadhyaya et al., 2017), showing that exposure to a HFD from preconception through to pregnancy is able to reprogram offspring cardiac tissue.

1.12 Conclusion

The regulation of DNA and H3K4 methylation, and metabolic imbalances appear to be intricately linked in embryos; but there are little to no mechanistic studies confirming this concept. Therefore, there is a current need for a model that demonstrates that an alteration to mitochondrial function increases or decreases DNA methylation and H3K4me3, either at a global level or at an allele specific level.

1.12.1 Research hypothesis and aims

My hypothesis is that disruptions in mitochondrial activity (due to environmental disruption in the form of maternal HFD or increased BMI or due to *in vitro* manipulations such as IVM) modifies the availability of metabolic cofactors required by TET and KDM5 protein families for methylation, thereby altering DNA and histone methylation marks in the oocyte and embryo.

This will address the knowledge gap of whether there are differences in TET transcription and translation in oocytes and embryos obtained from modes of metabolic perturbation including maternal obesity. This study will also investigate whether the activity of TETs in the preimplantation embryo are altered under mitochondrial stress caused by the consumption of a high fat diet. Additionally, direct inhibition or stimulation of α-ketoglutarate binding using supplementary α-ketoglutarate or 2HG in culture media will more directly address whether alteration in α-ketoglutarate availability decreases, or increases DNA and H3K4 methylation, and subsequent embryo development.

Aim 1: To use a mouse model of maternal obesity to establish the effects of obesity on oocyte metabolism, TET protein expression and activity in oocytes, and progression of DNA methylation in the 2-cell embryo due to elevated substrate availability.

Aim 2: To establish embryo culture models of α-ketoglutarate stimulation and 2-hydroxyglutarate inhibition of TET protein function to determine if increasing α-ketoglutarate availability in the early embryo increases progression of DNA demethylation, and inhibition to decrease progression, with subsequent impacts to embryo development.

Aim 3: To establish a model of TET inhibition using 2-hydroxyglutarate during oocyte maturation and its interaction with *in vitro* maturation to examine the inhibition on histone 3 lysine 4 methylation, blastocyst development and cell counts through reduced α-ketoglutarate availability.

Aim 4: To determine if increased maternal BMI (overweight/obese) increases the expression of *TET1*, *TET2* or *TET3* in cumulus and granulosa cells and determine if changes to *TET* expression are predictive of embryo development rates or pregnancy and live birth.

1.13 References

ABE, K.-I., FUNAYA, S., TSUKIOKA, D., KAWAMURA, M., SUZUKI, Y., SUZUKI, M. G., SCHULTZ, R. M. & AOKI, F. 2018. Minor zygotic gene activation is essential for mouse preimplantation development. *Proceedings of the National Academy of Sciences,* 115**,** E6780.

ABS 2011-2012. Australian Health Survey: First Results, Canberra, Australian Capital Territory , Canberra, Australian Capital Territory. http://www.abs.gov.au/ausstats/abs@.nsf/Lookup/by%20Subject/4338.0~2011-13~Main%20Features~Overweight%20and%20obesity~10007. Accessed 22 July 2019 7 /06/2013. Report No.: 4338.

ACTON, B., JURISICOVA, A., JURISICA, I. & CASPER, R. 2004. Alterations in mitochondrial membrane potential during preimplantation stages of mouse and human embryo development. *Molecular Human Reproduction,* 10**,** 23-32.

ADENOT, P. G., MERCIER, Y., RENARD, J.-P. & THOMPSON, E. M. 1997. Differential H4 acetylation of paternal and maternal chromatin precedes DNA replication and differential transcriptional activity in pronuclei of 1-cell mouse embryos. *Development,* 124**,** 4615-4625.

AMIR, R. E., VAN DEN VEYVER, I. B., WAN, M., TRAN, C. Q., FRANCKE, U. & ZOGHBI, H. Y. 1999. Rett syndrome is caused by mutations in X-linked MECP2, encoding methyl-CpG-binding protein 2. *Nature Genetics,* 23**,** 185-188.

AMOUROUX, R., NASHUN, B., SHIRANE, K., NAKAGAWA, S., HILL, P. W. S., D'SOUZA, Z., NAKAYAMA, M., MATSUDA, M., TURP, A., NDJETEHE, E., ENCHEVA, V., KUDO, N. R., KOSEKI, H., SASAKI, H. & HAJKOVA, P. 2016. De novo DNA methylation drives 5hmC accumulation in mouse zygotes. *Nature Cell Biology,* 18**,** 225-233.

AN, Y., XU, W., LI, H., LEI, H., ZHANG, L., HAO, F., DUAN, Y., YAN, X., ZHAO, Y., WU, J., WANG, Y. & TANG, H. 2013. High-Fat Diet Induces Dynamic Metabolic Alterations in Multiple Biological Matrices of Rats. *Journal of Proteome Research,* 12**,** 3755-3768.

ANDREU-VIEYRA, C. V., CHEN, R., AGNO, J. E., GLASER, S., ANASTASSIADIS, K., STEWART, A. F. & MATZUK, M. M. 2010. MLL2 Is Required in Oocytes for Bulk Histone 3 Lysine 4 Trimethylation and Transcriptional Silencing. *PLOS Biology,* 8**,** e1000453.

AUGUSTIN, R., POCAR, P., NAVARRETE-SANTOS, A., WRENZYCKI, C., GANDOLFI, F., NIEMANN, H. & FISCHER, B. 2001. Glucose transporter expression is developmentally regulated in in vitro derived bovine preimplantation embryos. *Molecular Reproduction and Development,* 60**,** 370-376.

AUSTIN, C. R. 1962. Fertilization of Mammalian Eggs in Vitro. *In:* BOURNE, G. H. & DANIELLI, J. F. (eds.) *International Review of Cytology.* Academic Press.

AUTA, J., SMITH, R. C., DONG, E., TUETING, P., SERSHEN, H., BOULES, S., LAJTHA, A., DAVIS, J. & GUIDOTTI, A. 2013. DNA-methylation gene network dysregulation in peripheral blood lymphocytes of schizophrenia patients. *Schizophrenia Research,* 150**,** 312-318.

BABAYEV, E. & SELI, E. 2015. Oocyte mitochondrial function and reproduction. *Current Opinion in Obstetrics and Gynecology,* Publish Ahead of Print.

BACHMAN, M., URIBE-LEWIS, S., YANG, X., BURGESS, H. E., IURLARO, M., REIK, W., MURRELL, A. & BALASUBRAMANIAN, S. 2015. 5-Formylcytosine can be a stable DNA modification in mammals. *Nature Chemical Biology,* 11**,** 555-557.

BANWELL, K. M., LANE, M., RUSSELL, D. L., KIND, K. L. & THOMPSON, J. G. 2007. Oxygen concentration during mouse oocyte in vitro maturation affects embryo and fetal development. *Human Reproduction,* 22**,** 2768-2775.

BARKER, D. J. P. & OSMOND, C. 1986. INFANT MORTALITY, CHILDHOOD NUTRITION, AND ISCHAEMIC HEART DISEASE IN ENGLAND AND WALES. *The Lancet,* 327**,** 1077-1081.

BARNES, F. L., FLORMAN, H. M., SIRARD, M. A., LEIBFRIED-RUTLEDGE, M. L., SIMS, M. L. & FIRST, N. L. 1989. Timing of Nuclear Progression and Protein Synthesis Necessary for Meiotic Maturation of Bovne Oocytes1. *Biology of Reproduction,* 40**,** 1257-1263.

BAVISTER, B. D. 1995. Culture of preimplantation embryos: facts and artifacts. *Human Reproduction Update,* 1**,** 91-148.

BAVISTER, B. D. & SQUIRRELL, J. M. 2000. Mitochondrial distribution and function in oocytes and early embryos. *Human Reproduction,* 15**,** 189-198.

BIGGERS, J. D. & STERN, S. 1973. Metabolism of the preimplantation mammalian embryo. *Adv Reprod Physiol,* 6**,** 1-59.

BONEY, C. M., VERMA, A., TUCKER, R. & VOHR, B. R. 2005. Metabolic syndrome in childhood: association with birth weight, maternal obesity, and gestational diabetes mellitus. *Pediatrics,* 115**,** e290-e296.

BORRA, M. T., SMITH, B. C. & DENU, J. M. 2005. Mechanism of Human SIRT1 Activation by Resveratrol. *Journal of Biological Chemistry,* 280**,** 17187-17195.

BOUDOURES, A. L., CHI, M., THOMPSON, A., ZHANG, W. & MOLEY, K. H. 2016. The effects of voluntary exercise on oocyte quality in a diet-induced obese murine model. *Reproduction,* 151**,** 261-270.

BRAUDE, P., BOLTON, V. & MOORE, S. 1988. Human gene expression first occurs between the four- and eight-cell stages of preimplantation development. *Nature,* 332**,** 459-461.

BRINSTER, R. L. & THOMSON, J. L. 1966. Development of eight-cell mouse embryos in vitro. *Experimental Cell Research,* 42**,** 308-315.

BRISON, D. R. & LEESE, H. J. 1991. Energy metabolism in late preimplantation rat embryos. *Journal of Reproduction and Fertility,* 93**,** 245-251.

BRISON, D. R. & LEESE, H. J. 1994. Blastocoel cavity formation by preimplantation rat embryos in the presence of cyanide and other inhibitors of oxidative phosphorylation. *Journal of Reproduction and Fertility,* 101**,** 305-309.

BROWN, H., TAN, T. & THOMPSON, J. 2015. Metaboloepigenetics: providing alternate hypotheses for regulation of gene expression in the early embryo. *Animal Reproduction,* 12**,** 437-443.

CALARCO, P. G. & BROWN, E. H. 1969. An ultrastructural and cytological study of preimplantation development of the mouse. *Journal of Experimental Zoology,* 171**,** 253-283.

CANO-RODRIGUEZ, D., GJALTEMA, R. A. F., JILDERDA, L. J., JELLEMA, P., DOKTER-FOKKENS, J., RUITERS, M. H. J. & ROTS, M. G. 2016. Writing of H3K4Me3 overcomes epigenetic silencing in a sustained but context-dependent manner. *Nature Communications,* 7**,** 12284-12284.

CAO, Z., ZHANG, M., XU, T., CHEN, Z., TONG, X., ZHANG, D., WANG, Y., ZHANG, L., GAO, D., LUO, L., KHAN, I. M. & ZHANG, Y. 2019. Vitrification of murine mature metaphase II oocytes perturbs DNA methylation reprogramming during preimplantation embryo development. *Cryobiology,* 87**,** 91-98.

CARAYANNOPOULOS, M. O., SCHLEIN, A., WYMAN, A., CHI, M., KEEMBIYEHETTY, C. & MOLEY, K. H. 2004. GLUT9 is differentially expressed and targeted in the preimplantation embryo. *Endocrinology,* 145**,** 1435-43.

CARDOZO, E. R., KARMON, A. E., GOLD, J., PETROZZA, J. C. & STYER, A. K. 2016. Reproductive outcomes in oocyte donation cycles are associated with donor BMI. *Human Reproduction,* 31**,** 385-392.

CAREY, B. W., FINLEY, L. W. S., CROSS, J. R., ALLIS, C. D. & THOMPSON, C. B. 2015. Intracellular [agr]-ketoglutarate maintains the pluripotency of embryonic stem cells. *Nature,* 518**,** 413-416.

CATALANO, P. M. & EHRENBERG, H. M. 2006. Review article: The short- and long-term implications of maternal obesity on the mother and her offspring. *BJOG: An International Journal of Obstetrics & Gynaecology,* 113**,** 1126-1133.

CHASON, R. J., CSOKMAY, J., SEGARS, J. H., DECHERNEY, A. H. & ARMANT, D. R. 2011. Environmental and epigenetic effects upon preimplantation embryo metabolism and development. *Trends in Endocrinology & Metabolism,* 22**,** 412-420.

CHENG, J., BLUM, R., BOWMAN, C., HU, D., SHILATIFARD, A., SHEN, S. & DYNLACHT, B. D. 2014. A role for H3K4 monomethylation in gene repression and partitioning of chromatin readers. *Molecular Cell,* 53**,** 979-992.

CHI, M. M., MANCHESTER, J. K., YANG, V. C., CURATO, A. D., STRICKLER, R. C. & LOWRY, O. H. 1988. Contrast in levels of metabolic enzymes in human and mouse ova. *Biology of Reproduction,* 39**,** 295-307.

CONAGHAN, J., HARDY, K., LEESE, H. J., WINSTON, R. M. & HANDYSIDE, A. H. 1998. Culture of human preimplantation embryos to the blastocyst stage: a comparison of 3 media. *International Journal of Developmental Biology,* 42**,** 885-893.

DAHL, J. A., JUNG, I., AANES, H., GREGGAINS, G. D., MANAF, A., LERDRUP, M., LI, G., KUAN, S., LI, B., LEE, A. Y., PREISSL, S., JERMSTAD, I., HAUGEN, M. H., SUGANTHAN, R., BJØRÅS, M., HANSEN, K., DALEN, K. T., FEDORCSAK, P., REN, B. & KLUNGLAND, A. 2016. Broad histone H3K4me3 domains in mouse oocytes modulate maternal-to-zygotic transition. *Nature,* 537**,** 548.

DANG, L., WHITE, D. W., GROSS, S., BENNETT, B. D., BITTINGER, M. A., DRIGGERS, E. M., FANTIN, V. R., JANG, H. G., JIN, S., KEENAN, M. C., MARKS, K. M., PRINS, R.

M., WARD, P. S., YEN, K. E., LIAU, L. M., RABINOWITZ, J. D., CANTLEY, L. C., THOMPSON, C. B., VANDER HEIDEN, M. G. & SU, S. M. 2009. Cancer-associated IDH1 mutations produce 2-hydroxyglutarate. *Nature,* 462**,** 739-744.

DEATON, A. M. & BIRD, A. 2011. CpG islands and the regulation of transcription. *Genes & Development,* 25**,** 1010-1022.

DI EMIDIO, G., FALONE, S., VITTI, M., D'ALESSANDRO, A. M., VENTO, M., DI PIETRO, C., AMICARELLI, F. & TATONE, C. 2014. SIRT1 signalling protects mouse oocytes against oxidative stress and is deregulated during aging. *Human Reproduction,* 29**,** 2006-2017.

DOHERTY, A. S., MANN, M. R., TREMBLAY, K. D., BARTOLOMEI, M. S. & SCHULTZ, R. M. 2000. Differential Effects of Culture on Imprinted H19 Expression in the Preimplantation Mouse Embryo 1. *Biology of Reproduction,* 62**,** 1526-1535.

DONOHOE, D. R. & BULTMAN, S. J. 2012. Metaboloepigenetics: interrelationships between energy metabolism and epigenetic control of gene expression. *Journal of Cellular Physiology,* 227**,** 3169-3177.

DU, Q., LUU, P.-L., STIRZAKER, C. & CLARK, S. J. 2015. Methyl-CpG-binding domain proteins: readers of the epigenome. *Epigenomics,* 7**,** 1051-1073.

DUMOLLARD, R., DUCHEN, M. & CARROLL, J. 2007. The Role of Mitochondrial Function in the Oocyte and Embryo. *In:* JUSTIN, C. S. J. (ed.) *Current Topics in Developmental Biology.* Academic Press.

ECKERSLEY-MASLIN, M. A., ALDA-CATALINAS, C. & REIK, W. 2018. Dynamics of the epigenetic landscape during the maternal-to-zygotic transition. *Nature Reviews Molecular Cell Biology,* 19**,** 436-450.

EPPIG, J. J., O'BRIEN, M. J., WIGGLESWORTH, K., NICHOLSON, A., ZHANG, W. & KING, B. A. 2009. Effect of in vitro maturation of mouse oocytes on the health and lifespan of adult offspring. *Human Reproduction (Oxford, England)*, 24**,** 922-928.

EVANS, B., GRINER, E. & REPRODUCIBILITY PROJECT: CANCER BIOLOGYIORNSELIZABETHSCIENCE EXCHANGE, P. A. C. L. U. K. E. P. A. C. E. P. A. C. F. O. S. C. V. 2015. Registered report: Oncometabolite 2-hydroxyglutarate is a competitive inhibitor of α-ketoglutarate-dependent dioxygenases. *eLife*, 4**,** e07420.

FLÉCHON, J. E., DEGROUARD, J., FLÉCHON, B., LEFÈVRE, F. & TRAUB, O. 2004. Gap Junction Formation and Connexin Distribution in Pig Trophoblast before Implantation. *Placenta*, 25**,** 85-94.

FRAUER, C., ROTTACH, A., MEILINGER, D., BULTMANN, S., FELLINGER, K., HASENÖDER, S., WANG, M., QIN, W., SÖDING, J., SPADA, F. & LEONHARDT, H. 2011. Different Binding Properties and Function of CXXC Zinc Finger Domains in Dnmt1 and Tet1. *PLOS ONE*, 6**,** e16627.

FULLSTON, T., MITCHELL, M., WAKEFIELD, S. & LANE, M. 2011. Mitochondrial inhibition during preimplantation embryogenesis shifts the transcriptional profile of fetal mouse brain. *Reproduction, Fertility and Development*, 23**,** 691-701.

GABUT, M., SAMAVARCHI-TEHRANI, P., WANG, X., SLOBODENIUC, V., O'HANLON, D., SUNG, H.-K., ALVAREZ, M., TALUKDER, S., PAN, Q., MAZZONI, ESTEBAN O., NEDELEC, S., WICHTERLE, H., WOLTJEN, K., HUGHES, TIMOTHY R., ZANDSTRA, P. W., NAGY, A., WRANA, JEFFREY L. & BLENCOWE, BENJAMIN J. 2011. An Alternative Splicing Switch Regulates Embryonic Stem Cell Pluripotency and Reprogramming. *Cell*, 147**,** 132-146.

GAO, Y., LIU, X., TANG, B., LI, C., KOU, Z., LI, L., LIU, W., WU, Y., KOU, X., LI, J., ZHAO, Y., YIN, J., WANG, H., CHEN, S., LIAO, L. & GAO, S. 2017. Protein Expression

Landscape of Mouse Embryos during Pre-implantation Development. *Cell Reports,* 21**,** 3957-3969.

GARDNER, D. & LANE, M. 1997. Culture and selection of viable blastocysts: a feasible proposition for human IVF? *Human Reproduction Update,* 3**,** 367-382.

GARDNER, D. K., LANE, M. & WATSON, A. J. 2004. *Laboratory Guide to the Mammalian Embryo,* Cary, NC, USA, Oxford University Press.

GARDNER, D. K. & LEESE, H. J. 1988. The role of glucose and pyruvate transport in regulating nutrient utilization by preimplantation mouse embryos. *Development,* 104**,** 423-429.

GARDNER, D. K. & LEESE, H. J. 1990. Concentrations of nutrients in mouse oviduct fluid and their effects on embryo development and metabolism in vitro. *Journal of Reproduction and Fertility,* 88**,** 361-368.

GARDNER, D. K. & SAKKAS, D. 1993. Mouse embryo cleavage, metabolism and viability: role of medium composition. *Human Reproduction,* 8**,** 288-295.

GARDNER, D. K., WALE, P. L., COLLINS, R. & LANE, M. 2011. Glucose consumption of single post-compaction human embryos is predictive of embryo sex and live birth outcome. *Human Reproduction*.

GASPAR, R. C., ARNOLD, D. R., CORRÊA, C. A. P., DA ROCHA, C. V., PENTEADO, J. C. T., DEL COLLADO, M., VANTINI, R., GARCIA, J. M. & LOPES, F. L. 2015. Oxygen tension affects histone remodeling of in vitro–produced embryos in a bovine model. *Theriogenology,* 83**,** 1408-1415.

GE, H., TOLLNER, T. L., HU, Z., DA, M., LI, X., GUAN, H., SHAN, D., LU, J., HUANG, C. & DONG, Q. 2012a. Impaired mitochondrial function in murine oocytes is associated with controlled ovarian hyperstimulationand in vitro maturation. *Reproduction, Fertility and Development,* 24**,** 945-952.

GE, H., TOLLNER, T. L., HU, Z., DAI, M., LI, X., GUAN, H., SHAN, D., ZHANG, X., LV, J., HUANG, C. & DONG, Q. 2012b. The importance of mitochondrial metabolic activity and mitochondrial DNA replication during oocyte maturation in vitro on oocyte quality and subsequent embryo developmental competence. *Molecular Reproduction and Development,* 79**,** 392-401.

GREEN, M. P., HARVEY, A. J., SPATE, L. D., KIMURA, K., THOMPSON, J. G. & ROBERTS, R. M. 2016. The effects of 2,4-dinitrophenol and d-glucose concentration on the development, sex ratio, and interferon-tau (IFNT) production of bovine blastocysts. *Molecular Reproduction and Development,* 83**,** 50-60.

GU, B. & LEE, M. G. 2013. Histone H3 lysine 4 methyltransferases and demethylases in self-renewal and differentiation of stem cells. *Cell & Bioscience,* 3**,** 39-39.

GU, L., LIU, H., GU, X., BOOTS, C., MOLEY, K. & WANG, Q. 2015. Metabolic control of oocyte development: linking maternal nutrition and reproductive outcomes. *Cellular and Molecular Life Sciences,* 72**,** 251-271.

GUILLEMETTE, B., DROGARIS, P., LIN, H.-H. S., ARMSTRONG, H., HIRAGAMI-HAMADA, K., IMHOF, A., BONNEIL, E., THIBAULT, P., VERREAULT, A. & FESTENSTEIN, R. J. 2011. H3 lysine 4 is acetylated at active gene promoters and is regulated by H3 lysine 4 methylation. *PLOS Genetics,* 7**,** e1001354-e1001354.

GUMBINER, B., STEVENSON, B. & GRIMALDI, A. 1988. The role of the cell adhesion molecule uvomorulin in the formation and maintenance of the epithelial junctional complex. *The Journal of Cell Biology,* 107**,** 1575-1587.

HAMATANI, T., CARTER, M. G., SHAROV, A. A. & KO, M. S. H. 2004. Dynamics of Global Gene Expression Changes during Mouse Preimplantation Development. *Developmental Cell,* 6**,** 117-131.

HAN, L., REN, C., LI, L., LI, X., GE, J., WANG, H., MIAO, Y.-L., GUO, X., MOLEY, K. H., SHU, W. & WANG, Q. 2018. Embryonic defects induced by maternal obesity in mice derive from Stella insufficiency in oocytes. *Nature Genetics,* 50**,** 432-442.

HANOVER, J. A., KRAUSE, M. W. & LOVE, D. C. 2012. Bittersweet memories: linking metabolism to epigenetics through O-GlcNAcylation. *Nature Reviews Molecular Cell Biology,* 13**,** 312-321.

HARVEY, A. J., KIND, K. L. & THOMPSON, J. G. 2004. Effect of the oxidative phosphorylation uncoupler 2,4-dinitrophenol on hypoxia-inducible factor-regulated gene expression in bovine blastocysts. *Reproduction, Fertility and Development,* 16**,** 665-673.

HEWITSON, L. C. & LEESE, H. J. 1993. Energy metabolism of the trophectoderm and inner cell mass of the mouse blastocyst. *Journal of Experimental Zoology,* 267**,** 337-343.

HEWITSON, L. C., MARTIN, K. L. & LEESE, H. J. 1996. Effects of metabolic inhibitors on mouse preimplantation embryo development and the energy metabolism of isolated inner cell masses. *Molecular Reproduction and Development,* 43**,** 323-330.

HOU, Y.-J., ZHU, C.-C., DUAN, X., LIU, H.-L., WANG, Q. & SUN, S.-C. 2016. Both diet and gene mutation induced obesity affect oocyte quality in mice. *Scientific Reports,* 6**,** 18858.

HOUGHTON, F. D. 2006. Energy metabolism of the inner cell mass and trophectoderm of the mouse blastocyst. *Differentiation,* 74**,** 11-18.

HOUGHTON, F. D., THOMPSON, J. G., KENNEDY, C. J. & LEESE, H. J. 1996. Oxygen consumption and energy metabolism of the early mouse embryo. *Molecular Reproduction and Development,* 44**,** 476-485.

HU, D., GAO, X., CAO, K., MORGAN, M. A., MAS, G., SMITH, E. R., VOLK, A. G., BARTOM, E. T., CRISPINO, J. D., DI CROCE, L. & SHILATIFARD, A. 2017. Not All H3K4 Methylations Are Created Equal: Mll2/COMPASS Dependency in Primordial Germ Cell Specification. *Molecular Cell,* 65**,** 460-475.e6.

HU, L., LI, Z., CHENG, J., RAO, Q., GONG, W., LIU, M., SHI, Y. G., ZHU, J., WANG, P. & XU, Y. 2013. Crystal Structure of TET2-DNA Complex: Insight into TET-Mediated 5mC Oxidation. *Cell,* 155**,** 1545-1555.

HUANG, X., GAO, X., LI, W., JIANG, S., LI, R., HONG, H., ZHAO, C., ZHOU, P., CHEN, H., BO, X. & LI, H. 2019. Stable H3K4me3 is associated with transcription initiation during early embryo development. *Bioinformatics,* 35**,** 3931-3936.

HUXLEY, R. R., SHIELL, A. W. & LAW, C. M. 2000. The role of size at birth and postnatal catch-up growth in determining systolic blood pressure: a systematic review of the literature. *Journal of Hypertension,* 18**,** 815-831.

IGOSHEVA, N., ABRAMOV, A. Y., POSTON, L., ECKERT, J. J., FLEMING, T. P., DUCHEN, M. R. & MCCONNELL, J. 2010. Maternal Diet-Induced Obesity Alters Mitochondrial Activity and Redox Status in Mouse Oocytes and Zygotes. *PLOS ONE,* 5**,** e10074.

INOUE, A., SHEN, L., DAI, Q., HE, C. & ZHANG, Y. 2011. Generation and replication-dependent dilution of 5fC and 5caC during mouse preimplantation development. *Cell Research,* 21**,** 1670-1676.

INOUE, A. & ZHANG, Y. 2011. Replication-Dependent Loss of 5-Hydroxymethylcytosine in Mouse Preimplantation Embryos. *Science (New York, N.Y.),* 334**,** 194-194.

IQBAL, K., JIN, S.-G., PFEIFER, G. P. & SZABÓ, P. E. 2011. Reprogramming of the paternal genome upon fertilization involves genome-wide oxidation of 5-methylcytosine. *Proceedings of the National Academy of Sciences of the United States of America,* 108**,** 3642-3647.

IURLARO, M., FICZ, G., OXLEY, D., RAIBER, E.-A., BACHMAN, M., BOOTH, M. J., ANDREWS, S., BALASUBRAMANIAN, S. & REIK, W. 2013. A screen for hydroxymethylcytosine and formylcytosine binding proteins suggests functions in transcription and chromatin regulation. *Genome Biology,* 14**,** R119-R119.

IYER, L. M., ABHIMAN, S. & ARAVIND, L. 2011. Natural history of eukaryotic DNA methylation systems. *Progress in Molecular Biololgy and Translational Science,* 101**,** 25-104.

JABBARI, K. & BERNARDI, G. 2004. Cytosine methylation and CpG, TpG (CpA) and TpA frequencies. *Gene,* 333**,** 143-149.

JEZIORSKA, D. M., MURRAY, R. J. S., DE GOBBI, M., GAENTZSCH, R., GARRICK, D., AYYUB, H., CHEN, T., LI, E., TELENIUS, J., LYNCH, M., GRAHAM, B., SMITH, A. J. H., LUND, J. N., HUGHES, J. R., HIGGS, D. R. & TUFARELLI, C. 2017. DNA methylation of intragenic CpG islands depends on their transcriptional activity during differentiation and disease. *Proceedings of the National Academy of Sciences,* 114**,** E7526-E7535.

JIA, Z., SHI, Y., ZHANG, L., REN, Y., WANG, T., XING, L., ZHANG, B., GAO, G. & BU, R. 2018. DNA methylome profiling at single-base resolution through bisulfite sequencing of 5mC-immunoprecipitated DNA. *BMC Biotechnology,* 18**,** 7.

JOBERTY, G., BOESCHE, M., BROWN, J. A., EBERHARD, D., GARTON, N. S., HUMPHREYS, P. G., MATHIESON, T., MUELBAIER, M., RAMSDEN, N. G., READER, V., RUEGER, A., SHEPPARD, R. J., WESTAWAY, S. M., BANTSCHEFF, M., LEE, K., WILSON, D. M., PRINJHA, R. K. & DREWES, G. 2016. Interrogating the Druggability of the 2-Oxoglutarate-Dependent Dioxygenase Target Class by Chemical Proteomics. *ACS Chemical Biology,* 11**,** 2002-2010.

JOHNSON, T. B. & COGHILL, R. D. 1925. RESEARCHES ON PYRIMIDINES. C111. THE DISCOVERY OF 5-METHYL-CYTOSINE IN TUBERCULINIC ACID, THE NUCLEIC ACID OF THE TUBERCLE BACILLUS1. *Journal of the American Chemical Society,* 47**,** 2838-2844.

KAELIN JR, WILLIAM G. & MCKNIGHT, STEVEN L. 2013. Influence of Metabolism on Epigenetics and Disease. *Cell,* 153**,** 56-69.

KAUPPINEN, R. A., SIHRA, T. S. & NICHOLLS, D. G. 1987. Aminooxyacetic acid inhibits the malate-aspartate shuttle in isolated nerve terminals and prevents the mitochondria from utilizing glycolytic substrates. *Biochimica et Biophysica Acta (BBA) - Molecular Cell Research,* 930**,** 173-178.

KELLEY, R. L. & GARDNER, D. K. 2019. Individual culture and atmospheric oxygen during culture affect mouse preimplantation embryo metabolism and post-implantation development. *Reproductive BioMedicine Online,* 39**,** 3-18.

KIM, C. H., LEE, E. K., CHOI, Y. J., AN, H. J., JEONG, H. O., PARK, D., KIM, B. C., YU, B. P., BHAK, J. & CHUNG, H. Y. 2016. Short-term calorie restriction ameliorates genomewide, age-related alterations in DNA methylation. *Aging Cell,* 15**,** 1074-1081.

KO, M. S. H. 2006. Expression profiling of the mouse early embryo: Reflections and perspectives. *Developmental Dynamics,* 235**,** 2437-2448.

KOPEINA, G. S., SENICHKIN, V. V. & ZHIVOTOVSKY, B. 2017. Caloric restriction - A promising anti-cancer approach: From molecular mechanisms to clinical trials. *Biochimica et Biophysica Acta (BBA) - Reviews on Cancer,* 1867**,** 29-41.

KREBS, H. A. & JOHNSON, W. A. 1937. Metabolism of ketonic acids in animal tissues. *Biochemical Journal,* 31**,** 645-660.

KUBISCH, H. M., LARSON, M. A., FUNAHASHI, H., DAY, B. N. & ROBERTS, R. M. 1995. Pronuclear visibility, development and transgene expression in IVM/IVF-derived porcine embryos. *Theriogenology,* 44**,** 391-401.

KWONG, W. Y., WILD, A. E., ROBERTS, P., WILLIS, A. C. & FLEMING, T. P. 2000. Maternal undernutrition during the preimplantation period of rat development causes blastocyst abnormalities and programming of postnatal hypertension. *Development,* 127**,** 4195-4202.

LANE, M. & GARDNER, D. K. 1992. Effect of incubation volume and embryo density on the development and viability of mouse embryos in vitro. *Human Reproduction,* 7**,** 558-562.

LANE, M. & GARDNER, D. K. 1998. Amino acids and vitamins prevent culture-induced metabolic perturbations and associated loss of viability of mouse blastocysts. *Human Reproduction,* 13**,** 991-997.

LANE, M. & GARDNER, D. K. 2000. Lactate Regulates Pyruvate Uptake and Metabolism in the PreimplantationMouse Embryo. *Biology of Reproduction,* 62**,** 16-22.

LANE, M. & GARDNER, D. K. 2005. Mitochondrial Malate-Aspartate Shuttle Regulates Mouse Embryo Nutrient Consumption. *Journal of Biological Chemistry,* 280**,** 18361-18367.

LANE, M., MCPHERSON, N. O., FULLSTON, T., SPILLANE, M., SANDEMAN, L., KANG, W. X. & ZANDER-FOX, D. L. 2014a. Oxidative Stress in Mouse Sperm Impairs Embryo Development, Fetal Growth and Alters Adiposity and Glucose Regulation in Female Offspring. *PLOS ONE,* 9**,** e100832.

LANE, M., ROBKER, R. L. & ROBERTSON, S. A. 2014b. Parenting from before conception. *Science,* 345**,** 756-760.

LEARY, C., LEESE, H. J. & STURMEY, R. G. 2015. Human embryos from overweight and obese women display phenotypic and metabolic abnormalities. *Human Reproduction,* 30**,** 122-132.

LEE, K., HAMM, J., WHITWORTH, K., SPATE, L., PARK, K.-W., MURPHY, C. N. & PRATHER, R. S. 2014. Dynamics of TET family expression in porcine preimplantation embryos is related to zygotic genome activation and required for the maintenance of NANOG. *Developmental Biology,* 386**,** 86-95.

LEESE, H. J. 2002. Quiet please, do not disturb: a hypothesis of embryo metabolism and viability. *BioEssays,* 24**,** 845-849.

LEESE, H. J. 2012. Metabolism of the preimplantation embryo: 40 years on. *Reproduction,* 143**,** 417-427.

LEESE, H. J. & BARTON, A. M. 1984. Pyruvate and glucose uptake by mouse ova and preimplantation embryos. *Journal of Reproduction and Fertility,* 72**,** 9-13.

LEPIKHOV, K. & WALTER, J. 2004. Differential dynamics of histone H3 methylation at positions K4 and K9 in the mouse zygote. *BMC Developmental Biology,* 4**,** 12.

LI, L., ZHENG, P. & DEAN, J. 2010. Maternal control of early mouse development. *Development (Cambridge, England),* 137**,** 859-870.

LI, Y., FENG, H.-L., CAO, Y.-J., ZHENG, G.-J., YANG, Y., MULLEN, S., CRITSER, J. K. & CHEN, Z.-J. 2006. Confocal microscopic analysis of the spindle and chromosome configurations of human oocytes matured in vitro. *Fertility and Sterility,* 85**,** 827-832.

LI, Y. & O'NEILL, C. 2012. Persistence of Cytosine Methylation of DNA following Fertilisation in the Mouse. *PLOS ONE,* 7**,** e30687.

LI, Y. & O'NEILL, C. 2013. 5′-methylcytosine and 5′-hydroxymethylcytosine Each Provide Epigenetic Information to the Mouse Zygote. *PLOS ONE,* 8**,** e63689.

LIANG, Q.-X., LIN, Y.-H., ZHANG, C.-H., SUN, H.-M., ZHOU, L., SCHATTEN, H., SUN, Q.-Y. & QIAN, W.-P. 2018. Resveratrol increases resistance of mouse oocytes to postovulatory aging in vivo. *Aging,* 10**,** 1586-1596.

LIU, M.-J., SUN, A.-G., ZHAO, S.-G., LIU, H., MA, S.-Y., LI, M., HUAI, Y.-X., ZHAO, H. & LIU, H.-B. 2018. Resveratrol improves in vitro maturation of oocytes in aged mice and humans. *Fertility and Sterility,* 109**,** 900-907.

LIU, Y., HE, X.-Q., HUANG, X., DING, L., XU, L., SHEN, Y.-T., ZHANG, F., ZHU, M.-B., XU, B.-H., QI, Z.-Q. & WANG, H.-L. 2013. Resveratrol protects mouse oocytes from methylglyoxal-induced oxidative damage. *PLOS ONE,* 8**,** e77960-e77960.

LIU, Y., JIANG, W., LIU, J., ZHAO, S., XIONG, J., MAO, Y. & WANG, Y. 2012. IDH1 mutations inhibit multiple α-ketoglutarate-dependent dioxygenase activities in astroglioma. *Journal of Neuro-Oncology,* 109**,** 253-260.

LUZZO, K. M., WANG, Q., PURCELL, S. H., CHI, M., JIMENEZ, P. T., GRINDLER, N., SCHEDL, T. & MOLEY, K. H. 2012. High Fat Diet Induced Developmental Defects in the Mouse: Oocyte Meiotic Aneuploidy and Fetal Growth Retardation/Brain Defects. *PLOS ONE,* 7**,** e49217.

MA, Y., MA, Y., WEN, L., LEI, H., CHEN, S. & WANG, X. 2019. Changes in DNA methylation and imprinting disorders in E9.5 mouse fetuses and placentas derived from vitrified eight-cell embryos. *Molecular Reproduction and Development,* 86**,** 404-415.

MAITI, A. & DROHAT, A. C. 2011. Thymine DNA Glycosylase Can Rapidly Excise 5-Formylcytosine and 5-Carboxylcytosine: POTENTIAL IMPLICATIONS FOR ACTIVE DEMETHYLATION OF CpG SITES. *The Journal of Biological Chemistry,* 286**,** 35334-35338.

MANN, M. R. W., LEE, S. S., DOHERTY, A. S., VERONA, R. I., NOLEN, L. D., SCHULTZ, R. M. & BARTOLOMEI, M. S. 2004. Selective loss of imprinting in the placenta following preimplantation development in culture. *Development,* 131**,** 3727-3735.

MARDINOGLU, A., KAMPF, C., ASPLUND, A., FAGERBERG, L., HALLSTRÖM, B. M., EDLUND, K., BLÜHER, M., PONTÉN, F., UHLEN, M. & NIELSEN, J. 2014. Defining the Human Adipose Tissue Proteome To Reveal Metabolic Alterations in Obesity. *Journal of Proteome Research,* 13**,** 5106-5119.

MATSUZUKA, T., OZAWA, M., NAKAMURA, A., USHITANI, A., HIRABAYASHI, M. & KANAI, Y. 2005. Effects of Heat Stress on the Redox Status in the Oviduct and Early Embryonic Development in Mice. *Journal of Reproduction and Development,* 51**,** 281-287.

MCPHERSON, N. O., BELL, V. G., ZANDER-FOX, D. L., FULLSTON, T., WU, L. L., ROBKER, R. L. & LANE, M. 2015. When two obese parents are worse than one! Impacts on embryo and fetal development. *American Journal of Physiology - Endocrinology and Metabolism,* 309**,** E568-E581.

MCPHERSON, N. O., FULLSTON, T., AITKEN, R. J. & LANE, M. 2014. Paternal Obesity, Interventions, and Mechanistic Pathways to Impaired Health in Offspring. *Annals of Nutrition and Metabolism,* 64**,** 231-238.

MEIRELLES, F. V., CAETANO, A. R., WATANABE, Y. F., RIPAMONTE, P., CARAMBULA, S. F., MERIGHE, G. K. & GARCIA, S. M. 2004. Genome activation and developmental block in bovine embryos. *Animal Reproduction Science,* 82–83**,** 13-20.

MENKE, T. M. & MCLAREN, A. 1970. Mouse blastocysts grown in vivo and in vitro: carbon dioxide production and trophoblast outgrowth. *Journal of Reproduction and Fertility,* 23**,** 117-127.

MICHAN, S. 2013. Calorie restriction and NAD^+/sirtuin counteract the hallmarks of aging. *Frontiers in Bioscience (Landmark edition),* 19**,** 1300-1319.

MITCHELL, M., CASHMAN, K. S., GARDNER, D. K., THOMPSON, J. G. & LANE, M. 2009. Disruption of Mitochondrial Malate-Aspartate Shuttle Activity in Mouse Blastocysts Impairs Viability and Fetal Growth. *Biology of Reproduction,* 80**,** 295-301.

MONNÉ, M., MINIERO, D. V., BISACCIA, F. & FIERMONTE, G. 2012. The mitochondrial oxoglutarate carrier: from identification to mechanism. *Journal of Bioenergetics and Biomembranes,* 45**,** 1-13.

MORGAN, H. D., SANTOS, F., GREEN, K., DEAN, W. & REIK, W. 2005. Epigenetic reprogramming in mammals. *Human Molecular Genetics,* 14**,** R47-R58.

NAKAGAWA, T., LV, L., NAKAGAWA, M., YU, Y., YU, C., D'ALESSIO, ANA C., NAKAYAMA, K., FAN, H.-Y., CHEN, X. & XIONG, Y. 2015. CRL4VprBP E3 Ligase

Promotes Monoubiquitylation and Chromatin Binding of TET Dioxygenases. *Molecular Cell,* 57**,** 247-260.

NERI, F., INCARNATO, D., KREPELOVA, A., PARLATO, C. & OLIVIERO, S. 2016. Methylation-assisted bisulfite sequencing to simultaneously map 5fC and 5caC on a genome-wide scale for DNA demethylation analysis. *Nature Protocols,* 11**,** 1191-1205.

NERI, F., INCARNATO, D., KREPELOVA, A., RAPELLI, S., ANSELMI, F., PARLATO, C., MEDANA, C., DAL BELLO, F. & OLIVIERO, S. 2015. Single-Base Resolution Analysis of 5-Formyl and 5-Carboxyl Cytosine Reveals Promoter DNA Methylation Dynamics. *Cell reports,* 10**,** 674-683.

NIAKAN, K. K., HAN, J., PEDERSEN, R. A., SIMON, C. & PERA, R. A. R. 2012. Human pre-implantation embryo development. *Development,* 139**,** 829-841.

NIKAS, G., AO, A., WINSTON, R. M. & HANDYSIDE, A. H. 1996. Compaction and surface polarity in the human embryo in vitro. *Biology of Reproduction,* 55**,** 32-37.

NIU, Y., DESMARAIS, T. L., TONG, Z., YAO, Y. & COSTA, M. 2015. Oxidative stress alters global histone modification and DNA methylation. *Free Radical Biology and Medicine,* 82**,** 22-28.

NOTO, V., CAMPO, R., ROZIERS, P., SWINNEN, K., VERCRUYSSEN, M. & GORDTS, S. 1993. Fertilization and early embryology: Mitochondrial distribution after fast embryo freezing. *Human Reproduction,* 8**,** 2115-2118.

OU, X.-H., LI, S., WANG, Z.-B., LI, M., QUAN, S., XING, F., GUO, L., CHAO, S.-B., CHEN, Z., LIANG, X.-W., HOU, Y., SCHATTEN, H. & SUN, Q.-Y. 2012. Maternal insulin resistance causes oxidative stress and mitochondrial dysfunction in mouse oocytes. *Human Reproduction,* 27**,** 2130-2145.

PAGE-LARIVIERE, F. & SIRARD, M. A. 2014. Spatiotemporal expression of DNA demethylation enzymes and histone demethylases in bovine embryos. *Cellular Reprogramming,* 16**,** 40-53.

PANTALEON, M., RYAN, J. P., GIL, M. & KAYE, P. L. 2001. An Unusual Subcellular Localization of GLUT1 and Link with Metabolism in Oocytes and Preimplantation Mouse Embryos. *Biology of Reproduction,* 64**,** 1247-1254.

PAREDES, R. M., QUINONES, M., MARBALLI, K., GAO, X., VALDEZ, C., AHUJA, S. S., VELLIGAN, D. & WALSS-BASS, C. 2014. Metabolomic profiling of schizophrenia patients at risk for metabolic syndrome. *International Journal of Neuropsychopharmacology,* 17**,** 1139-1148.

PASTOR, W. A., ARAVIND, L. & RAO, A. 2013. TETonic shift: biological roles of TET proteins in DNA demethylation and transcription. *Nature Reviews Molecular Cell Biology,* 14**,** 341-356.

PATEL, S. A., CHAUDHARI, A., GUPTA, R., VELINGKAAR, N. & KONDRATOV, R. V. 2016. Circadian clocks govern calorie restriction–mediated life span extension through BMAL1- and IGF-1-dependent mechanisms. *The FASEB Journal,* 30**,** 1634-1642.

PATRA, S. K., PATRA, A., ZHAO, H., CARROLL, P. & DAHIYA, R. 2003. Methyl-CpG–DNA binding proteins in human prostate cancer: expression of CXXC sequence containing MBD1 and repression of MBD2 and MeCP2. *Biochemical and Biophysical Research Communications,* 302**,** 759-766.

PEKOWSKA, A., BENOUKRAF, T., FERRIER, P. & SPICUGLIA, S. 2010. A unique H3K4me2 profile marks tissue-specific gene regulation. *Genome Research,* 20**,** 1493-1502.

PEÑA, P. V., HOM, R. A., HUNG, T., LIN, H., KUO, A. J., WONG, R. P. C., SUBACH, O. M., CHAMPAGNE, K. S., ZHAO, R., VERKHUSHA, V. V., LI, G., GOZANI, O. & KUTATELADZE, T. G. 2008. Histone H3K4me3 Binding Is Required for the DNA Repair

and Apoptotic Activities of ING1 Tumor Suppressor. *Journal of Molecular Biology,* 380**,** 303-312.

PENZIAS, A. S., ROSSI, G., GUTMANN, J. N., HAJ-HASSAN, L., LEYKIN, L. & DIAMOND, M. P. 1993. Dichloroacetic acid accelerates initial development of 2-cell murine embryos in vitro. *Metabolism,* 42**,** 1077-1080.

PETERS, H., BYSKOV, A. G., HIMELSTEIN-BRAW, R. & FABER, M. 1975. FOLLICULAR GROWTH: THE BASIC EVENT IN THE MOUSE AND HUMAN OVARY. *Journal of Reproduction and Fertility,* 45**,** 559-566.

PHIPPS, K., BARKER, D., HALES, C., FALL, C., OSMOND, C. & CLARK, P. 1993. Fetal growth and impaired glucose tolerance in men and women. *Diabetologia,* 36**,** 225-228.

PRIVAT, E. & SOWERS, L. C. 1996. Photochemical Deamination and Demethylation of 5-Methylcytosine. *Chemical Research in Toxicology,* 9**,** 745-750.

PURCELL, S. H. & MOLEY, K. H. 2009. Glucose transporters in gametes and preimplantation embryos. *Trends in Endocrinology & Metabolism,* 20**,** 483-489.

REIS SILVA, A. R., ADENOT, P., DANIEL, N., ARCHILLA, C., PEYNOT, N., LUCCI, C. M., BEAUJEAN, N. & DURANTHON, V. 2011. Dynamics of DNA methylation levels in maternal and paternal rabbit genomes after fertilization. *Epigenetics,* 6**,** 987-993.

REYNIER, P., MAY-PANLOUP, P., CHRÉTIEN, M.-F., MORGAN, C. J., JEAN, M., SAVAGNER, F., BARRIÈRE, P. & MALTHIÈRY, Y. 2001. Mitochondrial DNA content affects the fertilizability of human oocytes. *Molecular Human Reproduction,* 7**,** 425-429.

REYNOLDS, K. A., BOUDOURES, A. L., CHI, M. M.-Y., WANG, Q. & MOLEY, K. H. 2015. Adverse effects of obesity and/or high-fat diet on oocyte quality and metabolism are not reversible with resumption of regular diet in mice. *Reproduction, Fertility and Development,* 27**,** 716-724.

RIEGER, D., MCGOWAN, L. T., COX, S. F., PUGH, P. A. & THOMPSON, J. G. 2002. Effect of 2,4-dinitrophenol on the energy metabolism of cattle embryos produced by in vitro fertilization and culture. *Reproduction, Fertility and Development,* 14**,** 339-343.

RIETHMACHER, D., BRINKMANN, V. & BIRCHMEIER, C. 1995. A targeted mutation in the mouse E-cadherin gene results in defective preimplantation development. *Proceedings of the National Academy of Sciences,* 92**,** 855-859.

ROBERT, C., MCGRAW, S., MASSICOTTE, L., PRAVETONI, M., GANDOLFI, F. & SIRARD, M.-A. 2002. Quantification of Housekeeping Transcript Levels During the Development of Bovine Preimplantation Embryos. *Biology of Reproduction,* 67**,** 1465-1472.

ROBERTSON, K. D., UZVOLGYI, E., LIANG, G., TALMADGE, C., SUMEGI, J., GONZALES, F. A. & JONES, P. A. 1999. The human DNA methyltransferases (DNMTs) 1, 3a and 3b: coordinate mRNA expression in normal tissues and overexpression in tumors. *Nucleic Acids Research,* 27**,** 2291-2298.

SAKASHITA, A., KOBAYASHI, H., WAKAI, T., SOTOMARU, Y., HATA, K. & KONO, T. 2014. Dynamics of genomic 5-hydroxymethylcytosine during mouse oocyte growth. *Genes to Cells,* 19**,** 629-636.

SALEHNIA, M., TÖHÖNEN, V., ZAVAREH, S. & INZUNZA, J. 2013. Does Cryopreservation of Ovarian Tissue Affect the Distribution and Function of Germinal Vesicle Oocytes Mitochondria? *BioMed Research International,* 2013**,** 489032.

SANFINS, A., PLANCHA, C. E. & ALBERTINI, D. F. 2015. Pre-implantation developmental potential from in vivo and in vitro matured mouse oocytes: a cytoskeletal perspective on oocyte quality. *Journal of assisted reproduction and genetics,* 32**,** 127-136.

SANTOS, F., HENDRICH, B., REIK, W. & DEAN, W. 2002. Dynamic Reprogramming of DNA Methylation in the Early Mouse Embryo. *Developmental Biology,* 241**,** 172-182.

SASSONE-CORSI, P. 2013. When Metabolism and Epigenetics Converge. *Science,* 339**,** 148-150.

SATHANANTHAN, A. H. & TROUNSON, A. O. 2000. Mitochondrial morphology during preimplantational human embryogenesis. *Human Reproduction,* 15**,** 148-159.

SCHOMACHER, L., HAN, D., MUSHEEV, M. U., ARAB, K., KIENHOFER, S., VON SEGGERN, A. & NIEHRS, C. 2016. Neil DNA glycosylases promote substrate turnover by Tdg during DNA demethylation. *Nat Struct Mol Biol,* advance online publication.

SCHULTZ, R. M. 1993. Regulation of zygotic gene activation in the mouse. *BioEssays,* 15**,** 531-538.

SCOTT, L. A. & SMITH, S. 1998. The successful use of pronuclear embryo transfers the day following oocyte retrieval. *Human Reproduction,* 13**,** 1003-13.

SEIDLER, E. A. & MOLEY, K. H. Metabolic Determinants of Mitochondrial Function in Oocytes. Seminars in reproductive medicine, 2015. 396-400.

SHA, Q.-Q., DAI, X.-X., JIANG, J.-C., YU, C., JIANG, Y., LIU, J., OU, X.-H., ZHANG, S.-Y. & FAN, H.-Y. 2018. CFP1 coordinates histone H3 lysine-4 trimethylation and meiotic cell cycle progression in mouse oocytes. *Nature Communications,* 9**,** 3477.

SHAO, G.-B., CHEN, J.-C., ZHANG, L.-P., HUANG, P., LU, H.-Y., JIN, J., GONG, A.-H. & SANG, J.-R. 2014. Dynamic patterns of histone H3 lysine 4 methyltransferases and demethylases during mouse preimplantation development. *In Vitro Cellular & Developmental Biology - Animal,* 50**,** 603-613.

SHAO, G.-B., WANG, J., ZHANG, L.-P., WU, C.-Y., JIN, J., SANG, J.-R., LU, H.-Y., GONG, A.-H., DU, F.-Y. & PENG, W.-X. 2015. Aging alters histone H3 lysine 4 methylation in mouse germinal vesicle stage oocytes. *Reproduction, Fertility and Development,* 27**,** 419-426.

SHEN, L., INOUE, A., HE, J., LIU, Y., LU, F. & ZHANG, Y. 2014a. Tet3 and DNA Replication Mediate Demethylation of Both the Maternal and Paternal Genomes in Mouse Zygotes. *Cell Stem Cell,* 15**,** 459-470.

SHEN, L., SONG, C.-X., HE, C. & ZHANG, Y. 2014b. Mechanism and Function of Oxidative Reversal of DNA and RNA Methylation. *Annual Review of Biochemistry,* 83**,** 585-614.

SHIRASAWA, H. & TERADA, Y. 2017. In vitro maturation of human immature oocytes for fertility preservation and research material. *Reproductive Medicine and Biology,* 16**,** 258-267.

SHOGREN-KNAAK, M., ISHII, H., SUN, J.-M., PAZIN, M. J., DAVIE, J. R. & PETERSON, C. L. 2006. Histone H4-K16 acetylation controls chromatin structure and protein interactions. *Science,* 311**,** 844-847.

SPEAKMAN, J. R., MITCHELL, S. E. & MAZIDI, M. 2016. Calories or protein? The effect of dietary restriction on lifespan in rodents is explained by calories alone. *Experimental Gerontology,* 86**,** 28-38.

STEWART, K. R., VESELOVSKA, L., KIM, J., HUANG, J., SAADEH, H., TOMIZAWA, S.-I., SMALLWOOD, S. A., CHEN, T. & KELSEY, G. 2015. Dynamic changes in histone modifications precede de novo DNA methylation in oocytes. *Genes & Development,* 29**,** 2449-2462.

STOKES, P. J., ABEYDEERA, L. R. & LEESE, H. J. 2005. Development of porcine embryos in vivo and in vitro; evidence for embryo 'cross talk' in vitro. *Developmental Biology,* 284**,** 62-71.

TALBOT, P. 1985. Sperm penetration through oocyte investments in mammals. *American Journal of Anatomy,* 174**,** 331-346.

TELFORD, N. A., WATSON, A. J. & SCHULTZ, G. A. 1990. Transition from maternal to embryonic control in early mammalian development: a comparison of several species. *Molecular Reproduction and Development,* 26**,** 90-100.

THOMPSON, J., SIMPSON, A., PUGH, P., WRIGHT, R. & TERVIT, H. 1991. Glucose utilization by sheep embryos derived in vivo and in vitro. *Reproduction, Fertility and Development,* 3**,** 571-576.

TRIMARCHI, J. R., LIU, L., PORTERFIELD, D. M., SMITH, P. J. S. & KEEFE, D. L. 2000. Oxidative Phosphorylation-Dependent and -Independent Oxygen Consumption by Individual Preimplantation Mouse Embryos. *Biology of Reproduction,* 62**,** 1866-1874.

TSUKAMOTO, S., KUMA, A. & MIZUSHIMA, N. 2008a. The role of autophagy during the oocyte-to-embryo transition. *Autophagy,* 4**,** 1076-1078.

TSUKAMOTO, S., KUMA, A., MURAKAMI, M., KISHI, C., YAMAMOTO, A. & MIZUSHIMA, N. 2008b. Autophagy Is Essential for Preimplantation Development of Mouse Embryos. *Science,* 321**,** 117.

UPADHYAYA, B., LARSEN, T., BARWARI, S., LOUWAGIE, E. J., BAACK, M. L. & DEY, M. 2017. Prenatal Exposure to a Maternal High-Fat Diet Affects Histone Modification of Cardiometabolic Genes in Newborn Rats. *Nutrients,* 9**,** 407.

VAN BLERKOM, J., DAVIS, P. & ALEXANDER, S. 2000. Differential mitochondrial distribution in human pronuclear embryos leads to disproportionate inheritance between blastomeres: relationship to microtubular organization, ATP content and competence. *Human Reproduction,* 15**,** 2621-2633.

VAN BLERKOM, J., DAVIS, P., MATHWIG, V. & ALEXANDER, S. 2002. Domains of high-polarized and low-polarized mitochondria may occur in mouse and human oocytes and early embryos. *Human Reproduction,* 17**,** 393-406.

VAN BLERKOM, J., DAVIS, P. W. & LEE, J. 1995. Fertilization and early embryolgoy: ATP content of human oocytes and developmental potential and outcome after in-vitro fertilization and embryo transfer. *Human Reproduction,* 10**,** 415-424.

VAN DEN HURK, R. & ZHAO, J. 2005. Formation of mammalian oocytes and their growth, differentiation and maturation within ovarian follicles. *Theriogenology,* 63**,** 1717-1751.

VAN SOOM, A., BOERJAN, M. L., BOLS, P. E., VANROOSE, G., LEIN, A., CORYN, M. & DE KRUIF, A. 1997. Timing of compaction and inner cell allocation in bovine embryos produced in vivo after superovulation. *Biology of Reproduction,* 57**,** 1041-1049.

WAKEFIELD, S. L., LANE, M. & MITCHELL, M. 2011. Impaired Mitochondrial Function in the Preimplantation Embryo Perturbs Fetal and Placental Development in the Mouse. *Biology of Reproduction,* 84**,** 572-580.

WANG, S., KOU, Z., JING, Z., ZHANG, Y., GUO, X., DONG, M., WILMUT, I. & GAO, S. 2010. Proteome of mouse oocytes at different developmental stages. *Proceedings of the National Academy of Sciences,* 107**,** 17639-17644.

WARBURG, O. 1956. On the Origin of Cancer Cells. *Science,* 123**,** 309-314.

WATKINS, A. J., URSELL, E., PANTON, R., PAPENBROCK, T., HOLLIS, L., CUNNINGHAM, C., WILKINS, A., PERRY, V. H., SHETH, B., KWONG, W. Y., ECKERT, J. J., WILD, A. E., HANSON, M. A., OSMOND, C. & FLEMING, T. P. 2008a. Adaptive Responses by Mouse Early Embryos to Maternal Diet Protect Fetal Growth but Predispose to Adult Onset Disease. *Biology of Reproduction,* 78**,** 299-306.

WATKINS, A. J., WILKINS, A., CUNNINGHAM, C., PERRY, V. H., SEET, M. J., OSMOND, C., ECKERT, J. J., TORRENS, C., CAGAMPANG, F. R. A., CLEAL, J., GRAY, W. P., HANSON, M. A. & FLEMING, T. P. 2008b. Low protein diet fed exclusively during mouse oocyte maturation leads to behavioural and cardiovascular abnormalities in offspring. *The Journal of Physiology,* 586**,** 2231-2244.

WATSON, A. J. & BARCROFT, L. C. 2001. Regulation of blastocyst formation. *Frontiers in Bioscience,* 6**,** D708-30.

WATSON, A. J. & KIDDER, G. M. 1988. Immunofluorescence assessment of the timing of appearance and cellular distribution of Na/K-ATPase during mouse embryogenesis. *Developmental Biology,* 126**,** 80-90.

WHITTINGHAM, D. 1975. Fertilization, early development and storage of mammalian ova in vitro. *The Early Development of Mammals***,** 1-24.

WHITTINGHAM, D. G. 1969. The Failure of Lactate and Phosphoenolpyruvate to Support Development of the Mouse Zygote in Vitro. *Biology of Reproduction,* 1**,** 381-386.

WIESNER, R. J., RÜEGG, J. C. & MORANO, I. 1992. Counting target molecules by exponential polymerase chain reaction: Copy number of mitochondrial DNA in rat tissues. *Biochemical and Biophysical Research Communications,* 183**,** 553-559.

WILDING, M., DALE, B., MARINO, M., DI MATTEO, L., ALVIGGI, C., PISATURO, M. L., LOMBARDI, L. & DE PLACIDO, G. 2001. Mitochondrial aggregation patterns and activity in human oocytes and preimplantation embryos. *Human Reproduction,* 16**,** 909-917.

WU, H. & ZHANG, Y. 2011. Mechanisms and functions of Tet protein-mediated 5-methylcytosine oxidation. *Genes & Development,* 25**,** 2436-2452.

WU, H. & ZHANG, Y. 2012. Early Embryos Reprogram DNA Methylation in Two Steps. *Cell Stem Cell,* 10**,** 487-489.

WU, L. L.-Y., DUNNING, K. R., YANG, X., RUSSELL, D. L., LANE, M., NORMAN, R. J. & ROBKER, R. L. 2010. High-Fat Diet Causes Lipotoxicity Responses in Cumulus–Oocyte Complexes and Decreased Fertilization Rates. *Endocrinology,* 151**,** 5438-5445.

WU, L. L., RUSSELL, D. L., WONG, S. L., CHEN, M., TSAI, T.-S., ST JOHN, J. C., NORMAN, R. J., FEBBRAIO, M. A., CARROLL, J. & ROBKER, R. L. 2015a. Mitochondrial dysfunction in oocytes of obese mothers: transmission to offspring and reversal by pharmacological endoplasmic reticulum stress inhibitors. *Development,* 142**,** 681-691.

WU, Y., ZHANG, Z., LIAO, X. & WANG, Z. 2015b. High fat diet triggers cell cycle arrest and excessive apoptosis of granulosa cells during the follicular development. *Biochemical and Biophysical Research Communications,* 466**,** 599-605.

WYMAN, A., PINTO, A. B., SHERIDAN, R. & MOLEY, K. H. 2008. One-Cell Zygote Transfer from Diabetic to Nondiabetic Mouse Results in Congenital Malformations and Growth Retardation in Offspring. *Endocrinology,* 149**,** 466-469.

XU, K., CHEN, X., YANG, H., XU, Y., HE, Y., WANG, C., HUANG, H., LIU, B., LIU, W., LI, J., KOU, X., ZHAO, Y., ZHAO, K., ZHANG, L., HOU, Z., WANG, H., WANG, H., LI, J., FAN, H., WANG, F., GAO, Y., ZHANG, Y., CHEN, J. & GAO, S. 2017. Maternal Sall4 Is Indispensable for Epigenetic Maturation of Mouse Oocytes. *Journal of Biological Chemistry,* 292**,** 1798-1807.

XU, W., YANG, H., LIU, Y., YANG, Y., WANG, P., KIM, S.-H., ITO, S., YANG, C., WANG, P., XIAO, M.-T., LIU, L.-X., JIANG, W.-Q., LIU, J., ZHANG, J.-Y., WANG, B., FRYE, S., ZHANG, Y., XU, Y.-H., LEI, Q.-Y., GUAN, K.-L., ZHAO, S.-M. & XIONG, Y. 2011. Oncometabolite 2-Hydroxyglutarate Is a Competitive Inhibitor of α-Ketoglutarate-Dependent Dioxygenases. *Cancer Cell,* 19**,** 17-30.

YANG, H., LIN, H., XU, H., ZHANG, L., CHENG, L., WEN, B., SHOU, J., GUAN, K., XIONG, Y. & YE, D. 2014. TET-catalyzed 5-methylcytosine hydroxylation is dynamically regulated by metabolites. *Cell Research,* 24**,** 1017-1020.

YU, C., FAN, X., SHA, Q.-Q., WANG, H.-H., LI, B.-T., DAI, X.-X., SHEN, L., LIU, J., WANG, L., LIU, K., TANG, F. & FAN, H.-Y. 2017. CFP1 Regulates Histone H3K4 Trimethylation and Developmental Potential in Mouse Oocytes. *Cell Reports,* 20**,** 1161-1172.

YU, C., ZHANG, Y.-L., PAN, W.-W., LI, X.-M., WANG, Z.-W., GE, Z.-J., ZHOU, J.-J., CANG, Y., TONG, C., SUN, Q.-Y. & FAN, H.-Y. 2013. CRL4 Complex Regulates Mammalian

Oocyte Survival and Reprogramming by Activation of TET Proteins. *Science,* 342**,** 1518-1521.

ZAMBONI, L., CHAKRABORTY, J. & SMITH, D. M. 1972. First Cleavage Division of the Mouse Zygote: An Ultrastructural Study. *Biology of Reproduction,* 7**,** 170-193.

ZANDER-FOX, D., CASHMAN, K. S. & LANE, M. 2013. The presence of 1 mM glycine in vitrification solutions protects oocyte mitochondrial homeostasis and improves blastocyst development. *Journal of Assisted Reproduction and Genetics,* 30**,** 107-116.

ZANDER-FOX, D. L., FULLSTON, T., MCPHERSON, N. O., SANDEMAN, L., KANG, W. X., GOOD, S. B., SPILLANE, M. & LANE, M. 2015. Reduction of Mitochondrial Function by FCCP During Mouse Cleavage Stage Embryo Culture Reduces Birth Weight and Impairs the Metabolic Health of Offspring. *Biology of Reproduction,* 92, 1-11.

ZHANG, B., ZHENG, H., HUANG, B., LI, W., XIANG, Y., PENG, X., MING, J., WU, X., ZHANG, Y., XU, Q., LIU, W., KOU, X., ZHAO, Y., HE, W., LI, C., CHEN, B., LI, Y., WANG, Q., MA, J., YIN, Q., KEE, K., MENG, A., GAO, S., XU, F., NA, J. & XIE, W. 2016. Allelic reprogramming of the histone modification H3K4me3 in early mammalian development. *Nature,* 537**,** 553.

ZHANG, Z., HE, C., ZHANG, L., ZHU, T., LV, D., LI, G., SONG, Y., WANG, J., WU, H., JI, P. & LIU, G. 2019. Alpha-ketoglutarate affects murine embryo development through metabolic and epigenetic modulations. *Reproduction,* 158**,** 125-135.

ZHAO, S., LIN, Y., XU, W., JIANG, W., ZHA, Z., WANG, P., YU, W., LI, Z., GONG, L., PENG, Y., DING, J., LEI, Q., GUAN, K.-L. & XIONG, Y. 2009. Glioma-Derived Mutations in IDH1 Dominantly Inhibit IDH1 Catalytic Activity and Induce HIF-1α. *Science,* 324**,** 261-265.

ZHU, C., GAO, Y., GUO, H., XIA, B., SONG, J., WU, X., ZENG, H., KEE, K., TANG, F. & YI, C. 2017. Single-Cell 5-Formylcytosine Landscapes of Mammalian Early Embryos and ESCs at Single-Base Resolution. *Cell Stem Cell*, 20**,** 720-731.e5.

ZIOMEK, C. A., JOHNSON, M. H. & HANDYSIDE, A. H. 1982. The developmental potential of mouse 16-cell blastomeres. *Journal of Experimental Zoology*, 221**,** 345-355.

Chapter 2 Maternal high fat diet alters oocyte levels of Ten-Eleven Translocase (TET) proteins and methylation marks in mouse embryos

2.1 Statement of Authorship

Statement of Authorship

Title of Paper	Maternal High Fat Diet Alters Oocyte Levels of Ten-Eleven Translocase (TET) Proteins and Methylation Marks in Mouse Embryos.
Publication Status	☐ Published ☐ Accepted for Publication ☐ Submitted for Publication ☑ Unpublished and Unsubmitted work written in manuscript style
Publication Details	Currently written in the style for the Journal of Assisted Reproduction and Genetics (JARG).

Principal Author

Name of Principal Author (Candidate)	Alexander Penn		
Contribution to the Paper	Study design, performed experiments, analysed and interpreted data, wrote and edited the manuscript		
Overall percentage (%)	80%		
Certification:	This paper reports on original research I conducted during the period of my Higher Degree by Research candidature and is not subject to any obligations or contractual agreements with a third party that would constrain its inclusion in this thesis. I am the primary author of this paper.		
Signature		Date	16/07/2021

Co-Author Contributions

By signing the Statement of Authorship, each author certifies that:

i. the candidate's stated contribution to the publication is accurate (as detailed above);

ii. permission is granted for the candidate in include the publication in the thesis; and

iii. the sum of all co-author contributions is equal to 100% less the candidate's stated contribution.

Name of Co-Author	Nicole O McPherson		
Contribution to the Paper	Assisted in interpretation of data, and editing of the manuscript		
Signature		Date	16/07/2021

Name of Co-Author	Tod Fullston		
Contribution to the Paper	Assisted in interpretation of data, and editing of the manuscript		
Signature		Date	16/07/2021

Name of Co-Author	Michelle Lane (deceased)		
Contribution to the Paper	Study design, assisted in interpretation of data, and editing of the manuscript		
Signature		Date	

Name of Co-Author	Deirdre Zander-Fox		
Contribution to the Paper	Assisted in interpretation of data, and editing of the manuscript		
Signature		Date	16/07/2021

Please cut and paste additional co-author panels here as required.

2.2 Abstract

Purpose: Maternal obesity during the peri-conception period has implications for offspring metabolic health, however the precise mechanism for this programming is unknown. Ten-Eleven translocase (TET) enzymes and their adaptor protein VPRBP (adaptor protein viral protein R binding protein) actively demethylate DNA using the TCA cycle intermediary α-ketoglutarate and may play a role in programming offspring health. Whether these are disrupted by maternal obesity is unknown and will be investigated.

Methods: 5-6 week old C57Bl/6 female mice were fed either a control diet (N= 175, CD; 6% fat) or a high-fat diet (N= 158, HFD; 21% fat) for six weeks and oocytes were collected for measurement of gene expression and global protein levels of TET/VPRBP, as well as metabolic parameters. Females were mated and zygotes collected and cultured *in vitro* for measurements of embryo development and assessment of global DNA methylation for 5mC, 5hmC, 5fC and 5caC in the 2-cell embryo. A subset of these embryos was transferred into pseudopregnant Swiss females for day 18 foetal measurements.

Results: After HFD treatment; oocytes showed increased pyruvate oxidation and intracellular ROS. Gene expression for *Tet3* was unchanged, however TET3 protein in the oocyte was increased in HFD fed mice, coupled with decreased chromatin localisation. Gene expression of the adaptor protein *Vprbp* was increased with HFD with a decreased proportion of oocytes demonstrating presence of VPRBP protein co-localised with chromatin, similar to TET3. Immediately after 2-cell cleavage; global DNA methylation of 5hmC was reduced with a concomitant increase in 5fC.

Conclusion: Metabolic sensor proteins such as TETs may provide a link between maternal obesity induced oocyte mitochondrial dysfunction, and pre-implantation embryo methylation and programming changes.

2.3 Introduction

Currently in most Western societies, greater than 50% of reproductively aged women are overweight or obese (ABS, 2011-2012, Ng et al., 2014). Maternal obesity at conception is linked to increased time to pregnancy, elevated birth weights, metabolic syndrome, and insulin resistance and an increased risk of obesity in the resultant children (Boney et al., 2005). Moreover, studies in animal models have shown that even when exposure to a high fat diet (HFD) is limited to the peri-conception period, impairments to foetal development and subsequent adult metabolic health including alterations in insulin metabolism persist in offspring into adulthood (Sasson et al., 2015). Further, studies from donor *in vitro* fertilisation (IVF) cycles have shown that oocytes donated from women who are obese produce embryos that have reduced pregnancy rates irrespective of whether the recipient is of normal weight (Cardozo et al., 2016). This implies that exposure of oocytes to an obesogenic environment is sufficient to transmit altered health cues to the next generation. However, currently, the mechanism responsible for this peri-conception programming of health from maternal obesity is not well understood (Lane et al., 2014b).

A novel concept has emerged recently whereby the metabolic profile of a cell is believed to be directly linked to its epigenetic profile (Brown et al., 2015, Tzika et al., 2018). This concept is of interest in the realm of maternal programming as increasing data demonstrates that maternal obesity damages oocyte mitochondria resulting in perturbed metabolism of oocytes and subsequent early embryos, impairing viability and resultant offspring health (Bavister, 1995, Boots et al., 2016, Boudoures et al., 2017, Igosheva et al., 2010, Lane et al., 2014a, Luzzo et al., 2012, McPherson et al., 2015, Reynolds et al., 2015, Wu et al., 2015a, Wu et al., 2010). Directly reducing mitochondrial function in the very early embryo with chemical compounds such as amino-oxyacetate (AOA), ammonium, and carbonyl cyanide 4-(trifluoromethoxy) phenylhydrazone (FCCP), can result in similar changes to embryo development and impaired foetal health similar to those from maternal obesity (Fullston et al., 2011, Lane and Gardner, 1998, Mitchell et al., 2009a, Wakefield et al.,

2011, Zander-Fox et al., 2015). Therefore, maternal obesity may be transmitting altered health cues to the next generation via a disruption to metabolic processes in the oocyte and early embryo. However, to date the mechanistic links between altered mitochondrial metabolic profile in the oocyte and perturbed foetal health remains largely unknown.

One of the earliest epigenetic changes in the developing embryo is demethylation of the maternal and paternal genomes in the 1-cell embryo prior to embryonic genome activation at the 2-cell stage (Iqbal et al., 2011, Santos et al., 2005). This allows the erasure of methylation patterns originating in the sperm and egg (exceptions are imprinted regions), and formation of new methylation patterns for the developing embryo, which is particularly important for embryonic genome activation (Eckersley-Maslin et al., 2018). This process is mediated via the activity of the Ten-Eleven Translocase family (TET) metabolic sensing proteins (Bagci and Fisher, 2013, Ito et al., 2010). The TET proteins remove 5-methylcytocine (5mC) by oxidizing the base to 5-hydroxymethylcytosine (5hmC); and further onto 5-formylcytosine (5fC) and 5-carboxycytosine (5caC) using the tricarboxylic acid (TCA) cycle intermediary α-ketoglutarate as a cofactor. When this process is blocked via maternal TET3 knockout, the resulting embryos are depleted of 5hmC and enriched for 5mC (Amouroux et al., 2016, Guo et al., 2014, Inoue et al., 2015, Shen et al., 2014, Tsukada et al., 2015) resulting in reduced live birth rates and 34% neonatal lethality within the first 3 days of life (Inoue et al., 2015). Binding of TETs to DNA is facilitated by ubiquitination via the cullin RING ligase 4 (CRL4) complex and the adaptor protein viral protein R binding protein (VPRBP), which binds to the CRL4 complex via DNA damage-binding protein 1 (DDB1). Knockouts of the adapter protein VPRBP in oocytes prevents 5hmC formation in the paternal pronucleus and impairs embryo development (Nakagawa et al., 2015a). The activity of TET proteins is directly related to availability of mitochondrial substrates, in particular elevations in α-ketoglutarate increase TET mediated DNA demethylation in embryonic stem cells (Carey et al., 2015), thereby directly linking mitochondrial activity and DNA methylation. Whether a similar

interaction occurs in the early embryo is unclear and whether the metabolic disturbances in the oocyte from maternal obesity influences TET mediated demethylation is unknown.

Therefore, the aim of this study was to examine the capacity of a maternal high fat diet to impair oocyte mitochondrial metabolism, and further increase TET mediated demethylation in the early embryo through increased substrate availability.

2.4 Materials and Methods

2.4.1 Mice

All reagents and chemicals were obtained from Sigma Aldrich (St Louis, Missouri, USA) unless specified elsewhere. Female C57Bl/6 mice were fed *ad libitum* either a control diet (CD; SF04-057, 6% fat from canola oil, Specialty Feeds) or a high fat diet (HFD; SF00-219, 21% fat from clarified butter, Harlan Teklad TD 88137 equivalent, Specialty Feeds; Glen Forrest, Western Australia) for six weeks, with total bodyweight measured weekly (see Table S2.1 for detailed diet information). Mice were maintained in a 14 h: 10 h light: dark cycle with *ad libitum* supply of water in a conventional animal house (University of Adelaide Laboratory Animal Services). At six weeks of age, fasted glucose tolerance tests (GTT) were performed by administering an intraperitoneal (i.p.) injection of 2 $g.kg^{-1}$ of 25% glucose solution (Zander-Fox et al., 2015). Insulin tolerance tests (ITT) were performed 5 days later under fed conditions, with i.p. injection of 0.75 $IU.kg^{-1}$ insulin (Zander-Fox et al., 2015). Tail blood glucose concentrations were measured using a glucometer before glucose or insulin bolus (0 min), and 15, 30, 60, and 120 min post bolus. Data was expressed as area under the curve for glucose tolerance and area above the curve for insulin tolerance.

2.4.2 Oocyte and zygote collection

After six weeks of diet treatment, female mice were superovulated using an i.p. injection 10 IU of pregnant mare's serum gonadotrophin (PMSG, Folligon; Intervet, Bendigo East, Australia) and after 48 h and subsequent i.p. injection of 10 IU human chorionic gonadotrophin (hCG, Pregnyl; Organon, Oss, Netherlands). Females were then mated overnight with C57Bl/6 male mice fed standard chow.

For oocyte collection, ovulated oocytes were collected 13-15 h post- hCG (without mating), and embryos were collected at 18 h post-hCG (with mating). Oocytes/embryos were denuded from surrounding cumulus cells using 0.5mg/mL hyaluronidase in GMOPS + 5% HSA (Vitrolife).

2.4.3 Embryo culture

For embryo culture, collected presumed zygotes were cultured in 20 µL drops of medium G1 PLUS (Vitrolife) under Ovoil (Vitrolife; Gothenburg, Sweden) at 37°C at 6% CO_2, 5% O_2, and 89% N_2. Two-cells were collected from culture within 30 min of embryo cleavage to maintain consistent nuclear morphology and to measure methylation levels before embryonic genome activation. At 14 h post presumed fertilisation at mid-dark cycle (5 h of culture); dishes containing embryos were checked for cleaved embryos at 30 min intervals; with cleaved embryos being removed from culture immediately and fixed for immunohistochemical staining (see section below). For blastocyst culture, embryos were cultured in G1 PLUS as above for 45 h, and then washed and cultured for a further 46 h in G2 PLUS (Vitrolife) at 37°C at 6% CO_2, 5% O_2, and 89% N_2. Embryo morphology and development was assessed at 26 h for cleavage, at 74 h for percentage on time development to early/expanding blastocyst, and at 91 h for assessment of development to the expanded-hatching blastocyst stage (Mitchell et al., 2009a).

2.4.4 Pyruvate uptake

Pyruvate uptake was assayed using an ultramicrofluorimetric assay (Leese and Barton, 1984). Individual metaphase II oocytes were placed in 250 nL drops of GMOPS under oil at 37°C for 4 h. Pyruvate present in the resulting media was measured through NADH fluorescence (excitation 340 nm, emission 440-470 nm) through an enzyme coupled reaction (Leese and Barton, 1984), using a Leica DMIRB microscope with a photometer attachment (Leica Microsystems; Wetzlar, Germany). Pyruvate used from the initial concentration present in the media was calculated and expressed as picomoles per oocyte per hour (Gardner and Leese, 1986).

2.4.5 Pyruvate oxidation by TCA cycle

Pyruvate oxidation in oocytes was assessed by measuring oxidation of 2-^{14}C-pyruvate (GE Healthcare; Chicago, Illinois, USA, specific activity 0.014 mCi/mL) (Lane and Gardner, 1998). Oocytes were incubated in G1 PLUS medium (Vitrolife) for 3 h at 37°C at 6% CO_2, 5% O_2, and 89% N_2. Pyruvate oxidation was calculated based on the recovery efficiencies of the radiolabelled substrate and expressed as picomoles per oocyte per hour.

2.4.6 Reactive oxygen species (ROS)

Levels of intracellular ROS in individual oocytes was assessed by incubation with 1 µM DCFDA (Thermo Fisher; Waltham, Mass., USA, excitation 492-495 nm, emission 517-527 nm) in G1 medium (Vitrolife) for 30 min. ROS levels were measuring using fluorescent microscope with a photometer attachment (Leica Microsystems), with gain and voltage normalised to a CD oocyte (Wakefield et al., 2008).

2.4.7 Embryo transfer

To assess viability, cultured blastocysts were transferred to Swiss pseudopregnant females at day 3.5 of pregnancy. Blastocysts from CD or HFD were allocated to contralateral uterine horns (Zander et al., 2006). On day 18 of pregnancy mice were culled and number of implantation sites, foetal development as well as foetal length and the weight of foetus and placenta were assessed.

2.4.8 Gene expression

Total RNA was extracted from pools of 20 snap frozen oocytes using RNeasy Micro kit (QIAGEN; Hilden, Germany) according to the manufacturer's protocol, including addition of 20 ng carrier RNA per sample before homogenization, and DNAse treatment of samples. Reverse transcription was performed using Superscript III Reverse Transcriptase kit (Invitrogen; Carlsbad, California, USA), with 250 ng random primers (Invitrogen) and 10mM dNTPs (Invitrogen) at 65°C for 5 min before addition of 200U Superscript III, 0.1M DTT and Superscript III reverse transcriptase buffer at 50°C for 60 min and 70°C for 15 min.

qPCR was carried out using Taqman chemistry (Applied Biosystems; Foster City, California, USA) using 2X Gene Expression Master Mix (Applied Biosystems), and *18S* rRNA as an endogenous control (Fullston et al., 2011, Jeong et al., 2014). The QuantStudio 12K Flex (Applied Biosystems) was used to thermocycle samples using standard Taqman cycling conditions (in a 0.1 mL Fast plate, Applied Biosystems) using Taqman probes for *18S* (Mm03928990_g1), *Tet1* (Mm01169087_m1), *Tet2* (Mm00524395_m1), *and Tet3* (Mm00805756_m1), *Vprbp* (Mm01226815_m1), *and Ddb1* (Mm00497159_m1) (Applied Biosystems), with three technical replicates run for each pool. Thermocycling conditions were as follows: initial denaturation of 95^0C for 10 min, and 40 cycles of denaturation at 95^0C for 15 s and annealing/extension at 60^0C for 60 s. Samples were normalised to the endogenous control *18S* rRNA and then expressed as fold change compared to CD fed mice. *18S* was selected as a reference gene for qPCR as it shows

constant levels in oocytes and embryos through to the 8-cell stage in embryos and it not linked to metabolism, unlike *Gapdh* (Robert et al., 2002). Samples which returned a $Ct \geq 35$ were not deemed to have been expressed reliably and were excluded from analysis.

2.4.9 Immunocytochemical staining for proteins TET3 and VPRBP

Oocytes were fixed in 4% paraformaldehyde (PFA) in 1x PBS at 4^{o}C overnight. Fixed oocytes were washed in PBS + 4 mg/mL PVP before permeabilising in 0.25% Triton X-100 in PBS for 15 min at room temperature (RT), then blocked overnight in 10% Donkey serum in PBS.

Oocytes were washed once in 0.25% Triton X in PBS, and incubated with primary antibody (Mouse anti-TET3, or rabbit anti-VPRBP, Table S2.2), diluted in PBS for 1.5 h at 37°C. Negative control oocytes and embryos were incubated in PBS only for 1.5 h at 37°C Oocytes were then washed twice in 0.25% Triton X in PBS, then incubated in secondary antibody 1:100 Donkey anti-Rabbit conjugated to Alexa-488 (AB150073, Abcam, excitation 490 nm, emission 525 nm) for 2 h at RT followed by addition of 1mM DAPI in PBS (excitation 358 nm, emission 461 nm) for 5 min. Oocytes were then washed twice in GMOPS (Vitrolife), and imaged using the Leica SP5 scanning confocal microscope (Leica) using 40x magnification. Relative levels of TET3 and VPRBP were measured via densitometry of captured images using Fiji version 2.0.0-rc-43/1.50e (Schindelin et al., 2012), with both spindles captured separately and averaged, and chromatin measured in only those with positive chromatin staining (i.e. with distinct fluorescence matching that of the chromatin region confirmed via DAPI co-stain) via encircling the DAPI stained chromatin and recording the VPRBP/TET3 channel. Data was then calculated as a fold change relative to CD measurements.

2.4.10 Assessment of DNA methylation for 5mC, 5hmC, 5fC and 5caC in embryos

DNA methylation was measured in 2-cell embryos no further than 30 min post cleavage, with embryos assessed every 30 min until there was a 1.5 h period where no further embryos had cleaved as opposed to a timed collection, where delayed developing embryos could alter the result through altered nuclear morphology or differing stage of cell cycle (Kang et al., 2014).

After fixation as listed above, immunocytochemistry was performed as previously described (Li and O'Neill, 2012). 2-cell embryos were permeabilised in 0.5% Tween 20 + 0.5% Triton X-100 in PBS at RT for 40 min, then blocked overnight in 30% Donkey serum (DS) in PBS at 4°C. The following morning, DNA was denatured in 4N HCl at 37°C for 10 min, followed by antigen retrieval in 0.25% Trypsin + EDTA at 37°C for 45 s, followed by wash in 10% donkey serum. Embryos were then incubated with 1:100 mouse anti-5mC (Active Motif; Carlsbad, California, USA), and either 1:500 rabbit anti-5hmC (Active Motif), 1:200 rabbit anti-5fC (Active Motif), or 1:200 rabbit anti 5-caC (Active Motif) in 10% DS at 4°C for 17 h, plus 1 h at 37°C. Embryos were washed twice in 0.5% Triton-X, followed by incubation with secondary antibodies 1:200 donkey anti-mouse Alexa 594 (ab150108, Abcam; Cambridge, United Kingdom) and 1:250 donkey anti-rabbit Alexa 488 (A-21206, Life Technologies; Carlsbad, California, USA) in 10% DS at RT for 2 h before washing in GMOPS PLUS (Vitrolife) and imaged using the CV1000 spinning disk confocal microscope (Yokogawa; Musashino, Tokyo, Japan) using 40x magnification. Relative levels of methylation marks were measured via densitometry of captured images using Fiji version 2.0.0-rc-43/1.50e (Schindelin et al., 2012) using the freehand tool to select whole nuclear regions. Data was then calculated as a fold change relative to CD measurements, and calculated as a ratio of 5hmC, 5fC and 5caC to each respective cell's 5mC measurement.

2.4.11 Statistical analysis

Data are expressed as the mean ± SEM unless stated otherwise. Statistical analysis was performed using IBM SPSS version 24 with a P value of <0.05 been statistically significant. All data were assessed for normality using The Lilliefors modification to the Kolmogorov-Smirnov normality test. Equal variance was assessed using Levene's test. The total mouse weights between CD and HFD fed mice over six weeks were analysed using a repeated measures generalised linear model with a Gaussian distribution; with interactions between diet and week of diet in order to show statistically significant weight gain. Postmortem fat deposits and tissue weights were analysed using general linear models to take differences into account from different collection dates where normally distributed and via two sample Wilcoxon rank sum test where not normally distributed. Serum measures, gene expression and embryo metabolism were analysed using independent Student's T-tests. TET3 immunocytochemistry and DNA methylation were analysed via general linear models with replicate of ICC run as a covariate and two sample Wilcoxon tests were performed where data was not normally distributed. VPRBP and TET3 oocyte frequency of chromatin staining was analysed using Pearson chi square analysis on binomial data. Embryo development, implantation and foetal count was measured using binomial regression, and foetal and placental measured were analysed using generalised linear models with individual implantation host mothers run as a covariate.

2.5 Results

2.5.1 Six weeks of HFD feeding increases bodyweight and adiposity, and alters blood metabolites

Female mice maintained an increased total body weight after 1 week on the HFD ($P<0.01$) (Figure S2.1). After six weeks on the HFD, total fat mass in grams was significantly increased ($P<0.0001$) with no differences in organ and muscle weights (Table S2.3). When expressed as a percentage of bodyweight, total fat mass was significantly increased ($P<0.0001$); while the proportionate weight of kidneys ($P<0.001$), liver ($P<0.005$) and pancreas ($P<0.05$) were decreased (Table S2.3). There was no difference in glucose tolerance (Figure S2.2a-b) after 6 weeks on a HFD. However, there were signs of insulin resistance evident as an increased area above the curve during the ITT, particularly at 60 min post insulin bolus compared with CD mice (Figure S2.2c-d) ($P<0.05$). HFD feeding also increased fasting serum levels of high-density lipoprotein ($P<0.001$), cholesterol ($P<0.005$) and leptin ($P<0.001$) compared with CD mice, while fasting serum insulin and glucose concentrations were not significantly different between the two groups (Table S2.3).

2.5.2 Embryo development and pregnancy outcomes under maternal HFD

Feeding females a HFD did not affect embryo cleavage rates to the 2-cell or on-time blastocyst development on day 4 and day 5 (Table 2.1). After transfer of CD or HFD blastocysts to pseudopregnant females, on day 18 of pregnancy no differences were seen between diets for implantation rate per embryos transferred, nor foetuses developed as percentage of total implanted ($P=0.07$), however foetuses per embryos transferred was significantly reduced for embryos created from females fed a HFD compared with CD mice ($P<0.05$, Table 1). There was also a reduction in foetal length for HFD females compared with CD females ($P<0.01$, Table 1), however foetal weights, placental weights and foetal to placental weight ratios were not different ($P=0.083$, Table 1).

2.5.3 Impairment to mitochondrial function in oocytes under maternal HFD

Uptake of pyruvate was not altered in oocytes from females fed a HFD (Figure 2.1a), although pyruvate oxidation was increased compared with oocytes from CD females (Figure 2.1b) ($P<0.01$). This corresponded with a greater percentage of pyruvate oxidised within the TCA cycle in oocytes from females fed a HFD (CD 7.96%, HFD 12.73%) compared with females fed a CD. Reactive oxygen species (ROS) was increased in oocytes from females fed a HFD compared with CD females (Figure 2.1c) ($P<0.001$).

2.5.4 TET1-3, VPRBP and DDB1 gene expression changes in the oocyte under maternal HFD

Gene expression of *Tet1-3* and the ubiquitination machinery *Vprbp* and *Ddb1* were measured in oocytes to determine changes in maternal transcript concentration. *Tet1 and Tet2* were not detected in oocytes collected from mothers fed either a CD or HFD (*Tet1* Ct values >39, *Tet2* Ct values >35, which were both above our established cut-off of Ct ≥35 determined as not expressed). *Tet3* and *Ddb1* gene expression in oocytes were not found to be altered by diets (Figure 2.2). However, *Vprbp* gene expression levels were increased in HFD derived oocytes compared with oocytes from CD fed mice ($P<0.05$, Figure 2.2).

2.5.5 TET3/VPRBP localisation changes in the oocyte under maternal HFD

Oocytes derived from CD and HFD fed females were measured for global TET3 presence to determine any changes to TET3 protein levels or localisation following maternal HFD. TET3 appeared to be co-localised with the metaphase spindle and chromatin and therefore these regions of the oocyte were assessed and calculated separately for TET3 (Figure 2.3a). The proportion of

oocytes that had positive TET3 staining directly upon the chromatin was lower in HFD oocytes ($P<0.05$, Figure 2.3c).

TET3 intensity as measured by relative fluorescence was not increased in the mitotic spindle and or the chromatin of HFD oocytes compared with CD oocytes (Figure 2.3c).

VPRBP also appeared to be co-localised with the mitotic spindle (Figure 2.4a), and similarly to TET3 the chromatin was stained less frequently in oocytes from HFD females compared with CD fed females ($P<0.05$, Figure 2.4b).

VPRBP relative fluorescence levels in oocytes from HFD females compared with CD fed females showed no difference in spindle staining intensity, nor chromatin staining intensity (Figure 2.4c).

2.5.6 Increased progression of DNA demethylation under maternal HFD

To assess the impact of TET3 protein changes on methylation marks, 2-cell embryos derived from HFD females within 30 min of cleavage were assessed for the DNA methylation marks 5mC, 5hmC, 5fC and 5caC (Figure 2.5a) and compared to 2-cell embryos derived from CD females. This stage was selected as the position of the cell cycle and the morphology of the nucleus is consistent (Kang et al., 2014), while still being present before the second DNA replication phase in the embryo preceding embryonic genome activation. Cleavage times were not significantly different between CD and HFD (Figure S2.3).

There were no differences in 5mC or 5caC (relative fluorescence or normalised to CD) levels of 2-cell embryos from HFD compared to CD females (Figure 2.5b). However, 5hmC levels were decreased ($P<0.01$) while 5fC levels increased ($P<0.01$) in 2-cell embryos from HFD females, after normalization to CD levels (Figure 2.5b).

The demethylation ratio of 5hmC:5mC was not changed in 2-cell embryos from HFD females compared with CD females (Figure 2.5c), however the ratio of 5fC:5mC was increased ($P<0.01$), while the ratio of 5caC:5mC was decreased ($P<0.05$) in 2-cell embryos from HFD females compared with CD females (Figure 2.5c).

This suggests that embryos of HFD mothers may have progressed to further oxidation of 5mC, with 5hmC progressing to 5fC and 5fC progressing to 5caC.

2.6 Discussion

Maternal obesity during the peri-conceptual period is associated with reduced pregnancy rates, altered foetal development and increased risk of obesity, metabolic syndrome and insulin resistance in offspring (Han et al., 2018, Jungheim et al., 2010). However, the underpinning mechanism that causes maternal obesity to alter offspring health remains largely unknown. Here we show that in a mouse model of maternal HFD there are alterations to methylation patterns in the early 2-cell embryo, with a higher proportion of 5fC marks suggesting advanced progression down the demethylation pathway in these embryos as methylated marks are removed from the genome. This coincides with elevated levels of whole oocyte TET3 protein, which appeared to preferentially localise around the spindle on the metaphase plate. Overall, these findings suggest that maternal obesity appears to advance the removal of methylation marks in the early embryo and implicates this process as a component acting to program suboptimal health in offspring.

The HFD feeding of females in this study did not impact the rate of embryonic development to the blastocyst stage. This differs to other studies which have reported decreased *in vitro* fertilisation rates (Wu et al., 2010), as well as developmental delays in culture to blastocyst stage and increased rates of fragmentation when blastocysts were flushed on 3.5 days post coitum, where development was *in vivo* HFD environment (Han et al., 2018). However, it is difficult to directly compare studies due to differences in diet formulations including the proportion and source of fat 21.0% w/w clarified butter (40% energy from fat) vs 31.7% w/w lard plus 3.2% w/w soybean oil (60% energy from fat), and length of dietary feeding (6 weeks vs 16 weeks). In addition, the embryos in our study were removed from the tract for the preimplantation embryo developmental period, which suggests that there may be a further impact on development due to exposure to the reproductive tract of a female fed a HFD during the pre-implantation embryo development period. Despite this, transfers of these cultured blastocysts from HFD donors, resulted in lower foetal development rates and reduced foetal:placental weight and crown-rump lengths. These observations are consistent

with several other studies which have shown reduced crown:rump lengths when female mice are fed HFD during the pre- and peri-conception period (McPherson et al., 2015, Sasson et al., 2015), as well as through preconception and throughout gestation (Han et al., 2018, Jungheim et al., 2010, Musial et al., 2017, Samuelsson et al., 2008). Decreased foetal crown:rump lengths and alterations to foetal weight in offspring from mothers fed a high fat diet before conception is known to be associated with poorer health outcomes in the offspring; including increased appetite, increased adiposity, decrease to muscle mass, insulin insensitivity and glucose intolerance (Ashino et al., 2012, Ge et al., 2014), along with increased blood pressure and heart rate (Samuelsson et al., 2008). TET proteins alter DNA methylation by using α-ketoglutarate as a substrate to hydroxylate 5mC to 5hmC, then further oxidise to 5fC and 5caC (Ito et al., 2011). Given that TET proteins utilise a mitochondrial intermediate as a co-factor, DNA methylation concentrations have been shown to be dependent on mitochondrial function (Zhang et al., 2019). As maternal obesity is known to induce mitochondrial dysfunction in oocytes and the early embryo (McPherson et al., 2015, Wu et al., 2010), we surmised that this altered metabolic would lead to changes in TET protein levels and early embryo methylation.

We were unable to detect the presence of TET1 or TET2 transcripts or protein in oocytes regardless of diet intervention. This is in agreement with other studies which failed to detect TET2 in mouse embryos until the late preimplantation embryo (Gao et al., 2019) and transcription of *Tet2* occurring post fertilisation (Yu et al., 2013b). TET3 transcripts and protein concentrations were present in all the oocytes assessed, consistent with previous studies (Amouroux et al., 2016, Cao et al., 2019, Gu et al., 2011, Guo et al., 2014, Han et al., 2018, Inoue et al., 2012, Inoue et al., 2015, Kurotaki et al., 2015, Nakagawa et al., 2015a, Shen et al., 2014, Tsukada et al., 2015, Yu et al., 2013b, Zhang et al., 2014). Interestingly in our study there were no significant alterations to TET3 levels observed in oocytes from a maternal HFD, where alteration have been recorded in the maternal pronuclei from HFD embryos post fertilisation (Han et al., 2018). These alterations because of maternal HFD

may not be indicative of an increase in total TET3 protein, rather a re-distribution of the TET3 present and relative TET3 enrichment within the maternal pronucleus through increased nuclear targeting.

VPRBP localised to the same nuclear position as TET3 in the oocyte. VPRBP is an adaptor protein that binds the cullin-RING ligase complex in order to monoubquitinate TET proteins, which increases their affinity for methylated DNA (Nakagawa et al., 2015a). Interestingly, we showed increased gene expression of *Vprbp* in oocytes from females fed a HFD. VPRBP in oocytes is essential for establishment of 5hmC marks on the DNA (Yu et al., 2013b), however the exact mechanism in which ubiquitination of TET via VPRBP alters the function of TET is not known. However, VPRBP appears to be enriched in both maternal and paternal pronuclei post fertilisation similar to TET3 (Amouroux et al., 2016, Guo et al., 2014, Han et al., 2018, Yu et al., 2013a). Additionally, deletion of VPRBP in the oocyte results in a failure to cleave (Nakagawa et al., 2015b) and VPRBP knockout oocytes show elevated levels of 5mC (Nakagawa et al., 2015a, Yu et al., 2013b).

There was an observed disconnect between the relative increase in transcript level for *Vprbp* while observing no statistically significant changes in protein levels. Oocyte transcription occurs at a high rate throughout folliculogenesis, however by the GV stage the oocytes become transcriptionally quiet (Picton et al., 1998). This is followed by a large scale degradation of transcripts in the oocyte and early embryo leading up to embryonic genome activation at the 2-cell in mouse (Picton et al., 1998), where transcript may be present however it is degraded after fertilisation rather than translated. This may result in the observed disparity between transcript and protein abundance in our model.

Interestingly, we showed that chromatin localisation of VPRBP and TET3 was present in fewer oocytes obtained from mothers fed a HFD. This may be due to a delay in oocyte development under HFD conditions as oocytes were collected temporally and thus may not indicate differential

localisation at the same point of maturation. Co-localisation assays after fertilisation in the early pronuclear stages would need to be conducted to completely explain this phenomenon.

It should also be noted though that VPRBP also acts as an adaptor protein for many other enzymes, including p53, (Schabla et al., 2018) and therefore its function and changes in levels due to maternal obesity may not be limited to TETs. The spindle localisation of TETs is also not completely understood; however TETs have been shown to be bound to cyclin-dependent kinases, which are essential for correct cell cycle progression (Chrysanthou et al., 2018).

As maternal derived TET3 is required for establishment of 5hmC, 5fC and 5caC DNA marks post fertilisation (Amouroux et al., 2016, Guo et al., 2014, Han et al., 2018, Inoue et al., 2015, Shen et al., 2014, Tsukada et al., 2015), we investigated whether the changes seen in TET3 and VPRBP concentrations in the HFD oocyte were associated with changes in methylation marks in the early pre-implantation embryo. As stated previously, we assessed the methylation status of 2-cell embryos within 30 min of cleavage (prior to embryonic genome activation) to ensure the embryos were at the same developmental stage. The rationale for this is that DNA methylation is actively occurring in PN4-5 embryos, so would give a more "uniform" staging of the embryonic methylation status prior to the methylation changes that occur in the 2-cell during S phase (Inoue et al., 2011). Interestingly, we found that females fed an HFD had advancement in the DNA demethylation cycle, with 5hmC levels significantly decreased coupled with significant increased concentrations of 5fC methylation compared with 2-cells derived from CD females. This observation is supported by another study of maternal HFD fed mice (34.9% fat for 16 weeks) where late stage PN3-5 embryos from mothers fed an HFD also showed an enhanced progression of methylation marks with increased 5hmC levels in the maternal pronucleus relative to zygotes from CD mothers (Han et al., 2018). Our data suggests a progression after cleavage in the 2-cell, where the observed increase in 5hmC is further oxidised to 5fC, with a concomitant reduction in 5hmC. There is evidence in late pronuclear stage embryos that the paternal pronucleus is also

enriched for 5fC and 5caC (Amouroux et al., 2016), which may lead to the progression of 5fC to 5caC and removal of 5caC and at the next cell division. It is believed that DNA replication at cell division is required for the base excision repair pathway to remove 5fC and 5caC (Inoue et al., 2011). In mouse embryos initially there is an increasing level of 5hmC, 5fC and 5caC across pronuclear migration followed by both 5fC and 5caC halving at the 2-cell and halving again at cleavage to the 4-cell (Inoue et al., 2011). These alterations to DNA methylation status, particularly in promoter regions (Han et al., 2018) alter the binding of methyl-CpG binding proteins (Li and O'Neill, 2012). This in turn would alter expression of genes following embryonic genome activation (2-cell in the mouse), potentially altering the developmental trajectory of the preimplantation embryo and may be one of the mechanisms for the altered foetal growth observed in offspring from obese mothers. In further support of this, knockout of TET3 in mouse embryos halted progression of 5mC to 5hmC and beyond resulting in a marked reduction in live births, with very low neonatal survival (Tsukada et al., 2015).

One of the key co-factors for TET protein function is α-ketoglutarate, which is a TCA cycle intermediate (Loenarz and Schofield, 2008) and therefore TET protein function and methylation of the early embryo is heavily reliant on mitochondrial function. In rodents, maternal obesity alters the distribution of mitochondria (Igosheva et al., 2010), increases levels of reactive oxygen species (ROS) (Igosheva et al., 2010), lowers mitochondria membrane potential (Wu et al., 2015a, Wu et al., 2015b), reduces electron density (Boudoures et al., 2017), and decreases ATP content, all which directly correlate with downstream metabolic changes to the pre-implantation embryo and subsequent foetus (Boots et al., 2016). During preimplantation embryo development, the embryo relies on mitochondria for the generation of energy, where perturbations that either decrease or increase mitochondrial function, negatively influence preimplantation development and the resulting offspring (Brison and Leese, 1994, Fullston et al., 2011, Green et al., 2016, Hewitson et al., 1996, Lane and Gardner, 2005, McPherson et al., 2014, Mitchell et al., 2009a, Mitchell et al.,

2009b, Wakefield et al., 2011, Wu et al., 2015a, Zander et al., 2006, Zander-Fox et al., 2015). Increased pyruvate oxidation as observed in our HFD oocytes is an indication of increased TCA cycle activity. Pyruvate can be either converted to acetyl-CoA in the mitochondrial matrix to be used through the TCA cycle, or can be used in the cytoplasm by lactate dehydrogenase (Lane and Gardner, 2000). As there was no increase in pyruvate uptake in oocytes obtained from HFD females, this indicates that a greater percentage of the pyruvate was used in the TCA cycle and a lower proportion of pyruvate used for lactate based metabolism which would increase the level of α-ketoglutarate (Lane and Gardner, 2000). It also appears that ROS is likely increased due to increased pyruvate oxidation which is facilitated by increased substrate availability in HFD oocytes, and associated with reduced implantation rates (Conaghan et al., 1993, Turner et al., 1994).

It should be noted that the pyruvate uptake assay in our study was performed on mature oocytes with cumulus cells removed. The maturing oocyte from the GV stage to the MII stage obtains pyruvate from the cumulus cells surrounding the oocyte (Leese and Barton, 1985), so there may be further differences in oocytes with the cumulus intact (as would be found *in vivo*) compared to the data presented in this study. In addition maternal HFD is also associated with disruptions to these gap junctions between the cumulus cell and the oocyte (Ratchford et al., 2008, Wang et al., 2012, Wang et al., 2010). These disruptions may also reduce the *in vivo* pyruvate uptake in the oocyte, so the observed increase in pyruvate oxidation may be more significant if the starting pyruvate concentration was lower in the HFD oocytes. Increasing pyruvate oxidation through the TCA cycle increases the TCA cycle intermediaries such as α-ketoglutarate (Houghton et al., 1996, Maus and Peters, 2017), which could then be transported into the cytoplasm to be used by α-ketoglutarate dependent enzymes such as TETs. While we did not measure embryonic α-ketoglutarate concentrations directly, the aforementioned increase in TCA cycle based metabolism of pyruvate

may lead to increased α-ketoglutarate availability to be utilised via TETs however, this remains to be confirmed in future studies.

In non-embryonic systems; changes to metabolism are associated with changes to DNA methylation (Salminen et al., 2015). There are alterations to TCA cycle activity reported in Alzheimer's disease (Salminen et al., 2015), with a decrease in glutamate uptake (Nilsen et al., 2014), potentially affecting availability of α-ketoglutarate for use by TET proteins to demethylate DNA. A global increase in both 5mC 5hmC in grey matter is observed; similarly to PN5 embryos (Bradley-Whitman and Lovell, 2013, Coppieters et al., 2014); however there is a reduction in 5fC and 5caC in the hippocampus in both preclinical and late stage Alzheimer's with a concomitant increase in TET1 (Bradley-Whitman and Lovell, 2013). Additionally, cancers with mutations to isocitrate dehydrogenase I (IDH1) produce the oncometabolite 2-hydroxygutarate (2HG) instead of α-ketoglutarate (Figueroa et al., 2010, Xu et al., 2011). 2HG is a competitive inhibitor of all α-ketoglutarate dependent enzymes, including TETs. Supplementation with 2HG reduces the activity of TET (Yang et al., 2016), and cells containing IDH1 mutations show hypermethylation at 5mC (Figueroa et al., 2010), indicating lower demethylation to 5hmC and beyond.

In conclusion, metabolic sensor proteins such as TETs may provide the link between mitochondrial dysfunction in oocytes, as seen in obesity, and epigenetic changes within the resultant embryo. In turn these epigenetic changes may alter the transcription and translation of proteins in the early embryo, altering the growth and development of subsequent offspring and program suboptimal health.

2.7 Tables

Table 2.1 Embryo development from lean and obese females, including blastocyst viability and foetal/placental morphometry following transfer of blastocysts from lean or obese females into pseudopregnant recipient females

Parameter	CD	HFD	P
Cleavage	77.1%	78.4%	NS
On-time development on day 4	73.2%	78.1%	NS
On-time development on day 5	86.1%	92.4%	NS
Implantation/ET	72.2%	62.5%	NS
Foetus/ET	61.1%	33.3%	0.048
Foetus/Implantation	84.6%	53.3%	NS
Foetal weight (mg)	1037.2 ± 48.5	947.1 ± 36.0	NS
Placental weight (mg)	151.4 ± 8.6	152.8 ± 6.3	NS
Foetal:Placental weight ratio	7.1 ± 0.5	6.2 ± 0.4	0.083
Foetal length (mm)	21.5 ± 0.4	20.1 ± 0.3	0.002

Data represents mean ± standard error of the mean (SEM). CD = control diet, HFD = high fat diet. Blastocyst development expressed per 2-cell embryo. Values for embryo development are from n=124 CD and n=186 HFD embryos from n=25 and n=37 mice respectively. Foetal data represents mean ± SEM from 8 pregnancies from 10 female mice, with n=41 CD and n=62 HFD day 5 embryos transferred. Foetal and placental measures represent 15 and 29 foetuses and placentas from CD and HFD females respectively

2.8 Figures

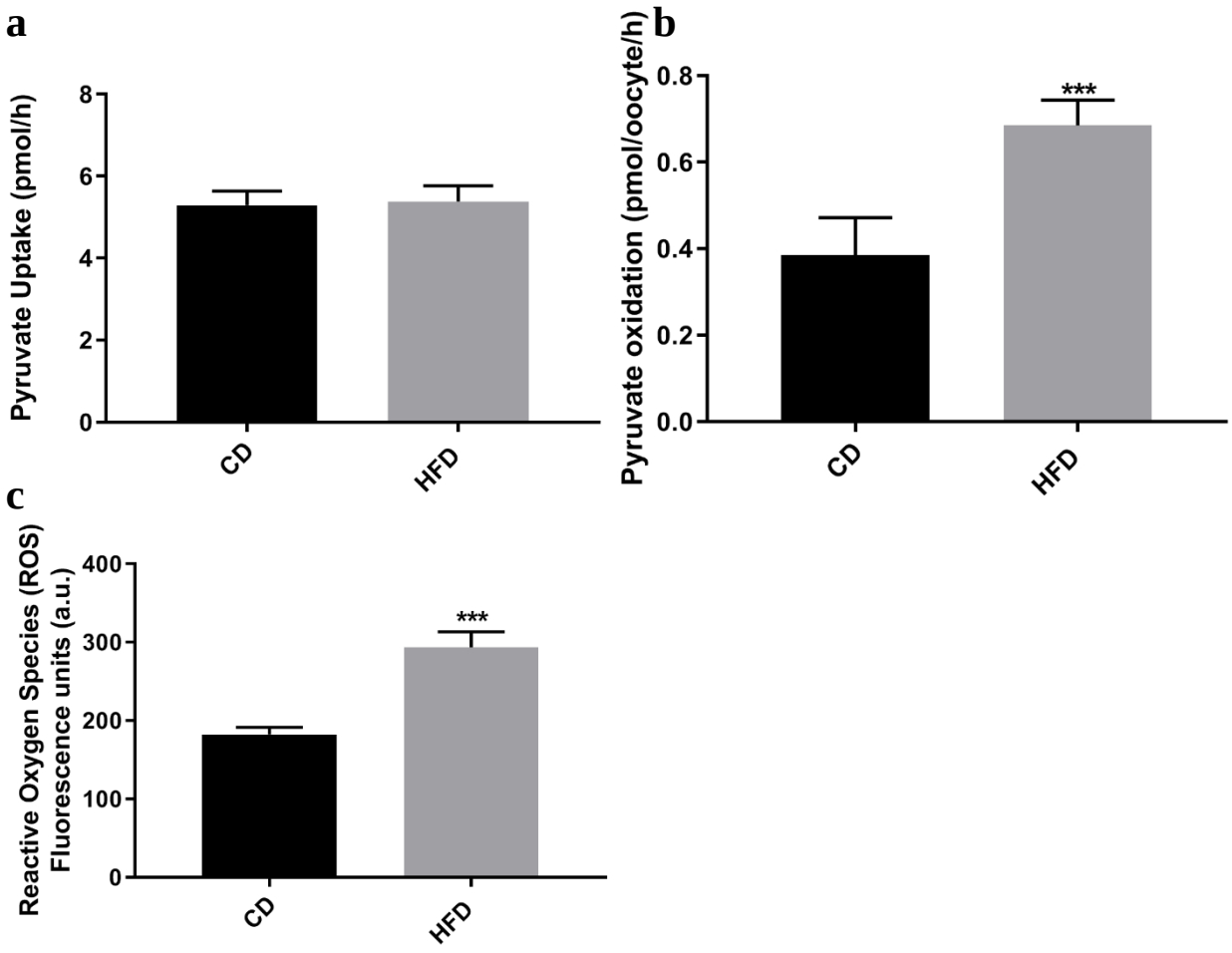

Figure 2.1 Effect of maternal high fat diet (HFD) on mitochondria and metabolism. All data is expressed as mean ± standard error of the mean SEM. **a** pyruvate uptake expressed as uptake (picomoles pyruvate/oocyte/h) n=32 control diet (CD) and n=36 HFD oocytes from n=7 CD and n=8 HFD mice **b** pyruvate oxidation expressed as uptake (picomoles pyruvate/oocyte/h) CD (n=11) and HFD (n=21) individual oocytes from n=2 CD and n= 7 HFD mice and **c** reactive oxygen species (ROS) in fluorescence units from n=39 CD and n=27 HFD oocytes from n=5 CD and n=7 HFD mice. *** P<0.001

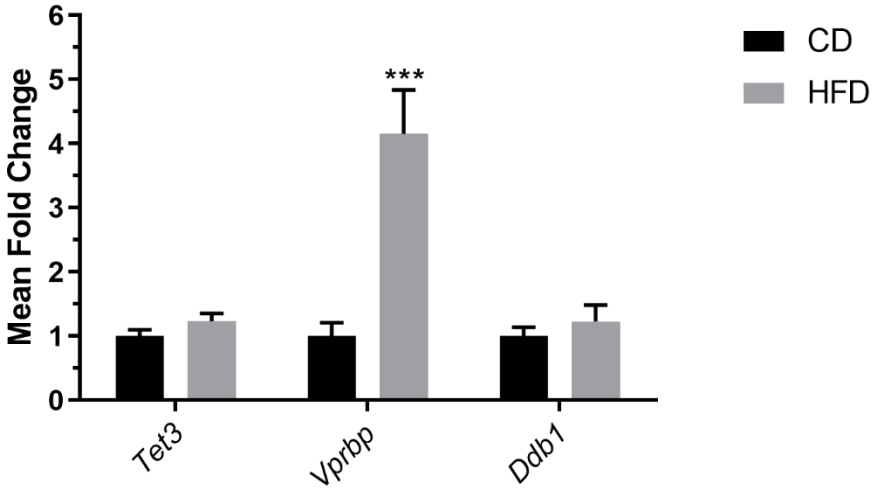

Figure 2.2 Effect of a maternal high fat diet (HFD) on oocyte gene expression of *Tet3*, *Vprbp* and *Ddb1*. Data expressed as fold change ± standard error of the mean (SEM). n=7 control diet (CD) and n=9 HFD pools of 20 oocytes/treatment from n=17 CD and n=17 HFD mice. *** P<0.001

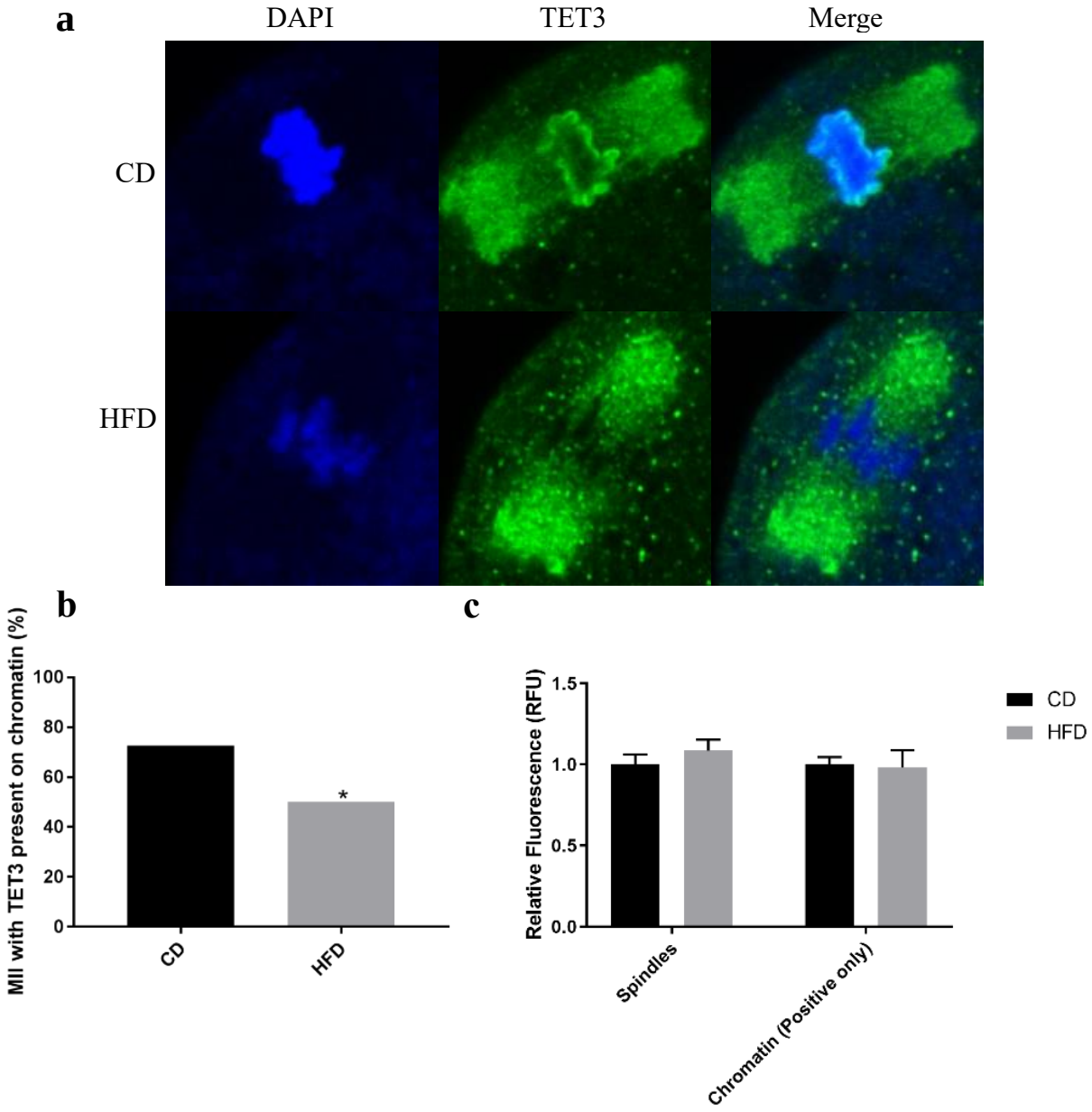

Figure 2.3 TET3 immunocytochemistry on oocytes from control diet (CD) or high fat diet (HFD) fed mothers. **a** Representative images of staining for TET3 (green) and nuclear reference 2-(4-amidinophenyl)-1H -indole-6-carboxamidine (DAPI) in blue. Difference in apparent size due to orientation of oocyte altering location of chromatin in z-space, **b** relative fluorescence levels for whole oocyte, cytoplasm and mitotic spindle area fluorescence from CD (n=26) or HFD (n=26) oocytes from n=4 CD and n=14 HFD mice and **c** Frequency of oocytes that have positive TET3 staining in the region of the chromatin expressed as mean ± standard error of the mean (SEM). * P<0.05, ** P<0.01

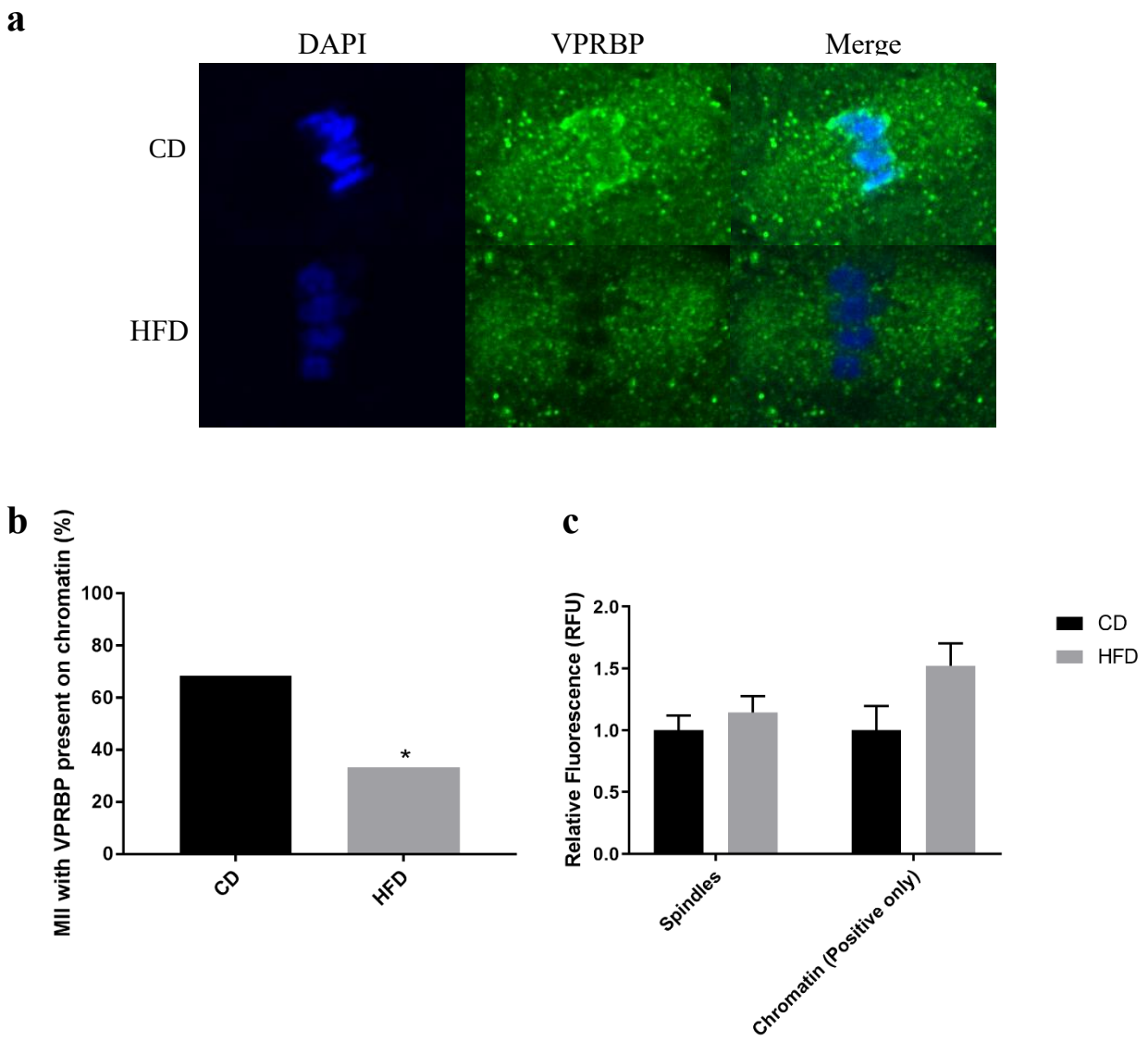

Figure 2.4 VPRBP immunocytochemistry on oocytes from control diet (CD) and high fat diet (HFD) fed mothers. **a** Classification of staining for VPRBP (green) as either present or not present at chromatin and nuclear reference 2-(4-amidinophenyl)-1H -indole-6-carboxamidine (DAPI) in blue in the chromatin in the mitotic spindle. Difference in apparent size due to orientation of oocyte altering location of chromatin in z-space **b** frequencies of oocytes that show presence of VPRBP directly upon the chromatin and **c** relative fluorescence levels for whole oocyte, cytoplasm and mitotic spindle area fluorescence from CD (n=19) or HFD (n=22) oocytes from n=3 CD and n=3 HFD females expressed as mean ± standard error of the mean (SEM). * P<0.05

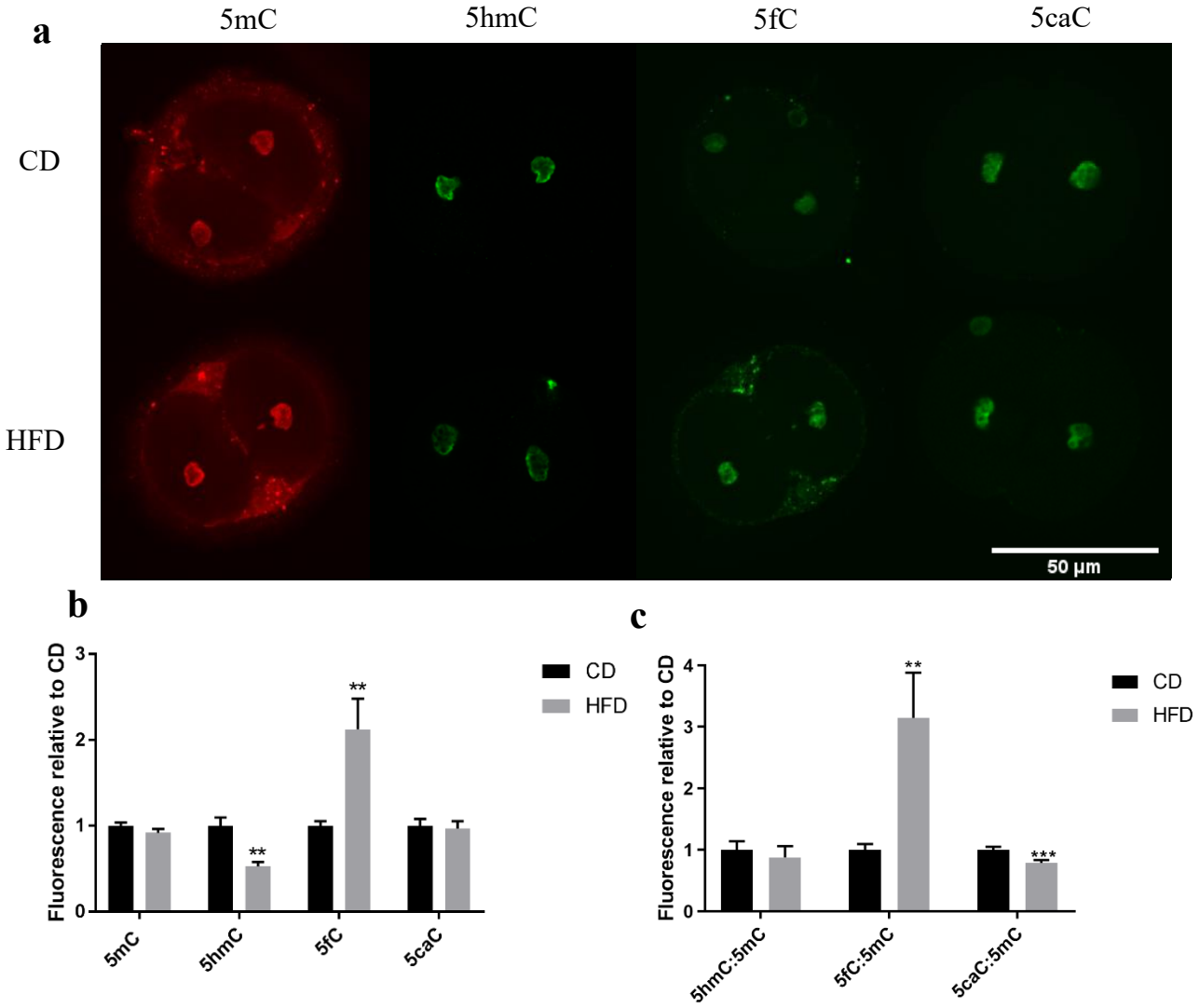

Figure 2.5 Immunocytochemistry on early 2-cell embryos for DNA methylation marks **a** representative images of 5-methylcytosine (5mC) 5-hydroxymethylcytosine (5hmC) 5-formylcytosine (5fC) and 5-carboxycytosine (5caC) in control diet (CD) and high fat diet (HFD) early 2-cells **b** Effect of maternal HFD on 5mC (n=54 CD, n=55 HFD from n=18 CD and n=7 HFD females) 5hmC (n=14 CD, n=15 HFD from n=4 CD and n=6 HFD females) 5fC(n=17 CD, n=20 HFD from n=11 CD and n=4 HFD females) and 5caC (n=22 CD, n=20 HFD from n=11 CD and n=4 HFD females) levels expressed as levels relative to CD in 2-cell embryos, and **c** the demethylation of 5mC to 5hmC 5fC and 5caC as a percentage of 5mC in the 2-cell embryo. Data expressed as fluorescence relative to CD ± standard error of the mean (SEM), * P<0.05, ** P<0.01, *** P<0.001

2.9 Supplementary Tables

Table S2.1 Composition of diet feeds

Ingredients	Control Diet (CD) SF04-04-57	High fat Diet (HFD) SF00-219 (Harlan Teklad TD88137 Equivalent)
Sucrose (%)	34.1	34.1
Casein acid (%)	19.5	19.5
Canola oil (%)	6.0	-
Clarified butter (%)	-	21.0
Cellulose (%)	5.0	5.0
Wheat starch (%)	30.5	15.5
Vitamins/Minerals (%)	4.9	4.9
Digestible Total Energy (kJ/g)	16.1	19.4
Digestible energy from Lipids (%)	21.0	40.0
Digestible energy from Protein (%)	14.0	17.0
Digestible energy from Carbohydrates (%)	65.0	43.0

Table S2.2 Table of antibodies used in this study

Protein name	Manufacturer	Catalogue Number)	Working Dilution	Antibody ID	Antibody Name	Reference
TET3	Abcam	ab174862	1:100	AB_2811266	Anti-TET3 antibody [clone 2B7] N terminal	Clone 2B7 (Weng et al., 2017)
VPRBP	Proteintech	11612-1-AP	1:100	AB_2216933	VPRBP antibody	(Nakagawa et al., 2015a, Yu et al., 2013b)
5mC	Active Motif	39649	1:100	AB_2687950	5-mC antibody (mAb), clone 33D3	(Zhai et al., 2018), Clone 33D3 (Amouroux et al., 2016, Han et al., 2018, Li and O'Neill, 2013, Li et al., 2016, Nakagawa et al., 2015a)
5hmC	Active Motif	39769	1:500	AB_10013602	5-hydroxymethylcytosine (5hmC) antibody (pAb)	(Han et al., 2018) (embryo)
5fC	Active Motif	61223	1:200	AB_2687953	5-formylcytosine (5fC) antibody (pAb)	(Nettersheim et al., 2013) (germ cells)
5caC	Active Motif	61225	1:200	AB_2793557	5-carboxylcytosine (5caC) antibody (pAb)	(Nettersheim et al., 2013) (germ cells)

Table S2.3 The effect of maternal high fat diet of six weeks in duration on mouse bodyweight, fat and organ mass, and blood serum metabolites. Data expressed as mean ± standard error of the mean SEM

Parameter	CD (g)	HFD (g)	P	CD (%)	HFD (%)	P
n	175	158				
Bodyweight at week 6	21.19±0.15	22.40±0.17	≤0.0001			
Fat Deposits						
Sum of Total Fat (g)	0.758±0.025	1.345±0.002	≤0.0001	3.424±0.096	5.425±0.183	≤0.0001
Gonadal Fat (g)	0.312±0.013	0.623±0.032	≤0.0001	1.401±0.052	2.516±0.104	≤0.0001
Peri-renal fat (g)	0.034±0.002	0.054±0.006	≤0.0001	0.158±0.007	0.221±0.023	≤0.0001
Retroperitoneal Fat (g)	0.047±0.003	0.105±0.006	≤0.0001	0.209±0.010	0.424±0.021	≤0.0001
Omental Fat (g)	0.177±0.006	0.243±0.010	≤0.0001	0.804±0.021	1.003±0.031	≤0.0001
Dorsal Fat (g)	0.188±0.006	0.301±0.011	≤0.0001	0.853±0.022	1.248±0.038	≤0.0001
Tissue Weights						
Vastus Lateralis (g)	0.107±0.003	0.121±0.010	NS	0.522±0.015	0.534±0.044	NS
Soleus (g)	0.0067±0.0005	0.0070±0.0002	NS	0.0322±0.0020	0.0309±0.0012	NS
Kidneys (g)	0.265±0.002	0.265±0.005	NS	1.225±0.012	1.011±0.033	≤0.0001
Liver (g)	1.193±0.020	1.21±0.021	NS	5.493±0.077	5.133±0.071	≤0.005
Pancreas (g)	0.108±0.008	0.098±0.002	NS	0.499±0.036	0.416±0.008	≤0.05
Blood Metabolites						
Triglyceride (mM)	0.279±0.012	0.238±0.016	NS			
Non-esterified Fatty Acids (NEFA) (mM)	0.486±0.036	0.443±0.030	≤0.05			
High Density Lipoprotein (HDL) (mM)	0.848±0.044	1.152±0.013	≤0.001			
Glucose (mM)	3.640±0.266	4.04±0.304	NS			
Insulin (ng/mL)	0.22±0.05	0.27±0.12	NS			
Leptin (ng/mL)	0.40±0.07	2.61±0.27	≤0.001			
Cholesterol (mM)	1.010±0.038	1.248±0.015	≤0.005			

CD= control diet, HFD= high fat diet

2.10 Supplementary Figures

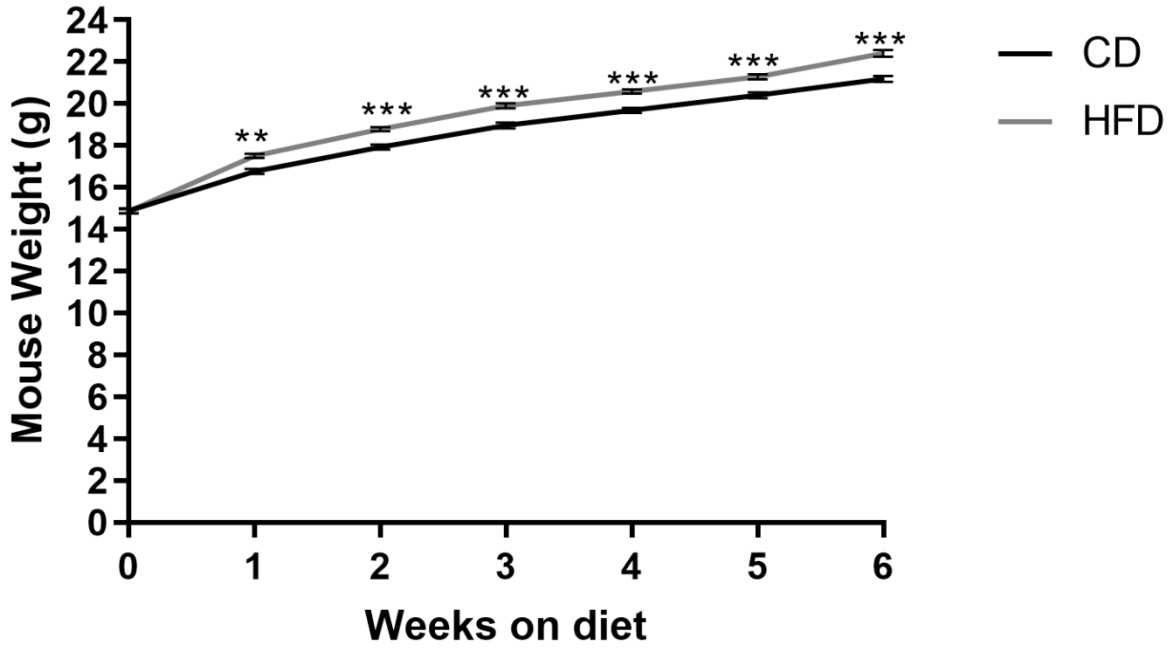

Figure S2.1 The effect of maternal high fat diet of six weeks in duration on mouse total body weight. Control diet (CD) n=175, high fat diet (HFD) n=158, data expressed as mean ± standard error of the mean (SEM), ** P<0.01 *** P<0.001

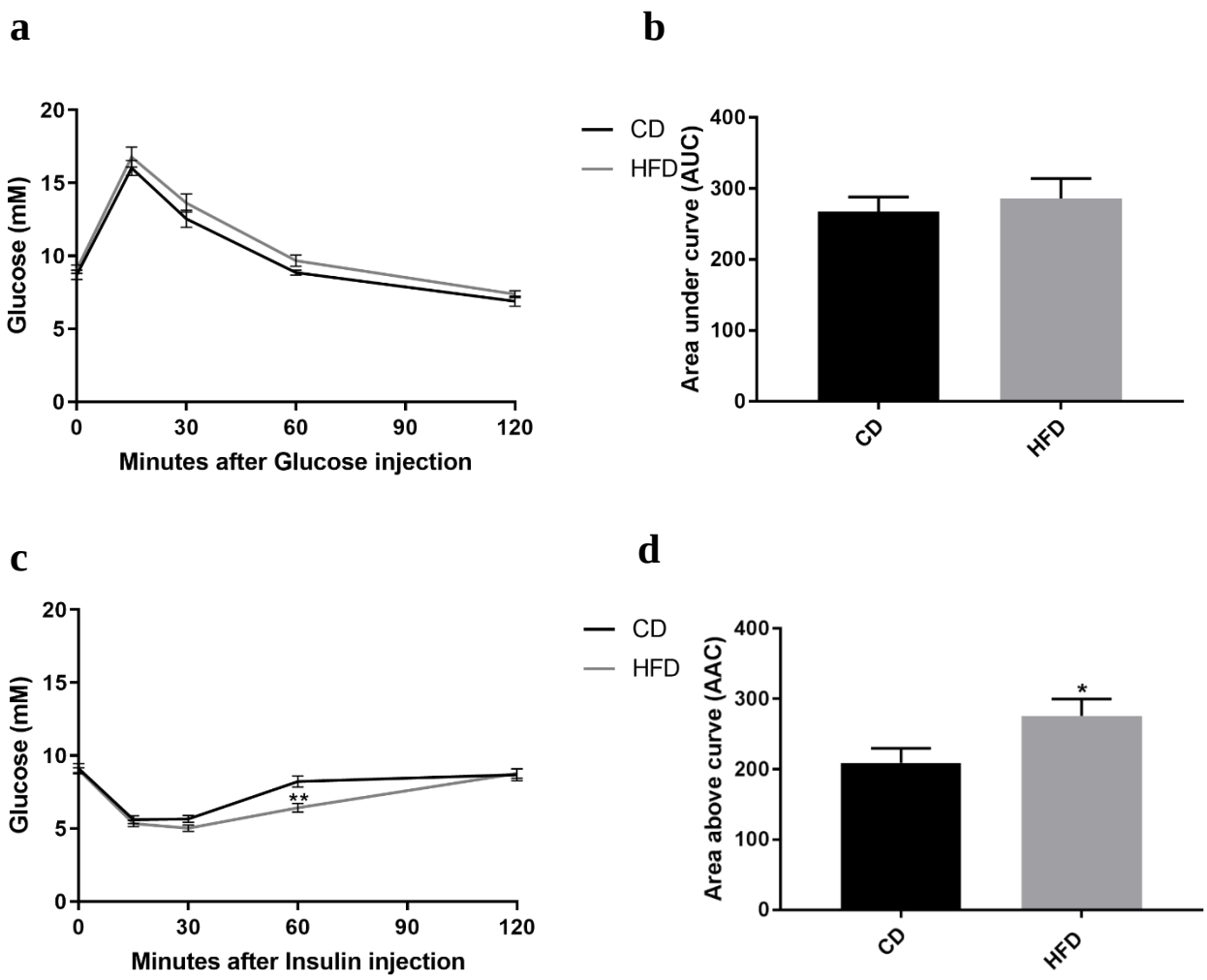

Figure S2.2 Effect of a maternal high fat diet (HFD) on glucose and insulin tolerance on mothers **a-b** glucose tolerance test from control diet (CD) (n=10) and HFD (n=10) female mice. **a** Blood glucose levels measured at 15 min, 30 min, 60 min, and 120min post glucose bolus **b** glucose sensitivity as area under the curve for the glucose tolerance test **c-d** insulin tolerance test from CD (n=10) and HFD (n=10) female mice **c** Blood glucose levels measured at 15min 30min 60min and 120min post insulin bolus and **d** insulin tolerance measured by above the curve (AAC) for the insulin tolerance test. Data represents mean ± standard error of the mean (SEM) * $P<0.05$, ** $P<0.01$

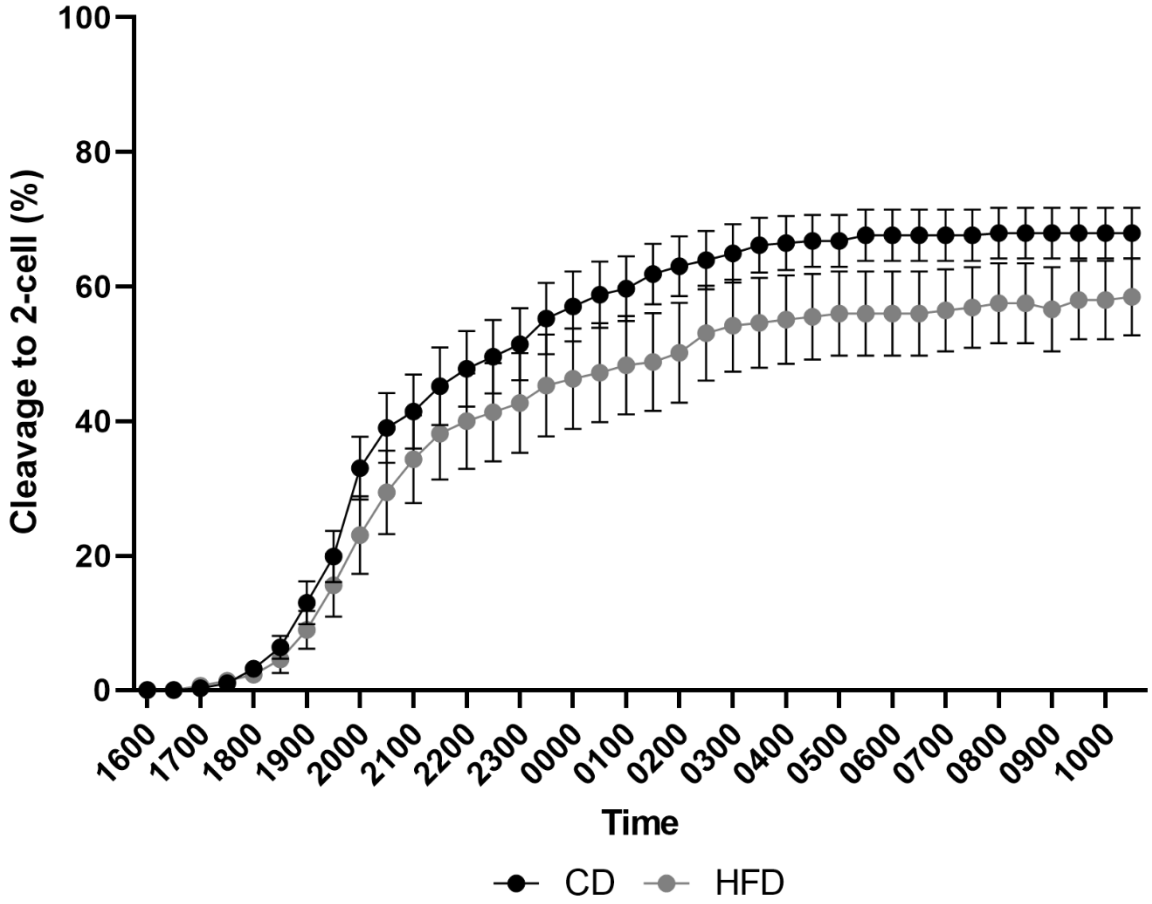

Figure S2.3 Effect of a maternal high fat diet (HFD) on cleavage times (time of day) to the 2-cell stage. Data from n=54 control diet (CD), n=55 HFD embryos cultured in n=34 CD and n=22 HFD culture wells, from n=18 CD and n=7 HFD females. Data represents mean ± standard error of the mean (SEM)

2.11 References

ABS 2011-2012. Australian Health Survey: First Results, Canberra, Australian Capital Territory , Canberra, Australian Capital Territory. http://www.abs.gov.au/ausstats/abs@.nsf/Lookup/by%20Subject/4338.0~2011-13~Main%20Features~Overweight%20and%20obesity~10007. Accessed 22 July 2019 7 /06/2013. Report No.: 4338.

AMOUROUX, R., NASHUN, B., SHIRANE, K., NAKAGAWA, S., HILL, P. W. S., D'SOUZA, Z., NAKAYAMA, M., MATSUDA, M., TURP, A., NDJETEHE, E., ENCHEVA, V., KUDO, N. R., KOSEKI, H., SASAKI, H. & HAJKOVA, P. 2016. De novo DNA methylation drives 5hmC accumulation in mouse zygotes. *Nature Cell Biology,* 18**,** 225-233.

ASHINO, N. G., SAITO, K. N., SOUZA, F. D., NAKUTZ, F. S., ROMAN, E. A., VELLOSO, L. A., TORSONI, A. S. & TORSONI, M. A. 2012. Maternal high-fat feeding through pregnancy and lactation predisposes mouse offspring to molecular insulin resistance and fatty liver. *The Journal of Nutritional Biochemistry,* 23**,** 341-348.

BAGCI, H. & FISHER, AMANDA G. 2013. DNA Demethylation in Pluripotency and Reprogramming: The Role of Tet Proteins and Cell Division. *Cell Stem Cell,* 13**,** 265-269.

BAVISTER, B. D. 1995. Culture of preimplantation embryos: facts and artifacts. *Human Reproduction Update,* 1**,** 91-148.

BONEY, C. M., VERMA, A., TUCKER, R. & VOHR, B. R. 2005. Metabolic syndrome in childhood: association with birth weight, maternal obesity, and gestational diabetes mellitus. *Pediatrics,* 115**,** e290-e296.

BOOTS, C. E., BOUDOURES, A., ZHANG, W., DRURY, A. & MOLEY, K. H. 2016. Obesity-induced oocyte mitochondrial defects are partially prevented and rescued by supplementation with co-enzyme Q10 in a mouse model. *Human Reproduction,* 31**,** 2090-2097.

BOUDOURES, A. L., SABEN, J., DRURY, A., SCHEAFFER, S., MODI, Z., ZHANG, W. & MOLEY, K. H. 2017. Obesity-exposed oocytes accumulate and transmit damaged mitochondria due to an inability to activate mitophagy. *Developmental Biology,* 426**,** 126-138.

BRADLEY-WHITMAN, M. A. & LOVELL, M. A. 2013. Epigenetic changes in the progression of Alzheimer's disease. *Mechanisms of Ageing and Development,* 134**,** 486-495.

BRISON, D. R. & LEESE, H. J. 1994. Blastocoel cavity formation by preimplantation rat embryos in the presence of cyanide and other inhibitors of oxidative phosphorylation. *Journal of Reproduction and Fertility,* 101**,** 305-309.

BROWN, H., TAN, T. & THOMPSON, J. 2015. Metaboloepigenetics: providing alternate hypotheses for regulation of gene expression in the early embryo. *Animal Reproduction,* 12**,** 437-443.

CAO, Z., ZHANG, M., XU, T., CHEN, Z., TONG, X., ZHANG, D., WANG, Y., ZHANG, L., GAO, D., LUO, L., KHAN, I. M. & ZHANG, Y. 2019. Vitrification of murine mature metaphase II oocytes perturbs DNA methylation reprogramming during preimplantation embryo development. *Cryobiology,* 87**,** 91-98.

CARDOZO, E. R., KARMON, A. E., GOLD, J., PETROZZA, J. C. & STYER, A. K. 2016. Reproductive outcomes in oocyte donation cycles are associated with donor BMI. *Human Reproduction,* 31**,** 385-392.

CAREY, B. W., FINLEY, L. W. S., CROSS, J. R., ALLIS, C. D. & THOMPSON, C. B. 2015. Intracellular [agr]-ketoglutarate maintains the pluripotency of embryonic stem cells. *Nature,* 518**,** 413-416.

CHRYSANTHOU, S., SENNER, C. E., WOODS, L., FINEBERG, E., OKKENHAUG, H., BURGE, S., PEREZ-GARCIA, V. & HEMBERGER, M. 2018. A Critical Role of TET1/2 Proteins in Cell-Cycle Progression of Trophoblast Stem Cells. *Stem Cell Reports,* 10**,** 1355-1368.

CONAGHAN, J., HARDY, K., HANDYSIDE, A. H., WINSTON, R. M. L. & LEESE, H. J. 1993. Selection criteria for human embryo transfer: A comparison of pyruvate uptake and morphology. *Journal of Assisted Reproduction and Genetics,* 10**,** 21-30.

COPPIETERS, N., DIERIKS, B. V., LILL, C., FAULL, R. L. M., CURTIS, M. A. & DRAGUNOW, M. 2014. Global changes in DNA methylation and hydroxymethylation in Alzheimer's disease human brain. *Neurobiology of Aging,* 35**,** 1334-1344.

ECKERSLEY-MASLIN, M. A., ALDA-CATALINAS, C. & REIK, W. 2018. Dynamics of the epigenetic landscape during the maternal-to-zygotic transition. *Nature Reviews Molecular Cell Biology,* 19**,** 436-450.

FIGUEROA, M. E., ABDEL-WAHAB, O., LU, C., WARD, P. S., PATEL, J., SHIH, A., LI, Y., BHAGWAT, N., VASANTHAKUMAR, A., FERNANDEZ, H. F., TALLMAN, M. S., SUN, Z., WOLNIAK, K., PEETERS, J. K., LIU, W., CHOE, S. E., FANTIN, V. R., PAIETTA, E., LÖWENBERG, B., LICHT, J. D., GODLEY, L. A., DELWEL, R., VALK, P. J. M., THOMPSON, C. B., LEVINE, R. L. & MELNICK, A. 2010. Leukemic IDH1 and IDH2 mutations result in a hypermethylation phenotype, disrupt TET2 function, and impair hematopoietic differentiation. *Cancer Cell,* 18**,** 553-567.

FULLSTON, T., MITCHELL, M., WAKEFIELD, S. & LANE, M. 2011. Mitochondrial inhibition during preimplantation embryogenesis shifts the transcriptional profile of fetal mouse brain. *Reproduction, Fertility and Development,* 23**,** 691-701.

GAO, W., YU, X., HAO, J., WANG, L., QI, M., HAN, L., LIN, C. & WANG, D. 2019. Ascorbic acid improves parthenogenetic embryo development through TET proteins in mice. *Bioscience Reports,* 39**,** BSR20181730.

GARDNER, D. K. & LEESE, H. J. 1986. Non-invasive measurement of nutrient uptake by single cultured pre-implantation mouse embryos. *Human Reproduction,* 1**,** 25-27.

GE, Z.-J., LUO, S.-M., LIN, F., LIANG, Q.-X., HUANG, L., WEI, Y.-C., HOU, Y., HAN, Z.-M., SCHATTEN, H. & SUN, Q.-Y. 2014. DNA Methylation in Oocytes and Liver of

Female Mice and Their Offspring: Effects of High-Fat-Diet–Induced Obesity. *Environmental Health Perspectives,* 122**,** 159-164.

GREEN, M. P., HARVEY, A. J., SPATE, L. D., KIMURA, K., THOMPSON, J. G. & ROBERTS, R. M. 2016. The effects of 2,4-dinitrophenol and d-glucose concentration on the development, sex ratio, and interferon-tau (IFNT) production of bovine blastocysts. *Molecular Reproduction and Development,* 83**,** 50-60.

GU, T.-P., GUO, F., YANG, H., WU, H.-P., XU, G.-F., LIU, W., XIE, Z.-G., SHI, L., HE, X., JIN, S.-G., IQBAL, K., SHI, Y. G., DENG, Z., SZABO, P. E., PFEIFER, G. P., LI, J. & XU, G.-L. 2011. The role of Tet3 DNA dioxygenase in epigenetic reprogramming by oocytes. *Nature,* 477**,** 606-610.

GUO, F., LI, X., LIANG, D., LI, T., ZHU, P., GUO, H., WU, X., WEN, L., GU, T.-P., HU, B., WALSH, COLUM P., LI, J., TANG, F. & XU, G.-L. 2014. Active and Passive Demethylation of Male and Female Pronuclear DNA in the Mammalian Zygote. *Cell Stem Cell,* 15**,** 447-458.

HAN, L., REN, C., LI, L., LI, X., GE, J., WANG, H., MIAO, Y.-L., GUO, X., MOLEY, K. H., SHU, W. & WANG, Q. 2018. Embryonic defects induced by maternal obesity in mice derive from Stella insufficiency in oocytes. *Nature Genetics,* 50**,** 432-442.

HEWITSON, L. C., MARTIN, K. L. & LEESE, H. J. 1996. Effects of metabolic inhibitors on mouse preimplantation embryo development and the energy metabolism of isolated inner cell masses. *Molecular Reproduction and Development,* 43**,** 323-330.

HOUGHTON, F. D., THOMPSON, J. G., KENNEDY, C. J. & LEESE, H. J. 1996. Oxygen consumption and energy metabolism of the early mouse embryo. *Molecular Reproduction and Development,* 44**,** 476-485.

IGOSHEVA, N., ABRAMOV, A. Y., POSTON, L., ECKERT, J. J., FLEMING, T. P., DUCHEN, M. R. & MCCONNELL, J. 2010. Maternal Diet-Induced Obesity Alters Mitochondrial Activity and Redox Status in Mouse Oocytes and Zygotes. *PLOS ONE,* 5**,** e10074.

INOUE, A., MATOBA, S. & ZHANG, Y. 2012. Transcriptional activation of transposable elements in mouse zygotes is independent of Tet3-mediated 5-methylcytosine oxidation. *Cell Research,* 22**,** 1640-1649.

INOUE, A., SHEN, L., DAI, Q., HE, C. & ZHANG, Y. 2011. Generation and replication-dependent dilution of 5fC and 5caC during mouse preimplantation development. *Cell Research,* 21**,** 1670-1676.

INOUE, A., SHEN, L., MATOBA, S. & ZHANG, Y. 2015. Haploinsufficiency, but Not Defective Paternal 5mC Oxidation, Accounts for the Developmental Defects of Maternal Tet3 Knockouts. *Cell Reports,* 10**,** 463-470.

IQBAL, K., JIN, S.-G., PFEIFER, G. P. & SZABÓ, P. E. 2011. Reprogramming of the paternal genome upon fertilization involves genome-wide oxidation of 5-methylcytosine. *Proceedings of the National Academy of Sciences of the United States of America,* 108**,** 3642-3647.

ITO, S., D'ALESSIO, A. C., TARANOVA, O. V., HONG, K., SOWERS, L. C. & ZHANG, Y. 2010. Role of Tet proteins in 5mC to 5hmC conversion, ES cell self-renewal, and ICM specification. *Nature,* 466**,** 1129-1133.

ITO, S., SHEN, L., DAI, Q., WU, S. C., COLLINS, L. B., SWENBERG, J. A., HE, C. & ZHANG, Y. 2011. Tet proteins can convert 5-methylcytosine to 5-formylcytosine and 5-carboxylcytosine. *Science,* 333**,** 1300-1303.

JEONG, J.-K., KANG, M.-H., GURUNATHAN, S., CHO, S.-G., PARK, C., SEO, H. G. & KIM, J.-H. 2014. Evaluation of reference genes in mouse preimplantation embryos for gene expression studies using real-time quantitative RT-PCR (RT-qPCR). *BMC Research Notes,* 7**,** 675.

JUNGHEIM, E. S., SCHOELLER, E. L., MARQUARD, K. L., LOUDEN, E. D., SCHAFFER, J. E. & MOLEY, K. H. 2010. Diet-Induced Obesity Model: Abnormal Oocytes and Persistent Growth Abnormalities in the Offspring. *Endocrinology,* 151**,** 4039-4046.

KANG, E., WU, G., MA, H., LI, Y., TIPPNER-HEDGES, R., TACHIBANA, M., SPARMAN, M., WOLF, D. P., SCHOLER, H. R. & MITALIPOV, S. 2014. Nuclear reprogramming by interphase cytoplasm of two-cell mouse embryos. *Nature,* 509**,** 101-104.

KUROTAKI, Y. K., HATANAKA, Y., KAMIMURA, S., OIKAWA, M., INOUE, H., OGONUKI, N., INOUE, K. & OGURA, A. 2015. Impaired active DNA demethylation in zygotes generated by round spermatid injection. *Human Reproduction,* 30**,** 1178-1187.

LANE, M. & GARDNER, D. K. 1998. Amino acids and vitamins prevent culture-induced metabolic perturbations and associated loss of viability of mouse blastocysts. *Human Reproduction,* 13**,** 991-997.

LANE, M. & GARDNER, D. K. 2000. Lactate Regulates Pyruvate Uptake and Metabolism in the PreimplantationMouse Embryo. *Biology of Reproduction,* 62**,** 16-22.

LANE, M. & GARDNER, D. K. 2005. Mitochondrial Malate-Aspartate Shuttle Regulates Mouse Embryo Nutrient Consumption. *Journal of Biological Chemistry,* 280**,** 18361-18367.

LANE, M., MCPHERSON, N. O., FULLSTON, T., SPILLANE, M., SANDEMAN, L., KANG, W. X. & ZANDER-FOX, D. L. 2014a. Oxidative Stress in Mouse Sperm Impairs Embryo Development, Fetal Growth and Alters Adiposity and Glucose Regulation in Female Offspring. *PLOS ONE,* 9**,** e100832.

LANE, M., ROBKER, R. L. & ROBERTSON, S. A. 2014b. Parenting from before conception. *Science,* 345**,** 756-760.

LEESE, H. J. & BARTON, A. M. 1984. Pyruvate and glucose uptake by mouse ova and preimplantation embryos. *Journal of Reproduction and Fertility,* 72**,** 9-13.

LEESE, H. J. & BARTON, A. M. 1985. Production of pyruvate by isolated mouse cumulus cells. *Journal of Experimental Zoology,* 234**,** 231-236.

LI, Y. & O'NEILL, C. 2012. Persistence of Cytosine Methylation of DNA following Fertilisation in the Mouse. *PLOS ONE,* 7**,** e30687.

LI, Y. & O'NEILL, C. 2013. 5′-methylcytosine and 5′-hydroxymethylcytosine Each Provide Epigenetic Information to the Mouse Zygote. *PLoS ONE,* 8**,** e63689.

LI, Y., SEAH, M. K. Y. & O'NEILL, C. 2016. Mapping global changes in nuclear cytosine base modifications in the early mouse embryo. *Reproduction (Cambridge, England),* 151**,** 83-95.

LOENARZ, C. & SCHOFIELD, C. J. 2008. Expanding chemical biology of 2-oxoglutarate oxygenases. *Nature Chemical Biology,* 4**,** 152.

LUZZO, K. M., WANG, Q., PURCELL, S. H., CHI, M., JIMENEZ, P. T., GRINDLER, N., SCHEDL, T. & MOLEY, K. H. 2012. High Fat Diet Induced Developmental Defects in the Mouse: Oocyte Meiotic Aneuploidy and Fetal Growth Retardation/Brain Defects. *PLoS ONE,* 7**,** e49217.

MAUS, A. & PETERS, G. J. 2017. Glutamate and α-ketoglutarate: key players in glioma metabolism. *Amino Acids,* 49**,** 21-32.

MCPHERSON, N. O., BELL, V. G., ZANDER-FOX, D. L., FULLSTON, T., WU, L. L., ROBKER, R. L. & LANE, M. 2015. When two obese parents are worse than one! Impacts on embryo and fetal development. *American Journal of Physiology - Endocrinology and Metabolism,* 309**,** E568-E581.

MCPHERSON, N. O., ZANDER-FOX, D. & LANE, M. 2014. Stimulation of mitochondrial embryo metabolism by dichloroacetic acid in an aged mouse model improves embryo development and viability. *Fertility and Sterility,* 101**,** 1458-1466.e5.

MITCHELL, M., CASHMAN, K. S., GARDNER, D. K., THOMPSON, J. G. & LANE, M. 2009a. Disruption of Mitochondrial Malate-Aspartate Shuttle Activity in Mouse Blastocysts Impairs Viability and Fetal Growth. *Biology of Reproduction,* 80**,** 295-301.

MITCHELL, M., SCHULZ, S. L., ARMSTRONG, D. T. & LANE, M. 2009b. Metabolic and Mitochondrial Dysfunction in Early Mouse Embryos Following Maternal Dietary Protein Intervention. *Biology of Reproduction,* 80**,** 622-630.

MUSIAL, B., VAUGHAN, O. R., FERNANDEZ-TWINN, D. S., VOSHOL, P., OZANNE, S. E., FOWDEN, A. L. & SFERRUZZI-PERRI, A. N. 2017. A Western-style obesogenic diet alters maternal metabolic physiology with consequences for fetal nutrient acquisition in mice. *The Journal of Physiology,* 595**,** 4875-4892.

NAKAGAWA, T., LV, L., NAKAGAWA, M., YU, Y., YU, C., D'ALESSIO, ANA C., NAKAYAMA, K., FAN, H.-Y., CHEN, X. & XIONG, Y. 2015a. CRL4VprBP E3 Ligase Promotes Monoubiquitylation and Chromatin Binding of TET Dioxygenases. *Molecular Cell,* 57**,** 247-260.

NAKAGAWA, T., LV, L., NAKAGAWA, M., YU, Y., YU, C., D'ALESSIO, ANA C., NAKAYAMA, K., FAN, H.-Y., CHEN, X. & XIONG, Y. 2015b. CRL4VprBP E3 Ligase Promotes Monoubiquitylation and Chromatin Binding of TET Dioxygenases. *Molecular Cell,* 57**,** 247-260.

NETTERSHEIM, D., HEUKAMP, L. C., FRONHOFFS, F., GREWE, M. J., HAAS, N., WAHA, A., HONECKER, F., WAHA, A., KRISTIANSEN, G. & SCHORLE, H. 2013. Analysis of TET Expression/Activity and 5mC Oxidation during Normal and Malignant Germ Cell Development. *PLOS ONE,* 8**,** e82881.

NG, M., FLEMING, T., ROBINSON, M., THOMSON, B., GRAETZ, N., MARGONO, C., MULLANY, E. C., BIRYUKOV, S., ABBAFATI, C., ABERA, S. F., ABRAHAM, J. P., ABU-RMEILEH, N. M. E., ACHOKI, T., ALBUHAIRAN, F. S., ALEMU, Z. A., ALFONSO, R., ALI, M. K., ALI, R., GUZMAN, N. A., AMMAR, W., ANWARI, P., BANERJEE, A., BARQUERA, S., BASU, S., BENNETT, D. A., BHUTTA, Z., BLORE, J., CABRAL, N., NONATO, I. C., CHANG, J.-C., CHOWDHURY, R., COURVILLE, K. J., CRIQUI, M. H., CUNDIFF, D. K., DABHADKAR, K. C., DANDONA, L., DAVIS, A., DAYAMA, A., DHARMARATNE, S. D., DING, E. L., DURRANI, A. M., ESTEGHAMATI, A., FARZADFAR, F., FAY, D. F. J., FEIGIN, V. L., FLAXMAN, A., FOROUZANFAR, M. H., GOTO, A., GREEN, M. A., GUPTA, R., HAFEZI-NEJAD, N., HANKEY, G. J., HAREWOOD, H. C., HAVMOELLER, R.,

HAY, S., HERNANDEZ, L., HUSSEINI, A., IDRISOV, B. T., IKEDA, N., ISLAMI, F., JAHANGIR, E., JASSAL, S. K., JEE, S. H., JEFFREYS, M., JONAS, J. B., KABAGAMBE, E. K., KHALIFA, S. E. A. H., KENGNE, A. P., KHADER, Y. S., KHANG, Y.-H., KIM, D., KIMOKOTI, R. W., KINGE, J. M., KOKUBO, Y., KOSEN, S., KWAN, G., LAI, T., LEINSALU, M., LI, Y., LIANG, X., LIU, S., LOGROSCINO, G., LOTUFO, P. A., LU, Y., MA, J., MAINOO, N. K., MENSAH, G. A., MERRIMAN, T. R., MOKDAD, A. H., MOSCHANDREAS, J., NAGHAVI, M., NAHEED, A., NAND, D., NARAYAN, K. M. V., NELSON, E. L., NEUHOUSER, M. L., NISAR, M. I., OHKUBO, T., OTI, S. O., PEDROZA, A., et al. 2014. Global, regional, and national prevalence of overweight and obesity in children and adults during 1980–2013: a systematic analysis for the Global Burden of Disease Study 2013. *The Lancet,* 384**,** 766-781.

NILSEN, L. H., WITTER, M. P. & SONNEWALD, U. 2014. Neuronal and astrocytic metabolism in a transgenic rat model of Alzheimer's disease. *Journal of Cerebral Blood Flow & Metabolism,* 34**,** 906-914.

PICTON, H., BRIGGS, D. & GOSDEN, R. 1998. The molecular basis of oocyte growth and development. *Molecular and Cellular Endocrinology,* 145**,** 27-37.

RATCHFORD, A. M., ESGUERRA, C. R. & MOLEY, K. H. 2008. Decreased oocyte-granulosa cell gap junction communication and connexin expression in a type 1 diabetic mouse model. *Molecular endocrinology (Baltimore, Md.),* 22**,** 2643-2654.

REYNOLDS, K. A., BOUDOURES, A. L., CHI, M. M.-Y., WANG, Q. & MOLEY, K. H. 2015. Adverse effects of obesity and/or high-fat diet on oocyte quality and metabolism are not reversible with resumption of regular diet in mice. *Reproduction, Fertility and Development,* 27**,** 716-724.

ROBERT, C., MCGRAW, S., MASSICOTTE, L., PRAVETONI, M., GANDOLFI, F. & SIRARD, M.-A. 2002. Quantification of Housekeeping Transcript Levels During the

Development of Bovine Preimplantation Embryos. *Biology of Reproduction,* 67**,** 1465-1472.

SALMINEN, A., HAAPASALO, A., KAUPPINEN, A., KAARNIRANTA, K., SOININEN, H. & HILTUNEN, M. 2015. Impaired mitochondrial energy metabolism in Alzheimer's disease: Impact on pathogenesis via disturbed epigenetic regulation of chromatin landscape. *Progress in Neurobiology,* 131**,** 1-20.

SAMUELSSON, A.-M., MATTHEWS, P. A., ARGENTON, M., CHRISTIE, M. R., MCCONNELL, J. M., JANSEN, E. H. J. M., PIERSMA, A. H., OZANNE, S. E., TWINN, D. F., REMACLE, C., ROWLERSON, A., POSTON, L. & TAYLOR, P. D. 2008. Diet-Induced Obesity in Female Mice Leads to Offspring Hyperphagia, Adiposity, Hypertension, and Insulin Resistance: A Novel Murine Model of Developmental Programming. *Hypertension,* 51**,** 383-392.

SANTOS, F., PETERS, A. H., OTTE, A. P., REIK, W. & DEAN, W. 2005. Dynamic chromatin modifications characterise the first cell cycle in mouse embryos. *Developmental Biology,* 280**,** 225-236.

SASSON, I., VITINS, A., MAINIGI, M., MOLEY, K. & SIMMONS, R. 2015. Pre-gestational vs gestational exposure to maternal obesity differentially programs the offspring in mice. *Diabetologia,* 58**,** 615-624.

SCHABLA, N. M., MONDAL, K. & SWANSON, P. C. 2018. DCAF1 (VprBP): emerging physiological roles for a unique dual-service E3 ubiquitin ligase substrate receptor. *Journal of Molecular Cell Biology*.

SCHINDELIN, J., ARGANDA-CARRERAS, I., FRISE, E., KAYNIG, V., LONGAIR, M., PIETZSCH, T., PREIBISCH, S., RUEDEN, C., SAALFELD, S. & SCHMID, B. 2012. Fiji: an open-source platform for biological-image analysis. *Nature Methods,* 9**,** 676.

SHEN, L., INOUE, A., HE, J., LIU, Y., LU, F. & ZHANG, Y. 2014. Tet3 and DNA Replication Mediate Demethylation of Both the Maternal and Paternal Genomes in Mouse Zygotes. *Cell Stem Cell,* 15**,** 459-470.

TSUKADA, Y.-I., AKIYAMA, T. & NAKAYAMA, K. I. 2015. Maternal TET3 is dispensable for embryonic development but is required for neonatal growth. *Scientific Reports,* 5**,** 15876.

TURNER, K., MARTIN, K. L., WOODWARD, B. J., LENTON, E. A. & LEESE, H. J. 1994. Fertilization and early embryology: Comparison of pyruvate uptake by embryos derived from conception and non-conception natural cycles. *Human Reproduction,* 9**,** 2362-2366.

TZIKA, E., DREKER, T. & IMHOF, A. 2018. Epigenetics and Metabolism in Health and Disease. *Frontiers in Genetics,* 9**,** 361-361.

WAKEFIELD, S. L., LANE, M. & MITCHELL, M. 2011. Impaired Mitochondrial Function in the Preimplantation Embryo Perturbs Fetal and Placental Development in the Mouse. *Biology of Reproduction,* 84**,** 572-580.

WAKEFIELD, S. L., LANE, M., SCHULZ, S. J., HEBART, M. L., THOMPSON, J. G. & MITCHELL, M. 2008. Maternal supply of omega-3 polyunsaturated fatty acids alter mechanisms involved in oocyte and early embryo development in the mouse. *American Journal of Physiology - Endocrinology And Metabolism,* 294**,** E425-E434.

WANG, Q., CHI, M. M. & MOLEY, K. H. 2012. Live Imaging Reveals the Link Between Decreased Glucose Uptake in Ovarian Cumulus Cells and Impaired Oocyte Quality in Female Diabetic Mice. *Endocrinology,* 153**,** 1984-1989.

WANG, Q., FROLOVA, A. I., PURCELL, S., ADASTRA, K., SCHOELLER, E., CHI, M. M., SCHEDL, T. & MOLEY, K. H. 2010. Mitochondrial dysfunction and apoptosis in cumulus cells of type I diabetic mice. *PLOS ONE,* 5**,** e15901-e15901.

WENG, Y.-L., AN, R., CASSIN, J., JOSEPH, J., MI, R., WANG, C., ZHONG, C., JIN, S.-G., PFEIFER, G. P., BELLACOSA, A., DONG, X., HOKE, A., HE, Z., SONG, H. & MING, G.-L. 2017. An Intrinsic Epigenetic Barrier for Functional Axon Regeneration. *Neuron,* 94**,** 337-346.e6.

WU, L. L.-Y., DUNNING, K. R., YANG, X., RUSSELL, D. L., LANE, M., NORMAN, R. J. & ROBKER, R. L. 2010. High-Fat Diet Causes Lipotoxicity Responses in Cumulus–Oocyte Complexes and Decreased Fertilization Rates. *Endocrinology,* 151**,** 5438-5445.

WU, L. L., RUSSELL, D. L., WONG, S. L., CHEN, M., TSAI, T.-S., ST JOHN, J. C., NORMAN, R. J., FEBBRAIO, M. A., CARROLL, J. & ROBKER, R. L. 2015a. Mitochondrial dysfunction in oocytes of obese mothers: transmission to offspring and reversal by pharmacological endoplasmic reticulum stress inhibitors. *Development,* 142**,** 681-691.

WU, Y., ZHANG, Z., LIAO, X. & WANG, Z. 2015b. High fat diet triggers cell cycle arrest and excessive apoptosis of granulosa cells during the follicular development. *Biochemical and Biophysical Research Communications,* 466**,** 599-605.

XU, W., YANG, H., LIU, Y., YANG, Y., WANG, P., KIM, S.-H., ITO, S., YANG, C., WANG, P., XIAO, M.-T., LIU, L.-X., JIANG, W.-Q., LIU, J., ZHANG, J.-Y., WANG, B., FRYE, S., ZHANG, Y., XU, Y.-H., LEI, Q.-Y., GUAN, K.-L., ZHAO, S.-M. & XIONG, Y. 2011. Oncometabolite 2-Hydroxyglutarate Is a Competitive Inhibitor of α-Ketoglutarate-Dependent Dioxygenases. *Cancer Cell,* 19**,** 17-30.

YANG, Q., LIANG, X., SUN, X., ZHANG, L., FU, X., ROGERS, C. J., BERIM, A., ZHANG, S., WANG, S., WANG, B., FORETZ, M., VIOLLET, B., GANG, D. R., RODGERS, B. D., ZHU, M.-J. & DU, M. 2016. AMPK/α-Ketoglutarate Axis Dynamically Mediates DNA Demethylation in the Prdm16 Promoter and Brown Adipogenesis. *Cell Metabolism,* 24**,** 542-554.

YU, C., ZHANG, Y.-L., PAN, W.-W., LI, X.-M., WANG, Z.-W., GE, Z.-J., ZHOU, J.-J., CANG, Y., TONG, C., SUN, Q.-Y. & FAN, H.-Y. 2013a. CRL4 Complex Regulates Mammalian Oocyte Survival and Reprogramming by Activation of TET Proteins. *Science,* 342**,** 1518-1521.

YU, C., ZHANG, Y.-L., PAN, W.-W., LI, X.-M., WANG, Z.-W., GE, Z.-J., ZHOU, J.-J., CANG, Y., TONG, C., SUN, Q.-Y. & FAN, H.-Y. 2013b. CRL4 Complex Regulates

Mammalian Oocyte Survival and Reprogramming by Activation of TET Proteins. *Science,* 342**,** 1518-1521.

ZANDER-FOX, D. L., FULLSTON, T., MCPHERSON, N. O., SANDEMAN, L., KANG, W. X., GOOD, S. B., SPILLANE, M. & LANE, M. 2015. Reduction of Mitochondrial Function by FCCP During Mouse Cleavage Stage Embryo Culture Reduces Birth Weight and Impairs the Metabolic Health of Offspring. *Biology of Reproduction,* 92, 1-11.

ZANDER, D. L., THOMPSON, J. G. & LANE, M. 2006. Perturbations in Mouse Embryo Development and Viability Caused by Ammonium Are More Severe after Exposure at the Cleavage Stages. *Biology of Reproduction,* 74**,** 288-294.

ZHAI, Y., ZHANG, Z., YU, H., SU, L., YAO, G., MA, X., LI, Q., AN, X., ZHANG, S. & LI, Z. 2018. Dynamic Methylation Changes of DNA and H3K4 by RG108 Improve Epigenetic Reprogramming of Somatic Cell Nuclear Transfer Embryos in Pigs. *Cellular Physiology and Biochemistry,* 50**,** 1376-1397.

ZHANG, Q., LIU, X., GAO, W., LI, P., HOU, J., LI, J. & WONG, J. 2014. Differential Regulation of the Ten-Eleven Translocation (TET) Family of Dioxygenases by O-Linked β-N-Acetylglucosamine Transferase (OGT). *The Journal of Biological Chemistry,* 289**,** 5986-5996.

ZHANG, Z., HE, C., ZHANG, L., ZHU, T., LV, D., LI, G., SONG, Y., WANG, J., WU, H., JI, P. & LIU, G. 2019. Alpha-ketoglutarate affects murine embryo development through metabolic and epigenetic modulations. *Reproduction,* 158**,** 125-135.

Chapter 3 The effect of altering the availability of a TET protein substrate (alpha ketoglutarate) on DNA methylation in the two-cell mouse embryo and its further development

3.1 Chapter Link

Chapter 2 examined the effects of maternal obesity on TET-mediated changes to DNA methylation form 5mC through to 5caC in the 2-cell embryo, showing that under a maternal HFD there was increased pyruvate uptake oxidation, and progressed DNA demethylation. This occurred with reductions in TET3 and VPRBP at chromatin regions, indicating that this progression was more likely due to metabolic alterations to the substrate α-ketoglutarate, the TCA cycle intermediary that acts as a cofactor for TET causing the increased DNA demethylation. However, as a maternal HFD alters many pathways and systems in the embryo, we sought to focus on one potentially key metabolite, α-ketoglutarate. This was achieved by either increasing α-ketoglutarate or decreasing availability of α-ketoglutarate for TET binding through addition of α-ketoglutarate or the competitive inhibitor 2-hydroxyglutarate. It was then investigated whether the direct modulation of the central metabolite α-ketoglutarate induced changes to DNA methylation similar to that of a maternal HFD model.

3.2 Statement of Authorship

Name of Co-Author	Nicole O McPherson		
Contribution to the Paper	Assisted in interpretation of data, and editing of the manuscript		
Signature	NMcPherson	Date	4/07/2021

Name of Co-Author	Tod Fullston		
Contribution to the Paper	Assisted in interpretation of data, and editing of the manuscript		
Signature		Date	02/07/2021

Name of Co-Author	Michelle Lane (deceased)		
Contribution to the Paper	Experimental design, assisted in interpretation of data, and editing of the manuscript		
Signature		Date	

Please cut and paste additional co-author panels here as required.

3.3 Abstract

Purpose Metabolic based disorders in mothers, including obesity, are linked to poor health outcomes in offspring. This may occur via epigenetic mechanisms that interact with key metabolites. The Ten-Eleven Translocase (TET) proteins demethylate DNA using α-ketoglutarate as a substrate, provide a link between metabolic disruptions caused by maternal obesity and altered demethylation in the embryo.

Methods In this study embryos were collected from CBAF1 mice and cultured in α-ketoglutarate supplemented media (0 mM, 1.4 mM, 3.5 mM or 14.0 mM) or with 2-hydroxyglutarate (0 mM or 20 mM), a competitive inhibitor of alpha ketoglutarate for TET proteins. At the 2-cell G2 phase measurements for DNA methylation of 5-methylcytosine (5mC), 5-hydroxymethylcytiosine (5hmC), 5-formylcytosine (5fC) and 5-carboxylcytosine (5caC) were performed. Embryos were also cultured as above for 96 h to assess blastocyst development and inner cell mass and trophectoderm proliferation differences.

Results Embryos cultured with 1.4 mM α-ketoglutarate had decreased 2-cell 5mC, whilst 14.0 mM α-ketoglutarate increased the 5hmC:5mC ratio. In contrast supplementation with 20 mM 2HG increased 5mC and concomitantly decreased the 5fC:5mC and 5caC:5mC ratios. α-ketoglutarate at concentrations up to 3.5 mM did not alter embryo development or blastocyst cell counts, whilst embryos cultured in 14.0 mM α-ketoglutarate were blocked at the 2-cell stage. Culture with 2HG reduced development past the 4-cell stage and decreased total blastocyst cell and inner cell mass cell count.

Conclusion We have demonstrated that the DNA demethylation that occurs post-fertilisation prior to embryonic genome activation in the preimplantation embryo is sensitive to alterations in TET protein substrate availability, providing a possible link between key metabolites and altered DNA methylation in the early embryo.

3.4 Introduction

Metabolic regulation in the preimplantation embryo is essential for normal embryonic development to the blastocyst stage and maintenance of optimal health in the resulting offspring. Environments which oversupply metabolites to the oocyte and preimplantation embryo during development, such as maternal obesity, alter oocyte mitochondrial function (Igosheva et al., 2010), reduce blastocyst development, and impair the health of subsequent offspring in animal models (Igosheva et al., 2010, Jungheim and Moley, 2010, Jungheim et al., 2010, McPherson et al., 2015). Similarly, human oocytes collected from obese women and transferred to recipients who have a normal BMI showed reduced pregnancy rates than those from lower bodyweight donors (Cardozo et al., 2016). Furthermore, in *in vitro* studies that pharmacologically reduce mitochondrial oxidative phosphorylation in the pre-implantation embryo using the malate aspartate inhibitor aminooxyacetate (AOA), and the oxidative phosphorylation uncoupler carbonyl cyanide–*p*-trifluoromethoxyphenylhydrazone (FCCP), result in a significant decrease in embryo implantation, foetal development, and foetal weights despite only a minor impairment being seen to blastocyst development (Wakefield et al., 2011, Zander-Fox et al., 2015). In addition maternal pre-conception exposure to obesity has been shown to alter methylation in the pronuclear embryo, with altered foetal outcomes after birth (Han et al., 2018). These alterations in offspring health after the application of a stressor during the time of preimplantation embryo development have been suggested to result from epigenetic programming changes (Lane et al., 2014). Together these studies suggest a link between embryo mitochondrial metabolism and epigenetic changes.

One pathway through which epigenetic alterations are believed to be transmitted is through DNA methylation, in a setting where the methylation level in the embryo immediately after fertilisation is rapidly changed throughout cleavage development (Iqbal et al., 2011, Santos et al., 2005). DNA methylation in the form of 5-methylcytosine (5mC) is altered in the genome by the Ten-Eleven Transolcase (TET) family of proteins, consisting of TET1, TET2 and TET3, using α-ketoglutarate as a cofactor (Ito et al., 2010). The TET family of proteins oxidise 5-

methylcytosine (5mC) to 5-hydroxymethylcytosine (5hmC), and then further oxidise 5hmC to 5-formylcytosine (5fC) and onto 5-carboxycytosine (5caC) prior to either the complete removal of the methyl mark or the reinstatement of it (Ito et al., 2011). The TET family of proteins are critical for embryo and foetal development with TET3 knockouts resulting in depleted 5hmC and enriched 5mC in the embryo and subsequently a high proportion of early neonatal deaths (Inoue et al., 2015). TET proteins require the TCA cycle intermediate α-ketoglutarate as a co-factor, thus providing a link between mitochondrial metabolism and DNA methylation (Ito et al., 2010, Koivunen et al., 2012, Shen et al., 2014b, Simmons et al., 2008, Tahiliani et al., 2009, Wu and Zhang, 2010).

α-ketoglutarate, the cofactor and energy donor for demethylation of 5mC, is produced in the TCA cycle, noting that the TCA cycle is the primary source of energy in the oocyte until the compaction stage (Dumollard et al., 2007, Houghton and Leese, 2004, Houghton et al., 1996, Lane and Gardner, 2005, Leese, 1991, Leese, 1995, Trimarchi et al., 2000, Whittingham, 1969). Previous studies have shown that the concentration of α-ketoglutarate present in the oocyte is at, or below, the K_m of TET3 (the only TET protein present in the cleavage stage embryo) (Sudhamalla et al., 2017). This therefore suggests that TET3 is exceedingly sensitive to any increase or decrease in α-ketoglutarate availability and will change the rate of TET-mediated demethylation dependent on the level of α-ketoglutarate available. This has been confirmed in studies using embryonic stem cells where modulating cellular α-ketoglutarate concentration changed the expression of genes required to maintain pluripotency (Carey et al., 2015).

2-hydroxyglutarate (2HG) is structurally similar to α-ketoglutarate and acts as a competitive inhibitor for α-ketoglutarate dependent enzymes (Chen et al., 2017, Dang et al., 2009, Joberty et al., 2016, Koivunen et al., 2012, Leonardi et al., 2012, Losman and Kaelin, 2013, Pope et al., 2012, Sasaki et al., 2012, Sudhamalla et al., 2017, Xu et al., 2011). Using 2HG as a competitive inhibitor decreases cellular 5hmC levels in cell culture, showing that inhibiting supply of α-ketoglutarate to TET proteins inhibits the process of DNA demethylation (Xu et al., 2011).

It is currently unknown whether supplementation of α-ketoglutarate, or inhibition of TET activity using 2HG, results in an alteration to the DNA methylation profile at the time of embryonic genome activation (EGA). Therefore, the objectives of this study were to determine if TET-mediated demethylation in preimplantation embryos is directly proportional to the amount of α-ketoglutarate present; and if removing α-ketoglutarate availability through competitive inhibition of TET results in a reduction of methylation past 5mC onto 5hmC, 5fC and 5caC.

3.5 Materials and Methods

3.5.1 Mice

Female C57Bl6 x CBA (CBAF1) mice aged 4-6 weeks were fed standard rodent chow (Specialty Feeds) with *ad libitum* access to food and water. Mice were maintained in a 12:12 h light: dark cycle. Mice were superovulated by an intraperitoneal (i.p.) injection of 5 IU pregnant mare's serum gonadotrophin (Folligon; Intervet, Bendigo East, Australia), followed 46-48 h later by an i.p. injection of 5 IU chorionic gonadotrophin (Chorulon, Intervet, Bendigo East, Australia). Females were mated overnight with CBAF1 male stud mice. Oviducts were collected and zygotes collected at 8 h post presumed fertilisation (i.e. mid-dark cycle), at 20 h post hCG. All animal work was approved by the University of Adelaide Animal Ethics committee (M-2015-259, M-2017-046 and M-119-13) and performed in accordance with the Australian Code for the Care and Use of Animals for Scientific Purposes 8th edition.

3.5.2 Media composition

All chemicals were purchased from Sigma-Aldrich (St Louis, Missouri, USA) unless otherwise stated. GMOPS (Vitrolife; Gothenburg, Sweden) supplemented with 5% human serum albumin (HSA, Vitrolife) was used for embryo collection and handling. Media for embryo culture for the α-ketoglutarate experiments was G1 and G2 (Vitrolife) supplemented with 5% HSA. 100 µL of α-ketoglutarate stock solution in Milli-Q water (Merck; Darmstadt, Germany) was added to 10mL culture media to final concentrations of 1.4 mM, 3.5 mM and 14.0 mM α-ketoglutarate, with 100 µL Milli-Q water as vehicle control for 0 mM α-ketoglutarate. Concentrations were selected as per (Lane and Gardner, 1995), where 3.5 mM and 14.0 mM α-ketoglutarate showed reduced blastocyst development and blastocyst cell number when cultured from the 2-cell stage to blastocyst (Lane and Gardner, 1995).

Media for the 2HG addition was G1 and G2 supplemented with 5% HSA prepared without addition of glutamine and glutamate, as these can be converted to α-ketoglutarate in the embryo through glutamate dehydrogenase (Gardner and Lane, 1993) (Table S4.1), with 0 mM or 20 mM (DL)-2-hydroxyglutarate (2HG) added to media. 20 mM was selected as this is the average cellular concentration of 2HG observed under Stage II and stage III glioma (cancer that creates 2HG *in vivo*) (Choi et al., 2012, Dang et al., 2009, Gross et al., 2010). 2HG is a competitive inhibitor for α-ketoglutarate as it binds the active site of α-ketoglutarate dependent enzymes such as TETs and cannot be converted to succinate thus blocking any further action of these proteins.

3.5.3 Embryo culture

Presumed zygotes were removed into GMOPS + 5% HSA and denuded of cumulus cells using 0.5mg/mL hyaluronidase in GMOPS + 5% HSA for less than 1 min then washed once in GMOPS + 5% HSA and cultured in 20 µL culture drops of media in groups of 10 at 37°C 6% CO_2, 5%O_2, 89% N_2. Embryos were cultured in medium G1+5% HSA for 48 h (Day 1 to Day 3) and then transferred into G2+5% HSA media for a further 48 h (Day 3 to Day 5).

3.5.4 Collection of 2-cell embryos pre- and post-embryonic genome activation

Two-cell embryos were assessed after embryonic genome activation as those before embryonic genome activation (collected within 30 min of the first cleavage division) showed no significant differences in DNA methylation for 5mC, 5hmC, 5fC nor 5caC (Figure S4.1).

Two-cell embryos post embryonic genome activation were collected and fixed at 28 h of culture, which was the time point selected as the point 30 min before cells began to cleave to 3-cells to confirm in late G2 phase (Kang et al., 2014). Embryos were fixed in 4% paraformaldehyde (PFA) in PBS at 4°C overnight. Fixed embryos were then stored in PBS + 4 mg/mL polyvinylpyrrolidone (PVP).

3.5.5 Embryo development

α-ketoglutarate treated embryos were cultured to the blastocyst in G1+5% HSA with the above concentrations of α-ketoglutarate for 48 h (Day 1 to Day 3), and then transferred to G2+5% HSA media supplemented with the same concentration of α-ketoglutarate for a further 48 h (Day 3 to Day 5).

2HG cultured embryos cultured in G1/G2 media without glutamine/glutamate supplemented with 20 mM 2HG throughout the entire culture period were unable to be cultured to the blastocyst stage, with embryo development significantly decreased after 48 h (Table S4.2), with no embryos reaching the blastocyst stage (Table S4.2) and only 10 embryos reaching the morula stage. Therefore, to assess the impact of 2HG on embryo development, embryos were cultured in G1 media without glutamine/glutamate (Table S4.1) and either 0 mM or 20 mM 2HG for 48 h until the 8-cell stage and then transferred to commercial G2 + 5% HSA media (Vitrolife) for a further 48 h.

Embryo development was scored after 24 h of culture (cleavage stage) for 1-cell, 2-cell or 3-cell, after 48 h (compaction stage) for development <4-cell, 4-cell, 6-cell, 8-cell or a compacting morula, after 79 h (early blastocyst stage) for development to morula, early blastocyst (blastocoel less than 50% total volume), blastocyst, expanded blastocyst or hatching blastocyst and after 96 h of culture (late blastocyst stage) for development to morula, early blastocyst (blastocoel less than 50% total volume), blastocyst, expanded blastocyst or hatching blastocyst. After 96 h of culture, blastocysts were then fixed in 4% PFA (as above) for cell counting.

3.5.6 Blastocyst cell counts

Blastocyst cell number, trophectoderm (TE) and inner cell mass (ICM) cell number were assessed using immunocytochemistry for Oct4, which in blastocysts will only be present in the inner cell mass coupled with a nuclear stain (Campbell et al., 2012, McPherson et al., 2014). Blastocysts were placed into 0.1 M glycine for 5 min at room temperature (RT), followed by permeabilisation in 0.25% Triton-X in PBS (TX) for 10 min at RT. Blastocysts were then blocked overnight in 10% donkey serum in PBS at 4ºC. Blastocysts were washed in 0.25% Triton-X (TX) and incubated in 1:100 goat anti-Oct3/4 (sc-362275, Santa Cruz; Dallas, Texas, USA) for 1.5 h at 37ºC. Blastocysts were washed twice in 0.25% Triton-X and incubated in secondary antibody 1:100 donkey anti-goat conjugated to Alexa-594 (Thermo Fisher A11058, excitation 590 nm emission 617 nm) at RT for 2 h covered in dark conditions. Blastocysts were again washed twice in 0.25% Triton-X and counterstained with 25 µg/mL Hoechst 33342 for 5 min. Blastocysts were transferred to PBS/PVP and mounted onto microscope slides in glycerol for cell counts. Blastocysts were counted using epifluorescence microscopy (Olympus BX51, Olympus; Shinjuku City, Tokyo, Japan), using the red channel (excitation filter 520-560 nm, emission from 420 nm) to count Oct4 in the inner cell mass and a count of total nuclei via Hoechst (excitation filter 330-385 nm, emission from 580 nm).

3.5.7 Immunocytochemical assessment of DNA methylation (5mC, 5hmC, 5fC and 5caC)

Two-cell embryos (post genome activation) were stained for both 5mC, and either 5hmC, 5fC or 5caC using a previously validated co-immunocytochemical a protocol (Li and O'Neill, 2013, Li and O'Neill, 2012).

After fixation, two-cell embryos were permeabilised in 0.5% Tween 20 + 0.5% Triton X-100 in PBS at RT for 40 min, then blocked overnight in 30% Donkey serum (DS) in PBS at 4°C. The following morning, DNA was denatured in 4 N HCl at 37°C for 10 min, followed by antigen retrieval in 0.25% Trypsin + EDTA at 37°C for 45 s, followed by wash in 10% donkey

serum. Embryos were then incubated with 1:100 mouse anti-5mC (Active Motif, Carlsbad, CA), and either 1:500 rabbit anti-5hmC (Active Motif), 1:200 rabbit anti-5fC (Active Motif), or 1:200 rabbit anti 5-caC (Active Motif) in PBS at 4°C for 17 h, plus 1 h at 37°C. Embryos were washed twice in 0.5% TX, followed by incubation with secondary antibodies 1:200 donkey anti-mouse Alexa 594 (ab150108, Abcam; Cambridge, United Kingdom) and 1:250 donkey anti-rabbit Alexa 488 (ab150073, Abcam) at RT for 2 h before washing in GMOPS (Vitrolife). A negative control was included for each experimental day and comprised a 2-cell embryo using the experimental protocol as above with omission of both anti-5mC and anti-5-hmC antibodies and incubated with PBS only. Embryos were imaged using the CV1000 spinning disk confocal microscope (Yokogawa) using 40x magnification, with consistent measurement settings used on each experimental day, with the results normalised by imaging green (excitation 450/480) and red/orange (excitation 565/580) 15 µm Fluospheres from Blood flow determination kit (Invitrogen; Carlsbad, California, USA) to control for changes to microscope over replicates. Relative levels of methylation marks were measured via densitometry of captured images using Fiji version 2.0.0-re-43 on ImageJ version 1.50e on whole nuclear regions. Data was then calculated as a fold change relative to CD measurements.

3.5.8 Statistical analysis

Statistics were performed using IBM SPSS Statistics version 26. All data is expressed as mean ± standard error of the mean (SEM) with normality assessed using the Kolmogorov-Smirnov test.

Embryo culture for both α-ketoglutarate and 2HG were measured via binomial regression using embryo culture replicate fitted as a cofactor. Blastocyst cell numbers were assessed using general linear models with culture replicate fitted as a cofactor. All DNA methylation was measured by normalizing results to the control. Normally distributed data was analysed by a general linear model with culture date fitted as cofactor, with non-normally distributed data analysed by a Kruskal-Wallis test. A-ketoglutarate cultured 2-cells were analysed for correlation of methylation increase with increasing α-ketoglutarate concentrations via two-sided Spearman correlation coefficient and presented as Spearman rho (ρ), with weak correlation determined at $\rho < \pm 0.3$, moderate correlation at $\rho = \pm 0.3\text{-}0.6$, and high correlation at $\rho > \pm 0.6$. Statistical differences were determined at $P<0.05$.

3.6 Results

3.6.1 Effect of culturing embryos with α-ketoglutarate on embryo development and blastocyst cell allocation

Culturing zygotes in 1.4 mM or 3.5 mM α-ketoglutarate did not impact cleavage rates to the 2-cell stage, embryo compaction or blastocyst development (Table 4.1). Embryos cultured in 14.0 mM α-ketoglutarate had arrested development at the 2-cell stage and were unable to be cultured past this point ($P>0.05$, Table 4.1).

There were no effects of α- ketoglutarate concentration on blastocyst total cell number, ICM cell number, trophectoderm cell number; or percent of ICM as a proportion of total cell number ($P>0.05$, Figure 4.1).

3.6.2 Effect of culturing embryos with α-ketoglutarate on DNA methylation in 2-cells post embryonic genome activation

The effect of culturing embryos in α-ketoglutarate on 2-cell DNA methylation was assessed at the end of the G2 phase, where embryonic genome activation has occurred (Figure 4.2a). The level of DNA 5mC was reduced following culturing in concentrations ≥1.4 mM of α-ketoglutarate ($P<0.05$, Figure 4.2b), with 5mC moderately correlated to α-ketoglutarate concentrations (Spearman $\rho = -0.353$, $P<0.001$). The concentration of 5hmC was only reduced at 14.0 mM α- ketoglutarate ($P<0.001$, Figure 4.2c); however linear regression showed a weak negative correlation with increasing concentrations (Spearman $\rho = -0.266$, $P<0.01$). Concentration of 5fC was decreased at 1.4 mM and 14.0 mM concentrations of α- ketoglutarate ($P<0.001$, Figure 4.2e), with a weak negative correlation across increasing concentrations (Spearman $\rho = -0.276$, $P<0.05$). The concentration of 5caC was only reduced at a concentration of 14.0 mM ($P<0.01$, Figure 4.2g), however a weak negative correlation was observed across increasing concentrations (Spearman $\rho = -0.228$, $P<0.01$).

When expressed as a ratio to each individual cell's 5mC fluorescence, the ratio of 5hmC:5mC increased with14.0 mM of α-ketoglutarate compared to control ($P<0.0001$, Figure 4.2d), with a moderate positive correlation across increasing concentrations (Spearman $\rho = 0.302$, $P<0.001$). The ratio of 5fC:5mC showed a weak positive correlation to α-ketoglutarate concentration (Spearman $\rho = 0.178$, $P<0.05$), but there were no individual significant differences between α-ketoglutarate concentrations ($P>0.05$, Figure 4.2f). The ratio of 5caC:5mC in DNA was not correlated to α-ketoglutarate concentrations (Spearman $\rho = -0.13$, $P>0.1$), but there was a significant reduction in 5caC:5mC under 14.0 mM α-ketoglutarate compared to 0 mM ($P<0.001$, Figure 4.2h). These data show a dose dependent progression of 5mC to 5hmC and 5fC due to culture of embryos in α-ketoglutarate supplemented media.

3.6.3 Effect of competitive inhibition of a-ketoglutarate with 2HG on embryo development and blastocyst cell numbers

Embryos were cultured with the α-ketoglutarate inhibitor 2HG, to determine the effect of reducing the α-ketoglutarate able to bind the TETs to demethylate DNA. In this experimental model glutamine and glutamate were removed from the culture media as these can be metabolised into α-ketoglutarate through glutamate dehydrogenase (Gardner and Lane, 1993, Gardner and Leese, 1990, Kramen and Biggers, 1971).

There was no effect of 20 mM 2HG culture on cleavage to the 2-cell stage (Table 4.2), however after 48 h of culture 8-cell rates were significantly reduced ($P<0.05$, Table 4.2), with an increased proportion of embryos below the 6-cell stage (Table 4.2). After transfer to G2 + 5% HSA media that did not contain 2HG, there was no further impact on development rates after 79 h or 96 h of culture under 20 mM 2HG treated embryos (Table 4.2).

20 mM of 2HG however significantly reduced total blastocyst cell number, ICM cell number and TE cell number compared with control ($P<0.04$, Figure 4.3) although the proportion of ICM to total cells was not affected ($P>0.05$, Figure 4.3).

3.6.4 Effect of culturing embryos with 2HG on DNA methylation in 2-cells post embryonic genome activation

DNA methylation was measured in the G2 phase 2-cell similarly to α-ketoglutarate culture to determine the effects of decreased α-ketoglutarate availability due to competitive inhibition (Figure 4.4a). Culture of zygotes with 20 mM 2HG, significantly increased the levels of 5mC DNA methylation compared with control ($P<0.01$, Figure 4.4b). There were no significant differences in 5hmC nor 5fC concentration under 20 mM 2HG ($P>0.05$, Figure 4.4c, e), however 5caC levels were reduced with 20 mM 2HG compared with control ($P<0.05$, Figure 4.4g).

When expressed as a ratio to each individual cell's 5mC fluorescence, there was a significant reduction in the ratio of 5hmC:5mC ($P<0.001$, Figure 4.4d), 5fC:5mC of DNA ($P<0.001$, Figure 4.4f), as well as the 5caC:5maC ratio ($P<0.001$, Figure 4.4h). This suggests that culture of embryos with the competitive inhibitor 2HG lowers oxidation of 5mC to the further demethylation bases.

3.7 Discussion

Control of DNA methylation/demethylation in a tightly regulated temporal spatial manner is essential for normal embryo development and for the maintenance of viability and offspring health (Inoue et al., 2015, Tsukada et al., 2015, Wu and Zhang, 2017, Zhu et al., 2018). Physiological alterations to metabolism, such as those that can be caused by obesity (Igosheva et al., 2010, Kubandová et al., 2014, Luzzo et al., 2012, McPherson et al., 2015), low dietary protein consumption (Fleming et al., 2012, Mitchell et al., 2009, Watkins et al., 2010, Watkins et al., 2011, Watkins et al., 2008a, Watkins et al., 2008b), and age (McPherson et al., 2014) have been shown to alter embryo TCA cycle function. In addition, these maternal phenotypes also result in compromised embryo development and offspring viability and health. Although such metabolic alterations are linked to epigenetic changes in the brain, and kidney of offspring (Dzitoyeva et al., 2012, Han et al., 2018, Kim et al., 2016); the underlying mechanistic link has not been identified to date. In addition, it is unknown whether such a mechanism would act as an active cellular response to the altered environment, or as a direct result of altered metabolite levels. Here we have demonstrated that the concentration of α-ketoglutarate during a single DNA replication event in the 2-cell embryo at the time-point of embryonic genome activation altered the removal of methylation marks from DNA.

Increasing the availability of α-ketoglutarate by direct supplementation to embryo culture media resulted in enhanced demethylation consistent with increased TET3 enzyme activity (Nettersheim et al., 2013). Previous research has also shown that supplemented embryo culture media with 150μM α-ketoglutarate (as compared to our concentrations of 1.4 mM to 14.0 mM) demonstrated reduced 5hmC and 5mC in mouse blastocysts (Zhang et al., 2019).

In this study, we have shown that addition of α-ketoglutarate similarly decreases 5mC and 5hmC, but also showed the same trend for 5fC and 5caC in a dose dependent manner, providing a mechanistic link between cellular alterations to α-ketoglutarate as a key substrate of TET enzymes and alterations to global methylation in embryos.

Previous findings from culture media supplemented with α-ketoglutarate resulted in reduced blastocyst rates and cell number at a 1.75 mM and above when incubated from the 2-cell stage onwards (Lane and Gardner 1995). In our study the concentrations of 3.5 mM and 14.0 mM are likely causing other cellular effects due to large alterations to the rate of TCA cycle, including increased amino acid turnover (Houghton et al., 2002) and altered nutrient balance (Lane and Gardner, 1997).

At 3.5 mM there was a trend towards an increased percentage of embryos at or above the 8-cell stage after 48 h of culture was evident. This could be expected due to enhancement of the TCA cycle, which is the primary source of energy during this stage of embryo development (Dumollard et al., 2007, Houghton and Leese, 2004, Houghton et al., 1996, Lane and Gardner, 2005, Leese, 1995, Trimarchi et al., 2000) and that the effects of altered embryo development may not be fully ascribed to altered DNA methylation alone.

It is possible that at the highest concentration used in this study (14.0 mM α-ketoglutarate) there may have been an increase in the generation of reactive oxygen species (ROS) though overstimulation of metabolism (Starkov et al., 2004). This has been shown in previous studies culturing embryos cultured with 150 μM α-ketoglutarate (Zhang et al., 2019). Notably, we also demonstrated a block in development at the two-cell stage at 14.0 mM α-ketoglutarate, providing evidence that embryonic genome activation was not able to occur.

Alternatively, α-ketoglutarate supplementation has been shown to alter other α-ketoglutarate dependent enzymes, such as the lysine demethylases in the KDM5 and KDM6 families (Tran et al., 2018) and therefore, this block to cleavage may also be due to histone hypermethylation blacking embryonic genome activation, effectively blocking process past the 2-cell.

Under α-ketoglutarate culture at concentrations of 1.4 mM and 3.5 mM there were no changes to blastocyst development or day 5 blastocyst cell numbers. These results are similar to that of embryos from mothers fed a high fat diet (HFD), where there are no differences in embryo development or changes in blastocyst cell numbers (McPherson et al., 2015). In these maternal HFD studies there were differences in resultant offspring characteristics, with a shorter

crown:rump length observed and differences in foetuses per embryo transferred despite the lack of visible embryo phenotype (Han et al., 2018, McPherson et al., 2015). This indicated that whilst there were no overt alterations to embryo development, there may be alterations to epigenetic marks, such as changed methylation profiles in these embryos. This implies that changes to DNA methylation in the preimplantation period may trigger changes in the resulting embryo that leads to poorer health outcomes. These results are also similar to that of incubation with the mitochondrial uncoupler carbonyl cyanide 4-(trifluoromethoxy) phenylhydrazone (FCCP), where a mild reduction in ICM was observed, resulting in reductions in female offspring birthweight and reduced fat mass and bone mass at weaning (Zander-Fox et al., 2015). α-ketoglutarate remains as a potential mediator of these events due to a plausible increase in its abundance in the 1-cell to 2-cell embryo caused by the maternal HFD.

2HG is produced by gliomal cancers that have a mutation to isocitrate dehydrogenase which normally canonically produces α-ketoglutarate from isocitrate via the TCA cycle (Chen et al., 2017, Dang et al., 2009, Figueroa et al., 2010, Guilhamon et al., 2013, Jin et al., 2011, Koivunen et al., 2012, Krell et al., 2011, Leonardi et al., 2012, Lu et al., 2012, Necula et al., 2015, Pfeifer et al., 2013, Sasaki et al., 2012, Scourzic et al., 2015, Xu et al., 2011, Ye et al., 2013). The modification caused by the mutant isocitrate dehydrogenase allows 2HG to function as a competitive inhibitor for α-ketoglutarate as it cannot be cleaved to be used as an energy source and carbon donor for all α-ketoglutarate dependent enzymes, including TETs. Therefore, we wanted to examine whether inverse alterations were observed under competitive inhibition. As 2HG is not metabolised by the embryo this allowed us to assess if the alterations to methylation and embryonic development are directly due to α-ketoglutarate's action on TET mediated demethylation.

Previous studies have used an inhibition model for α-ketoglutarate using 2HG in a cell free system that showed inhibition of TET function by the addition of either S-enantiomer or R-enantiomer of 2HG (Koivunen et al., 2012). The R-enantiomer is of interest as it is the product of the mutant IDH1 discussed previously, and biologically acts as a more potent inhibitor than the S-enantiomer, with IC_{50} at less than half that of the S- enantiomer (Sudhamalla et al., 2017). Glutamine and glutamate were omitted from the media as they can be converted to α-ketoglutarate, so we created a model of inhibiting TET activity by addition of the competitive inhibitor 2HG, plus removal of glutamine and glutamate so no α-ketoglutarate can be formed using this pathway. In our model using 2HG inhibition there was a significant reduction in development up to day 3. Upon transfer to standard G2 media these embryos developed to blastocyst and showed no differences in development throughout culture to day 4 or day 5 which implied some level of catch-up growth was occurring. If 2HG was present throughout the whole culture period embryos arrested at the cleavage stage. This indicates that removal of 2HG at prior to compaction is required for embryos to reach the blastocyst. Although formation of blastocysts was not delayed on day 5, these embryos had a reduced number of cells, indicating that these blastocysts were mitotically delayed relative to control embryos potentially as a result from the earlier delay and later catch-up growth. As the control media did not contain glutamine or glutamate and development persisted through to the blastocyst stage, the 4-cell block was not likely due to a depletion of glutamine and glutamate in these embryos.

Alterations to amino acid concentrations can have an impact on DNA methylation. It has been shown that intraperitoneal injection of glutamine and glutamate increases α-ketoglutarate in mouse livers leading to an increase of 5mC (Yang et al. 2014), showing a direct increase in methylation with an increase in substrate concentration. Therefore, for this model to show the effect of depleted α-ketoglutarate on embryonic methylation, glutamine and glutamate were omitted from the culture media to prevent endogenous production of α-ketoglutarate.

The presumed result of introducing the competitive inhibitor 2HG into the culture media was an increase in 5mC levels as TET-mediated oxidation cannot be carried out, with a concomitant decrease in further bases 5hmC, 5fC and 5caC. In the aforementioned gliomal cancers there is an observed hypermethylation of the genome, with reduced activity for TET2, the active TET in these cell types through production of 2HG (Figueroa et al., 2010). Our model of addition of 2HG in racemic form (i.e. D-2HG and L-2HG in 50:50 ratio) shows significant increases in 5mC, with decreased relative 5caC, and significantly reduced 5hmC:5mC, 5fC:5mC and 5caC:5mC.

The establishment of correct DNA methylation status is critical for the initiation of the maternal to embryonic transition in embryos (Lee et al., 2014, Shen et al., 2014a). The early embryo is a critical period of time for changes in methylation to occur; where the methylation is actively removed from the genome, with the greatest reduction seen in the paternal pronucleus (Santos et al., 2002). The largest period of active demethylation occurs in the pronuclei during the S phase (DNA replication) stage of the cell cycle (Amouroux et al., 2016). We have supplemented culture media from 8 h after presumed fertilisation with α-ketoglutarate and 2HG (which is from PN4 stage of pronuclear migration and development). This time point proceeds the first S-phase in the 1-cell embryo; thus it is unlikely that the α-ketoglutarate was available to the TET proteins to actively demethylate DNA in the G1 phase of the newly formed 2-cell. This is consistent with our observations of no significant trend in reduction of 5mC or increase in 5hmC, 5fC or 5caC at this stage. After the second embryonic S phase in the 2-cell embryo, we saw significant changes in methylation with supplementation of α-ketoglutarate and 2HG. Therefore, we can see that the effects of α-ketoglutarate availability are because of the modulation of TET-mediated demethylation caused by the manipulation of substrate concentration.

Our model demonstrates that competitive inhibition of α-ketoglutarate to bind TET can create a phenotype of elevated 5mC methylation and reduced active progression of demethylation by TET proteins. This demonstrates that DNA methylation can be controlled via either elevated or decreased supply of α-ketoglutarate in the early embryo, however further research is required to examine the degree to which demethylation can be recovered, if the altered methylation persists to the blastocyst, or if this catch-up growth has any long term effects.

In conclusion, we have shown that supplementation of embryo culture media with α-ketoglutarate decreases 5mC in a dose-dependent manner in the G2 phase 2-cell, with a concomitant increase in 5hmc:5mC ratio. While in contrast competitive inhibition of α-ketoglutarate increased 5mC and decreased 5hmC:5mC, 5fC:5mC and 5caC:5mC in the G2 2-cell. Competitive inhibition with 20 mM 2HG reduced development through cleavage stages, blocking development to the blastocyst, but recovery in normal media (from the 8-cell stage) allowed blastocyst formation, albeit of a somewhat compromised quality (reduced inner cell mass and trophectoderm cells). Here we provide evidence of a direct metabolic link (availability of α-ketoglutarate) to alterations in methylation and disruptions in development of the early embryo that suggests a mechanism that acts before and during embryonic genome activation in the mouse embryo and may result in long-term effects in offspring.

Declarations

Acknowledgements

We would like to thank Bridget Arman and Lauren Sandeman for technical assistance, and we would like to thank Vitrolife for gifting the Vitrolife G1+5% HSA and G2+5% HSA culture media, and G-MOPS+5% HSA handling media used for this study.

3.8 Tables

Table 3.1 Effect of culturing embryos with 0, 1.4, 3.5 and 14.0 mM α-ketoglutarate on embryo development

	0 mM	1.4 mM	3.5 mM	14.0 mM
Day 2				
Cleavage on day 2 (%)	83.87	92.68	85.20	81.97
Day 3				
≤6 cell (% 2-cell)	11.76 [a]	7.50 [a]	1.89 [a^]	100 [b]
6-cell (% 2-cell)	5.88	7.50	5.66	0
8-cell (% 2-cell)	58.82 [a]	62.50 [a]	64.15 [a]	0 [b]
Compacting (% 2-cell)	23.53 [a]	22.50 [a]	28.30 [a]	0 [b]
8 cell plus compacting (% 2-cell)	82.35 [a]	85.00 [a]	94.23 [a#]	0 [b]
Day 4				
Total Blastocyst (% 2-cell)	90.38	82.93	86.27	0 *
Early Blast (% of total blast)	17.02	30.30	29.55	0 *
Blastocyst	27.66	21.21	29.54	0 *
Expanded Blast (%)	48.94	45.45	38.64	0 *
Hatching Blast (%)	6.38	3.03	2.27	0 *
				0 *
Day 5				
Total Blast (% 2-cell)	100	97.30	96.23	0 *
Early Blast (% of total blast)	0.00	2.78	1.96	0 *
Blastocyst (% of total blast)	11.54	8.33	9.80	0 *
Expanded Blast (% of total blast)	28.85	33.33	33.33	0 *
Hatching Blast (% of total blast)	59.62	55.56	54.90	0 *

0 mM n=62, 1.4 mM n=41, 3.5 mM n=61, 14.0 mM n=61. Differing letters denotes statistically significant difference P= <0.05.* No statistics were run against 14.0 mM embryos on Day 4 or Day 5 as no embryos were transferred to G2+5% human serum albumin (HSA) due to arrested development. ^ P=0.057 compared with 0 mM. [#] P=0.072 compared with 0 mM

Table 3.2 Embryo development on day 3, day 4 and day 5 on embryos cultured in G1 ± 20 mM 2-hydroxyglutarate (2HG) without glutamine/glutamate for 48 h and transferred into G2 + 5% HSA for 48 h until day 5 of culture

	0 mM	20 mM
Day 2		
Cleavage (%)	89.00	81.00
Day 3		
<6 cell (% 2-cell)	29.21 [a]	55.56 [b]
6 cell (% 2-cell)	11.24 [a]	22.22 [a] (P=0.058)
8-cell (% 2-cell)	58.43 [a]	22.22 [b]
Compacting (% 2-cell)	1.12	0.00
8-cell plus compacting (% 2-cell)	59.55 [a]	22.22 [b]
Day 4		
Total Blastocyst (% 2-cell)	50.00 [a]	41.03 [a]
Early Blast (% of total blast)	54.55	56.25
Blastocyst (% of total blast)	18.18	25.00
Expanded Blast (% of total blast)	22.73	6.25
Hatching Blast (% of total blast)	4.55	12.50
Day 5		
Total Blast (% 2-cell)	85.39	87.65
Early Blast (% of total blast)	5.26	4.23
Blastocyst (% of total blast)	9.21 [a]	2.82 [a] (P=0.077)
Expanded Blast (% of total blast)	26.32	22.54
Hatching Blast (% of total blast)	59.21 [a]	70.42 [a] (P=0.108)

0 mM n=89, 20 mM n=81. Differing letters denotes statistically significant differences (P<0.05)

3.9 Figures

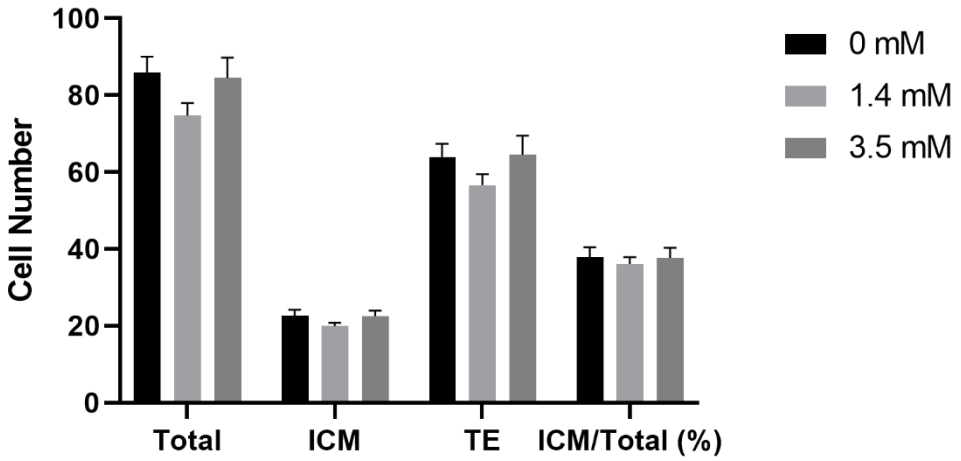

Figure 3.1 Blastocyst cell numbers after co-culture in 0, 1.4, or 3.5 mM α-ketoglutarate. Total cell number was determined with Hoechst 33342 and inner cell mass cells via Oct4 staining, with cells counterstained. 0 mM n=20, 1.4 mM n=22, 3.5 mM n=20. Data expressed as mean ± standard error of the mean (SEM). No statistical differences were found between concentrations

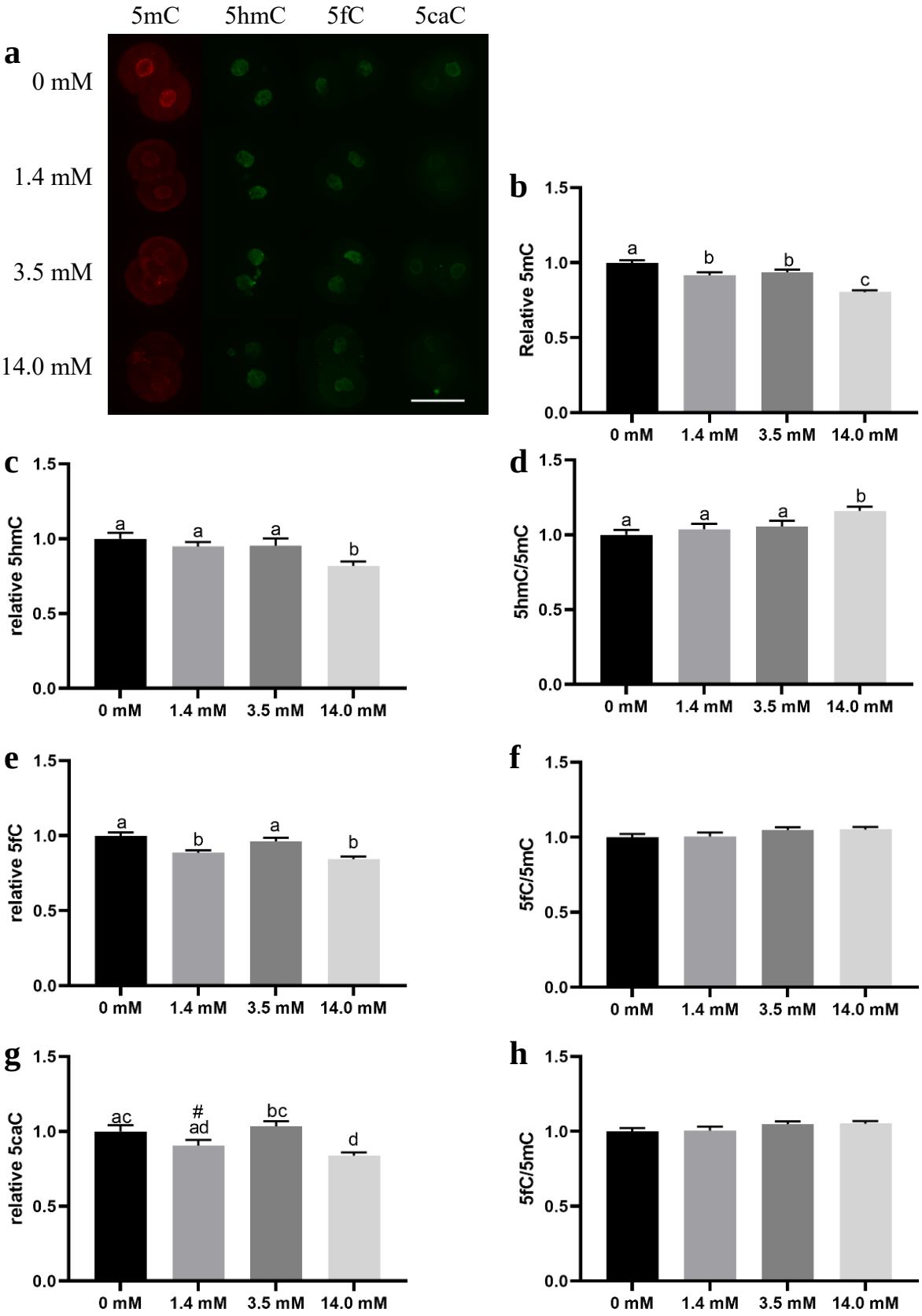
a
5mC
5hmC
5fC
5caC
0 mM
1.4 mM
3.5 mM
14.0 mM
b
Relative 5mC
c
relative 5hmC
d
5hmC/5mC
e
relative 5fC
f
5fC/5mC
g
relative 5caC
h
5fC/5mC
0 mM
1.4 mM
3.5 mM
14.0 mM

Figure 3.2 Effect of culturing embryos to the late G2 2-cell in media containing 0 mM, 1.4 mM, 3.5 mM and 14.0 mM α-ketoglutarate on DNA methyl marks. **a** representative images of G2 phase 2-cells on 5mC (red), 5hmC, 5fC and 5caC (green) **b** Relative 5mC values in G2 2-cell embryos after cuture in media containing α-ketoglutarate (n=54 0 mM, n=54 1.4 mM, n=54 3.5 mM, n=54 14.0 mM), **c** relative 5hmC values and **d** relative 5hmC:5mC ratio (n=16 0 mM, n=16 1.4 mM, n=16 3.5 mM, n=16 14.0 mM). **e** Relative 5fC values and **f** relative 5fC:5mC ratio (n=21 0 mM, n=23 1.4 mM, n=22 3.5 mM, n=18 14.0 mM). **g** Relative 5caC values and **h** relative 5caC:5mC ratio (n=17 0 mM, n=15 1.4 mM, n=16 3.5 mM, n=20 14.0 mM). Data expressed as mean ± standard error of the mean (SEM)., with different letters denoting significance $P<0.05$, and where letters are not present, no significant differences are present. # $P=0.068$ compared to 0.0 mM α-ketoglutarate. Scale bar = 50 μm

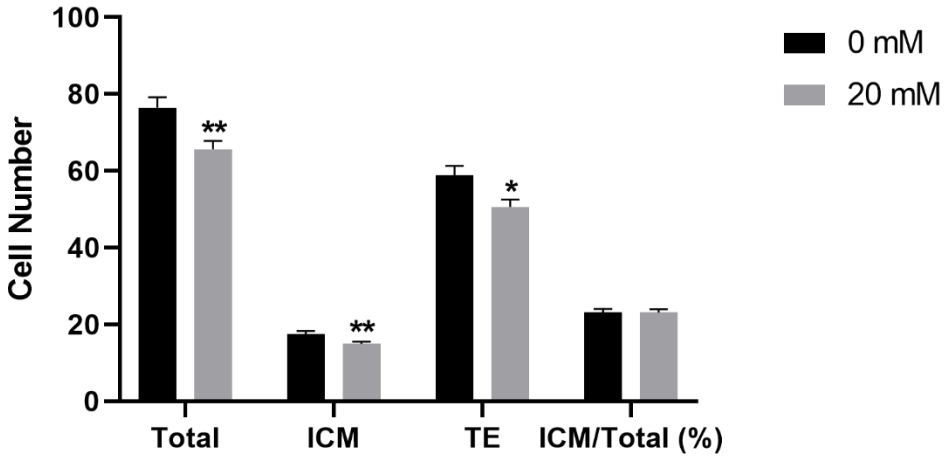

Figure 3.3 Day 5 blastocyst total cell number and cell differentiation into inner cell mass (ICM), trophectoderm (TE) on embryos cultured in G1 ± 20 mM 2-hydroxyglutarate (2HG) without glutamine/glutamate for 48 h and transferred into G2 + 5% HSA for 48 h until day 5 of culture. 0 mM n=40, 20 mM n=41. Data expressed as mean ± standard error of the mean (SEM). * $P<0.05$, ** $P<0.01$

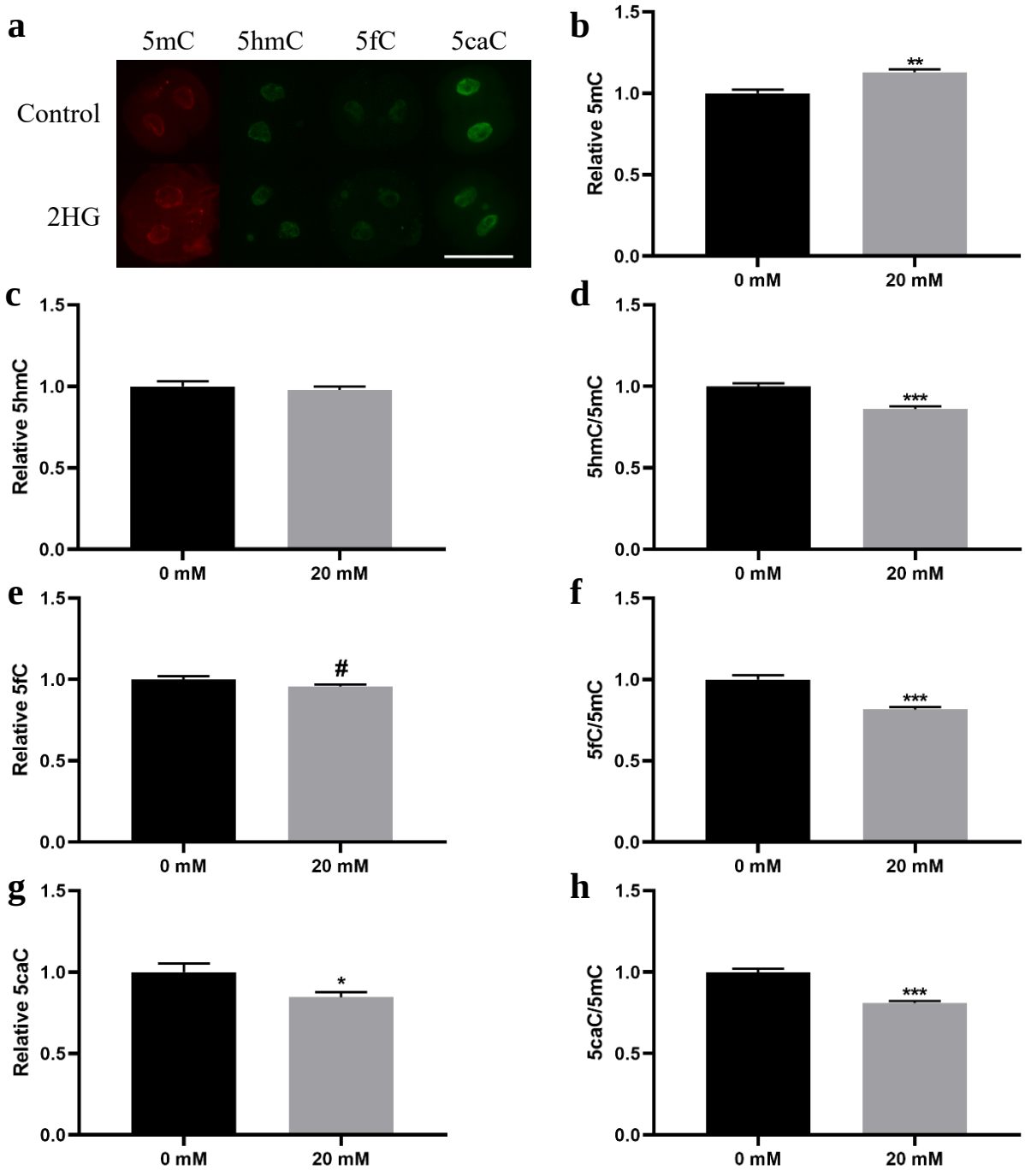

Figure 3.4 Effect of culturing embryos in G1 media containing 0 mM or 20 mM 2-hydroxyglutarate (2HG) with glutamine and glutamate removed. **a** Representative images of control and 2HG cultured embryos for 5mC (red), 5hmC, 5fC and 5caC (green), **b** levels of 5mC (0 mM n=69, 20 mM n=59), and **c** 5hmC values, **d** the ratio of 5hmC:5mC (0 mM n=23, 20 mM n=16), **e** 5fC values, **f** 5fC:5mC ratio (0 mM n=19, 20 mM n=23), **g** 5caC values and **h** 5caC:5mC ratio (0 mM n=25, 20 mM n=20). Data is normalised to the average for 0 mM 5mC and is expressed as mean ± standard error of the mean (SEM). # P= 0.056 * P<0.05 ** P<0.01 *** P<0.001. Scale bar = 50 µm

3.10 Supplementary Tables

Table S3.1 Media formulation

Component	G1.2 No glutamine/ glutamate (mM)	G1.2 + 2HG (mM)	G2.2 No glutamine/ glutamate (mM)	G2.2 + 2HG (mM)
NaCl	90.1	90.1	90.1	90.1
KCl	5.5	5.5	5.5	5.5
$NaHPO_4.2H_2O$	0.25	0.25	0.25	0.25
$MgSO_4.7H_2O$	1.0	1.0	1.0	1.0
$NaHCO_3$	25.0	25.0	25.0	25.0
$CaCl_2.2H_2O$	1.8	1.8	1.8	1.8
Glucose	0.5	0.5	3.15	3.15
Na Lactate	10.5	10.5	5.87	5.87
Na Pyruvate	0.32	0.32	0.1	0.1
EDTA	0.01	0.01		
Alanine	0.1	0.1	0.1	0.1
Arginine			0.6	0.6
Asparagine	0.1	0.1	0.1	0.1
Aspartate	0.1	0.1	0.1	0.1
Cystine			0.1	0.1
Glycine	0.1	0.1	0.1	0.1
Histidine			0.2	0.2
Isoleucine			0.4	0.4
Leucine			0.4	0.4
Lysine			0.4	0.4
Methionine			0.1	0.1
Phenylalanine			0.2	0.2
Proline	0.1	0.1	0.1	0.1
Serine	0.1	0.1	0.1	0.1
Taurine				
Threonine			0.4	0.4
Tryptophan			0.5	0.5
Tyrosine			0.2	0.2
Valine			0.4	0.4
Choline chloride			0.0072	0.0072
Folic Acid			0.0023	0.0023
Inositol			0.01	0.01
Nicotinamide			0.0082	0.0082
Pantothenate			0.0042	0.0042
Pyridoxal			0.0049	0.0049
Riboflavin			0.00027	0.00027
Thiamine			0.00296	0.00296
(DL) 2-hydroxyglutarate	0	20	0	20

Table S3.2 Embryo development on day 3, day 4 and day 5 on embryos cultured in G1 ± 20 mM 2-hydroxyglutarate (2HG) without glutamine/glutamate and transferred into G2 ± 20 mM 2HG without glutamine/glutamate

	0 mM	20 mM
Day 2		
Cleavage (%)	87.16	88.28
Day 3 (% 2-cell)		
≤6 cell (not degenerate)	25.90	100.00
6 cell	23.02	0.00
8-cell	35.25	0.00
Compacting	15.83	0.00
Day 5 (% 2-cell)		
Total Blast (%)	92.25	0.00
Early Blast-Blast (%)	23.26	0.00
Expanded Blast (%)	32.56	0.00
Hatching Blast (%)	36.43	0.00

Data from collected embryos 0 mM n=148 from n=16 mice, 20 mM n=130 from n=16 mice

3.11 Supplementary Figures

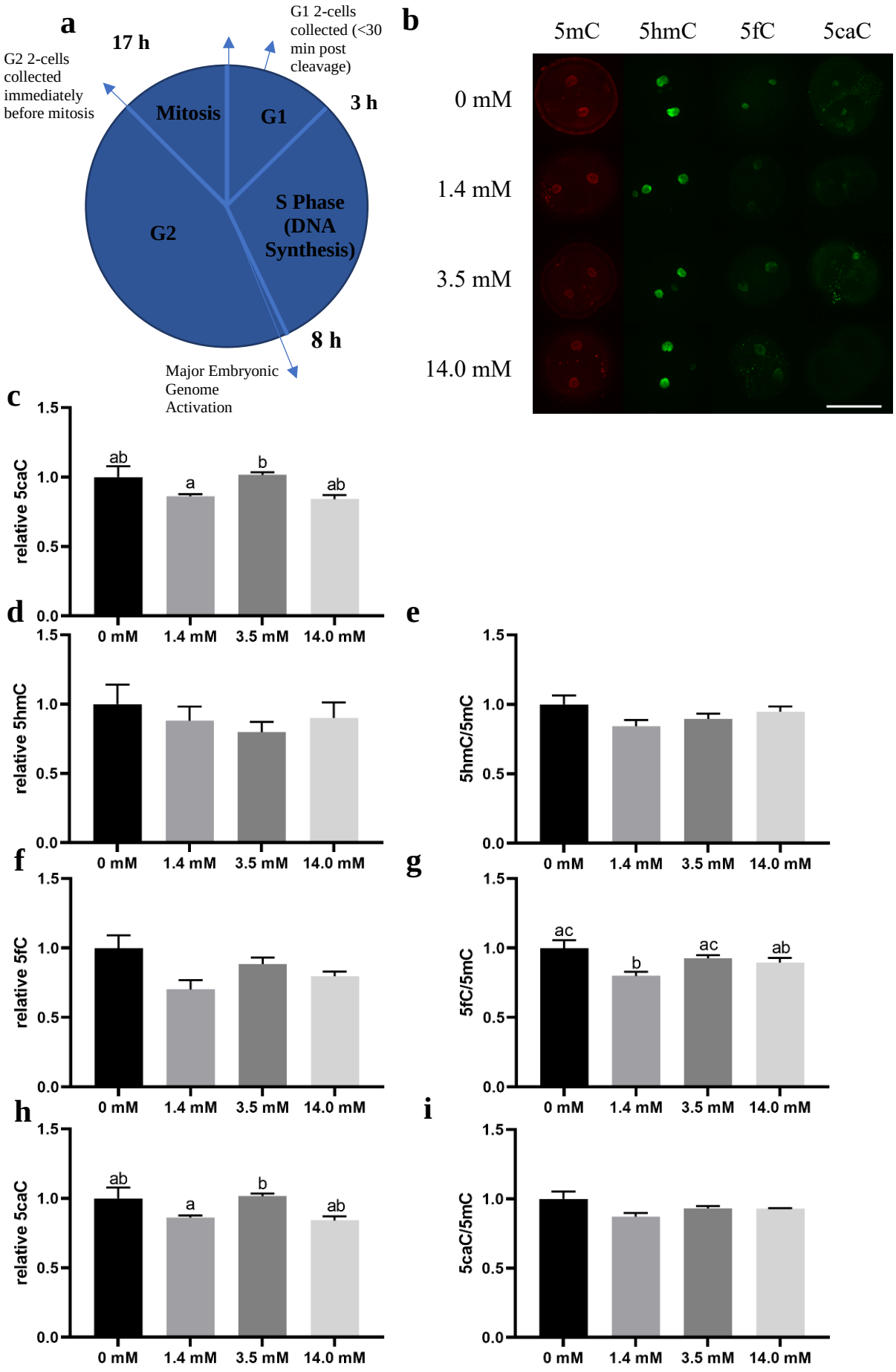

Figure S3.1 Effect of culture of embryos with α-ketoglutarate (0, 1.4, 3.5 or 14.0 mM) on 2-cells collected in the G1 phase (immediately after mitosis) on DNA methylation **a** cell cycle timings in the 2-cell adapted from (Kang et al., 2014), with collection times for G1 and G2 embryos, **b** representative images of G1 phase 2-cells on 5mC (red), 5hmC, 5fC and 5caC (green) **c** relative 5mC values in G1 embryos (n=27 0 mM, n=26 1.4 mM, n=42 3.5 mM, n=21 14.0 mM), **d** relative 5hmC values in G1 embryos, and **e** relative 5hmC:5mC ratio (n=14 0 mM, n=18 1.4 mM, n=16 3.5 mM, n=11 14.0 mM. **f** Relative 5fC levels and **g** relative 5fC:5mC ratio (n=11 0 mM, n=6 1.4 mM, n=23 3.5 mM, n=8 14.0 mM). **h** Relative 5caC levels and **i** 5caC:5mC ratio (n=4 0 mM, n=4 1.4 mM, n=3 3.5 mM, n=2 14.0 mM). Data expressed as mean ± standard error of the mean (SEM). Differing letters denote significant differences at $P<0.05$. Scale bar = 50 µm

3.12 References

AMOUROUX, R., NASHUN, B., SHIRANE, K., NAKAGAWA, S., HILL, P. W. S., D'SOUZA, Z., NAKAYAMA, M., MATSUDA, M., TURP, A., NDJETEHE, E., ENCHEVA, V., KUDO, N. R., KOSEKI, H., SASAKI, H. & HAJKOVA, P. 2016. De novo DNA methylation drives 5hmC accumulation in mouse zygotes. *Nature Cell Biology,* 18**,** 225-233.

CAMPBELL, J. M., NOTTLE, M. B., VASSILIEV, I., MITCHELL, M. & LANE, M. 2012. Insulin Increases Epiblast Cell Number of In Vitro Cultured Mouse Embryos via the PI3K/GSK3/p53 Pathway. *Stem Cells and Development,* 21**,** 2430-2441.

CARDOZO, E. R., KARMON, A. E., GOLD, J., PETROZZA, J. C. & STYER, A. K. 2016. Reproductive outcomes in oocyte donation cycles are associated with donor BMI. *Human Reproduction,* 31**,** 385-392.

CAREY, B. W., FINLEY, L. W. S., CROSS, J. R., ALLIS, C. D. & THOMPSON, C. B. 2015. Intracellular [agr]-ketoglutarate maintains the pluripotency of embryonic stem cells. *Nature,* 518**,** 413-416.

CHEN, F., BIAN, K., TANG, Q., FEDELES, B. I., SINGH, V., HUMULOCK, Z. T., ESSIGMANN, J. M. & LI, D. 2017. Oncometabolites d- and l-2-Hydroxyglutarate Inhibit the AlkB Family DNA Repair Enzymes under Physiological Conditions. *Chemical Research in Toxicology,* 30**,** 1102-1110.

CHOI, C., GANJI, S. K., DEBERARDINIS, R. J., HATANPAA, K. J., RAKHEJA, D., KOVACS, Z., YANG, X.-L., MASHIMO, T., RAISANEN, J. M., MARIN-VALENCIA, I., PASCUAL, J. M., MADDEN, C. J., MICKEY, B. E., MALLOY, C. R., BACHOO, R. M. & MAHER, E. A. 2012. 2-hydroxyglutarate detection by magnetic resonance spectroscopy in IDH-mutated patients with gliomas. *Nature Medicine,* 18**,** 624-629.

DANG, L., WHITE, D. W., GROSS, S., BENNETT, B. D., BITTINGER, M. A., DRIGGERS, E. M., FANTIN, V. R., JANG, H. G., JIN, S., KEENAN, M. C., MARKS, K. M.,

PRINS, R. M., WARD, P. S., YEN, K. E., LIAU, L. M., RABINOWITZ, J. D., CANTLEY, L. C., THOMPSON, C. B., VANDER HEIDEN, M. G. & SU, S. M. 2009. Cancer-associated IDH1 mutations produce 2-hydroxyglutarate. *Nature,* 462**,** 739-744.

DUMOLLARD, R., WARD, Z., CARROLL, J. & DUCHEN, M. R. 2007. Regulation of redox metabolism in the mouse oocyte and embryo. *Development,* 134**,** 455.

DZITOYEVA, S., CHEN, H. & MANEV, H. 2012. Effect of aging on 5-hydroxymethylcytosine in brain mitochondria. *Neurobiology of Aging,* 33**,** 2881-2891.

FIGUEROA, M. E., ABDEL-WAHAB, O., LU, C., WARD, P. S., PATEL, J., SHIH, A., LI, Y., BHAGWAT, N., VASANTHAKUMAR, A., FERNANDEZ, H. F., TALLMAN, M. S., SUN, Z., WOLNIAK, K., PEETERS, J. K., LIU, W., CHOE, S. E., FANTIN, V. R., PAIETTA, E., LÖWENBERG, B., LICHT, J. D., GODLEY, L. A., DELWEL, R., VALK, P. J. M., THOMPSON, C. B., LEVINE, R. L. & MELNICK, A. 2010. Leukemic IDH1 and IDH2 mutations result in a hypermethylation phenotype, disrupt TET2 function, and impair hematopoietic differentiation. *Cancer Cell,* 18**,** 553-567.

FLEMING, T. P., VELAZQUEZ, M. A., ECKERT, J. J., LUCAS, E. S. & WATKINS, A. J. 2012. Nutrition of females during the peri-conceptional period and effects on foetal programming and health of offspring. *Animal Reproduction Science,* 130**,** 193-197.

GARDNER, D. K. & LANE, M. 1993. Amino acids and ammonium regulate mouse embryo development in culture. *Biology of Reproduction,* 48**,** 377-385.

GARDNER, D. K. & LEESE, H. J. 1990. Concentrations of nutrients in mouse oviduct fluid and their effects on embryo development and metabolism in vitro. *Journal of Reproduction and Fertility,* 88**,** 361-368.

GROSS, S., CAIRNS, R. A., MINDEN, M. D., DRIGGERS, E. M., BITTINGER, M. A., JANG, H. G., SASAKI, M., JIN, S., SCHENKEIN, D. P., SU, S. M., DANG, L., FANTIN, V. R. & MAK, T. W. 2010. Cancer-associated metabolite 2-hydroxyglutarate accumulates in acute myelogenous leukemia with isocitrate dehydrogenase 1 and 2 mutations. *The Journal of Experimental Medicine,* 207**,** 339-344.

GUILHAMON, P., ESKANDARPOUR, M., HALAI, D., WILSON, G. A., FEBER, A., TESCHENDORFF, A. E., GOMEZ, V., HERGOVICH, A., TIRABOSCO, R., FERNANDA AMARY, M., BAUMHOER, D., JUNDT, G., ROSS, M. T., FLANAGAN, A. M. & BECK, S. 2013. Meta-analysis of IDH-mutant cancers identifies EBF1 as an interaction partner for TET2. *Nature Communications,* 4**,** 2166.

HAN, L., REN, C., LI, L., LI, X., GE, J., WANG, H., MIAO, Y.-L., GUO, X., MOLEY, K. H., SHU, W. & WANG, Q. 2018. Embryonic defects induced by maternal obesity in mice derive from Stella insufficiency in oocytes. *Nature Genetics,* 50**,** 432-442.

HOUGHTON, F. D., HAWKHEAD, J. A., HUMPHERSON, P. G., HOGG, J. E., BALEN, A. H., RUTHERFORD, A. J. & LEESE, H. J. 2002. Non-invasive amino acid turnover predicts human embryo developmental capacity. *Human reproduction (Oxford, England),* 17**,** 999-1005.

HOUGHTON, F. D. & LEESE, H. J. 2004. Metabolism and developmental competence of the preimplantation embryo. *European Journal of Obstetrics & Gynecology and Reproductive Biology,* 115**,** S92-S96.

HOUGHTON, F. D., THOMPSON, J. G., KENNEDY, C. J. & LEESE, H. J. 1996. Oxygen consumption and energy metabolism of the early mouse embryo. *Molecular Reproduction and Development,* 44**,** 476-485.

IGOSHEVA, N., ABRAMOV, A. Y., POSTON, L., ECKERT, J. J., FLEMING, T. P., DUCHEN, M. R. & MCCONNELL, J. 2010. Maternal Diet-Induced Obesity Alters Mitochondrial Activity and Redox Status in Mouse Oocytes and Zygotes. *PLOS ONE,* 5**,** e10074.

INOUE, A., SHEN, L., MATOBA, S. & ZHANG, Y. 2015. Haploinsufficiency, but Not Defective Paternal 5mC Oxidation, Accounts for the Developmental Defects of Maternal Tet3 Knockouts. *Cell Reports,* 10**,** 463-470.

IQBAL, K., JIN, S.-G., PFEIFER, G. P. & SZABÓ, P. E. 2011. Reprogramming of the paternal genome upon fertilization involves genome-wide oxidation of 5-methylcytosine.

Proceedings of the National Academy of Sciences of the United States of America, 108**,** 3642-3647.

ITO, S., D'ALESSIO, A. C., TARANOVA, O. V., HONG, K., SOWERS, L. C. & ZHANG, Y. 2010. Role of Tet proteins in 5mC to 5hmC conversion, ES cell self-renewal, and ICM specification. *Nature,* 466**,** 1129-1133.

ITO, S., SHEN, L., DAI, Q., WU, S. C., COLLINS, L. B., SWENBERG, J. A., HE, C. & ZHANG, Y. 2011. Tet proteins can convert 5-methylcytosine to 5-formylcytosine and 5-carboxylcytosine. *Science,* 333**,** 1300-1303.

JIN, S.-G., JIANG, Y., QIU, R., RAUCH, T. A., WANG, Y., SCHACKERT, G., KREX, D., LU, Q. & PFEIFER, G. P. 2011. 5-Hydroxymethylcytosine Is Strongly Depleted in Human Cancers but Its Levels Do Not Correlate with IDH1 Mutations. *Cancer Research,* 71**,** 7360-7365.

JOBERTY, G., BOESCHE, M., BROWN, J. A., EBERHARD, D., GARTON, N. S., HUMPHREYS, P. G., MATHIESON, T., MUELBAIER, M., RAMSDEN, N. G., READER, V., RUEGER, A., SHEPPARD, R. J., WESTAWAY, S. M., BANTSCHEFF, M., LEE, K., WILSON, D. M., PRINJHA, R. K. & DREWES, G. 2016. Interrogating the Druggability of the 2-Oxoglutarate-Dependent Dioxygenase Target Class by Chemical Proteomics. *ACS Chemical Biology,* 11**,** 2002-2010.

JUNGHEIM, E. S. & MOLEY, K. H. 2010. Current knowledge of obesity's effects in the pre- and periconceptional periods, and avenues for future research. *American Journal of Obstetrics and Gynecology,* 203**,** 525-530.

JUNGHEIM, E. S., SCHOELLER, E. L., MARQUARD, K. L., LOUDEN, E. D., SCHAFFER, J. E. & MOLEY, K. H. 2010. Diet-Induced Obesity Model: Abnormal Oocytes and Persistent Growth Abnormalities in the Offspring. *Endocrinology,* 151**,** 4039-4046.

KANG, E., WU, G., MA, H., LI, Y., TIPPNER-HEDGES, R., TACHIBANA, M., SPARMAN, M., WOLF, D. P., SCHOLER, H. R. & MITALIPOV, S. 2014. Nuclear reprogramming by interphase cytoplasm of two-cell mouse embryos. *Nature,* 509**,** 101-104.

KIM, C. H., LEE, E. K., CHOI, Y. J., AN, H. J., JEONG, H. O., PARK, D., KIM, B. C., YU, B. P., BHAK, J. & CHUNG, H. Y. 2016. Short-term calorie restriction ameliorates genomewide, age-related alterations in DNA methylation. *Aging Cell,* 15**,** 1074-1081.

KOIVUNEN, P., LEE, S., DUNCAN, C. G., LOPEZ, G., LU, G., RAMKISSOON, S., LOSMAN, J. A., JOENSUU, P., BERGMANN, U., GROSS, S., TRAVINS, J., WEISS, S., LOOPER, R., LIGON, K. L., VERHAAK, R. G. W., YAN, H. & KAELIN, W. G., JR. 2012. Transformation by the (R)-enantiomer of 2-hydroxyglutarate linked to EGLN activation. *Nature,* 483**,** 484-488.

KRAMEN, M. A. & BIGGERS, J. D. 1971. Uptake of Tricarboxylic Acid Cycle Intermediates by Preimplantation Mouse Embryos In Vitro. *Proceedings of the National Academy of Sciences of the United States of America,* 68**,** 2656-2659.

KRELL, D., ASSOKU, M., GALLOWAY, M., MULHOLLAND, P., TOMLINSON, I. & BARDELLA, C. 2011. Screen for IDH1, IDH2, IDH3, D2HGDH and L2HGDH Mutations in Glioblastoma. *PLoS ONE,* 6**,** e19868.

KUBANDOVÁ, J., ČIKOŠ, Š., BURKUŠ, J., CZIKKOVÁ, S., KOPPEL, J. & FABIAN, D. 2014. Amount of maternal body fat significantly affected the quality of isolated mouse preimplantation embryos and slowed down their development. *Theriogenology,* 81**,** 187-195.

LANE, M. & GARDNER, D. 1997. Differential regulation of mouse embryo development and viability by amino acids. *Reproduction,* 109**,** 153-164.

LANE, M. & GARDNER, D. K. 1995. Removal of embryo-toxic ammonium from the culture medium by in situ enzymatic conversion to glutamate. *Journal of Experimental Zoology,* 271**,** 356-363.

LANE, M. & GARDNER, D. K. 2005. Mitochondrial Malate-Aspartate Shuttle Regulates Mouse Embryo Nutrient Consumption. *Journal of Biological Chemistry,* 280**,** 18361-18367.

LANE, M., ROBKER, R. L. & ROBERTSON, S. A. 2014. Parenting from before conception. *Science,* 345**,** 756-760.

LEE, K., HAMM, J., WHITWORTH, K., SPATE, L., PARK, K.-W., MURPHY, C. N. & PRATHER, R. S. 2014. Dynamics of TET family expression in porcine preimplantation embryos is related to zygotic genome activation and required for the maintenance of NANOG. *Developmental Biology,* 386**,** 86-95.

LEESE, H. 1991. Metabolism of the preimplantation mammalian embryo. *Oxford Reviews of Reproductive Biology,* 13**,** 35.

LEESE, H. J. 1995. Metabolic control during preimplantation mammalian development. *Human Reproduction Update,* 1**,** 63-72.

LEONARDI, R., SUBRAMANIAN, C., JACKOWSKI, S. & ROCK, C. O. 2012. Cancer-associated isocitrate dehydrogenase mutations inactivate NADPH-dependent reductive carboxylation. *Journal of Biological Chemistry,* 287**,** 14615-14620.

LI, Y. & O'NEILL, C. 2012. Persistence of Cytosine Methylation of DNA following Fertilisation in the Mouse. *PLOS ONE,* 7**,** e30687.

LI, Y. & O'NEILL, C. 2013. 5′-methylcytosine and 5′-hydroxymethylcytosine Each Provide Epigenetic Information to the Mouse Zygote. *PLOS ONE,* 8**,** e63689.

LOSMAN, J.-A. & KAELIN, W. G. 2013. What a difference a hydroxyl makes: mutant IDH, (R)-2-hydroxyglutarate, and cancer. *Genes & Development,* 27**,** 836-852.

LU, C., WARD, P. S., KAPOOR, G. S., ROHLE, D., TURCAN, S., ABDEL-WAHAB, O., EDWARDS, C. R., KHANIN, R., FIGUEROA, M. E., MELNICK, A., WELLEN, K. E., O/'ROURKE, D. M., BERGER, S. L., CHAN, T. A., LEVINE, R. L., MELLINGHOFF, I. K. & THOMPSON, C. B. 2012. IDH mutation impairs histone demethylation and results in a block to cell differentiation. *Nature,* 483**,** 474-478.

LUZZO, K. M., WANG, Q., PURCELL, S. H., CHI, M., JIMENEZ, P. T., GRINDLER, N., SCHEDL, T. & MOLEY, K. H. 2012. High Fat Diet Induced Developmental Defects

in the Mouse: Oocyte Meiotic Aneuploidy and Fetal Growth Retardation/Brain Defects. *PLOS ONE,* 7**,** e49217.

MCPHERSON, N. O., BELL, V. G., ZANDER-FOX, D. L., FULLSTON, T., WU, L. L., ROBKER, R. L. & LANE, M. 2015. When two obese parents are worse than one! Impacts on embryo and fetal development. *American Journal of Physiology - Endocrinology and Metabolism,* 309**,** E568-E581.

MCPHERSON, N. O., ZANDER-FOX, D. & LANE, M. 2014. Stimulation of mitochondrial embryo metabolism by dichloroacetic acid in an aged mouse model improves embryo development and viability. *Fertility and Sterility,* 101**,** 1458-1466.e5.

MITCHELL, M., SCHULZ, S. L., ARMSTRONG, D. T. & LANE, M. 2009. Metabolic and Mitochondrial Dysfunction in Early Mouse Embryos Following Maternal Dietary Protein Intervention. *Biology of Reproduction,* 80**,** 622-630.

NECULA, L. G., MAMBET, C., ALBULESCU, R. & DIACONU, C. C. 2015. Epigenetics in Gastric Carcinogenesis: Tet Genes as Important Players. *Journal of Immunoassay and Immunochemistry,* 36**,** 445-455.

NETTERSHEIM, D., HEUKAMP, L. C., FRONHOFFS, F., GREWE, M. J., HAAS, N., WAHA, A., HONECKER, F., WAHA, A., KRISTIANSEN, G. & SCHORLE, H. 2013. Analysis of TET Expression/Activity and 5mC Oxidation during Normal and Malignant Germ Cell Development. *PLOS ONE,* 8**,** e82881.

PFEIFER, G. P., KADAM, S. & JIN, S.-G. 2013. 5-hydroxymethylcytosine and its potential roles in development and cancer. *Epigenetics & Chromatin,* 6**,** 10-10.

POPE, W., PRINS, R., ALBERT THOMAS, M., NAGARAJAN, R., YEN, K., BITTINGER, M., SALAMON, N., CHOU, A., YONG, W., SOTO, H., WILSON, N., DRIGGERS, E., JANG, H., SU, S., SCHENKEIN, D., LAI, A., CLOUGHESY, T., KORNBLUM, H., WU, H., FANTIN, V. & LIAU, L. 2012. Non-invasive detection of 2-hydroxyglutarate and other metabolites in IDH1 mutant glioma patients using magnetic resonance spectroscopy. *Journal of Neuro-Oncology,* 107**,** 197-205.

SANTOS, F., HENDRICH, B., REIK, W. & DEAN, W. 2002. Dynamic Reprogramming of DNA Methylation in the Early Mouse Embryo. *Developmental Biology,* 241**,** 172-182.

SANTOS, F., PETERS, A. H., OTTE, A. P., REIK, W. & DEAN, W. 2005. Dynamic chromatin modifications characterise the first cell cycle in mouse embryos. *Developmental Biology,* 280**,** 225-236.

SASAKI, M., KNOBBE, C. B., ITSUMI, M., ELIA, A. J., HARRIS, I. S., CHIO, I. I. C., CAIRNS, R. A., MCCRACKEN, S., WAKEHAM, A., HAIGHT, J., TEN, A. Y., SNOW, B., UEDA, T., INOUE, S., YAMAMOTO, K., KO, M., RAO, A., YEN, K. E., SU, S. M. & MAK, T. W. 2012. D-2-hydroxyglutarate produced by mutant IDH1 perturbs collagen maturation and basement membrane function. *Genes & Development,* 26**,** 2038-2049.

SCOURZIC, L., MOULY, E. & BERNARD, O. A. 2015. TET proteins and the control of cytosine demethylation in cancer. *Genome Medicine,* 7**,** 9.

SHEN, L., INOUE, A., HE, J., LIU, Y., LU, F. & ZHANG, Y. 2014a. Tet3 and DNA Replication Mediate Demethylation of Both the Maternal and Paternal Genomes in Mouse Zygotes. *Cell Stem Cell,* 15**,** 459-470.

SHEN, L., SONG, C.-X., HE, C. & ZHANG, Y. 2014b. Mechanism and Function of Oxidative Reversal of DNA and RNA Methylation. *Annual Review of Biochemistry,* 83**,** 585-614.

SIMMONS, J. M., MÜLLER, T. A. & HAUSINGER, R. P. 2008. Fe(II)/alpha-ketoglutarate hydroxylases involved in nucleobase, nucleoside, nucleotide, and chromatin metabolism. *Dalton Transactions (Cambridge, England : 2003)***,** 5132-5142.

STARKOV, A. A., FISKUM, G., CHINOPOULOS, C., LORENZO, B. J., BROWNE, S. E., PATEL, M. S. & BEAL, M. F. 2004. Mitochondrial α-Ketoglutarate Dehydrogenase Complex Generates Reactive Oxygen Species. *The Journal of Neuroscience,* 24**,** 7779-7788.

SUDHAMALLA, B., DEY, D., BRESKI, M. & ISLAM, K. 2017. A rapid mass spectrometric method for the measurement of catalytic activity of ten-eleven translocation enzymes. *Analytical Biochemistry,* 534**,** 28-35.

TAHILIANI, M., KOH, K. P., SHEN, Y., PASTOR, W. A., BANDUKWALA, H., BRUDNO, Y., AGARWAL, S., IYER, L. M., LIU, D. R., ARAVIND, L. & RAO, A. 2009. Conversion of 5-Methylcytosine to 5-Hydroxymethylcytosine in Mammalian DNA by MLL Partner TET1. *Science (New York, N.Y.),* 324**,** 930-935.

TRAN, K. A., DILLINGHAM, C. M. & SRIDHARAN, R. 2018. The role of α-ketoglutarate-dependent proteins in pluripotency acquisition and maintenance. *Journal of Biological Chemistry,* 294, 5408-5419.

TRIMARCHI, J. R., LIU, L., PORTERFIELD, D. M., SMITH, P. J. S. & KEEFE, D. L. 2000. Oxidative Phosphorylation-Dependent and -Independent Oxygen Consumption by Individual Preimplantation Mouse Embryos. *Biology of Reproduction,* 62**,** 1866-1874.

TSUKADA, Y.-I., AKIYAMA, T. & NAKAYAMA, K. I. 2015. Maternal TET3 is dispensable for embryonic development but is required for neonatal growth. *Scientific Reports,* 5**,** 15876.

WAKEFIELD, S. L., LANE, M. & MITCHELL, M. 2011. Impaired Mitochondrial Function in the Preimplantation Embryo Perturbs Fetal and Placental Development in the Mouse. *Biology of Reproduction,* 84**,** 572-580.

WATKINS, A., LUCAS, E., TORRENS, C., CLEAL, J., GREEN, L., OSMOND, C., ECKERT, J., GRAY, W., HANSON, M. & FLEMING, T. 2010. Maternal low-protein diet during mouse pre-implantation development induces vascular dysfunction and altered renin-angiotensin-system homeostasis in the offspring. *The British Journal of Nutrition,* 103**,** 1762-1770.

WATKINS, A. J., LUCAS, E. S., WILKINS, A., CAGAMPANG, F. R. & FLEMING, T. P. 2011. Maternal periconceptional and gestational low protein diet affects mouse

offspring growth, cardiovascular and adipose phenotype at 1 year of age. *PLoS One,* 6**,** e28745.

WATKINS, A. J., URSELL, E., PANTON, R., PAPENBROCK, T., HOLLIS, L., CUNNINGHAM, C., WILKINS, A., PERRY, V. H., SHETH, B., KWONG, W. Y., ECKERT, J. J., WILD, A. E., HANSON, M. A., OSMOND, C. & FLEMING, T. P. 2008a. Adaptive Responses by Mouse Early Embryos to Maternal Diet Protect Fetal Growth but Predispose to Adult Onset Disease. *Biology of Reproduction,* 78**,** 299-306.

WATKINS, A. J., WILKINS, A., CUNNINGHAM, C., PERRY, V. H., SEET, M. J., OSMOND, C., ECKERT, J. J., TORRENS, C., CAGAMPANG, F. R. A., CLEAL, J., GRAY, W. P., HANSON, M. A. & FLEMING, T. P. 2008b. Low protein diet fed exclusively during mouse oocyte maturation leads to behavioural and cardiovascular abnormalities in offspring. *The Journal of Physiology,* 586**,** 2231-2244.

WHITTINGHAM, D. G. 1969. The Failure of Lactate and Phosphoenolpyruvate to Support Development of the Mouse Zygote in Vitro. *Biology of Reproduction,* 1**,** 381-386.

WU, S. C. & ZHANG, Y. 2010. Active DNA demethylation: many roads lead to Rome. *Nature Reviews Molecular Cell Biology,* 11**,** 607.

WU, X. & ZHANG, Y. 2017. TET-mediated active DNA demethylation: mechanism, function and beyond. *Nature Reviews Genetics,* 18**,** 517.

XU, W., YANG, H., LIU, Y., YANG, Y., WANG, P., KIM, S.-H., ITO, S., YANG, C., WANG, P., XIAO, M.-T., LIU, L.-X., JIANG, W.-Q., LIU, J., ZHANG, J.-Y., WANG, B., FRYE, S., ZHANG, Y., XU, Y.-H., LEI, Q.-Y., GUAN, K.-L., ZHAO, S.-M. & XIONG, Y. 2011. Oncometabolite 2-Hydroxyglutarate Is a Competitive Inhibitor of α-Ketoglutarate-Dependent Dioxygenases. *Cancer Cell,* 19**,** 17-30.

YE, D., MA, S., XIONG, Y. & GUAN, K.-L. 2013. R-2-hydroxyglutarate as the key effector of IDH mutations promoting oncogenesis. *Cancer Cell,* 23**,** 274-276.

ZANDER-FOX, D. L., FULLSTON, T., MCPHERSON, N. O., SANDEMAN, L., KANG, W. X., GOOD, S. B., SPILLANE, M. & LANE, M. 2015. Reduction of Mitochondrial

Function by FCCP During Mouse Cleavage Stage Embryo Culture Reduces Birth Weight and Impairs the Metabolic Health of Offspring. *Biology of Reproduction,* 92, 1-11.

ZHANG, Z., HE, C., ZHANG, L., ZHU, T., LV, D., LI, G., SONG, Y., WANG, J., WU, H., JI, P. & LIU, G. 2019. Alpha-ketoglutarate affects murine embryo development through metabolic and epigenetic modulations. *Reproduction,* 158**,** 123-133.

ZHU, Q., STÖGER, R. & ALBERIO, R. 2018. A Lexicon of DNA Modifications: Their Roles in Embryo Development and the Germline. *Frontiers in Cell and Developmental Biology,* 6**,** 24.

Chapter 4 *In vitro* maturation impairs the ability of lysine demethylases to remove H3K4 methylation in mouse oocytes

4.1 Chapter Link

In Chapter 3, the effects of α-ketoglutarate and 2-hydroxyglutarate supplemented media on *in vivo* fertilised embryos were explored, where it was clearly shown that 2HG supplementation increased 5mC and reduced 5caC, suggesting that less TET-mediated DNA demethylation was occurring. Given these suggested changes to programming in the early embryo through modulation of metabolism altering TET mediated DNA demethylation, we sought to determine if altering the environment throughout the maturation of the oocyte *in vitro* could alter programming of histone methylation, which is removed through lysine demethylases that also utilise α-ketoglutarate as a substrate.

In vitro maturation (IVM) is another model of environmental perturbation, which may induce similar perturbations in methylation trajectories as observed under modulation of α-ketoglutarate in the preimplantation embryo development form fertilisation to the blastocyst. In addition to the impact of the *in vitro* culture of oocytes, we also sought to examine if the presence of 2-hydroxyglutarate during the IVM period would further impact the oocyte methylation status. We also examined the histone methylation mark H3K4me3, which is removed by the lysine demethylases KDM5s that also uses α-ketoglutarate as a substrate, to assess if other metabolically sensitive proteins would be altered by this inhibition.

4.2 Statement of Authorship

Statement of Authorship

Title of Paper	In vitro maturation impairs the ability of lysine demethylases to remove H3K4 methylation in mouse oocytes
Publication Status	☐ Published ☐ Accepted for Publication ☐ Submitted for Publication ☑ Unpublished and Unsubmitted work written in manuscript style
Publication Details	Written in the style for Journal of Assisted Reproduction and Genetics (JARG)

Principal Author

Name of Principal Author (Candidate)	Alexander Penn
Contribution to the Paper	Study design, performed experiments, analysed and interpreted data, wrote and edited the manuscript
Overall percentage (%)	80%
Certification:	This paper reports on original research I conducted during the period of my Higher Degree by Research candidature and is not subject to any obligations or contractual agreements with a third party that would constrain its inclusion in this thesis. I am the primary author of this paper.
Signature	Date 16/07/2021

Co-Author Contributions

By signing the Statement of Authorship, each author certifies that:

i. the candidate's stated contribution to the publication is accurate (as detailed above);

ii. permission is granted for the candidate in include the publication in the thesis; and

iii. the sum of all co-author contributions is equal to 100% less the candidate's stated contribution.

Name of Co-Author	Deirdre Zander-Fox		
Contribution to the Paper	Assisted in interpretation of data, and editing of the manuscript		
Signature		Date	28/06/2021

Name of Co-Author	Nicole O McPherson		
Contribution to the Paper	Assisted in interpretation of data, and editing of the manuscript		
Signature		Date	4/07/2021

Name of Co-Author	Tod Fullston		
Contribution to the Paper	Assisted in interpretation of data, and editing of the manuscript		
Signature		Date	02/07/2021

Name of Co-Author	Michelle Lane (deceased)		
Contribution to the Paper	Experimental design, assisted in interpretation of data, and editing of the manuscript		
Signature		Date	

Please cut and paste additional co-author panels here as required.

4.3 Abstract

Purpose Oocyte maturation is critical period where the surrounding environment can ensure correct embryonic development and offspring health, e.g. via nutrient supply or can program aberrant outcomes. During this period, the KDM5 lysine demethylase enzyme family removes methylation on histone 3 lysine 4 trimethylation (H3K4me3) to dimethylation (H3K4me2) and monomethylation (H3K4me1). It uses the TCA cycle intermediary α-ketoglutarate as a substrate, sourced from the nutrient supply, which may provide an epigenetic link between nutrient supply and altered gene expression of genes post fertilisation, thus modulating embryonic genome activation and embryo development. Whether oocyte *in vitro* maturation (IVM) alters this process compared with ovulated oocytes will be examined.

Methods Immature CBAF1 cumulus enclosed oocytes (COCs) were aspirated and matured *in vitro* with or without 2-hydroxyglutarate (0 mM or 20 mM), a competitive inhibitor of α-ketoglutarate, and compared with ovulated oocytes. After maturation, oocytes were compared for cumulus expansion, global KDM5A and KDM5C concentration and localisation (by densitometry), and global levels of H3K4me3, H3K4me2 and H3K4me1. Oocytes were fertilised and cultured to the 2-cell stage and compared with in-vivo fertilised and flushed 2-cells for global levels of H3K4me3, H3K4me2 and H3K4me1. Embryos were also cultured as above for 96 h to assess blastocyst development rates and inner cell mass and trophectoderm proliferation differences.

Results We demonstrated that culture with the inhibitor 2-hydroxyglutarate (IVM + 2HG) reduced cumulus expansion after *in vitro* maturation and increased whole oocyte KDM5A in the region of mitotic spindles relative to standard IVM. Further, in whole IVM derived oocytes, global concentration of KDM5A is increased compared with ovulated MII, and further increased under IVM + 2HG. Oocyte global H3K4me3 is increased in IVM and IVM + 2HG compared with ovulated MII, with H3K4me1 levels being unchanged.

2-cell H3K4me3 was increased in IVF compared to flushed 2-cells, with further increase in IVM and IVM + 2HG. 2-cell H3K4me2 was increased in IVM and IVM + 2HG relative to both

IVF and flushed 2-cells, with no difference between IVF and flushed, and IVM and IVM + 2HG respectively. 2-cell H3K4me1 increases in IVF and IVM compared to flushed 2-cells, but not IVM + 2HG.

Embryo development under IVM and IVM + 2HG on day 3 had more 4-6 cell embryos and fewer 8-cell and compacting embryos relative to IVF, and fewer hatching blastocysts on day 5 with decreased inner cell mass and total cell count in IVM + 2HG compared to IVF and IVM compared to IVF.

Conclusion We have demonstrated that oocyte IVM alters H3K4me3 and H3K4me2 both in the oocyte and in the 2-cell embryo. The addition of 2HG during this period caused further delays in embryo development and reduced inner cell mass cell numbers. This shows that the period of oocyte maturation is sensitive to alterations in lysine demethylase substrate availability, suggesting a possible epigenetic mechanism linking sub-optimal oocyte/ovarian environment with compromised embryo and offspring health as seen from IVM.

4.4 Introduction

There is a significant body of research demonstrating the effects of environmental factors impacting chromatin methylation and structure in the developing embryo which can in turn program offspring developmental health trajectory (Akiyama et al., 2011, Bakhtari et al., 2014, Madogwe et al., 2020, Maekawa et al., 2016, Niu et al., 2015, Salminen et al., 2014). In particular, there has been significant focus on epigenetic alterations due to maternal obesity in embryos after fertilisation (Han et al., 2018), with alterations due to the presence of metabolic disruption (Zhang et al., 2019), which again can program offspring to be at increased risk of obesity, hypertension and metabolic syndrome (Ge et al., 2014, Grindler and Moley, 2013, Gu et al., 2015, Han et al., 2018, Jungheim et al., 2010, Luzzo et al., 2012, Sinclair et al., 2007). However, there has been less focus on the impact of environmental impacts during oocyte maturation from immature germinal vesicle (GV) oocytes that are arrested at metaphase I through to mature oocytes at metaphase II (MII). This oocyte maturation usually occurs *in vivo*, however, can also occur *in vitro* through *in vitro* maturation (IVM) in both the primary industry and the human setting.

IVM of oocytes is routinely carried out in domestic animals for the production of oocytes and embryos to be used for breeding (Camargo et al., 2019, Gegenfurtner et al., 2020, Geshi et al., 2000, Green et al., 2016, Kubisch et al., 1995, Rizos et al., 2002, Stokes et al., 2005, Wrenzycki and Stinshoff, 2013). It can also be used in human assisted reproduction, predominantly due to requirement of reduced hormone concentrations for ovarian stimulation thus minimising risk of ovarian hyperstimulation syndrome (OHSS) (Vuong et al., 2018, Vuong et al., 2020), or for fertility preservation especially in oncology patients (Yin et al., 2016).

Despite improvements to culture systems used for the maturation of oocytes, oocytes matured *in vitro* still result in poorer pregnancy rates in clinical cycles (Buckett et al., 2008) and poorer offspring health outcomes that include reduced adult cardiac output and pulse rate in animal models compared with *in vivo* ovulated oocytes (Eppig et al., 2009). These alterations shown in offspring health, presumably due to metabolic perturbations during oocyte growth, have been

suggested to be transmitted into offspring via epigenetic programming changes in the oocyte/embryo (Oblette et al., 2019).

Epigenetic programming can occur through DNA methylation as presented in Chapter 2 and Chapter 3, however can also be controlled through changes to histones, which bind DNA to package it into chromatin. Chromatin can be modified through chemical modifications to histones, including addition of methyl groups to specific lysine residues. Histone methylation in the form of histone 3 lysine 4 trimethylation (H3K4me3) signals for increased transcription of the DNA (Guillemette et al., 2011). Dimethylation (H3K4me2) is also associated with gene activation, however to a lesser magnitude and extent as H3K4me3 (Cheng et al., 2014, Peña et al., 2008). Monomethylation (H3K4me1) is more context dependent (i.e. dependent on the area of genome and other histone modifications present), though appears to be generally associated with repression of transcription (Cheng et al., 2014) (See Chapter 1.10.3 for more detailed information on the cellular effects of each H3K4 variant). Alterations to the metabolic environment within the developing oocyte and embryo have been shown to result in alterations to chromatin structure (Liu et al., 2015).

Histone methylation can be removed by the lysine demethylase 5 (KDM5) family of proteins, consisting of KDM5A-D (also known as JARID1A-D), all of which remove methylation from H3K4 using α-ketoglutarate as a substrate (Gu and Lee, 2013, Joberty et al., 2016, Kaelin Jr and McKnight, 2013, Tran et al., 2018, Xu et al., 2011). KDM5s oxidise the methyl bond to stepwise remove the methylation from H3K4me3 to H3K4me2, and further to H3K4me1 (He and Kidder, 2017). In oocytes, over three quarters of the genes involved in embryonic genome activation (Dahl et al., 2016, Park et al., 2013) are marked by H3K4me3, particularly at promoter regions. Further, in normal *in vitro* maturation, H3K4me3 reduces linearly over time (Sha et al., 2018), with H3K4me2 increasing from 10 h of IVM and H3K4me1 from 2 h (Sha et al., 2018).

It has been shown in animal models that KDM5 processes are critical for survival, with a knockdown of KDM5 proteins within the embryo leading to neonatal death in the first few days after birth (Albert et al., 2013, Catchpole et al., 2011). Similar to TET proteins, KDM5A-D require α-ketoglutarate as a cofactor and, therefore, they are influenced by mitochondrial metabolism and substrate concentration/availability (See Chapter 4.3) (Albert et al., 2013, Donohoe and Bultman, 2012, Gu and Lee, 2013, He and Kidder, 2017, Jensen et al., 2005, Joberty et al., 2016, Niu et al., 2015). The cofactor for KDM5A-D is α-ketoglutarate and is produced through the TCA cycle, which uses pyruvate as the initial cofactor. Throughout oocyte maturation, pyruvate is essential oocyte development and is delivered to the oocyte by the surrounding cumulus cells (Yeo et al., 2009).

2-hydroxyglutarate (2HG) is structurally similar to α-ketoglutarate (Figure 1.2b), acting as a competitive inhibitor as it binds the active site of KDM5A-D, however, cannot be cleaved as an energy source for α-ketoglutarate dependent enzymes, including KDM5s. We have previously demonstrated the effects of 2HG on DNA methylation when added to preimplantation embryo culture (See Chapter 3.3).

While there is an observed impact of the addition of 2HG into development post fertilisation, there is no known impact of competitive inhibition of α -ketoglutarate on KDM5 proteins in the maturing oocyte, with little information specifically on the impact of IVM±2HG on H3K4 methylation dynamics in the post embryonic genome activation (EGA) 2-cell embryo and development to the blastocyst stage.

The objectives of this study are to demonstrate the effect of IVM with or without supplementation of 2HG (which will competitively inhibit α–ketoglutarate binding) on KDM5 protein concentration or localisation in the mature oocyte as compared with ovulated oocytes. In addition, this study will also investigate the effects of IVM and 2HG on H3K4me1-3 methylation in the 2-cell post embryonic genome activation to highlight any global trends for gene activation or repression and determine their effects on embryo development and blastocyst cell numbers.

4.5 Materials and Methods

4.5.1 Mice

All animal work has been approved by the University of Adelaide Animal Ethics committee (M-2015-259, M-2017-046 and M-119-13) and performed in accordance with the Australian Code for the Care and Use of Animals for Scientific Purposes 8th edition. Female C57Bl6 x CBA (CBAF1) mice aged 4-6 weeks were fed standard rodent chow (Specialty Feeds, Glen Forrest, Western Australia, Australia) with *ad libitum* access to food and water. Mice were maintained in a 12:12 h light: dark cycle. For collection of immature oocytes, mice were superovulated by intraperitoneal (i.p.) injection of 5 IU pregnant mare's serum gonadotrophin (PMSG, Folligon; Intervet, Bendigo East, Australia). 46 h after PMSG administration, immature oocytes were collected. For collection of mature oocytes and 2-cell embryos, superovulation with 5 IU PMSG was followed 48h later by i.p. injection of 5 IU chorionic gonadotrophin (hCG, Chorulon; Intervet). Mature oocytes were collected from oviducts 13h-15 h post hCG, while 2-cell embryos were flushed from the oviduct at 46 h post hCG.

4.5.2 Media composition

All chemicals were purchased from Sigma-Aldrich (St Louis, Missouri, USA) unless otherwise stated. GMOPS (Vitrolife; Gothenburg, Sweden) + 5% human serum albumin (HSA, Vitrolife) was used for embryo collection and handling. Immature COCs were handled in GMOPS + 5% foetal bovine serum (FBS, Gibco). Oocytes were matured in Defined IVM (D-IVM) medium, formulated from commercial G2 Plus (Vitrolife) supplemented with 0.055 g/L pyruvic acid, 1 mg/mL fetuin, 50 mIU/mL recombinant follicle stimulating hormone (FSH, Merck Serono) and10 ng/mL epidermal-like growth factor (EGF). 2HG media was base D-IVM media supplemented with 20 mM DL-α-hydroxyglutaric acid (2HG). Media used for sperm handling and insemination was G-IVF Plus which contains 5% HSA (Vitrolife). Media used for embryo culture was commercial G1 Plus and G2 Plus media which is also pre-supplemented with 5% HSA (Vitrolife).

4.5.3 Oocyte and 2-cell embryo collection

COCs were aspirated from the ovaries of mice 46 h after PMSG injection. COCs were aspirated into GMOPS + 10% FBS and matured. Mature oocytes were collected from oviducts 13-15 h post hCG into GMOPS Plus and either fertilised and cultured as per Section 4.5.6 or fixed for immunocytochemistry. For MII oocytes for immunocytochemistry, oocytes were collected into GMOPS Plus containing 1mg/mL hyaluronidase (Type IV-S), with cumulus cells removed via repeated pipetting and washed in GMOPS Plus, and then fixed in 4% paraformaldehyde in PBS (PFA) overnight at 4ºC, and then stored in PBS + 4.0 mg/mL polyvinylpyrrolidone (PBS/PVP) at 4ºC for use as MII oocytes for immunocytochemistry. In-vivo derived 2-cell embryos were flushed from the oviduct 32 h post putative fertilisation at mid dark cycle into GMOPS Plus and fixed in 4% PFA overnight, and then stored in PBS/PVP at 4ºC to then undergo immunocytochemistry.

4.5.4 *In vitro* maturation of mouse cumulus oocyte complexes (COCs)

Aspirated and collected cumulus-oocyte complexes (COCs) were added to 35mm dishes containing D-IVM media, or D-IVM media supplemented with 20 mM 2HG, with ~10 COCs per mL of maturation media. Dishes were lightly agitated to separate COCs to allow independent cumulus expansion and maturation. COCs were matured at 37ºC 6% CO_2 5%O_2 for 16 h. The 2HG concentration of 20 mM was selected as this was the 2HG concentration observed in gliomal cancers (Choi et al., 2012, Dang et al., 2009, Gross et al., 2010), and to mirror the concentration of 2HG used in Chapter 3.

4.5.5 Scoring mature COCs for cumulus expansion

Cumulus expansion was assessed (blinded to treatment group) according to the 0-4 scale as described previously (Vanderhyden et al., 1990). On this scale, an expansion class 0 indicates no cumulus expansion characterised by adherence of cumulus cells to the culture dish, a class 1 the minimum response where cumulus cells have a glistening appearance and very few cells attach to the dish, a class 2 shows expansion of the outer layers of cumulus cells only, a class 3 indicates expansion of all layers of cumulus cells save the layer immediately next to the zona pellucida (corona radiata), and a class 4 indicates the maximum expansion, with expansion of all layers including the corona radiata (Figure S4.2). After scoring, mature COCs were either washed in GMOPS + 5% HSA and used for *in vitro* fertilisation, or were denuded mechanically via pipetting in GMOPS Plus, and fixed in 4% paraformaldehyde in PBS (4% PFA) overnight, then stored in PBS/PVP at 4ºC for immunofluorescence staining.

4.5.6 *In vitro* fertilisation and embryo culture

Approximately 30 min before fertilisation, sperm was collected from a CBAF1 male mouse of proven fertility (i.e., male previously used for natural mating), with sperm collected from the cauda epididymis and vas deferens (Yeo et al., 2009). Sperm was collected and capacitated in equilibrated G-IVF Plus for ~30 min at 37°C 6% CO_2. After 18 ± 0.5 h of IVM, matured oocytes used for *in vitro* fertilisation were removed from IVM media, washed in GMOPS + 5% HSA, and added to drops of G-IVF Plus containing capacitated sperm for 3-4 h at 37°C, 6% CO_2, 5% O_2. Mature ovulated MII oocytes were collected from GMOPS plus and the grouping of oocytes from one oviduct (approximately 15 oocytes) were added per drop of G-IVF Plus containing capacitated sperm for 3-4 h at 37°C, 6% CO_2, 5% O_2.

After fertilisation, presumed zygotes were washed in GMOPS + 5% HSA to remove most of the cumulus cells and placed into culture in groups of 10 putative embryos per 10 µl drop in G1 Plus at 37°C 6% CO_2 5% O_2. For collection of 2-cell embryos, presumed zygotes were cultured for 30 h until late G2 2-cell phase (33 h post insemination). For blastocyst collection, embryos

were cultured in G1 Plus for 50 h (with check for 2-cell at 20 h and move to fresh G1 Plus to remove from any remaining cumulus cells after IVF), then washed in equilibrated G2 Plus and then cultured in G2 Plus for a further 47 h (97 h total culture).

Embryo development was scored on day 2 of culture (20 h, cleavage stage) for 1-cell, 2-cell or 3-cell, day 3 at changeover (50 h, compaction stage) for development <4-cell, 4-cell, 6-cell, 8-cell or a compacting morula, and on day 5 of culture (97 h, late blastocyst stage) for development to morula, early blastocyst (blastocoel less than 50% total embryonic volume), blastocyst, expanded blastocyst or hatching blastocyst. After 97 h of culture (Day 5), blastocysts were then fixed in 4%PFA (as above) and stored in PBS/PVP for cell counting.

4.5.7 Immunofluorescence staining for KDM5A-C in oocytes

Fixed oocytes that have been stored in PBS/PVP were permeabilised in 0.25% Triton X-100 in PBS (TX) for 15 min at room temperature (RT), then blocked overnight in 10% donkey serum (DS) in PBS. Oocytes were then washed once in 0.25% TX, and incubated with primary antibody (Rabbit anti-KDM5A (Abcam; Cambridge, United Kingdom, ab70892), or KDM5C (ab190181, Abcam; Cambridge, United Kingdom)), diluted 1:100 in PBS for 1.5 h at 37°C. Negative control oocytes and embryos (which were undertaken on each experimental day) were incubated in PBS only for 1.5 h at 37°C (therefore omitting the primary antibody). Oocytes were then washed twice in 0.25% TX in PBS, then incubated in secondary antibody 1:100 Donkey anti-Rabbit conjugated to Alexa-488 (ab150073, Abcam), excitation 490 nm, emission 525 nm) for 2 h at room temperature (RT) followed by addition of 1 mM DAPI in PBS (excitation 358 nm, emission 461 nm) for 5 min. Oocytes were then washed twice in GMOPS (Vitrolife), and imaged using the CV1000 spinning disk confocal microscope (Yokogawa; Musashino, Tokyo, Japan) using 40x magnification. Experiments on different days were normalised using green fluorescent beads (Invitrogen; Carlsbad, California, USA, excitation 450 nm, emission 480 nm) run on each day. The positive control used were day 5 blastocysts (Shao et al., 2014), where KDM presence has been previous confirmed. Levels of KDMs were

measured via densitometry of captured images using ImageJ version 1.50e (Schindelin et al., 2012), with captures of whole cytoplasm, in addition to classification of spindle or chromatin staining presence, as characterised by presence of green fluorescence at a level higher than cytoplasmic presence at the region of the mitotic spindles, or directly on top of the DAPI signal for chromatin presence. Oocytes not having reached MII as determined by chromatin alignment on the metaphase plate were excluded from analysis.

4.5.8 Immunofluorescence staining for H3K4me3, me2 and me1 in MII oocytes

Oocytes were stained for H3K4me3, H3K4me2 and H3K4me1 individually. Oocytes were measured using a microscope with photometer to minimise the effect of oocyte loading direction affecting the reading of fluorescence through changes to chromatin orientation, instead capturing total fluorescence through a wider focal plane. Oocytes were permeabilised in 0.5% TX for 15 min at room temperature (RT) and then blocked overnight in 10% DS in PBS at 4°C. Oocytes were then incubated in the primary antibody (rabbit anti-H3K4me3 (ab8580, Abcam); rabbit anti-H3K4me2 (ab7766, Abcam); or rabbit anti-H3K4me1 (ab8895, Abcam) at 1:100 dilution in PBS for 1.5 h at 37°C. Negative control oocytes were prepared via omission of primary antibody (i.e. incubated for the same period in PBS). Oocytes were then washed twice in 0.5% TX and incubated in the secondary antibody. Donkey anti-Rabbit Alexa 488 conjugate (ab150073, Abcam, excitation 490 nm, emission 525 nm) diluted 1:200 in PBS for 2 h at RT protected from light. Oocytes were then washed twice in 0.5% TX.

Oocytes were then placed into confocal loading media (MOPS-HSA) and then mounted onto glass slides in drops of glycerol. Oocytes were then measured for fluorescence on a Leica DMIRB fluorescence microscope with a photometer attachment (Leica; Wetzlar, Germany), taking care to not include polar body in the fluorescence measurement area. Sample readings were auto adjusted to the first IVM *in vitro* matured oocyte measured on each day. Negative control oocytes and mounting media were also measured to measure background fluorescence levels and autofluorescence. After measurement, oocytes were viewed under epifluorescence and chromatin stage was recorded, with oocytes not having reached MII were excluded from analysis.

4.5.9 Immunofluorescence staining for H3K4me3, me2 and me1 in 2-cell embryos

Due to the shape of 2-cell embryos, the fluorescence was measured using confocal microscopy and densitometry. 2-Cell embryos were permeabilised in 0.5% Triton X-100 in PBS (0.5% TX) for 15 min at room temperature (RT) and then blocked overnight in 10% donkey serum in PBS at 4°C. Embryos were then incubated in the primary antibody (rabbit anti-H3K4me3; rabbit anti-H3K4me2; or rabbit anti-H3K4me1) at 1:100 dilution in PBS for 1.5 h at 37°C. Negative control embryos were prepared via omission of primary antibody (i.e. incubated for the same period in PBS). Embryos were then washed twice in 0.5% TX and incubated in the secondary antibody. Donkey anti-Rabbit Alexa 488 conjugate diluted 1:200 in PBS for 2 h at RT protected from light. Oocytes/embryos were then washed twice.

Embryos were counterstained with 0.5µg/mL Hoechst 33342 (Life Technologies; Carlsbad, California, USA) for 5 min at RT covered to protect from light and then washed twice in PBS and stored in MOPS-HSA for mounting. Embryos were imaged using the CV1000 spinning disk confocal microscope (Yokogawa) using 40x magnification. Experiments on different days were normalised using fluorescent beads (Invitrogen, excitation 450 nm, emission 480 nm) run on each day as a normaliser. Whole nuclear fluorescence was measured using via densitometry of captured images using ImageJ version 1.50e (Schindelin et al., 2012), with captures of whole

nucleus using the freehand tool. No positive control was performed as antibody performance for 2-cells mirrored that previously published H3K4me3-1 (Shao et al., 2014), and matched the patterns observed for H3K4me2 and H3K4me1 (Shao et al., 2014).

4.5.10 Day 5 blastocyst cell counts using Oct4 immunocytochemistry

Blastocyst cell number, TE and ICM cell number were assessed using immunocytochemistry for Oct4 which is a marker of pluripotency and thus indicative of inner cell mass cells. Blastocysts were placed into 0.1M glycine for 5 min at room temperature (RT), followed by permeabilisation in 0.25% Triton-X in PBS for 10 min at RT. Blastocysts were then blocked overnight in 10% donkey serum in PBS at 4ºC. Blastocysts were washed in 0.25% Triton-X and incubated in 1:100 goat anti-Oct3/4 (sc-8628, Santa Cruz; Dallas, Texas, USA) for 1.5 h at 37ºC. Embryos were washed twice in 0.25% Triton-X and incubated in secondary antibody 1:100 donkey anti-goat conjugated to Alexa-594 (A11058, Thermo Fisher, excitation 590 nm emission 617 nm) at RT for 2 h covered in dark conditions. Blastocysts were again washed twice in 0.25% Triton-X and counterstained with 25 µg/mL Hoechst 33342 for 5 min. Blastocysts were transferred to PBS/PVP and mounted onto microscope slides in glycerol for cell counts. Blastocysts were counted using epifluorescence microscopy (Olympus BX51, Olympus; Shinjuku City, Tokyo, Japan), using the red channel (excitation filter 520-560 nm, emission from 420 nm) to count Oct4 in the inner cell mass and a count of total nuclei via Hoechst (excitation filter 330-385 nm, emission from 580 nm).

4.5.11 Statistical analysis

Statistics were performed using IBM SPSS Statistics version 26. All data is expressed as mean ± standard error of the mean (SEM), with normality assessed using the Kolmogorov-Smirnov normality test, and statistical differences was determined at $P<0.05$ unless otherwise indicated. Cumulus expansion was measured via binary logistic generalised linear models to compare the number of class 1, class 2, class 3, and class 4 between groups. KDM5A and KDM5C proportions of presence of staining in chromatin and spindles was measured via binary logistic generalised linear model. KDM5A and KDM5C densitometry was measured by univariate general linear model if normally distributed, and via one-way Kruskal-Wallis test if not normally distributed. H3K4me3-1 in the MII oocyte was measured by general linear model. H3K4me3-1 in the 2-cell embryo was measured by general linear model if normally distributed, and via one-way Kruskal-Wallis test if not normally distributed. Embryo culture was measured via binary logistic generalised linear model. Blastocyst cell counts for ICM, TE and Total cell and ICM/Total were measured via general linear model.

4.6 Results

4.6.1 Reduced cumulus expansion and oocyte maturation after IVM ± 20 mM 2HG

To determine any changes in the cumulus oocyte complexes (COCs) after IVM, we first established if there were any differences in cumulus cell expansion with the addition of 20 mM 2HG. After 16 h of IVM ± 20 mM 2HG, there was a lower proportion of COCs reaching maximum grading of cumulus expansion after IVM+2HG, with more COCs in class 1 ($P<0.05$), class 2 ($P<0.01$), and class 3 ($P<0.05$), and fewer in class 4 ($P<0.001$, Figure 4.1a) compared to control IVM.

4.6.2 Altered localisation and abundance of KDM5A in MII oocytes after IVM ± 20 mM 2HG

KDM5A, the first member of the α-ketoglutarate dependent lysine demethylases for H3K4me3 (see Section 1.10.4 for more information), was observed in the MII oocyte to determine if any changes in distribution was present within the oocyte, and if the chromatin and spindle regions showed increased presence after IVM±20 mM 2HG. KDM5A appeared to be co-localised to the chromatin in 100% of ovulated oocytes (Figure 4.2a-b), however this localisation pattern was not present in IVM derived oocytes where no co-localisation was observed, and only one oocyte from IVM+20 mM 2HG showed similar co-localisation with chromatin (Figure 4.2b). Conversely in mitotic spindles, no co-localisation was observed in ovulated MII oocytes, and this was comparable with IVM± 20 mM 2HG (Figure 4.2b).

Due to these differences in localisations within the MII, KDM5A relative presence was measured specifically in chromatin or spindle regions for only those with positive co-localisation, while whole oocyte MII was measured for all oocytes regardless of where KDM5A was localised.

KDM5A was more abundant in the spindles in IVM+20 mM 2HG oocytes relative to IVM oocytes ($P<0.01$, Figure 4.2c), with no statistics performed against ovulated MII oocytes due to the lack of positive staining. Whole oocyte KDM5A was increased in the IVM cohort relative to ovulated MII oocytes ($P<0.05$). IVM+20 mM 2HG further increased oocyte KDM5A relative to ovulated MII oocytes ($P<0.001$) and IVM ($P<0.001$, Figure 4.2c). KDM5B was not assessed as it has been previously shown not to be expressed in MII oocytes(Page-Lariviere and Sirard, 2014).

4.6.3 KDM5C is unaltered in MII oocytes after IVM ± 20 mM 2HG

Similarly to KDM5A, co-localisation of KDM5C to the chromatin and region of mitotic spindles was established to determine the frequency of co-localised protein across the sample population (Figure 4.3a). There were no differences in chromatin nor in spindle co-localisation frequencies between ovulated MII oocytes compared with MII oocytes obtained from IVM± 20 mM 2HG (Figure 4.3b).

Global KDM5C was then measured in the chromatin and spindle co-localised regions for those oocytes with positive co-localisation, as well as whole oocyte presence of KDM5C. Of the oocytes with positive co-localisation, there was a significant increase in KDM5C on the chromatin in IVM + 20 mM 2HG oocytes relative to IVM oocytes ($P<0.05$), however, this was not different compared with ovulated MII oocytes ($P=0.051$, Figure 4.3c) There were no differences between treatment groups in KDM5C fluorescence levels on the spindles, or KDM5C for the whole oocyte (Figure 4.3c).

4.6.4 Histone methylation increased in MII oocytes after IVM±20 mM 2HG

Histone methylation at H3K4me3, H3K4me2 and H3K4me1 was measured in MII oocytes and to determine any changes to global histone methylation status after IVM±20mM 2HG.

For H3K4me3, both IVM and IVM+20 mM 2HG oocytes had increased abundance compared with ovulated oocytes ($P<0.001$, Figure 4.4a), with no differences between IVM and IVM+ 20 mM 2HG.

For H3K4me2, there was a similar increase in staining in IVM and IVM+20 mM 2HG oocytes compared with ovulated oocytes ($P<0.05$, Figure 4.4b), with no differences between IVM and IVM+20mM 2HG.

For H3K3me1, there were no statistically significant differences in global H3K4me1 florescence between ovulated oocytes, IVM, nor IVM+20 mM 2HG (Figure 4.4c).

4.6.5 Histone methylation increased post embryonic genome activation after IVM±20 mM 2HG

H3K4 methylation was further measured in the 2-cell embryo to determine any changes in histone methylation immediately after major embryonic genome activation (EGA) (See Section 1.2.3 for more information). Ovulated oocytes and IVM±20 mM 2HG oocytes were fertilised *in vitro*, and in-vivo fertilised and flushed 2-cells were also measured as a comparison group (5.5a, c, e).

H3K4me3 was increased in *in vitro* fertilisation (IVF) derived 2-cells compared with flushed 2-cells ($P<0.01$, Figure 4.5b), with further increases H3K4me3 in IVM and IVM+20 mM 2HG derived 2-cells relative to flushed ($P<0.001$ IVM, $P<0.001$ 2HG, Figure 4.5b) and IVF ($P<0.01$ IVM, $P<0.05$ IVM+2HG, Figure 4.5b).

H3K4me2 was increased in IVM and IVM+20mM 2HG 2-cells relative to flushed ($P<0.001$ IVM, $P<0.001$ IVM+20mM 2HG, Figure 4.5d) and IVF ($P<0.001$ IVM, $P<0.001$ IVM+20 mM 2HG, Figure 4.5d), with no change observe between IVM and IVM+20 mM 2HG or IVF vs flushed (Figure 4.5d).

H3K4me1 was increased in IVF 2-cells relative to flushed 2-cells (P<0.001, Figure 4.5f). IVM 2-cells shows increased H3K4me1 relative to flushed 2-cells (P<0.01, Figure 4.5f), however were not altered relative to IVF nor IVM+20 mM 2HG. IVM+20mM 2HG was decreased relative to IVF embryos (P<0.05, Figure 4.5f), however was not statistically significantly different to flushed 2-cells nor IVM derived embryos (Figure 4.5f).

4.6.6 Embryo development altered dynamics after IVM ± 20 mM 2HG

Embryos were fertilised and cultured to the blastocyst stage to determine the effect of IVM and IVM+20 mM 2HG on key developmental outcomes (Table 4.1). There was a statistically significant increase in cleavage rates in IVM embryos compared with IVF embryos in IVM (P<0.01) and IVM+20 mM 2HG (P<0.01, Table 4.1), with no differences between IVM and IVM+20 mM 2HG.

On day 3 for embryos that had cleaved, the proportion of embryos at the 8-cell stage was reduced in IVM+20 mM 2HG relative to IVF (P<0.001), and further reduced under IVM (P<0.001 IVF, P<0.01 IVM+20 mM 2HG). Compacting embryo rate was also reduced under IVM (P<0.01) and IVM+20 mM 2HG (P<0.05), with no difference between IVM and IVM+20 mM 2HG.

On Day 5 for embryos that had cleaved, total blastocyst development rates were not different. Blastocyst rate (>50% area blastocoel) was not changed from IVF to IVM but was increased in IVM+20 mM 2HG (P<0.05 IVF, P<0.05 IVM).

When grouping early blastocysts, blastocysts, expanded blastocysts (i.e., all blastocyst development stages below hatching), there was a significant increase in this category with IVM+20 mM 2HG relative to IVF (P<0.01) and IVM (P<0.01, Table 4.1) and this was due to decreased rates of hatching blastocysts (P<0.01). This shows that of cleaved embryos, IVM or IVM+20 mM 2HG were able to reach the blastocyst on day 5, however were delayed in their progress compared to the IVF cohort (where maturation occurred *in vivo*).

4.6.7 Blastocyst cell counts reduced after IVM ± 20 mM 2HG

After development to the blastocyst, there was a significant decrease in total cell count and ICM cell count in day 5 blastocysts in IVM+20 mM 2HG compared with IVF ($P<0.001$), with no difference in trophectoderm cell count or ICM as a percentage of total cells (Figure 4.6). Inner cell mass cell count was also reduced in IVM+20 mM 2HG relative to IVM ($P<0.05$) (Figure 4.6).

4.7 Discussion

The metabolic environment present for the final stages of oocyte maturation (from the germinal vesicle stage through to metaphase II (MII) for ovulation) is critical for successful embryo development and subsequent adult health (Banwell et al., 2007, Barnes et al., 1989, Brown et al., 2017, Camargo et al., 2019, del Collado et al., 2017, Dunning et al., 2011, Dunning et al., 2007, Gegenfurtner et al., 2020, Harris et al., 2009, Jones et al., 2008, Rizos et al., 2002, Romar et al., 2011, Schulte et al., 2015, Thompson et al., 1991, Thompson et al., 1996, Yeo et al., 2009). The model in this study used 2HG during *in vitro* maturation to competitively inhibit α-ketoglutarate, which was designed to create a further metabolic disruption over IVM alone. This disruption was then used to determine whether changing the amount of α-ketoglutarate available to bind KDM5A-C resulted in changes to global demethylation of H3K4me3 and H3K4me2. This metabolic change to methylation-altering proteins may provide insight into other model systems where increases or decreases to metabolic precursors may also act via α-ketoglutarate, such as those observed with maternal high fat diet.

The KDM5 family of lysine demethylases has been comprehensively studied using knockout models of its role in alterations and maintenance of H3K4 methylation in the preimplantation embryo, particularly for its contribution to embryonic genome activation (Albert et al., 2013, Cao et al., 2015, Catchpole et al., 2011, Dahl et al., 2016, Huang et al., 2015, Zhang et al., 2016). These knockout studies however cannot focus on specific windows of time when critical events occur, for example oocyte maturation, which is a much less studied area in terms of lysine demethylases, and the dynamics of H3K4me3. While KDM5B is the lysine demethylase that is essential for embryo development past the 2-cell (Dahl et al., 2016), there are no proteomic studies available to confirm its presence before fertilisation. There is however, suggestion that KDM5A and KDM5C may be present before fertilisation (due to confirmation of *Kdm5a* and *Kdm5c* transcript presence in GV oocytes (Shao et al., 2014)). In our study we have showed that KDM5A global concentration in the oocyte was increased after IVM and further increased under IVM+20mM 2HG compared with ovulated oocytes, indicating that

KDM5 protein is also present before fertilisation and can be modulated by the environment during the time of oocyte maturation.

These differences in KDM5 presence were observed for IVM relative to ovulated oocyte control, with no further alteration to KDM5 protein under IVM + 20 mM 2HG. Given that there was no additional difference in H3K4me3, H3K4me2 or H3K4me1 in IVM compared with IVM+20mM 2HG, it seems that we could not exceed the inhibition on oocyte and embryo development caused by IVM alone. This suggests that IVM itself is able to reduce the progression of histone demethylation, with no progression to H3K4me1 to be removed by to methylated H3K4.

The observed changes in histone methylation in the oocyte and 2-cell embryo coupled with altered blastocyst rates after IVM indicate that metabolic changes during oocyte maturation can result in embryonic consequences. Throughout the first 10 h of oocyte maturation in the oocyte (GV stage: prophase I of meiosis 1), it has been previously shown that H3K4me3 was reduced with a concomitant increase in H3K4me2 and H3K4me1 (Sha et al., 2018). It has also been demonstrated in oocytes, genes involved in embryonic genome activation overlap with regions of H3K4me3 enrichment (Dahl et al., 2016). Together, these indicate that removal of H3K4me3 occurs during oocyte maturation, with key regions remaining unchanged for embryonic genome activation to properly occur. As such alterations to the enzymes or substrate availability responsible for this process could directly alter the histone methylation status of the mature oocyte and affect early preimplantation development if aberrant removal or maintenance of H3K4me3 occurs during oocyte maturation.

There have been studies investigating CXXC zinc finger protein 1 (CFP1) which is required to maintain H3K4me3 methylation marks in the oocyte (Sha et al., 2018, Yu et al., 2017). Knockouts of CFP1 in the oocyte results in a reduction in H3K4me3 than is observed in wild type mice (Yu et al., 2017) and although are fertilised at a similar rate to wild type oocytes, fewer of these embryos cleaved and arrested at the 2-cell stage (Yu et al., 2017). This indicates that correct maintenance of H3K4me3 is not necessarily essential for embryo fertilisation, however, is critical for embryonic genome activation and embryonic development. It must be noted that this knockout model did not limit the CFP1 removal to the oocyte stage only, as its absence would also continue throughout embryo development, unlike in our model where *in vivo* matured IVF derived 2-cell embryos display lower global H3K4me3 and H3K4me2 compared with IVM derived embryos and flushed 2-cells (matured *in vivo* and fertilised *in vivo*). At present, there have been no other studies showing oocyte specific direct alterations to KDM5 proteins. Furthermore, the study of this oocyte maturation period remains a challenge without overlap with fertilisation and early embryonic effects, nor controlling for the limitation of the additional effects due to the IVM environment itself as we have demonstrated.

It must also be noted that our model system does not denude the oocytes from their cumulus-oocyte complexes before IVM treatment, so changes to cumulus cells must be considered. It was observed that there were significant differences in cumulus and granulosa cell morphology, with reduced cumulus expansion under 2HG exposure. There are few studies showing H3K4 methylation changes in cumulus or granulosa cells (Madogwe et al., 2020, Maekawa et al., 2016), however this change may be due to 2HG-mediated retention of H3K4me3 altering expression in the cumulus cells, which may influence nutrient uptake for the oocyte, such as *Glut1* for glucose uptake (Han et al., 2012). As such, our model of IVM mediated changes to H3K4 methylation and embryo development may be more related to metabolic changes during oocyte maturation as opposed to alterations to transcription mediated by modifications to H3K4me3 in the oocyte itself. While these alterations to H3K4me3 due to exposure to IVM with or without 2HG suggest epigenetic alterations, clinical outcomes are yet to be studied,

which is pressing given the current clinical use of human IVM (Basatemur and Sutcliffe, 2011, Chian et al., 2014, Jones et al., 2008, Vuong et al., 2018, Vuong et al., 2020).

Comparisons between ovulated and *in vitro* matured oocytes are relatively uncommon in the literature, with many studies examining changes during *in vitro* culture conditions not including ovulated oocytes as a control. In bovine oocytes, IVM derived mature oocytes (oocytes that have reached metaphase II) display a metabolic environment similar to that of GV stage oocytes (del Collado et al., 2017), with increased ROS and glutathione and decreased neutral lipids, leading to reduced fertilisation (Leibfried-Rutledge et al., 1987) and decreased blastocyst development (Holm et al., 2002). Interestingly, a phenomenon in *in vitro* matured cattle embryos relative to *in vivo*, artificial insemination, termed bovine large offspring syndrome (LOS) may be due to *in vitro* culture conditions, however will not be discussed here due to no current studies on this syndrome specifically on the oocyte IVM period compared to post-maturation in-vivo conditions. Transcription of *GDF9*, which is required in the signalling from the oocyte to the cumulus cells (Gilchrist et al., 2004, Yeo et al., 2009, Yeo et al., 2008), was also reduced in IVM oocytes relative to ovulated oocytes (Camargo et al., 2019). These alterations to the signalling between the cumulus cells and the oocyte itself may alter nutrient uptake into the oocyte, in turn altering development of the oocyte. Specifically, in mouse oocytes, IVM produces far fewer oocytes matured to MII per mouse, not only reducing the number of possible embryos that can be fertilised (Eppig, 1996, Eppig et al., 1992, Nishi et al., 2003) but also reducing the fertilisation of these oocytes. Human oocytes showed a similar trend to bovine and murine, where matured oocytes that had progressed to MII still had a metabolic and transcriptional content more similar to GV stage oocytes than to ovulated oocytes (Jones et al., 2008, Pereira et al., 2016). Specifically, microarrays of gene expression between germinal vesicle stage oocytes, IVM MII oocytes, and ovulated MII oocytes show via principal component analysis (PCA) distinct differences in expression profiles between the groups (Jones et al., 2008), which resulted in over twofold increased expression in over 2,000 genes from IVM relative to ovulated MII oocytes (Jones et al., 2008). These results may confirm the

differences in number of viable oocytes, and thus embryos available for transfer. As a result of these metabolic and transcriptional alterations during IVM, the development of embryos may also be altered, with resulting foetal development and adult health ramifications. We have shown in our study the alterations that can occur because of IVM, where embryo development on day 3 was reduced with greater effects seen with the α-ketoglutarate inhibitor 2HG present. Although there was some evidence of recovery by day 5, more embryos were observed at the early blastocyst to expanded blastocyst stages and less at the hatching stage for IVM+2HG compared with IVM and IVF. This is also evidenced by the reduced inner cell mass cell count, which is indicative of slowed development, with reduced inner cell mass leading to poorer clinical pregnancy rates (Gardner and Schoolcraft, 1999, Lee et al., 2015). Similar trends have been observed previously, with IVM embryos reporting reduced blastocyst formation (Eppig, 1996, Eppig et al., 1992).

As seen in Chapter 2, there were no overt changes to embryo development under maternal HFD, although after embryo transfer there was reduced foetal crown:rump length and increased foetal to placental weight ratio outcome when embryos were transferred to normal weight donor mothers (See Chapter 2 Table 2.1). While no embryo transfer experiments and foetal outcome experiments were performed using 2HG during the IVM window, this treatment may produce a similar result due to the disruption to KDMs under the same exposure window as the maternal HFD. However, it remains to be seen if these alterations under IVM + 20 mM 2HG would be exacerbated in comparison to any changes that would occur under IVM alone. When observing differences between IVM and IVF under human clinical cycles in singleton pregnancies, it was demonstrated that IVM resulted in increased birthweight compared with IVF (Fadini et al., 2012), and in twin births IVM/ICSI oocytes report a lower mean gestational age at birth (Fadini et al., 2012) and as such birth outcomes of IVM + 20 mM 2HG derived embryos are warranted to assess impact on offspring phenotype. Together, these findings indicate that IVM with or without 20 mM 2HG compared with *in vivo* development have altered embryo development,

however given the alterations seen in epigenetic proteins, this may result in wider implications to the resulting offspring via alterations to histone methylation pathways.

In addition, a randomised control trial, allocating patients with high antral follicle counts (at least 24 follicles in both ovaries) to either IVM or IVF treatment with matched patient populations showed significantly lower oocytes collected, with fewer mature oocytes, reduced fertilisation, and fewer embryos suitable for freezing on day 3 after IVM compared with IVF. Furthermore, the cumulative pregnancy rates at 6 months and one year were also significantly lower after IVM compared with IVF (Vuong et al., 2020). One limitation is that the selection for high antral follicle count may be selecting for younger patients in both groups (mean age below 30 years in both groups), where differences may be more profound from patients with a normal or reduced ovarian reserve who may also be more sensitised due to a baseline of metabolic disturbances, such as advanced maternal age (Pacella et al., 2012). Analyses of children from IVM cycles indicate no significant differences in birthweight, gestational age at birth, height, nor head circumference (Chian et al., 2014, Shu-Chi et al., 2006), however only one randomised controlled trial has been registered which is currently ongoing (Vuong, 2020). Other research groups have observed increase in miscarriages under IVM with a concomitant decrease in live birth rates (Buckett et al., 2008), however this was from total pregnancies rather than number of embryo transferred. Other studies have reported similar miscarriage rates (Söderström-Anttila et al., 2005); however did not control against IVF cycles, rather reporting increased over typical miscarriage rates in the same clinic (Söderström-Anttila et al., 2005). Overall, this indicates IVM impacts on the fertilisation potential of oocytes which then reduces the number of high quality embryos that are available per patient that are able to be transferred (Fadini et al., 2012, Shu-Chi et al., 2006, Vuong et al., 2020).

The true impact of IVM on offspring health remains to be thoroughly investigated. This could be assessed in animal models through randomised controlled segregation of model animals to IVM or IVF groups, with measurements of offspring characteristics (F1), and two subsequent generations (F2 and F3). The study of F2 and F3 generations are required for the confirmation

of maternal epigenetic transmission, as changes to the F2 generation can occur whilst in-utero in the F1 generation, even if mated normally, and the F3 generation is the first generation clear of the original exposure (Skinner, 2008).

In conclusion, here we have demonstrated that IVM alters early embryonic development and increases global H3K4me3 and H3K4me2 in mature oocytes and 2-cell embryos. The addition of the KDM5 inhibitor 2-hydroxyglutarate into IVM conditions further reduces embryo development and alters inner cell mass cell counts of blastocysts, however with no statistically significant further changes to H3K4me3, H3K4me2 nor H3K4me1 in oocytes or 2-cell embryos. This demonstrates that environmental changes to *in vitro* maturation conditions are able to alter epigenetic histone marks in the embryo and impact embryonic development.

4.8 Tables

Table 4.1 Embryo development from *in vitro* matured oocytes (IVM), or IVM in media containing 20 mM 2-hydroxyglutarate (2HG) fertilised *in vitro* (IVF) and cultured to blastocyst in commercial G1 and G2 Plus media

	IVF	IVM	IVM + 20 mM 2HG
Day 2			
Cleavage Rate (%)	80.61 [a]	90.99 [b]	91.16 [b]
Day 3			
(% of cleaved 2-cells)			
Degenerate	2.26 [a]	1.47 [a]	0.51 [a]
Below 4-cell	1.50 [a]	3.92 [a]	3.03 [a]
4-cell	7.52 [a]	36.76 [b]	24.75 [c]
6-cell	9.77 [a]	21.57 [b]	20.20 [b]
4-6 cell	17.29 [a]	58.33 [b]	44.951 [c]
8-cell	70.68 [a]	34.80 [b]	48.99 [c]
Compacting	8.27 [a]	1.47 [b]	2.53 [b]
Day 5			
(% of cleaved 2-cells)			
Cleaved	3.76 [a]	4.41 [a]	2.53 [a]
Degenerate/≤8-cell	9.02 [a]	9.80 [a]	9.09 [a]
Morula	2.26 [a]	5.88 [a]	3.03 [a]
Early Blast	8.27 [a]	11.27 [a]	14.14 [a]
Blastocyst	12.78 [a]	13.73 [a]	21.72 [b]
Expanded Blastocyst	7.52 [a]	13.24 [a]	16.16 [a]
Early Blast + Blastocyst + Expanded Blastocyst	28.57 [a]	38.24 [a]	52.02 [b]
Hatching Blastocyst	56.39 [a]	41.67 [ab]	33.33 [b]

Data from: IVF n=165, IVM n=222, IVM + 20 mM 2HG n=215. Differing letters denote statistically significant results ($P<0.05$). Mouse numbers per treatment group detailed in Figure S4.1

4.9 Figures

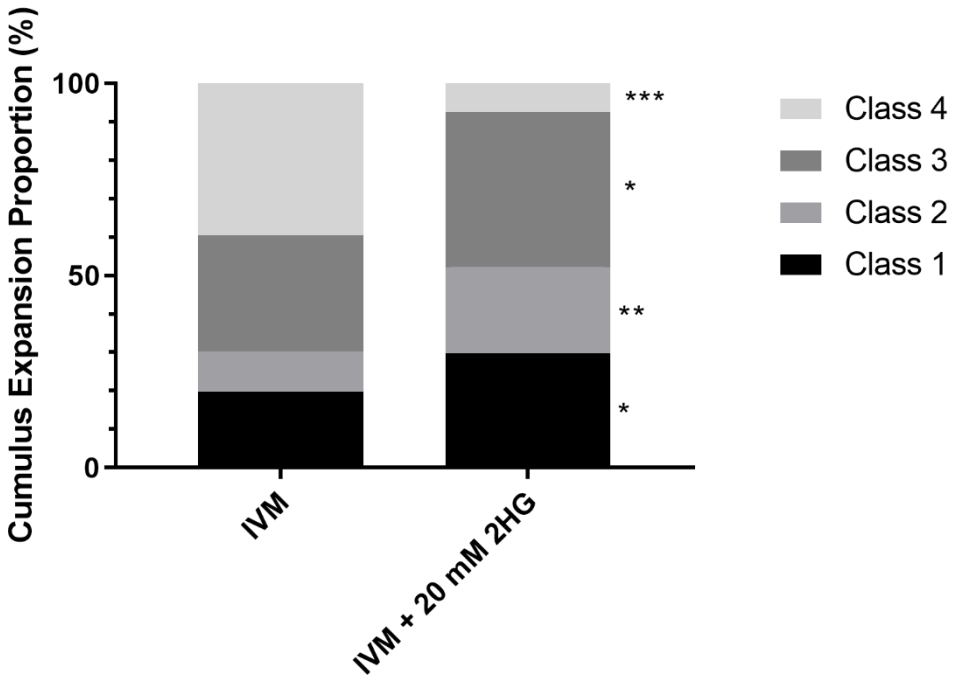

Figure 4.1 Cumulus expansion scoring according to classifications from (Vanderhyden et al., 1990) for *in vitro* matured oocytes (IVM) or oocytes matured in media containing 20 mM 2-hydroxyglutarate (2HG). IVM n=162, IVM + 20 mM 2HG n=161. * P<0.05 ** P<0.01 *** P<0.001 for comparison between differences between class numbers between IVM and IVM+20mM 2HG. Mouse numbers per treatment group detailed in Figure S4.1

a

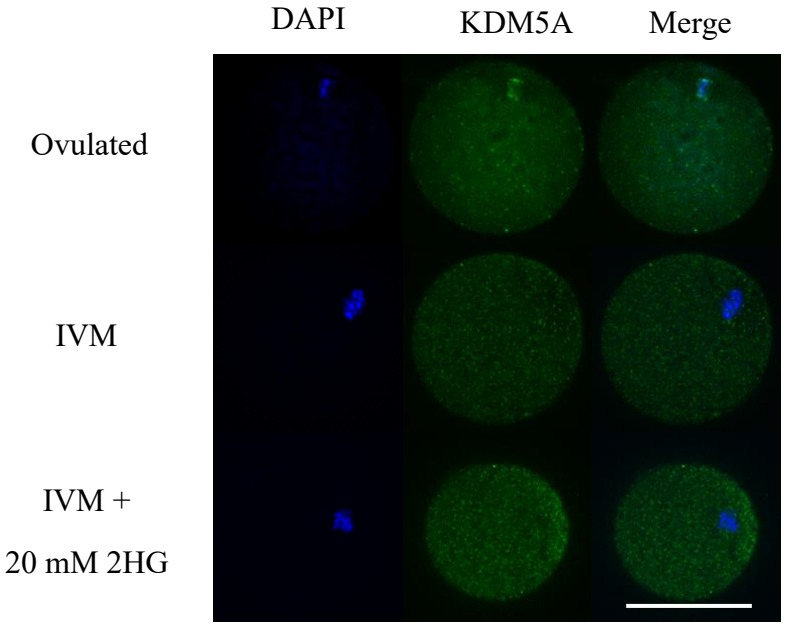
DAPI
KDM5A
Merge
Ovulated
IVM
IVM +
20 mM 2HG

b

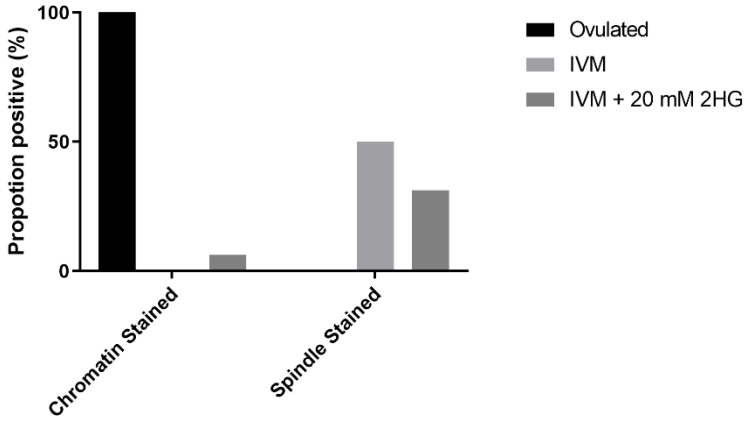
Propotion positive (%)
100
50
0
Chromatin Stained
Spindle Stained
Ovulated
IVM
IVM + 20 mM 2HG

c

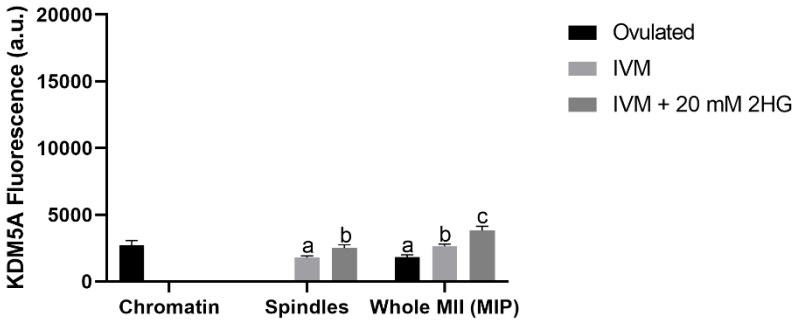
KDM5A Fluorescence (a.u.)
20000
15000
10000
5000
0
a
b
a
b
c
Chromatin
Spindles
Whole MII (MIP)
Ovulated
IVM
IVM + 20 mM 2HG

Figure 4.2 Chromatin and spindle staining for KDM5A in ovulated metaphase II (MII) oocytes, or *in vitro* matured (IVM) oocytes matured in control media or 20 mM 2-hydroxyglutarate (2HG) supplemented media. **a** Representative images for KDM5A (green) and the DNA intercalator 2-(4-amidinophenyl)-1H -indole-6-carboxamidine (DAPI) (blue) in MII oocytes, **b** Co-localisation frequencies for the percentages of oocytes with positive co-localisation in the chromatin and the region of mitotic spindles, **c** KDM5A fluorescence measured on the chromatin, region of mitotic spindles, and for whole oocyte measured on maximum image projection (MIP) of all confocal slices through the oocyte. Ovulated MII n=20, IVM n=22, IVM+20mM 2HG n=19. Differing letters denote statistical significance $P<0.05$. Data expressed as mean ± standard error of the mean (SEM). Where no letters present no statistically significant differences were observed, and where no columns present no staining presence was detected in any measured oocytes. Scale bar = 50μm. Mouse numbers per treatment group detailed in Figure S4.1

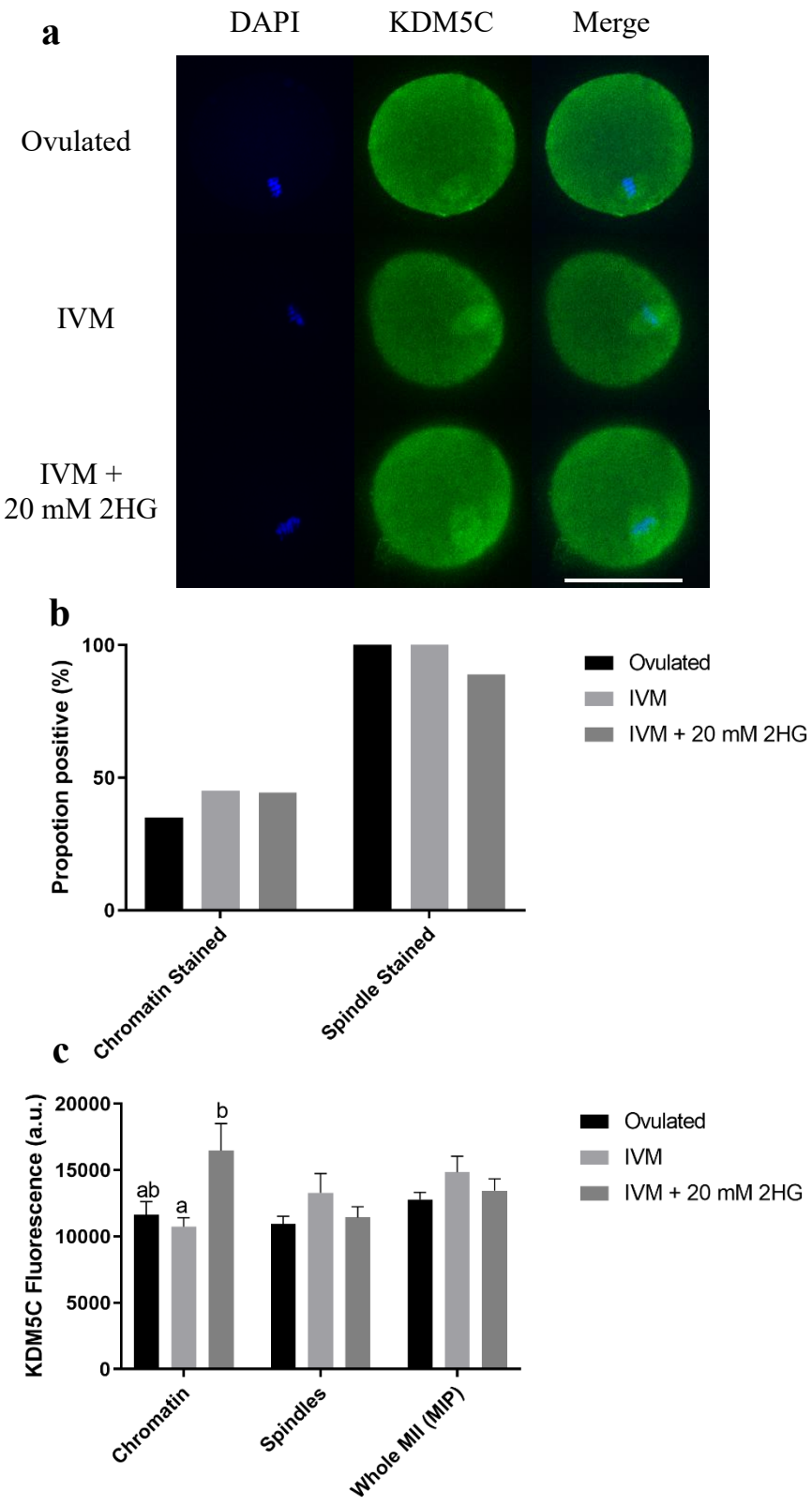
a
DAPI
KDM5C
Merge
Ovulated
IVM
IVM +
20 mM 2HG
b
Propotion positive (%)
100
50
0
Chromatin Stained
Spindle Stained
Ovulated
IVM
IVM + 20 mM 2HG
c
KDM5C Fluorescence (a.u.)
20000
15000
10000
5000
0
ab
a
b
Chromatin
Spindles
Whole MII (MIP)
Ovulated
IVM
IVM + 20 mM 2HG

Figure 4.3 Chromatin and spindle staining for KDM5C in ovulated metaphase II (MII) oocytes, or *in vitro* matured (IVM) oocytes matured in control media or 20 mM 2-hydroxyglutarate (2HG) supplemented media. **a** Representative images for KDM5C (green) and the DNA intercalator 2-(4-amidinophenyl)-1H -indole-6-carboxamidine (DAPI) (blue) in MII oocytes, **b** frequencies for the percentages of oocytes with positive signal that was visually determined to be in the chromatin and at the region of mitotic spindles **c** KDM5C fluorescence measured on the chromatin, region of mitotic spindles, and for whole oocyte measured on maximum image projection (MIP) of all confocal slices through the oocyte, with data expressed as mean ± standard error of the mean (SEM). Ovulated MII n=20, IVM n=22, IVM+20mM 2HG n=19. Scale bar = 50μm. Differing letters denote statistical significance $P<0.05$. Where no letters present no statistical significance was observed. Mouse numbers per treatment group detailed in Figure S4.1

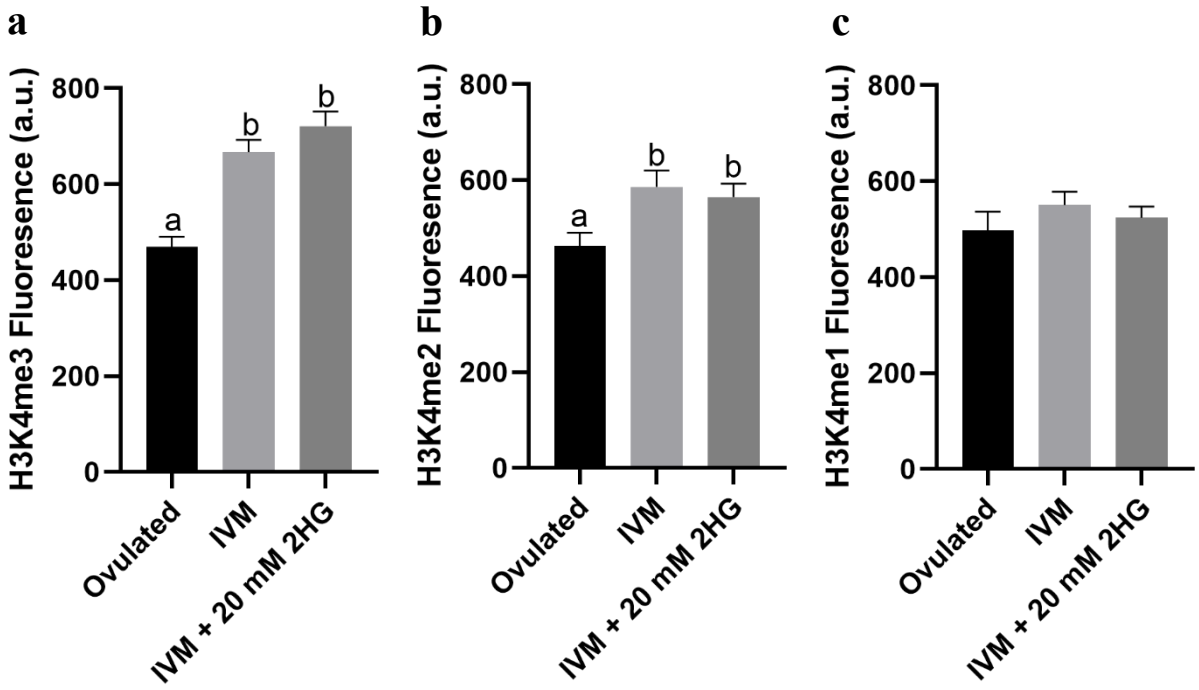

Figure 4.4 Relative H3K4 methylation in ovulated metaphase II (MII) oocytes, or *in vitro* matured (IVM) oocytes matured in control media or 20 mM 2-hydroxyglutarate (2HG) supplemented media. **a** Global H3K4me3 methylation fluorescence **b** global H3K4me2 methylation fluorescence **c** global H3K4me1 methylation fluorescence. H3K4me3 ovulated MII n=17, IVM n=18, IVM+20mM 2HG n=20, H3K4me2 ovulated MII n=19, IVM n=20, IVM+20mM 2HG n=18, H3K4me1 ovulated MII n=16, IVM n=24, IVM +20 mM 2HG n=22. Data expressed as mean ± standard error of the mean (SEM), with differing letters denote statistically significant results ($P \leq 0.05$). Where no letters present no statistical significance is present. Mouse numbers per treatment group detailed in Figure S4.1

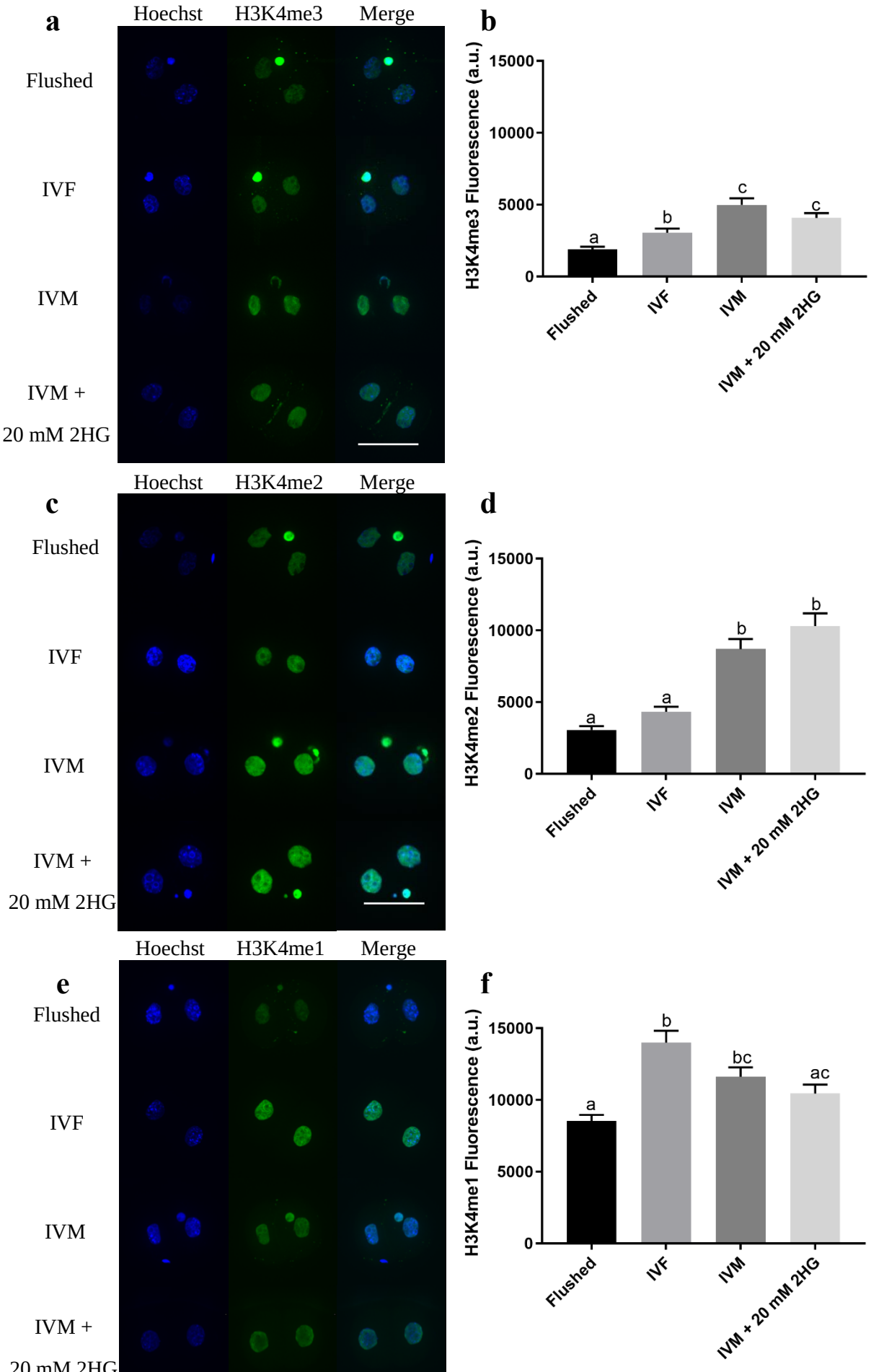
a
Hoechst
H3K4me3
Merge
Flushed
IVF
IVM
IVM +
20 mM 2HG
b
H3K4me3 Fluorescence (a.u.)
15000
10000
5000
0
a
b
c
c
Flushed
IVF
IVM
IVM + 20 mM 2HG
c
Hoechst
H3K4me2
Merge
Flushed
IVF
IVM
IVM +
20 mM 2HG
d
H3K4me2 Fluorescence (a.u.)
15000
10000
5000
0
a
a
b
b
Flushed
IVF
IVM
IVM + 20 mM 2HG
e
Hoechst
H3K4me1
Merge
Flushed
IVF
IVM
IVM +
20 mM 2HG
f
H3K4me1 Fluorescence (a.u.)
15000
10000
5000
0
a
b
bc
ac
Flushed
IVF
IVM
IVM + 20 mM 2HG

Figure 4.5 H3K4 methylation in the late 2-cell, of *in vivo* 2-cells from *in vitro* fertilised (IVF) oocytes, or *in vitro* matured (IVM) oocytes matured in control media or 20 mM 2-hydroxyglutarate (2HG) supplemented media. **a** Representative images of H3K4me3 (green) and DNA intercalator Hoechst 33342 (Hoechst, blue) in 2-cells **b** H3K4me3 fluorescence levels in 2-cell embryo nuclei, **c** representative images of H3K4me2 (green) and Hoechst 33342 (blue) in 2-cells, **d** H3K4me2 fluorescence levels in 2-cell embryo nuclei, **e** representative images of H3K4me1 (green) and Hoechst (blue in 2-cells, **f** H3K4me1 fluorescence levels in 2-cell embryo nuclei. H3K4me3 Flushed 2-cell n=29, IVF 2-cell 34, IVM n=27 and IVM+20mM 2HG n=31, H3K4me2 Flushed 2-cell n=29, IVF 2-cell n=35, IVM n=29 and IVM+20mM 2HG n=30, H3K4me1 Flushed 2-cell n=30, IVF 2-cell n=30, IVM n=30 and IVM+20mM 2HG n=33. Data expressed as mean ± standard error of the mean (SEM), with differing letters denote significance $P<0.05$. Scale bar = 50μm. Mouse numbers per treatment group detailed in Figure S4.1

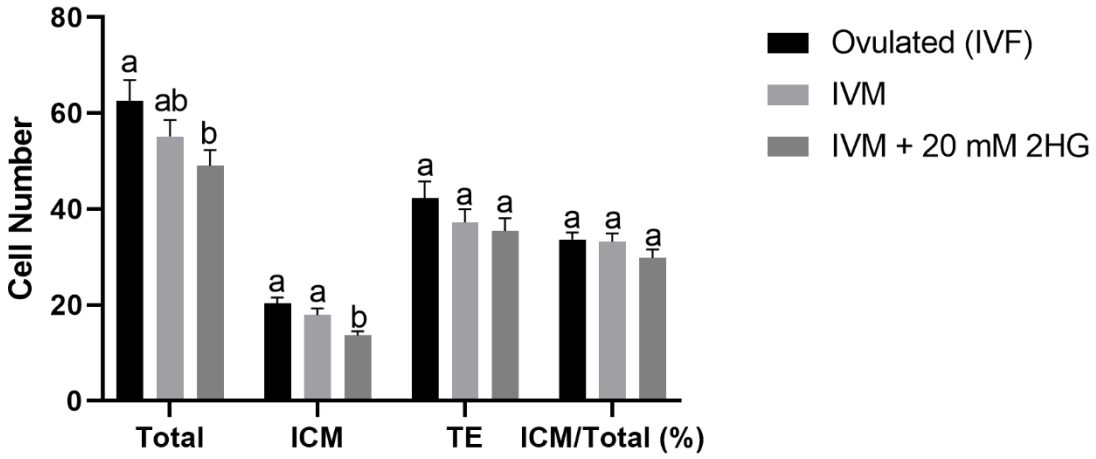

Figure 4.6 Cell counts of total cells, inner cell mass (ICM) and trophectoderm (TE) in blastocysts from *in vitro* fertilised (IVF) oocytes, or *in vitro* matured (IVM) oocytes matured in control media or 20 mM 2-hydroxyglutarate (2HG) supplemented media. IVF 2-cell n=29, IVM n=29 and IVM + 2HG n=32. Data expressed as mean ± standard error of the mean (SEM), with differing letters denote significant differences within each cell type $P<0.05$. Mouse numbers per treatment group detailed in Figure S4.1

4.10 Supplementary Figures

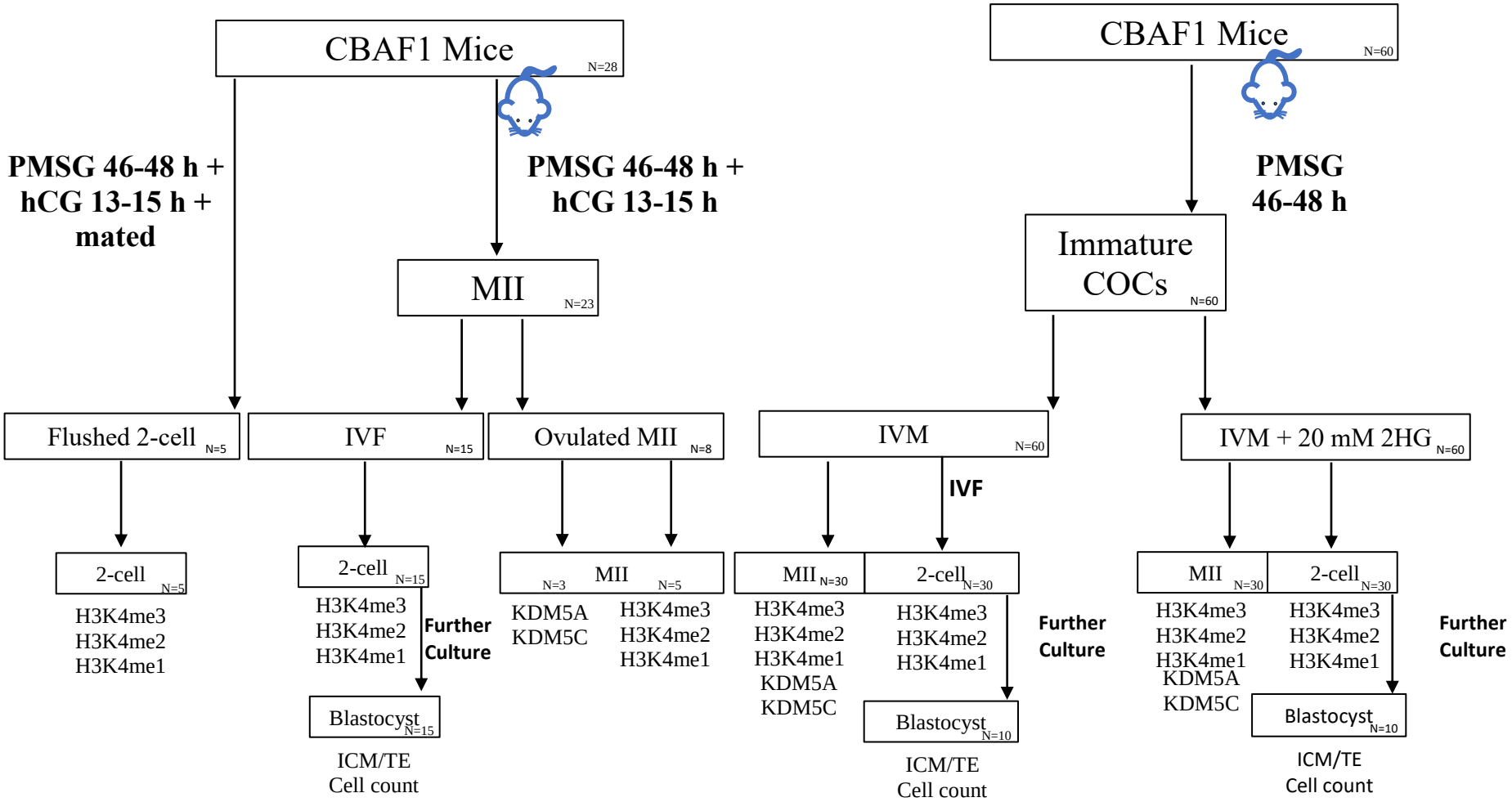

Figure S4.1 Experimental design for *in vitro* maturation (IVM), with mouse numbers used for pooled samples

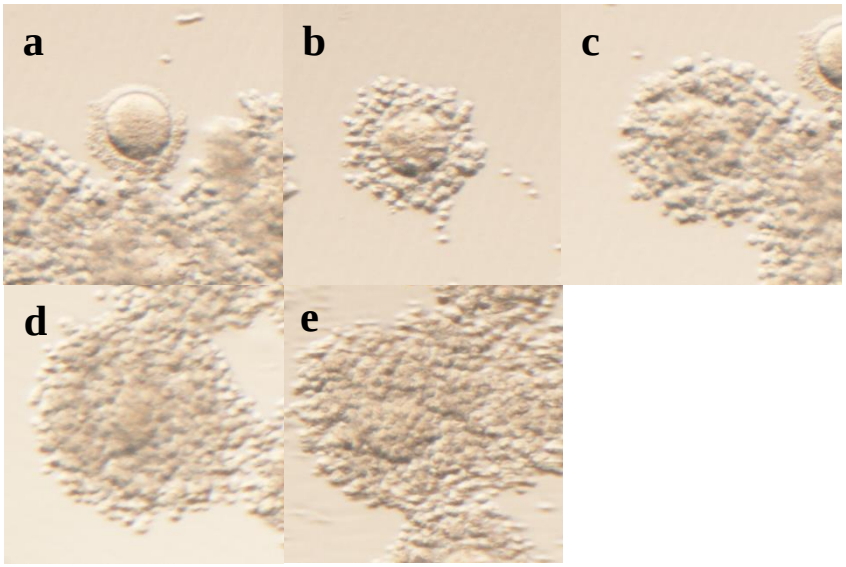

Figure S4.2 Representative images of cumulus expansion **a** Class 0, **b** Class 1, **c** Class 2, **d** Class 3, and **e** Class 4, with classes as described previously (Vanderhyden et al., 1990). Images provided by Anmol Saini

4.11 References

AKIYAMA, T., SUZUKI, O., MATSUDA, J. & AOKI, F. 2011. Dynamic replacement of histone H3 variants reprograms epigenetic marks in early mouse embryos. *PLOS Genetics,* 7**,** e1002279-e1002279.

ALBERT, M., SCHMITZ, S. U., KOOISTRA, S. M., MALATESTA, M., MORALES TORRES, C., REKLING, J. C., JOHANSEN, J. V., ABARRATEGUI, I. & HELIN, K. 2013. The histone demethylase Jarid1b ensures faithful mouse development by protecting developmental genes from aberrant H3K4me3. *PLOS Genetics,* 9**,** e1003461-e1003461.

BAKHTARI, A., RAHMANI, H.-R., BONAKDAR, E., JAFARPOUR, F., ASGARI, V., HOSSEINI, S.-M., HAJIAN, M., EDRISS, M.-A. & NASR-ESFAHANI, M.-H. 2014. The interfering effects of superovulation and vitrification upon some important epigenetic biomarkers in mouse blastocyst. *Cryobiology,* 69**,** 419-427.

BANWELL, K. M., LANE, M., RUSSELL, D. L., KIND, K. L. & THOMPSON, J. G. 2007. Oxygen concentration during mouse oocyte in vitro maturation affects embryo and fetal development. *Human Reproduction,* 22**,** 2768-2775.

BARNES, F. L., FLORMAN, H. M., SIRARD, M. A., LEIBFRIED-RUTLEDGE, M. L., SIMS, M. L. & FIRST, N. L. 1989. Timing of Nuclear Progression and Protein Synthesis Necessary for Meiotic Maturation of Bovne Oocytes. *Biology of Reproduction,* 40**,** 1257-1263.

BASATEMUR, E. & SUTCLIFFE, A. 2011. Health of IVM children. *Journal of Assisted Reproduction and Genetics,* 28**,** 489-493.

BROWN, H. M., DUNNING, K. R., SUTTON-MCDOWALL, M., GILCHRIST, R. B., THOMPSON, J. G. & RUSSELL, D. L. 2017. Failure to launch: aberrant cumulus gene expression during oocyte in vitro maturation. *Reproduction (Cambridge, England),* 153**,** R109-R120.

BUCKETT, W. M., CHIAN, R.-C., DEAN, N. L., SYLVESTRE, C., HOLZER, H. E. G. & TAN, S. L. 2008. Pregnancy loss in pregnancies conceived after in vitro oocyte maturation, conventional in vitro fertilization, and intracytoplasmic sperm injection. *Fertility and Sterility,* 90**,** 546-550.

CAMARGO, L. S. A., MUNK, M., SALES, J. N., WOHLRES-VIANA, S., QUINTÃO, C. C. R. & VIANA, J. H. M. 2019. Differential gene expression between in vivo and in vitro maturation: a comparative study with bovine oocytes derived from the same donor pool. *JBRA Assisted Reproduction,* 23**,** 7-14.

CAO, Z., LI, Y., CHEN, Z., WANG, H., ZHANG, M., ZHOU, N., WU, R., LING, Y., FANG, F., LI, N. & ZHANG, Y. 2015. Genome-Wide Dynamic Profiling of Histone Methylation during Nuclear Transfer-Mediated Porcine Somatic Cell Reprogramming. *PLOS ONE,* 10**,** e0144897.

CATCHPOLE, S., SPENCER-DENE, B., HALL, D., SANTANGELO, S., ROSEWELL, I., GUENATRI, M., BEATSON, R., SCIBETTA, A. G., BURCHELL, J. M. & TAYLOR-PAPADIMITRIOU, J. 2011. PLU-1/JARID1B/KDM5B is required for embryonic survival and contributes to cell proliferation in the mammary gland and in ER+ breast cancer cells. *International Journal of Oncology,* 38**,** 1267-1277.

CHENG, J., BLUM, R., BOWMAN, C., HU, D., SHILATIFARD, A., SHEN, S. & DYNLACHT, B. D. 2014. A role for H3K4 monomethylation in gene repression and partitioning of chromatin readers. *Molecular Cell,* 53**,** 979-992.

CHIAN, R. C., XU, C. L., HUANG, J. Y. J. & ATA, B. 2014. Obstetric outcomes and congenital abnormalities in infants conceived with oocytes matured in vitro. *Facts, Views & Vision in Obstetrics and Gynaecology,* 6**,** 15-18.

CHOI, C., GANJI, S. K., DEBERARDINIS, R. J., HATANPAA, K. J., RAKHEJA, D., KOVACS, Z., YANG, X.-L., MASHIMO, T., RAISANEN, J. M., MARIN-VALENCIA, I., PASCUAL, J. M., MADDEN, C. J., MICKEY, B. E., MALLOY, C. R., BACHOO, R. M. & MAHER, E. A. 2012. 2-hydroxyglutarate detection by magnetic

resonance spectroscopy in IDH-mutated patients with gliomas. *Nature Medicine,* 18**,** 624-629.

DAHL, J. A., JUNG, I., AANES, H., GREGGAINS, G. D., MANAF, A., LERDRUP, M., LI, G., KUAN, S., LI, B., LEE, A. Y., PREISSL, S., JERMSTAD, I., HAUGEN, M. H., SUGANTHAN, R., BJØRÅS, M., HANSEN, K., DALEN, K. T., FEDORCSAK, P., REN, B. & KLUNGLAND, A. 2016. Broad histone H3K4me3 domains in mouse oocytes modulate maternal-to-zygotic transition. *Nature,* 537**,** 548.

DANG, L., WHITE, D. W., GROSS, S., BENNETT, B. D., BITTINGER, M. A., DRIGGERS, E. M., FANTIN, V. R., JANG, H. G., JIN, S., KEENAN, M. C., MARKS, K. M., PRINS, R. M., WARD, P. S., YEN, K. E., LIAU, L. M., RABINOWITZ, J. D., CANTLEY, L. C., THOMPSON, C. B., VANDER HEIDEN, M. G. & SU, S. M. 2009. Cancer-associated IDH1 mutations produce 2-hydroxyglutarate. *Nature,* 462**,** 739-744.

DEL COLLADO, M., DA SILVEIRA, J. C., OLIVEIRA, M. L. F., ALVES, B. M. S. M., SIMAS, R. C., GODOY, A. T., COELHO, M. B., MARQUES, L. A., CARRIERO, M. M., NOGUEIRA, M. F. G., EBERLIN, M. N., SILVA, L. A., MEIRELLES, F. V. & PERECIN, F. 2017. In vitro maturation impacts cumulus–oocyte complex metabolism and stress in cattle. *Reproduction,* 154**,** 881-893.

DONOHOE, D. R. & BULTMAN, S. J. 2012. Metaboloepigenetics: interrelationships between energy metabolism and epigenetic control of gene expression. *Journal of Cellular Physiology,* 227**,** 3169-3177.

DUNNING, K. R., AKISON, L. K., RUSSELL, D. L., NORMAN, R. J. & ROBKER, R. L. 2011. Increased Beta-Oxidation and Improved Oocyte Developmental Competence in Response to l-Carnitine During Ovarian In Vitro Follicle Development in Mice. *Biology of Reproduction,* 85**,** 548-555.

DUNNING, K. R., LANE, M., BROWN, H. M., YEO, C., ROBKER, R. L. & RUSSELL, D. L. 2007. Altered composition of the cumulus-oocyte complex matrix during in vitro maturation of oocytes. *Human Reproduction,* 22**,** 2842-2850.

EPPIG, J. J. 1996. Coordination of nuclear and cytoplasmic oocyte maturation in eutherian mammals. *Reproduction, Fertility and Development,* 8**,** 485-489.

EPPIG, J. J., O'BRIEN, M. J., WIGGLESWORTH, K., NICHOLSON, A., ZHANG, W. & KING, B. A. 2009. Effect of in vitro maturation of mouse oocytes on the health and lifespan of adult offspring. *Human Reproduction,* 24**,** 922-928.

EPPIG, J. J., SCHROEDER, A. C. & BRIEN, M. J. O. 1992. Developmental capacity of mouse oocytes matured in vitro: effects of gonadotrophic stimulation, follicular origin and oocyte size. *Reproduction,* 95**,** 119-127.

FADINI, R., MIGNINI RENZINI, M., GUARNIERI, T., DAL CANTO, M., DE PONTI, E., SUTCLIFFE, A., SHEVLIN, M., COMI, R. & COTICCHIO, G. 2012. Comparison of the obstetric and perinatal outcomes of children conceived from in vitro or in vivo matured oocytes in in vitro maturation treatments with births from conventional ICSI cycles. *Human Reproduction,* 27**,** 3601-3608.

GARDNER, D. K. & SCHOOLCRAFT, W. B. 1999. In-vitro culture of human blastocyst. *Towards reproductive certainty: infertility and genetics beyond 1999***,** 378-388.

GE, Z.-J., LUO, S.-M., LIN, F., LIANG, Q.-X., HUANG, L., WEI, Y.-C., HOU, Y., HAN, Z.-M., SCHATTEN, H. & SUN, Q.-Y. 2014. DNA Methylation in Oocytes and Liver of Female Mice and Their Offspring: Effects of High-Fat-Diet–Induced Obesity. *Environmental Health Perspectives,* 122**,** 159-164.

GEGENFURTNER, K., FLENKENTHALER, F., FRÖHLICH, T., WOLF, E. & ARNOLD, G. J. 2020. The impact of transcription inhibition during in vitro maturation on the proteome of bovine oocytes†. *Biology of Reproduction,* 103**,** 1000-1011.

GESHI, M., TAKENOUCHI, N., YAMAUCHI, N. & NAGAI, T. 2000. Effects of Sodium Pyruvate in Nonserum Maturation Medium on Maturation, Fertilization, and Subsequent Development of Bovine Oocytes With or Without Cumulus Cells. *Biology of Reproduction,* 63**,** 1730-1734.

GILCHRIST, R. B., RITTER, L. J. & ARMSTRONG, D. T. 2004. Oocyte–somatic cell interactions during follicle development in mammals. *Animal Reproduction Science,* 82-83**,** 431-446.

GREEN, M. P., HARVEY, A. J., SPATE, L. D., KIMURA, K., THOMPSON, J. G. & ROBERTS, R. M. 2016. The effects of 2,4-dinitrophenol and d-glucose concentration on the development, sex ratio, and interferon-tau (IFNT) production of bovine blastocysts. *Molecular Reproduction and Development,* 83**,** 50-60.

GRINDLER, N. M. & MOLEY, K. H. 2013. Maternal obesity, infertility and mitochondrial dysfunction: potential mechanisms emerging from mouse model systems. *Molecular Human Reproduction,* 19**,** 486-494.

GROSS, S., CAIRNS, R. A., MINDEN, M. D., DRIGGERS, E. M., BITTINGER, M. A., JANG, H. G., SASAKI, M., JIN, S., SCHENKEIN, D. P., SU, S. M., DANG, L., FANTIN, V. R. & MAK, T. W. 2010. Cancer-associated metabolite 2-hydroxyglutarate accumulates in acute myelogenous leukemia with isocitrate dehydrogenase 1 and 2 mutations. *Journal of Experimental Medicine,* 207**,** 339-344.

GU, B. & LEE, M. G. 2013. Histone H3 lysine 4 methyltransferases and demethylases in self-renewal and differentiation of stem cells. *Cell & Bioscience,* 3**,** 39-39.

GU, L., LIU, H., GU, X., BOOTS, C., MOLEY, K. & WANG, Q. 2015. Metabolic control of oocyte development: linking maternal nutrition and reproductive outcomes. *Cellular and Molecular Life Sciences,* 72**,** 251-271.

GUILLEMETTE, B., DROGARIS, P., LIN, H.-H. S., ARMSTRONG, H., HIRAGAMI-HAMADA, K., IMHOF, A., BONNEIL, E., THIBAULT, P., VERREAULT, A. & FESTENSTEIN, R. J. 2011. H3 lysine 4 is acetylated at active gene promoters and is regulated by H3 lysine 4 methylation. *PLOS Genetics,* 7**,** e1001354-e1001354.

HAN, L., REN, C., LI, L., LI, X., GE, J., WANG, H., MIAO, Y.-L., GUO, X., MOLEY, K. H., SHU, W. & WANG, Q. 2018. Embryonic defects induced by maternal obesity in mice derive from Stella insufficiency in oocytes. *Nature Genetics,* 50**,** 432-442.

HAN, Y., YAN, J., ZHOU, J., TENG, Z., BIAN, F., GUO, M., MAO, G., LI, J., WANG, J., ZHANG, M. & XIA, G. 2012. Acute fasting decreases the expression of GLUT1 and glucose utilisation involved in mouse oocyte maturation and cumulus cell expansion. *Reproduction, Fertility and Development,* 24**,** 733-742.

HARRIS, S. E., LEESE, H. J., GOSDEN, R. G. & PICTON, H. M. 2009. Pyruvate and oxygen consumption throughout the growth and development of murine oocytes. *Molecular Reproduction and Development,* 76**,** 231-238.

HE, R. & KIDDER, B. L. 2017. H3K4 demethylase KDM5B regulates global dynamics of transcription elongation and alternative splicing in embryonic stem cells. *Nucleic Acids Research,* 45**,** 6427-6441.

HOLM, P., BOOTH, P. J. & CALLESEN, H. 2002. Kinetics of early in vitro development of bovine in vivo- and in vitro-derived zygotes produced and/or cultured in chemically defined or serum-containing media. *Reproduction,* 123**,** 553-65.

HUANG, J., ZHANG, H., WANG, X., DOBBS, K. B., YAO, J., QIN, G., WHITWORTH, K., WALTERS, E. M., PRATHER, R. S. & ZHAO, J. 2015. Impairment of Preimplantation Porcine Embryo Development by Histone Demethylase KDM5B Knockdown Through Disturbance of Bivalent H3K4me3-H3K27me3 Modifications. *Biology of Reproduction,* 92**,** 72, 1-11.

JENSEN, L. R., AMENDE, M., GUROK, U., MOSER, B., GIMMEL, V., TZSCHACH, A., JANECKE, A. R., TARIVERDIAN, G., CHELLY, J., FRYNS, J.-P., VAN ESCH, H., KLEEFSTRA, T., HAMEL, B., MORAINE, C., GECZ, J., TURNER, G., REINHARDT, R., KALSCHEUER, V. M., ROPERS, H.-H. & LENZNER, S. 2005. Mutations in the JARID1C gene, which is involved in transcriptional regulation and chromatin remodeling, cause X-linked mental retardation. *American Journal of Human Genetics,* 76**,** 227-236.

JOBERTY, G., BOESCHE, M., BROWN, J. A., EBERHARD, D., GARTON, N. S., HUMPHREYS, P. G., MATHIESON, T., MUELBAIER, M., RAMSDEN, N. G.,

READER, V., RUEGER, A., SHEPPARD, R. J., WESTAWAY, S. M., BANTSCHEFF, M., LEE, K., WILSON, D. M., PRINJHA, R. K. & DREWES, G. 2016. Interrogating the Druggability of the 2-Oxoglutarate-Dependent Dioxygenase Target Class by Chemical Proteomics. *ACS Chemical Biology,* 11**,** 2002-2010.

JONES, G. M., CRAM, D. S., SONG, B., MAGLI, M. C., GIANAROLI, L., LACHAM-KAPLAN, O., FINDLAY, J. K., JENKIN, G. & TROUNSON, A. O. 2008. Gene expression profiling of human oocytes following in vivo or in vitro maturation. *Human Reproduction,* 23**,** 1138-1144.

JUNGHEIM, E. S., SCHOELLER, E. L., MARQUARD, K. L., LOUDEN, E. D., SCHAFFER, J. E. & MOLEY, K. H. 2010. Diet-Induced Obesity Model: Abnormal Oocytes and Persistent Growth Abnormalities in the Offspring. *Endocrinology,* 151**,** 4039-4046.

KAELIN JR, WILLIAM G. & MCKNIGHT, STEVEN L. 2013. Influence of Metabolism on Epigenetics and Disease. *Cell,* 153**,** 56-69.

KUBISCH, H. M., LARSON, M. A., FUNAHASHI, H., DAY, B. N. & ROBERTS, R. M. 1995. Pronuclear visibility, development and transgene expression in IVM/IVF-derived porcine embryos. *Theriogenology,* 44**,** 391-401.

LEE, Y. S. L., THOUAS, G. A. & GARDNER, D. K. 2015. Developmental kinetics of cleavage stage mouse embryos are related to their subsequent carbohydrate and amino acid utilization at the blastocyst stage. *Human Reproduction,* 30**,** 543-552.

LEIBFRIED-RUTLEDGE, M. L., CRITSER, E. S., EYESTONE, W. H., NORTHEY, D. L. & FIRST, N. L. 1987. Development Potential of Bovine Oocytes Matured in Vitro or in Vivo. *Biology of Reproduction,* 36**,** 376-383.

LIU, X.-S., LITTLE, J. B. & YUAN, Z.-M. 2015. Glycolytic metabolism influences global chromatin structure. *Oncotarget,* 6**,** 4214-4225.

LUZZO, K. M., WANG, Q., PURCELL, S. H., CHI, M., JIMENEZ, P. T., GRINDLER, N., SCHEDL, T. & MOLEY, K. H. 2012. High Fat Diet Induced Developmental Defects

in the Mouse: Oocyte Meiotic Aneuploidy and Fetal Growth Retardation/Brain Defects. *PLOS ONE,* 7**,** e49217.

MADOGWE, E., TANWAR, D. K., TAIBI, M., SCHUERMANN, Y., ST-YVES, A. & DUGGAVATHI, R. 2020. Global analysis of FSH-regulated gene expression and histone modification in mouse granulosa cells. *Molecular Reproduction and Development,* 87**,** 1082-1096.

MAEKAWA, R., LEE, L., OKADA, M., ASADA, H., SHINAGAWA, M., TAMURA, I., SATO, S., TAMURA, H. & SUGINO, N. 2016. Changes in gene expression of histone modification enzymes in rat granulosa cells undergoing luteinization during ovulation. *Journal of Ovarian Research,* 9**,** 15.

NISHI, Y., TAKESHITA, T., SATO, K. & ARAKI, T. 2003. Change of the Mitochondrial Distribution in Mouse OoplasmDuring In Vitro Maturation. *Journal of Nippon Medical School,* 70**,** 408-415.

NIU, Y., DESMARAIS, T. L., TONG, Z., YAO, Y. & COSTA, M. 2015. Oxidative stress alters global histone modification and DNA methylation. *Free Radical Biology and Medicine,* 82**,** 22-28.

OBLETTE, A., RONDEAUX, J., DUMONT, L., DELESSARD, M., SAULNIER, J., RIVES, A., RIVES, N. & RONDANINO, C. 2019. DNA methylation and histone post-translational modifications in the mouse germline following in-vitro maturation of fresh or cryopreserved prepubertal testicular tissue. *Reproductive BioMedicine Online,* 39**,** 383-401.

PACELLA, L., ZANDER-FOX, D. L., ARMSTRONG, D. T. & LANE, M. 2012. Women with reduced ovarian reserve or advanced maternal age have an altered follicular environment. *Fertility and Sterility,* 98**,** 986-994.e2.

PAGE-LARIVIERE, F. & SIRARD, M. A. 2014. Spatiotemporal expression of DNA demethylation enzymes and histone demethylases in bovine embryos. *Cell Reprogramming,* 16**,** 40-53.

PARK, S.-J., KOMATA, M., INOUE, F., YAMADA, K., NAKAI, K., OHSUGI, M. & SHIRAHIGE, K. 2013. Inferring the choreography of parental genomes during fertilization from ultralarge-scale whole-transcriptome analysis. *Genes & Development,* 27**,** 2736-2748.

PEÑA, P. V., HOM, R. A., HUNG, T., LIN, H., KUO, A. J., WONG, R. P. C., SUBACH, O. M., CHAMPAGNE, K. S., ZHAO, R., VERKHUSHA, V. V., LI, G., GOZANI, O. & KUTATELADZE, T. G. 2008. Histone H3K4me3 Binding Is Required for the DNA Repair and Apoptotic Activities of ING1 Tumor Suppressor. *Journal of Molecular Biology,* 380**,** 303-312.

PEREIRA, N., NERI, Q. V., LEKOVICH, J. P., PALERMO, G. D. & ROSENWAKS, Z. 2016. The role of in-vivo and in-vitro maturation time on ooplasmic dysmaturity. *Reproductive BioMedicine Online,* 32**,** 401-406.

RIZOS, D., FAIR, T., PAPADOPOULOS, S., BOLAND, M. P. & LONERGAN, P. 2002. Developmental, qualitative, and ultrastructural differences between ovine and bovine embryos produced in vivo or in vitro. *Molecular Reproduction and Development,* 62**,** 320-327.

ROMAR, R., DE SANTIS, T., PAPILLIER, P., PERREAU, C., THÉLIE, A., DELL'AQUILA, M. E., MERMILLOD, P. & DALBIÈS-TRAN, R. 2011. Expression of Maternal Transcripts During Bovine Oocyte In Vitro Maturation is Affected by Donor Age. *Reproduction in Domestic Animals,* 46**,** e23-e30.

SALMINEN, A., KAARNIRANTA, K., HILTUNEN, M. & KAUPPINEN, A. 2014. Krebs cycle dysfunction shapes epigenetic landscape of chromatin: Novel insights into mitochondrial regulation of aging process. *Cellular Signalling,* 26**,** 1598-1603.

SCHINDELIN, J., ARGANDA-CARRERAS, I., FRISE, E., KAYNIG, V., LONGAIR, M., PIETZSCH, T., PREIBISCH, S., RUEDEN, C., SAALFELD, S. & SCHMID, B. 2012. Fiji: an open-source platform for biological-image analysis. *Nature Methods,* 9**,** 676.

SCHULTE, M. M. B., TSAI, J.-H. & MOLEY, K. H. 2015. Obesity and PCOS: The Effect of Metabolic Derangements on Endometrial Receptivity at the Time of Implantation. *Reproductive Sciences,* 22**,** 6-14.

SHA, Q.-Q., DAI, X.-X., JIANG, J.-C., YU, C., JIANG, Y., LIU, J., OU, X.-H., ZHANG, S.-Y. & FAN, H.-Y. 2018. CFP1 coordinates histone H3 lysine-4 trimethylation and meiotic cell cycle progression in mouse oocytes. *Nature Communications,* 9**,** 3477.

SHAO, G.-B., CHEN, J.-C., ZHANG, L.-P., HUANG, P., LU, H.-Y., JIN, J., GONG, A.-H. & SANG, J.-R. 2014. Dynamic patterns of histone H3 lysine 4 methyltransferases and demethylases during mouse preimplantation development. *In Vitro Cellular & Developmental Biology - Animal,* 50**,** 603-613.

SHU-CHI, M., JIANN-LOUNG, H., YU-HUNG, L., TSENG-CHEN, S., MING-I, L. & TSU-FUH, Y. 2006. Growth and development of children conceived by in-vitro maturation of human oocytes. *Early Human Development,* 82**,** 677-682.

SINCLAIR, K. D., ALLEGRUCCI, C., SINGH, R., GARDNER, D. S., SEBASTIAN, S., BISPHAM, J., THURSTON, A., HUNTLEY, J. F., REES, W. D., MALONEY, C. A., LEA, R. G., CRAIGON, J., MCEVOY, T. G. & YOUNG, L. E. 2007. DNA methylation, insulin resistance, and blood pressure in offspring determined by maternal periconceptional B vitamin and methionine status. *Proceedings of the National Academy of Sciences,* 104**,** 19351-19356.

SKINNER, M. K. 2008. What is an epigenetic transgenerational phenotype? F3 or F2. *Reproductive Toxicology (Elmsford, N.Y.),* 25**,** 2-6.

SÖDERSTRÖM-ANTTILA, V., MÄKINEN, S., TUURI, T. & SUIKKARI, A.-M. 2005. Favourable pregnancy results with insemination of in vitro matured oocytes from unstimulated patients. *Human Reproduction,* 20**,** 1534-1540.

STOKES, P. J., ABEYDEERA, L. R. & LEESE, H. J. 2005. Development of porcine embryos in vivo and in vitro; evidence for embryo 'cross talk' in vitro. *Developmental Biology,* 284**,** 62-71.

THOMPSON, J., SIMPSON, A., PUGH, P., WRIGHT, R. & TERVIT, H. 1991. Glucose utilization by sheep embryos derived in vivo and in vitro. *Reproduction, Fertility and Development,* 3**,** 571-576.

THOMPSON, J. G., PARTRIDGE, R. J., HOUGHTON, F. D., COX, C. I. & LEESE, H. J. 1996. Oxygen uptake and carbohydrate metabolism by in vitro derived bovine embryos. *Journal of Reproduction and Fertility,* 106**,** 299-306.

TRAN, K. A., DILLINGHAM, C. M. & SRIDHARAN, R. 2018. The role of α-ketoglutarate-dependent proteins in pluripotency acquisition and maintenance. *Journal of Biological Chemistry*.

VANDERHYDEN, B. C., CARON, P. J., BUCCIONE, R. & EPPIG, J. J. 1990. Developmental pattern of the secretion of cumulus expansion-enabling factor by mouse oocytes and the role of oocytes in promoting granulosa cell differentiation. *Developmental Biology,* 140**,** 307-317.

VUONG, L. N. 2020. *Health of IVF Versus IVM Children (FM-BABIES)* [Online]. https://ClinicalTrials.gov/show/NCT04296357. [Accessed 1 March 2021].

VUONG, L. N., HO, V. N. A., HO, T. M., DANG, V. Q., PHUNG, T. H., GIANG, N. H., LE, A. H., PHAM, T. D., WANG, R., NORMAN, R. J., SMITZ, J., GILCHRIST, R. B. & MOL, B. W. 2018. Effectiveness and safety of in vitro maturation of oocytes versus in vitro fertilisation in women with high antral follicle count: study protocol for a randomised controlled trial. *BMJ Open,* 8**,** e023413-e023413.

VUONG, L. N., HO, V. N. A., HO, T. M., DANG, V. Q., PHUNG, T. H., GIANG, N. H., LE, A. H., PHAM, T. D., WANG, R., SMITZ, J., GILCHRIST, R. B., NORMAN, R. J. & MOL, B. W. 2020. In-vitro maturation of oocytes versus conventional IVF in women with infertility and a high antral follicle count: a randomized non-inferiority controlled trial. *Human Reproduction,* 35**,** 2537-2547.

WRENZYCKI, C. & STINSHOFF, H. 2013. Maturation Environment and Impact on Subsequent Developmental Competence of Bovine Oocytes. *Reproduction in Domestic Animals,* 48**,** 38-43.

XU, W., YANG, H., LIU, Y., YANG, Y., WANG, P., KIM, S.-H., ITO, S., YANG, C., WANG, P., XIAO, M.-T., LIU, L.-X., JIANG, W.-Q., LIU, J., ZHANG, J.-Y., WANG, B., FRYE, S., ZHANG, Y., XU, Y.-H., LEI, Q.-Y., GUAN, K.-L., ZHAO, S.-M. & XIONG, Y. 2011. Oncometabolite 2-Hydroxyglutarate Is a Competitive Inhibitor of α-Ketoglutarate-Dependent Dioxygenases. *Cancer Cell,* 19**,** 17-30.

YEO, C. X., GILCHRIST, R. B. & LANE, M. 2009. Disruption of bidirectional oocyte-cumulus paracrine signaling during in vitro maturation reduces subsequent mouse oocyte developmental competence. *Biology of Reproduction,* 80**,** 1072-1080.

YEO, C. X., GILCHRIST, R. B., THOMPSON, J. G. & LANE, M. 2008. Exogenous growth differentiation factor 9 in oocyte maturation media enhances subsequent embryo development and fetal viability in mice. *Human Reproduction,* 23**,** 67-73.

YIN, H., JIANG, H., KRISTENSEN, S. G. & ANDERSEN, C. Y. 2016. Vitrification of in vitro matured oocytes collected from surplus ovarian medulla tissue resulting from fertility preservation of ovarian cortex tissue. *Journal of Assisted Reproduction and Genetics,* 33**,** 741-746.

YU, C., FAN, X., SHA, Q.-Q., WANG, H.-H., LI, B.-T., DAI, X.-X., SHEN, L., LIU, J., WANG, L., LIU, K., TANG, F. & FAN, H.-Y. 2017. CFP1 Regulates Histone H3K4 Trimethylation and Developmental Potential in Mouse Oocytes. *Cell Reports,* 20**,** 1161-1172.

ZHANG, B., ZHENG, H., HUANG, B., LI, W., XIANG, Y., PENG, X., MING, J., WU, X., ZHANG, Y., XU, Q., LIU, W., KOU, X., ZHAO, Y., HE, W., LI, C., CHEN, B., LI, Y., WANG, Q., MA, J., YIN, Q., KEE, K., MENG, A., GAO, S., XU, F., NA, J. & XIE, W. 2016. Allelic reprogramming of the histone modification H3K4me3 in early mammalian development. *Nature,* 537**,** 553.

ZHANG, Z., HE, C., ZHANG, L., ZHU, T., LV, D., LI, G., SONG, Y., WANG, J., WU, H., JI, P. & LIU, G. 2019. Alpha-ketoglutarate affects murine embryo development through metabolic and epigenetic modulations. *Reproduction,* 158**,** 125-135.

Chapter 5 Effects of elevated maternal body mass index on expression of *TET1-3* in human follicular cells, and its impact on embryo quality and cycle outcome

5.1 Chapter Link

In Chapter 4, under IVM conditions we have observed significant changes to cumulus cell expansion, which may lead to oocyte changes through nutrient uptake and perturbed signalling. Furthermore, in our HFD model in Chapter 3, we observed alterations to pyruvate oxidation in the oocyte without increased uptake of pyruvate, which is transported into the oocyte from the cumulus cells. In Chapter 2, in an HFD mouse model we observed a decrease in TET3 protein presence upon the chromatin, with increased pyruvate oxidation in the mitochondria, indicating increased TCA cycle based metabolism of pyruvate. It is unknown if any of these observed changes to availability of TCA cycle intermediaries as observed in Chapter 2 translate to changes in human samples, and clinical markers relevant to the IVF clinic.

In this study we will examine human cumulus and granulosa cells for expression of the *TET1-3* genes, to determine if elevated maternal body mass index alters gene expression. In addition, as a secondary outcome we will investigate whether *TET1-3* gene expression correlates with any aspect of IVF cycle outcome regardless of maternal BMI including fertilisation, embryo quality and embryo utilisation. Experiments were performed using cDNA created from extraction of total RNA from cumulus and granulosa samples from previous studies (REC 1677/2/2008 for patients collected 2006-2007, and REC 2114/10/11 for patients collected in 2009).

Cumulus and granulosa cells were examined as gene expression could not be directly examined in the oocytes from these patients due to both ethical considerations, and to also use cumulus and granulosa cells from oocytes that were cultured and used for embryo transfer. This will allow for examination of the effects of *TET1-3* expression in the cumulus and granulosa cells and correlation with cycle characteristic and outcome.

5.2 Author Declaration

Statement of Authorship

Title of Paper	Effects of elevated maternal body mass index on expression of *TET1-TET3* in human follicular cells, and its impact on embryo quality and cycle outcome
Publication Status	☐ Published ☐ Accepted for Publication ☐ Submitted for Publication ☑ Unpublished and Unsubmitted work written in manuscript style
Publication Details	Written in the style for Journal of Assisted Reproduction and Genetics (JARG)

Principal Author

Name of Principal Author (Candidate)	Alexander Penn		
Contribution to the Paper	Study design, performed experiments, analysed and interpreted data, wrote and edited the manuscript		
Overall percentage (%)	80%		
Certification:	This paper reports on original research I conducted during the period of my Higher Degree by Research candidature and is not subject to any obligations or contractual agreements with a third party that would constrain its inclusion in this thesis. I am the primary author of this paper.		
Signature		Date	16/07/2021

Co-Author Contributions

By signing the Statement of Authorship, each author certifies that:

i. the candidate's stated contribution to the publication is accurate (as detailed above);

ii. permission is granted for the candidate in include the publication in the thesis; and

iii. the sum of all co-author contributions is equal to 100% less the candidate's stated contribution.

Name of Co-Author	Deirdre Zander-Fox		
Contribution to the Paper	Experimental design, assisted in interpretation of data, and editing of the manuscript		
Signature		Date	28/06/2021

Name of Co-Author	Nicole O McPherson		
Contribution to the Paper	Assisted in interpretation of data, statistical analyses and editing of the manuscript		
Signature		Date	4/07/2021

Name of Co-Author	Tod Fullston		
Contribution to the Paper	Assisted in interpretation of data, and editing of the manuscript		
Signature		Date	02/07/2021

Name of Co-Author	Michelle Lane (deceased)		
Contribution to the Paper	Experimental design and assisted in interpretation of data.		
Signature		Date	

Please cut and paste additional co-author panels here as required.

5.3 Abstract

Purpose The rates of maternal overweight and obesity is increasing worldwide and is associated with reduced live birth rates. These poorer pregnancy outcomes seen in obese women may be in part influenced by altered cumulus and granulosa metabolism. This in turn may alter gene expression through changes via epigenetic mechanisms, such as DNA methylation 5mC, which is demethylated by the activity of Ten-Eleven Translocase (TET) proteins. The presence and function of these proteins have been explored in detail in oocytes in animal models, however expression in human cumulus and granulosa cells and their relationship with subsequent embryo development and pregnancy outcomes have never been assessed.

Methods Women undergoing routine IVF/ICSI fertility treatment (n=74) were recruited for the study. Female participants were classified as normal weight (BMI 18-25, n=38) or overweight/obese (BMI >25, n=36). Cumulus cells and granulosa cells were separated and collected from the oocytes obtained as part of the patient's normal ART cycle. Total RNA was extracted and expression of *TET1, TET2* and *TET3* assessed via quantitative PCR. These results were compared for expression changes based on maternal BMI via linear regression. Correlations between fertilisation, embryo quality and cycle outcomes and *TET1-3* expression (irrespective of maternal BMI) were also examined.

Results Maternal overweight/obesity did not alter expression of *TET1-3* in cumulus or granulosa cells, nor was there an observed linear relationship between maternal BMI and *TET1-3* expression. Overweight/obesity was associated with a reduced number of oocytes collected, however did not alter pregnancy or live birth rates. Decreased *TET2* expression in granulosa cells was associated with an increased proportion of slow growing embryos on day 3. Regression analysis also demonstrated that decreased *TET1* expression in granulosa cells was associated with increased fertilisation rate.

Conclusion We have demonstrated that *TET1-3* expression in human cumulus and granulosa cells does not appear to be influenced by maternal BMI, however independently their abundance considered alone may provide insight into embryo quality and fertilisation rates.

5.4 Introduction

38% of women entering into a pregnancy in Australia and other Western countries, are considered overweight or obese (Ng et al., 2014). Maternal obesity decreases oocyte quality, and thus embryo quality and pregnancy outcomes (Zander-Fox et al., 2012, Sermondade et al., 2019, Luke, 2017, Kaye et al., 2016, Mahmadaliyeva et al., 2018, Supramaniam et al., 2018, Bartolacci et al., 2019, Zhu et al., 2019, Brunet et al., 2020, Desmet et al., 2020). The mitochondrial activity of cumulus cells has been examined in relation to maternal obesity (Gorshinova et al., 2017), where obesity (BMI > 30) reduced the number of active mitochondria (Gorshinova et al., 2017). Additionally, obese women also have altered levels of key nutrients in their follicular fluid including glucose, triglyceride and free fatty acids (Robker et al., 2009). It has also been shown that impairment through lipid toxicity from endoplasmic reticulum (ER) stress from exposure to lipid rich follicular fluid from obese women impairs the maturation of oocytes (Yang et al., 2012). This may then in turn alter the metabolic environment of the cumulus oocyte complex (COC), modifying the metabolic profile of the oocyte.

It has been previously established through exploration of the Barker Hypothesis that maternal oocyte and foetal exposures to environmental cues can alter the health of subsequent children (Barker and Osmond, 1986). Maternal obesity has proven ability to alter foetal programming, where children born to obese mothers have increased bodyweight (Ovesen et al., 2011), increased energy intake (Brion et al., 2010) and increased cardiovascular risk (Forsén et al., 1997). These results indicate that exposure to obesity from before and during conception can result in poorer childhood health outcomes, suggesting a mechanism behind the heredity of this phenotype.

The oocyte is surrounded by layers of cumulus and granulosa cells, where cumulus cells provide energy to the oocyte, through the breakdown of glucose to form pyruvate, in addition to the beta oxidation of lipids (Dunning et al., 2011). Granulosa cells form the remainder of the ovarian follicle, which provide other growth factors for oocyte development, such as insulin-like growth factor 1 (IGF1) (Hammond et al., 1985). Granulosa cells influence oocyte

development through paracrine signalling and are susceptible to alterations in the metabolic environment, unlike cumulus cells which supply energy to the oocyte (Su et al., 2009).

Maternal obesity has previously been shown to decrease supply of lactate in follicular fluid, with a concomitant increase in glucose concentration, where elevated glucose was correlated with lower pregnancy rates (Wallace et al., 2012). These disruptions result from maternal obesity and can alter expression of key transcripts, where in human cumulus cells, BMI $\geq$ 25 kg/m^2 resulted in differential expression in 107 genes (Merhi et al., 2015). In particular, there was a positive association between increasing BMI and expression of *KIAA1234L*, a bone morphogenetic protein (BMP) regulator, where correct signalling is essential for correct embryo development (Zhu et al., 1999). Furthermore, in granulosa cells expression of insulin regulated genes, *CD36* and *SRBI* were increased under elevated maternal BMI (Robker et al., 2009). This highlights that the oocyte maturation period is sensitive to obesity/metabolic syndrome.

These modifications from maternal obesity can change IVF cycle outcomes even when the developing embryo has been removed from the maternal environment. There is an observed increase in live birth rates when using donor oocyte cycles with maternal obesity compared to autologous oocytes (Luke et al., 2011, Styne-Gross et al., 2005). This suggests that maternal obesity is reducing oocyte viability from before ovulation and preimplantation development as autologous oocytes are treated equally to donor oocytes within the *in vitro* fertilisation laboratory save the maternal environment (Luke et al., 2011). While modern *in vitro* culture of embryos created from oocytes obtained from obese women are able to produce high quality blastocysts and successful pregnancies after transfer to lower BMI mothers, biochemical and clinical pregnancy rates are still reduced relative to lower BMI donors (Cardozo et al., 2016). This suggests that these changes due to maternal obesity are programmed into the oocyte itself, and causes changes in the resulting embryo, even when transferred to a reduced stress environment.

The Ten-Eleven translocase (TET) family of proteins is responsible for the demethylation of 5-methylcytosine and are therefore linked to programming through the ability to alter the transcription of developmental genes. TET family members have been thoroughly examined in both HFD mouse models (Han et al., 2018), and studies directly on *Tet1-3* (1986, Inoue and Zhang, 2011, Ito et al., 2010, Ito et al., 2011, Koivunen et al., 2012, Shen et al., 2014, Simmons et al., 2008, Tahiliani et al., 2009, Wu and Zhang, 2010, Zhang et al., 2019), with very few human studies focused on TET protein expression in human oocytes (Efimova et al., 2015, Guo et al., 2014, Zhang et al., 2012). As TET proteins require α-ketoglutarate, a TCA cycle intermediary, as an energy source to oxidise 5mC to 5 hydroxymethylcytosine (5hmC), alterations to the cumulus oocyte complex (COC) metabolic environment seen in maternal overweight and obesity may directly alter TET activity in cumulus and granulosa cells. This may partly explain reported changes to oocyte quality, fertilisation and embryo development rates. Currently, there are no reported studies in the human of a link between *TET1-3* expression and maternal obesity.

Therefore, the objective of this study was to determine if increased maternal BMI (overweight/obese) alters the expression of *TET1*, *TET2* or *TET3* in cumulus and granulosa cells and determine if changes to *TET* expression are predictive of embryo development rates or pregnancy and live birth.

5.5 Materials and Methods

5.5.1 Patient recruitment

Women undergoing *in vitro* fertilisation (IVF) or intracytoplasmic sperm injection (ICSI) with a fresh embryo transfer were recruited from Repromed between April 2006 and December 2009.

Patients were grouped as normal weight (NW, BMI 18.5 – 25.0 kg/m^2, n=38) or overweight/obese (OW/OB, BMI >25.0 kg/m^2, n=36). Patients with polycystic ovary syndrome (PCOS) were excluded from this study as would confound results, as well as any cycles with donor recipient cycles, or preimplantation genetic testing (PGT) cycles.

This study was performed on biobanked cumulus cell and granulosa cell cDNA previously collected (Pacella-Ince et al., 2014b, Pacella-Ince et al., 2014a, Robker et al., 2009), with ethical approval from the Women's and Children's hospital REC 1677/2/2008 for patients collected 2006-2007, and REC 2114/10/11 for patients collected in 2009.

5.5.2 Clinical protocol

The clinical protocol used was as previously described in (Pacella-Ince et al., 2014b, Pacella-Ince et al., 2014a, Robker et al., 2009). Patients were administered daily recombinant follicle stimulating hormone (FSH, Gonal F, (Serono; Geneva, Switzerland), or Puregon, (Organon; Oss, Netherlands)) beginning on day 2 of the menstrual cycle. The gonadotrophin-releasing hormone (GnRH), 250 μg Orgalutran, Schering-Plough; Kenilworth, New Jersey, USA) was started on day 5-6 of stimulation and continued until human chorionic gonadotrophin (hCG) trigger administration (5000 IU Pregnyl, Schering-Plough, 250 μg Ovidrel, Serono). The hCG trigger was administered when two or more follicles were determined to be ≥ 17 mm diameter via ultrasound. Oocyte retrieval was performed transvaginally 36 h post hCG trigger under sedation.

5.5.3 Collection of granulosa and cumulus cells

Granulosa cells were collected at oocyte retrieval from surplus follicular fluid into 1X phosphate buffered saline (PBS, Sigma-Aldrich; St Louis, Missouri, USA). These collected granulosa cells were purified via density gradient centrifugation, where cells were first overlaid on a 60%/40% silica solution (Spermgrad; Vitrolife; Gothenburg, Sweden) and centrifuged at 470g for 30 min. Cumulus cells were collected by trimming cumulus-oocyte-complexes of their outer layers, then washing through PBS immediately after oocyte collection. Cells were dissociated by pipetting, and cumulus and granulosa cell counts were performed using a haemocytometer and diluted to a concentration of $1x10^6$ per mL, snap frozen in liquid nitrogen (LN_2) and stored at -80°C until RNA extraction was performed.

5.5.4 RNA isolation and quantitative PCR

Granulosa and cumulus cell RNA was extracted according to manufacturer's instructions using an RNEasy Mini kit (Qiagen; Hilden, Germany), or via a modification to the standard Tri-Reagent protocol (Simms et al., 1993, Chomczynski, 1993), where precipitation was instead performed overnight at -20°C, with final pellet dissolved in 25 µL ultrapure water (Robker et al., 2009). RNA concentration was determined using the Nanodrop 1000 spectrophotometer (Thermo Fisher; Waltham, Mass., USA). Reverse transcription to complementary DNA (cDNA) was performed using Superscript III Reverse Transcriptase kit (Invitrogen; Carlsbad, California, USA) as per manufacturer's instructions and stored at -20°C until real-time reverse transcription PCR (qPCR).

PCR was carried out using Taqman chemistry (Applied Biosystems; Foster City, California, USA) using Universal Master Mix without UNG (Applied Biosystems), using ribosomal protein *L19* (Hs02338565_gH) as an endogenous control. *L19* was selected as it is stably expressed in cumulus cells (Frota et al., 2011), while not altered by changes to metabolism (Robker et al., 2009), as may be observed with maternal obesity.

Best coverage probes were selected for *TET1* (Hs04189344_g1), *TET2* (Hs00325999_m1) and *TET3* (Hs00896441_m1) (Thermo Fisher). Samples were prepared in10uL reactions in a 0.1ml Fast plate (Life Tech) and cycled using standard Taqman cycling conditions (denaturation of 95^0C for 10 min, and 40 cycles of denaturation at 95^0C for 15 s and annealing/extension at 60^0C for 60 s) using the QuantStudio 3 Real-Time PCR system (Thermo Fisher). Samples were normalised to the endogenous control *RPL19* (ΔCt), and then OW/OB was expressed as fold change compared to NW. Samples which returned a Ct ≥ 35 were not deemed to have been expressed/detected and were excluded from analysis. All statistics were performed on ΔCt values.

5.5.5 Fertilisation protocol, embryo culture and embryo quality

Oocyte numbers at the time of oocyte pickup (OPU) were recorded and fertilised via either traditional *in vitro* insemination (IVF) in G-IVF Plus media (Vitrolife) or via intracytoplasmic sperm injection (ICSI) in G1 Plus media (Vitrolife). Embryos were cultured in G1 Plus from day 1 to day 3 of culture and changed over on day 3 into G2 Plus for culture to day 6.

Embryo quality was scored on day 3, on a scale of 1-4 (with 1 being the highest grade). On day 3 embryos were classified as cleavage stage embryos and graded based on cell number and fragmentation percentage (Veeck, 1999). In addition to comparison between embryo grades 1-4 between BMI groups, grade 1+2 and 3+4 were combined to determine any effect on "high quality" embryo development rates versus low quality.

Day 4 embryos were graded according to criteria as described previously (Feil et al., 2008). Day 5 and day 6 embryos were graded as blastocysts according to inner cell mass and trophectoderm cell counts and quality (Gardner and Schoolcraft, 1999).

Embryo transfers were performed on day 2-5 embryos under ultrasound guidance. Patients were in the care of their treating IVF physician until confirmation of a viable pregnancy following an ultrasound at 6-8 weeks gestation by the presence of a foetal pole and heartbeat.

5.5.6 Statistical analysis

Statistical analysis was performed using IBM SPSS Version 26. Normality was assessed using the Kolmogorov-Smirnov normality test. A P-value of <0.05 was considered statistically significant.

Differences in patient cohort were compared using general linear models if normally distributed or a one-way Kruskal-Wallis analysis of variance (ANOVA) if data was not normally distributed.

Infertility diagnoses were compared using binary logistic generalised linear models, with each diagnosis analysed separately.

The cycle cohort characteristics were compared using general linear models, except for the comparison between insemination methods (IVF/ICSI), which were compared using binary logistic generalised linear model.

TET1-3 expression differences grouped by BMI category were analysed using univariate general linear models if normally distributed, and one way Kruskal-Wallis ANOVA if not. Statistical analyses were performed on ΔCt values, with data presented as ΔCt, alongside fold change for linear interpretation of differences in expression

Linear regressions analysed the effect of BMI on patient and cycle characteristics. Maternal age, number of previous fresh cycles, starting FSH dose, and total FSH dose were included in the adjusted model.

TET1, *TET2* or *TET3* expression in cumulus or granulosa cells against embryo quality on day 3, fertilisation rate, number of embryos transferred, total embryo utilization from either total inseminated/injected oocytes or total fertilised embryos, biochemical pregnancy, foetal heart at pole scan, live birth rate, gestation length and birth rate were analysed using linear regression. Maternal BMI, maternal age, number of previous fresh cycles, starting FSH dose, and total FSH dose were included in the adjusted model.

5.6 Results

5.6.1 Patient demographics

A total of 74 patents were included in the analysis (Table 5.1), with n=38 (51.4%) patients presenting with BMI <25 kg/m^2 (normal weight, NW) and n=36 (48.7%) presenting with a BMI >25 kg/m^2 (overweight /obese OW/OB). Patient age was significantly higher in the overweight/obesity OW/OB group (P<0.01), along with increased BMI (P<0.001) and starting FSH dose (P<0.05, Table 5.1). There were no significant differences in total FSH dose (P=0.057), nor infertility diagnoses (Table 5.1).

5.6.2 Cycle characteristics

Cycle characteristics were compared to determine differences in oocyte collection and embryo outcome as a result of increased maternal BMI. There was a reduction in total oocyte number collected in OW/OB women compared to those with a normal BMI (11.5±6.6 NW, 8.4±6.5 OW/OB, P<0.05), although no difference were seen between insemination methods (IVF or ICSI), total fertilisation rate, embryo utilization per inseminated or injected oocyte, or embryo utilization per fertilised embryo (Table 5.2).

Biochemical pregnancy rate was numerically reduced due to overweight and obesity (39.4% NW vs 25.8% OW/OB), however was not statistically significant (Table 5.2). A similar numerical reduction was observed for foetal heart (33.3% NW vs 22.6% OW/OB) and live birth rates (27.3% NW vs 22.6% OW/OB, Table 5.2) however neither were statistically significant. Gestational length and infant birthweight were unaffected due to maternal overweight and obesity (Table 5.2).

5.6.3 Effect of overweight/obesity on *TET1-3* expression in cumulus and granulosa cells

Gene expression of *TET1*, *TET2* and *TET3* was assessed in NW and OW/OB cumulus or granulosa cells.

In both cumulus and granulosa cells, there were no significant differences in *TET1* (Figure 5.1a-b, Figure 5.2a-b), *TET2* (Figure 5.1c-d, Figure 5.2c-d) or *TET3* (Figure 5.1e-f, Figure 5.2e-f) expression when comparing between NW and OW/OB. The same results were also found for a linear regression across increasing BMI, where a per unit increase in BMI had no influence on *TET1*, *TET2* or *TET3* expression in granulosa and cumulus cells (Table 5.3). Table S5.1 shows the outcomes of the full adjusted model which in cumulus cells, increased starting FSH dose was related to increased *TET1* (β=0.053, CI [-0.005-0.100], P<0.05) and *TET2* expression (β= 0.036 CI [-0.004-0.068], P<0.05, Table S5.1), while in granulosa cells, increased previous number of cycles was related to increased *TET3* expression (β=0.452, CI [0.108-0.795], P<0.05, Table S5.1).

5.6.4 Effect of maternal BMI on embryo quality grading through preimplantation embryo development

Differences of embryo quality on day 3 were assessed between NW and OW/OB women (Table S5.2).

No statistically significant changes to embryo quality were observed for grade 1, grade 2, grade 3, grade 4, or grade 1+2 embryos on day 3 of embryo culture (Table S5.2). This demonstrates that patient BMI does not significantly alter embryo quality at this stage of development.

5.6.5 Effect of *TET1-3* expression on day 3 embryo quality

The effects of *TET1-3* expression in cumulus and granulosa cells on day 3 embryo quality was examined. Differences in embryo quality as grade 1, grade 2, grade 3 and grade 4 were compared, alongside grade 1 + 2 (high quality) and grade 3 + 4 (low quality).

In cumulus cells, a per unit decrease in *TET1*, *TET2*, or *TET3* expression did not alter embryo quality on day 3 of culture in both the unadjusted and adjusted models (Table S5.3). Further statistics on additional imputations are presented in Appendix A1.

Granulosa cell expression was also examined, as the different cell type has shown changes in expression profile. In granulosa cells, the unadjusted model showed that decreasing *TET1* expression was correlated with a decreased proportion of grade 2 embryos on day 3 (β=-0.069, CI [-0.137-0.002], P<0.05), however this was no longer significant in the adjusted model (β=-0.067 [-0.146-0.012], P=0.093) (Table S5.4).

In the unadjusted model, decreasing *TET2* was related to decreased proportion of grade 2 embryos on day 3 (β=-0.044, CI [-0.085- -0.002], P<0.05), however this was no longer evident in the adjusted model (β=-0.038, CI [-0.081-0.006], P=0.089). Further, in the adjusted model decreasing *TET2* was related to increased grade 4 embryos on day 3 (β=0.038, CI [0.011-0.066], P<0.01).

In both unadjusted and adjusted models, decreasing *TET3* did not correlate with embryo quality on day 3 (Table S5.4). Further statistics on additional imputations are presented in Appendix A1.

It should be noted that analyses of the relationship of *TET1-3* in cumulus and granulosa to embryo quality was not performed beyond day 3 as the proportion of embryos remaining on day4, 5 and 6 varied due to transfer and freezing on varying days and therefore those that remained were not an accurate representation of overall quality and results would be confounded.

5.6.6 Effect of *TET1-3* expression on oocyte fertilisation, embryo transfer results and pregnancy and live birth

The effects of *TET1-3* expression in cumulus and granulosa cells on fertilisation rate, embryo utilization, biochemical pregnancy, foetal heart, live birth, gestation length and birthweight were examined. Gestation length and birthweight were not analysed for cumulus cells as the degrees of freedom required were more than the total number of patients with these values available (Table S5.6).

In cumulus cells, in both the unadjusted and adjusted model *TET1* and *TET3* expression did not correlate with fertilisation rate, embryo transfer number, embryo utilization, biochemical pregnancy rate, foetal heart nor live birth rates (Table S5.6). Decreasing *TET2* expression in the unadjusted model correlated with increased fertilisation rate (β = 5.214, CI [0.785-9.643], $P<0.05$), however, this was no longer evident in the adjusted model (β = 4.625, CI [-0.206-9.456], P=0.060, Table S5.6). Embryos transferred, embryo utilization, biochemical pregnancy rate, foetal heart nor live birth were not significantly influenced by *TET2* gene expression.

Like *TET1*, decreasing *TET3* expression in an adjusted model did not significantly correlate with fertilisation rate, embryo utilization, biochemical pregnancy rate, foetal heart nor live birth rates (Table S5.6). Further statistics on additional imputations are presented in Appendix A2.

In granulosa cell in *TET2* or *TET3* and in the unadjusted model *TET1* expression did correlate with fertilisation rate, embryo utilization, biochemical pregnancy rate, foetal heart nor live birth rates (Table S5.7). However, in the adjusted model, decreasing *TET1* expression correlated with increased fertilisation rate (β=7.272 CI [1.610-12.933], $P<0.05$, Table S5.7), with no correlation seen with embryo utilization, biochemical pregnancy rate, foetal heart nor live birth. Further statistics on additional imputations are presented in Appendix A2

5.7 Discussion

Multiple reports have examined the effects of elevated maternal BMI on embryo quality and ART cycle outcomes (Zander-Fox et al., 2012, Sermondade et al., 2019, Luke, 2017, Kaye et al., 2016, Mahmadaliyeva et al., 2018, Supramaniam et al., 2018, Bartolacci et al., 2019, Zhu et al., 2019, Brunet et al., 2020, Desmet et al., 2020), with many reported a decrease in clinical pregnancy and live birth rates with maternal obesity (BMI > 30 kg/m^2) (Bartolacci et al., 2019, Brunet et al., 2020, Luke et al., 2011, Mahmadaliyeva et al., 2018, Sermondade et al., 2019, Zander-Fox et al., 2012). We attempted to extend these findings to assess if changes to gene expression of epigenetic regulators *TET1-3* in cumulus and granulosa cells from obese women could help explain these findings. Our study has demonstrated that like previous studies, maternal overweight/obesity is associated with reduced oocyte number at oocyte retrieval, despite increased FSH start dose and trending higher total dose. Additionally, we observed that decreasing expression of *TET2* in granulosa cells correlated with an increased proportion of poor grade embryos (grade 4 embryos) on day 3, whilst decreasing expression of *TET1* in granulosa cells was associated with increased fertilisation rates. However, this study was unable to demonstrate a correlation with *TET1-3* expression in granulosa and cumulus cells and female overweight/obesity. Whilst we did not find any link between maternal BMI and cumulus and granulosa *TET1-3* gene expression, other groups investigating gene expression changes in maternal overweight/obesity have shown alterations to other metabolically linked genes, including decreased expression in the glucose transporter *GLUT4*, and increased expression of insulin receptor substrate 2 (*IRS2*) in granulosa cells (Robker et al., 2009). Relating these changes to granulosa cell expression changes to clinical outcomes, oocytes from obese (BMI > 30 kg/m^2) women were fertilised at a lower rate compared to normal weight women (BMI 18-25 kg/m^2) (Robker et al., 2009). This supports our hypothesis that obesity is associated with alterations to metabolic profiles of cumulus oocytes complexes, which could be modifying the abundance of metabolic co-factors required for DNA and histone methylation.

The oocyte and early embryo rely on pyruvate based metabolism through the TCA cycle as a primary source of energy, however the cumulus and granulosa cells rely more on glucose metabolism and oxidative phosphorylation (Downs, 1995, Downs et al., 2002, Sutton-McDowall et al., 2004). Given that *TET1-3* use the TCA cycle intermediary α-ketoglutarate as a substrate, the decreased glucose uptake due to maternal obesity may reduce the available pyruvate pool and thus α-ketoglutarate (Leese and Barton, 1985) to be used by TETs. The regulation of DNA methylation changes in cumulus and granulosa cells and the oocyte will be the focus of future studies. Another report has shown that embryos generated from obese women consume less glucose, glutamine and glutamate from the media, with BMI being a negative predictor of glucose uptake (Leary et al., 2015). As glutamine and glutamate can be enzymatically converted to α-ketoglutarate via glutamate dehydrogenase in the embryo, this suggests that the obese egg would have reduced α-ketoglutarate concentrations.

While there were no alterations to *TET1-3* expression as a result of overweight/obesity in this study, there was an observed link between *TET1* expression in granulosa cells and fertilisation rate. Therefore, *TET1-3* levels may be playing a role in determining oocyte fertilisation and embryo developmental potential. There is precedent in the literature for gene expression changes in granulosa and cumulus cells to relate with clinical outcomes, where increased expression of *VERSICAN*, which binds with hyaluronan to form the extracellular matrix, and prostaglandin-endoperoxide synthase 2 (*PTGS2*), which forms part of the inflammation response, positively correlated with increased live birth rates and infant birthweight (Gebhardt et al., 2011). In addition, there has also been an observed correlation between mitochondrial DNA (mtDNA) copy number in cumulus cells and IVF cycle outcomes, including embryo quality (Ogino et al., 2016, Desquiret-Dumas et al., 2017). This is of interest as increased mtDNA copy number may be a sign of mitochondrial dysfunction (Gu et al., 2013), and therefore could indicate altered α-ketoglutarate availability and TET activity.

The effects of expression of *TET1-3* in cumulus and granulosa cells has been studied for its effects in bovine and murine studies, in order to examine changes to *TET* expression in both the oocyte and these cells, which is not possible in human studies for oocytes that are to be used for fertility treatments. In bovine cumulus cells, *TET3* has been found to be expressed at a 350 fold lower relative to the oocyte (Uh et al., 2020), suggesting that *TET3* is less important in cumulus cells than in the oocyte itself. TET3 is essential for demethylation of the paternal genome after fertilisation in preparation for embryonic genome activation (Gu et al., 2011, Lee et al., 2014). In the mouse, knockout of *TET2* in both oocytes and granulosa cells led to decrease in 5hmC in granulosa cells (Wang et al., 2020), suggesting that granulosa cells are equally sensitive to alterations to TET programming. Although oocytes from this knockout model matured normally, with no differences in oocyte number retrieved, they did find increased spindle abnormalities and reduced blastocyst formation, demonstrating the importance of *TET*2 in oocyte quality and developmental potential (Wang et al., 2020). This is of interest as increased spindle abnormalities are commonly seen in oocytes of infertile women and correlate with poorer embryonic outcomes following IVF or ICSI insemination (Tomari et al., 2018, Asa et al., 2017). Therefore, *TET2* may be important in the regulation of oocyte and embryo developmental potential.

Direct measurements of maternal BMI on epigenetic marks of cumulus and granulosa cells are limited, with most studies focussing on the oocyte. One study in mice examined the effects of obesity through high sugar feeding on cumulus gene expression (Chaffin et al., 2014). A high sugar diet was associated with increased gene expression of 35 transcripts and decreased gene expression of nine transcripts in cumulus cells (Chaffin et al., 2014), with particular alterations to amphiregulin (*AREG*), which binds the epidermal-like growth factor (EGF) receptor important for oocyte maturation to the MII stage (Peluffo et al., 2012), and *SPOCK3*, which is implicated in calcium binding, where calcium binding is essential in the oocyte for activation and resumption of meiosis after fertilisation. These results indicate that increased sugar intake to induce obesity can directly alter expression of key genes in cumulus cells, however this study

did not investigate whether these changes were due to modifications to DNA methylation, however does indicate that preconception poor diet can alter expression of genes critical to embryonic growth in cumulus and granulosa cells.

There were also observed effects on *TET* expression negatively associated with maternal age, the number of previous cycles, and also on total embryo utilization (although these were not significant given the number of samples in this study). Advanced maternal age is already associated with reduced mitochondrial ATP production in bovine oocytes (Iwata et al., 2011), which may in turn alter TET expression through changes to α-ketoglutarate availability and TCA cycle activity. We also noted an increased maternal age in our overweight and obese cohort, with this positive relationship being reported previously (van Harmelen et al., 2003). Even though we have shown few changes directly to *TET1-3* expression in cumulus and granulosa cells, there may still be altered methylation patterns in these cells, and the oocyte itself, as in a previous report it was shown that modifications to substrate availability (α-ketoglutarate) to oocyte culture media has the ability to alter 5mC, without any changes to TET1-2 abundance (Zhang et al., 2019).

Under maternal obesity it has been demonstrated that embryos consume less glucose from the media, with maternal BMI being a significant predictor of glucose uptake (Leary et al., 2015), as well as decreased uptake of glutamine and glutamate and no change in pyruvate uptake (Leary et al., 2015). As glutamine and glutamate can be enzymatically converted to α-ketoglutarate via glutamate dehydrogenase in the embryo, this suggests an overall reduction in metabolic energy uptake in the embryo., This was observed even during culture and *in vitro* fertilisation, which resulted in reduced blastocyst total cell count, inner cell mass (ICM) and trophectoderm (TE) cell counts, indicating that the reduced nutrient uptake results in slowed development. Overall, this shows that the maternal environment has epigenetically programmed the oocyte for its nutrient uptake, and thus growth trajectory post fertilisation.

The novel aspects and strengths of this study are that for the first time it investigated *TET* gene expression in human granulosa and cumulus cells to investigate whether maternal obesity was

associated with changes their expression, which can be associated to DNA methylation and thus form the possible basis of embryo programming.

The limitations of this study include the use of cDNA previously collected from two different patient cohorts, where one cohort was collected for analyses on maternal ovarian reserve and advanced maternal age (Pacella-Ince et al., 2014b, Pacella-Ince et al., 2014a). This can be observed where the maternal OW/OB patients also were significantly older, where aging also alters COC metabolic health (Pacella et al., 2012). Clinical protocol were similar between cohorts, with identical media and culture times and conditions, however, different FSH and hCG sources and doses were used which could be producing differing stimulation. In addition, these patients were all recruited from fertility clinic populations with no other lifestyle and biological factors were reordered, so despite the stated exclusions there may be additional comorbidities contributing to their subfertility other than maternal obesity (i.e. smoking, alcohol consumption) which have been linked to epigenetic regulation in other tissues (Zeilinger et al., 2013, Philibert et al., 2012).

In conclusion, this is the first study to examine if alterations to *TET1-3* expression in the cumulus and granulosa cells are associated with fertilisation, embryo quality and utilization rates in the human. We have established that increased maternal BMI (overweight/obesity) is not associated with any changes to *TET1-3* cumulus and granulosa gene expression in our cohort of patients. Independent of BMI, decreased *TET2* expression in granulosa cells was associated with reduced embryo quality on day 3. Additionally, increasing *TET1* expression in granulosa cells was associated with increased fertilisation rates. The future focus of this work will include analysis of TET activity in cumulus and granulosa cells (a better indicator of TET function) coupled with investigations into availability of metabolic co-factors such as α-ketoglutarate to provide further insight into epigenetic regulation via TETs. In addition, an increased sample size alongside assessment of changes to 5mC itself, will allow for further understanding of the effect that maternal overweight/obesity on the machinery responsible for DNA methylation and embryo programming.

Declarations

Acknowledgements

We would like to thank Leanne Pacella-Ince for de-identified data collection, and Jack Turner for technical assistance

5.8 Tables

Table 5.1 Patient Demographics as a total cohort, and for normal weight (NW, body mass index (BMI) 18.5-25 kg/m^2), overweight/obese (OW/OB, BMI >25 kg/m^2) patients

	Total	NW	OW/OB	P value
Number of patients	74	38	36	
Age Mean (±Std. Deviation)	35.89 ± 5.49	34.07 ± 5.32	37.61 ± 5.13	0.003
BMI Mean (±Std. Deviation)	28.10 ± 7.88	22.08 ± 1.79	34.28 ± 6.85	<0.001
Previous fresh cycles Median [range]	1.00 [0-9]	1.00 [0-9]	1.00 [0-8]	0.925
Starting FSH Dose Median [range]	300 [112-375]	225 [125-375]	300 [112-375]	0.016
Total FSH dose Median [range]	2700 [1250-4875]	2375 [1250-4200]	3000 [1344-4875]	0.057
Infertility Diagnosis Count (%)				
Tubular	9 (12.2%)	4 (10.5%)	5 (13.9%)	0.788
Endometrial	3 (4.1%)	2 (5.3%)	1 (2.8%)	0.594
Ovarian/Other	28 (37.8%)	15 (39.5%)	13 (36.1%)	0.766
Unexplained	9 (12.2%)	4 (10.5%)	5 (13.9%)	0.659
Male factor	46 (62.2%)	22 (57.9%)	24 (66.7%)	0.438

Where data normally distributed presented as Mean ± standard deviation (Std. Deviation), and where not normally distributed presented as median with range [minimum-maximum]. BMI = body mass index, FSH = Follicle stimulating hormone

Table 5.2 Cycle characteristics for oocyte collection, fertilisation rates and pregnancy results for the total cohort, normal weight (NW, body mass index (BMI) 18.5-25 kg/m^2), overweight/obese (OW/OB, BMI >25 kg/m^2)

	Total	NW	OW/OB	P-value
Number of patients	74 (72 IVF/ICSI, 64 ET)	38*	36*	
Oocytes collected	10.00 ± 6.20	11.47 ± 6.57	8.44 ± 5.46	**0.035**
IVF (n (%))	15 (20.8%)	10 (27.0%)	5 (14.3%)	0.189 (IVF
ICSI (n (%))	57 (79.2%)	27 (73.0%)	30 (85.7%)	vs ICSI)
IVF Fertilisation %	57.5	59.8	53.5	0.552
ICSI Fertilisation %	61.9	60.9	62.8	0.810
Total Fertilisation %	60.2	60.1	60.4	0.955
Total frozen + total transferred median [range]	2.00 [0-11]	3.00 [0-11]	2.00 [0-10]	0.122
Embryo utilisation (%) (per number of oocytes inseminated/injected)	40.92 (median 33.33)	38.5 (median 30.00)	43.56 (median 40.00)	0.439
Embryo utilisation (%) (per number of fertilised embryos)	62.61 (median 58.33)	58.97 (median 50.00)	66.37 (median 66.67)	0.194
Patients undergoing fresh embryo transfer	64	33	31	
Number of embryos transferred per patient Median [range]	1.00 [0-2]	1.00 [0-2]	1.00 [0-2]	0.512
Biochemical Pregnancy (from # ET) n (%)	21 (32.8%)	13 (39.4%)	8 (25.8%)	0.165
Foetal Heart (from ET) n (%)	18 (28.1%)	11 (33.3%)	7^ (22.6%)	0.341
Live Birth (from ET) n (%)	16 (25.0%)	9 (27.3%)	7^ (22.6%)	0.720
Singleton Gestation length (weeks) Mean± Std. Deviation	39.379 ± 1.21	39.650 ± 1.22	39.017 ± 1.21	0.352
Singleton Birth weight (g) Mean± Std. Deviation	3436 ± 408	3364 ± 318	3520 ± 511	0.514

*Both NW and OW/OB groups include a single patient in each group who did not undergo fertilisation. ^ includes one twin patient, reported as single data point, and excluded from gestation length and birthweight. Data presented as percentage where appropriate, and data not normally distributed presented as median with range [minimum-maximum]

Table 5.3 Gene expression regression against patient body mass index (BMI) for *TET1*, *TET2* and *TET3* in cumulus cells and granulosa cells

	Adjusted/ Unadjusted	Unstandardised β	95% Confidence Interval (CI)	P-value
TET1 Cumulus	Unadjusted	-0.25	-0.168 – 0.117	0.717
	Adjusted	-0.097	-0.29 – 0.096	0.307
TET2 Cumulus	Unadjusted	-0.044	-0.153 – 0.065	0.418
	Adjusted	-0.039	-0.175 – 0.097	0.560
TET3 Cumulus	Unadjusted	-0.112	-0.263 – 0.038	0.138
	Adjusted	-0.135	-0.332 – 0.063	0.173
TET1 Granulosa	Unadjusted	-0.057	-0.142 – 0.027	0.177
	Adjusted	-0.072	-0.164 – 0.019	0.117
TET2 Granulosa	Unadjusted	-0.028	-0.108 – 0.052	0.491
	Adjusted	-0.013	-0.102 – 0.07	0.774
TET3 Granulosa	Unadjusted	-0.074	-0.171 – 0.023	0.130
	Adjusted	-0.045	-0.150 – 0.059	0.383

Adjusted for age, previous cycles, oocytes collected, starting FSH dose, Total FSH Dose, Total fertilisation rate (both ICSI and IVF)

5.9 Figures

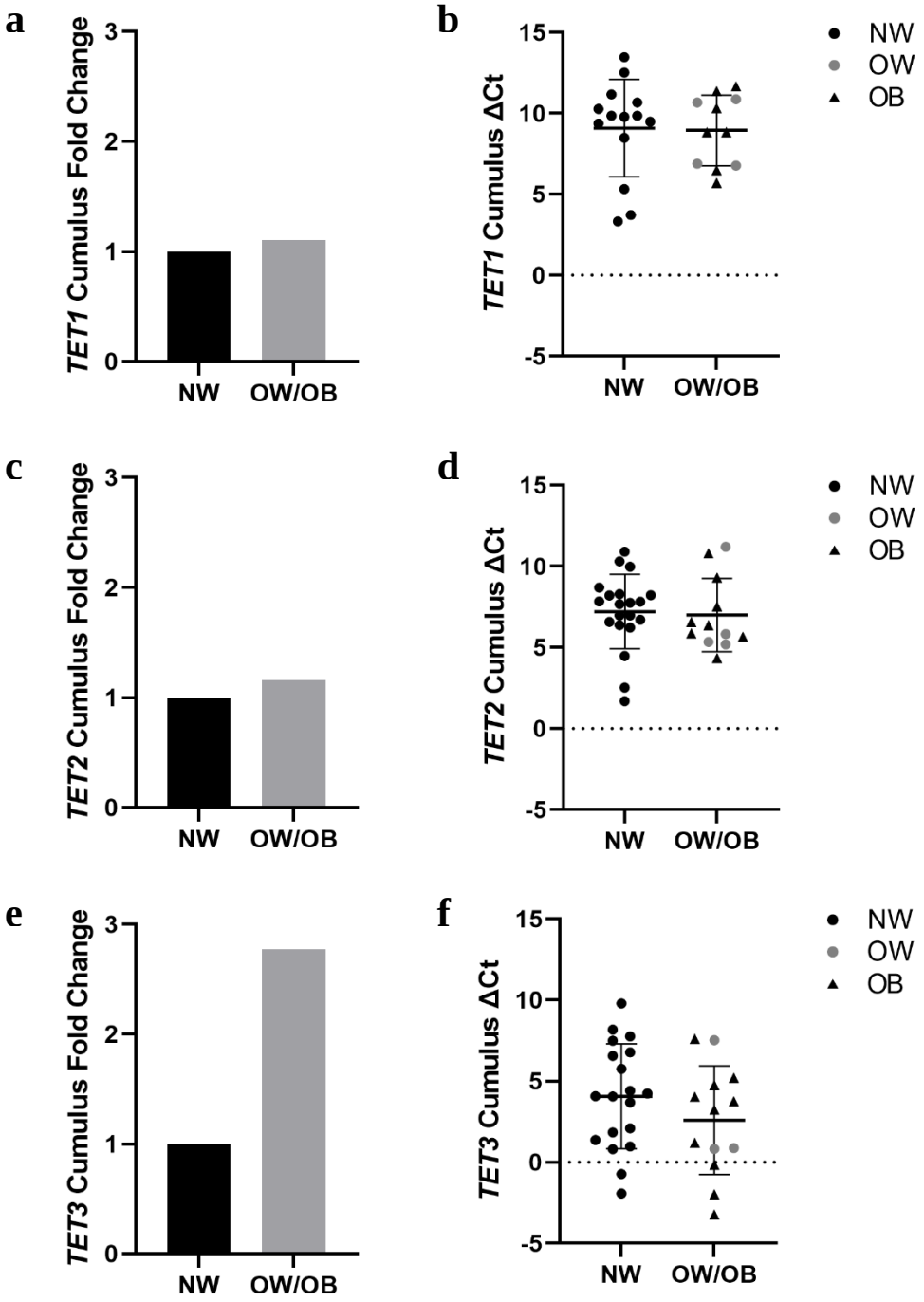

Figure 5.1 Gene expression of *TET1-3* in cumulus cells split by normal weight (NW, body mass index (BMI) 18.5-25 kg/m^2) and overweight/obese (OW/OB, BMI >25 kg/m^2). **a** *TET1* fold change ($2^{-\Delta\Delta Ct}$) **b** *TET1* expression ΔCt ± standard deviation (SD) , **c** *TET2* fold change ($2^{-\Delta\Delta Ct}$) and **d** *TET2* expression ΔCt ± SD, **e** TET3 fold change ($2^{-\Delta\Delta Ct}$) and **f** *TET3* expression ΔCt ± SD. Statistics performed on ΔCt values for *TET1-TET3*. Data from patients n=14 NW, n=11 OW/OB *TET1*, n=20 NW, n=12, OW/OB *TET2* and n=19 NW, and n=13 OW/OB *TET3*

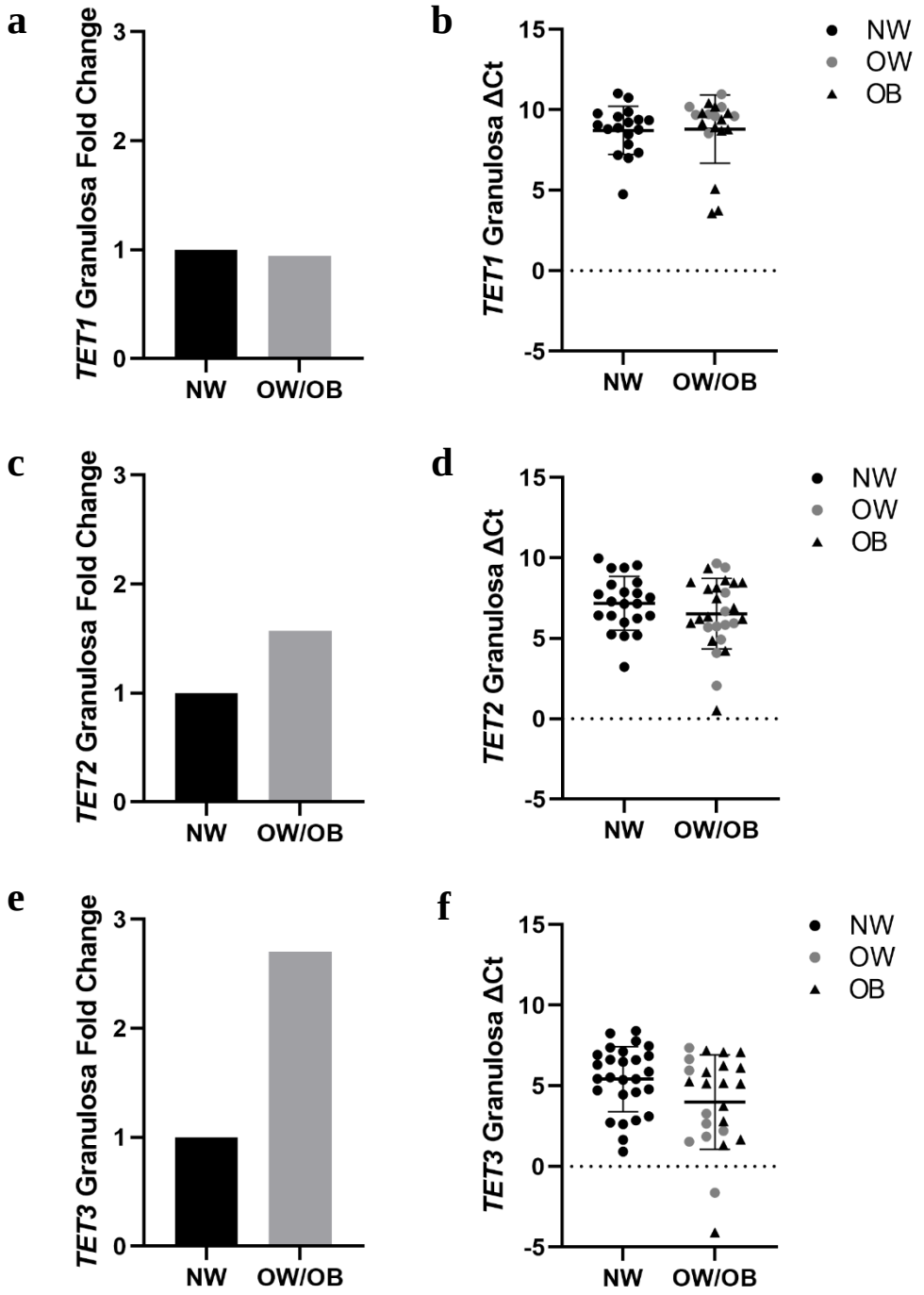

Figure 5.2 Gene expression of *TET1-3* in granulosa cells split by patients cells split by normal weight (NW, body mass index (BMI) 18.5-25 kg/m^2) and overweight/obese (OW/OB, BMI >25 kg/m^2). **a** *TET1* fold change ($2^{-\Delta\Delta Ct}$) **b** TET1 expression ΔCt ± standard deviation (SD) , **c** *TET2* fold change ($2^{-\Delta\Delta Ct}$) and **d** *TET2* expression ΔCt ± SD, **e** *TET3* fold change ($2^{-\Delta\Delta Ct}$) and **f** *TET3* expression ΔCt ± SD. Statistics performed on ΔCt values for *TET1-TET3*, with no significant differences present. Data from patients n=18 NW, n=20, OW/OB *TET1*, n=22 NW, n=27 OW/OB *TET2*, n=27 NW, and n=24 OW/OB *TET3*

5.10 Supplementary Tables

Table S5.1 Multiple imputed regression estimates for Table 5.3

Outcome	Variable	Est [95%CI] P-value
TET1 Cumulus	BMI	-0.097 [-0.290-0.096] P=0.307
	Age	-0.048 [-0.280-0.185] P=0.673
	Previous Cycles	-0.674 [-1.558-0.211] P=0.673
	Starting FSH	**0.053 [0.005-0.100] P=0.032**
	Total FSH	-0.003 [-0.007-0.000] P=0.064
TET2 Cumulus	BMI	-0.039 [-0.175-0.097] P=0.560
	Age	-0.111 [-0.293-0.071] P=0.221
	Previous Cycles	-0.109 [-0.687-0.470] P=0.703
	Starting FSH	**0.036 [0.004-0.068] P=0.031**
	Total FSH	-0.002 [-0.005-0.000] P=0.057
TET3 Cumulus	BMI	-0.135 [-0.332-0.063] P=0.173
	Age	-0.116 [-0.418-0.186] P=0.436
	Previous Cycles	-0.295 [-1.179-0.589] P=0.499
	Starting FSH	0.034 [-0.013-0.080] P=0.148
	Total FSH	-0.002 [-0.005-0.002] P=0.321
TET1 Granulosa	BMI	-0.072 [-0.164-0.019] P=0.117
	Age	0.100 [-0.051-0.251] P=0.185
	Previous Cycles	0.154 [-0.141-0.448] P=0.296
	Starting FSH	-0.023 [-0.050-0.005] P=0.107
	Total FSH	0.002 [-0.001-0.004] P=0.144
TET2 Granulosa	BMI	-0.013 [-0.102-0.077] P=0.774
	Age	-0.011 [-0.163-0.140] P=0.880
	Previous Cycles	0.260 [-0.045-0.566] P=0.093
	Starting FSH	-0.010 [-0.036-0.016] P=0.457
	Total FSH	0.000 [-0.002-0.002] P=0.820
TET3 Granulosa	BMI	-0.045 [-0.150-0.059] P=0.383
	Age	-0.101 [-0.280-0.078] P=0.260
	Previous Cycles	**0.452 [0.108-0.795] P=0.011**
	Starting FSH	-0.002 [-0.034-0.031] P=0.924
	Total FSH	0.000 [-0.003-0.002] P=0.837

Adjusted for body mass index (BMI), age, number of previous fresh cycles, starting follicle stimulating hormone (FSH dose), and total FSH dose. BMI = body mass index, CI = confidence interval

Table S5.2 Differences in embryo development for fertilised embryos for the total cohort, normal weight (NW, body mass index (BMI) 18.5-25 kg/m^2), overweight/obese (OW/OB, BMI >25 kg/m^2) on day 3 grouped by embryo grade on each day

	Total	NW (%)	OW/OB (%)	P value
D3 Grade 1 (median)	33.3	40.0	20.0	0.094
D3 Grade 2 (median)	14.8	14.3	23.1	0.668
D3 Grade 3 (median)	16.7	14.3	33.3	0.176
D3 Grade 4 (median)	0.0	0.0	0.0	0.526
D3 Grade 1+2 (median)	75.0	77.5	71.4	0.333
D3 Grade 3+4 (median)	25.0	22.5	28.6	0.333

Data presented as median percentage of all embryos in each grade per culture day, as all samples were not normally distributed

Table S5.3 Alterations to percentage embryo grades on each culture day from changes to *TET1*, *TET2* and *TET3* expression in cumulus cells

	TET1 Cumulus Cells		*TET2* Cumulus Cells		*TET3* Cumulus Cells	
	Unadjusted	Adjusted	Unadjusted	Adjusted	Unadjusted	Adjusted
D3 Grade 1	0.000 [-0.058-0.059] P=0.999	0.028 [-0.044-0.100] P=0.410	0.000 [-0.064-0.064] P=0.996	0.018 [-0.059-0.096] P=0.623	0.028 [-0.009-0.066] P=0.132	0.028 [-0.010-0.066] P=0.145
D3 Grade 2	0.002 [-0.053-0.057] P=0.937	0.001 [-0.070-0.071] P=0.982	0.001 [-0.050-0.051] P=0.974	-0.009 [-0.076-0.057] P=0.769	-0.019 [-0.047-0.009] P=0.166	-0.020 [-0.051-0.012] P=0.208
D3 Grade 3	-0.018 [-0.061-0.025] P=0.391	-0.039 [-0.087-0.008] P=0.096	-0.016 [-0.067-0.035] P=0.521	-0.012 [-0.079-0.055] P=0.713	-0.015 [-0.044-0.014] P=0.304	-0.008 [-0.042-0.025] P=0.607
D3 Grade 4	0.016 [-0.003-0.034] P=0.087	0.010 [-0.016-0.037] P=0.403	0.015 [-0.012-0.042] P=0.251	0.003 [-0.029-0.035] P=0.854	0.006 [-0.010-0.021] P=0.449	0.000 [-0.017-0.017] P=0.993
D3 Grade 1+Grade 2	0.002 [-0.050-0.054] P=0.933	0.029 [-0.036-0.093] P=0.346	0.001 [-0.058-0.060] P=0.973	0.009 [-0.071-0.089] P=0.813	0.009 [-0.025-0.043] P=0.593	0.008 [-0.031-0.048] P=0.664
D3 Grade 3+Grade 4	-0.002 [-0.054-0.050] P=0.933	-0.029 [-0.093-0.036] P=0.346	-0.001 [-0.060-0.058] P=0.973	-0.009 [-0.089-0.071] P=0.813	-0.009 [-0.043-0.025] P=0.593	-0.008 [-0.048-0.031] P=0.664

Adjusted for body mass index (BMI), age, number of previous fresh cycles, starting follicle stimulating hormone (FSH) dose, and total FSH dose. See Table S5.5 for statistics on adjustments

Table S5.4 Alterations to percentage embryo grades on each culture day from changes to *TET1*, *TET2* and *TET3* expression in granulosa cells

	TET1 Granulosa Cells		*TET2* Granulosa Cells		*TET3* Granulosa Cells	
	Unadjusted	Adjusted	Unadjusted	Adjusted	Unadjusted	Adjusted
D3 Grade 1	0.036 [-0.050-0.122] P=0.398	0.021 [-0.068-0.110] P=0.631	0.043 [-0.015-0.100] P=0.139	0.014 [-0.040-0.068] P=0.606	0.028 [-0.004-0.085] P=0.075	0.021 [-0.029-0.070] P=0.402
D3 Grade 2	**-0.069 [-0.137- -0.002] P=0.044**	-0.067 [-0.146-0.012] P=0.093	**-0.044 [-0.085- - 0.002] P=0.041**	-0.038 [-0.081-0.006] P=0.089	-0.021 [-0.057-0.014] P=0.229	-0.020 [-0.062-0.022] P=0.332
D3 Grade 3	0.012 [-0.050-0.075] P=0.687	0.019 [-0.054-0.093] P=0.590	-0.025 [-0.070-0.021] P=0.281	-0.015 [-0.063-0.034] P=0.545	-0.031 [-0.035-0.003] P=0.076	-0.023 [-0.064-0.017] P=0.254
D3 Grade 4	0.021 [-0.021-0.063] P=0.312	0.027 [-0.017-0.071] P=0.218	0.026 [-0.002-0.053] P=0.069	**0.038 [0.011-0.066] P=0.007**	0.012 [-0.009-0.033] P=0.265	0.023 [-0.001-0.046] P=0.056
D3 Grade 1+Grade 2	-0.033 [-0.109-0.042] P=0.371	-0.046 [-0.128-0.036] P=0.254	-0.001 [-0.055-0.053] P=0.972	-0.024 [-0.079-0.031] P=0.385	0.019 [-0.021-0.059] P=0.337	0.000 [-0.045-0.046] P=0.990
D3 Grade 3+Grade 4	0.033 [-0.042-0.109] P=0.371	0.046 [-0.036-0.128] P=0.254	0.001 [-0.053-0.055] P=0.972	0.024 [-0.031-0.079] P=0.385	-0.019 [-0.059-0.021] P=0.337	0.000 [-0.046-0.045] P=0.990

Adjusted for body mass index (BMI), age, number of previous fresh cycles, starting follicle stimulating hormone (FSH) dose, and total FSH dose. See Table S5.5 for statistics on adjustments

Table S5.5 Multiple imputed regression estimates for Table S5.3 and S5.4

Transcript	Outcome	Variable	Est [95% CI] P-value
TET1 Cumulus	D3 Grade 1	TET	0.028 [-0.044-0.100] P=0.410
		BMI	0.001 [-0.028-0.030] P=0.931
		Age	-0.010 [-0.047-0.027] P=0.551
		Previous Cycles	0.012 [-0.105-0.129] P=0.823
		Starting FSH	-0.005 [-0.013-0.003] P=0.170
		Total FSH	0.001 [0.000-0.001] P=0.066
	D3 Grade 2	TET	0.001 [-0.070-0.071] P=0.982
		BMI	0.012 [-0.016-0.040] P=0.369
		Age	0.007 [-0.029-0.043] P=0.684
		Previous Cycles	0.042 [-0.072-0.156] P=0.436
		Starting FSH	0.001 [-0.006-0.009] P=0.688
		Total FSH	0.000 [-0.001-0.000] P=0.630
	D3 Grade 3	TET	-0.039 [-0.087-0.008] P=0.096
		BMI	-0.010 [-0.029-0.010] P=0.294
		Age	0.003 [-0.022-0.027] P=0.811
		Previous Cycles	-0.063 [-0.140-0.014] P=0.099
		Starting FSH	0.003 [-0.003-0.008] P=0.232
		Total FSH	0.000 [-0.001-0.000] P=0.082
	D3 Grade 4	TET	0.010 [-0.016-0.037] P=0.403
		BMI	-0.004 [-0.014-0.007] P=0.468
		Age	0.001 [-0.013-0.014] P=0.900
		Previous Cycles	0.009 [-0.034-0.052] P=0.655
		Starting FSH	0.001 [-0.002-0.004] P=0.535
		Total FSH	0.000 [0.000-0.000] P=0.432
	D3 Grade 1+Grade 2	TET	0.029 [-0.036-0.093] P=0.346
		BMI	0.013 [-0.013-0.039] P=0.285
		Age	-0.004 [-0.037-0.030] P=0.819
		Previous Cycles	0.054 [-0.050-0.159] P=0.278
		Starting FSH	-0.004 [-0.011-0.003] P=0.256
		Total FSH	0.000 [0.000-0.001] P=0.108
	D3 Grade 3+Grade 4	TET	-0.029 [-0.093-0.036] P=0.346
		BMI	-0.013 [-0.039-0.013] P=0.285
		Age	0.004 [-0.030-0.037] P=0.819
		Previous Cycles	-0.054 [-0.159-0.050] P=0.278
		Starting FSH	0.004 [-0.003-0.011] P=0.256
		Total FSH	0.000 [-0.001-0.000] P=0.108

Table S5.5 Continued

Transcript	Outcome	Variable	Est [95% CI] P-value
TET2 Cumulus	D3 Grade 1	TET	0.018 [-0.059-0.096] P=0.623
		BMI	-0.013 [-0.036-0.010] P=0.245
		Age	-0.005 [-0.042-0.031] P=0.752
		Previous Cycles	-0.009 [-0.107-0.089] P=0.852
		Starting FSH	-0.004 [-0.011-0.003] P=0.292
		Total FSH	0.000 [0.000-0.001] P=0.147
	D3 Grade 2	TET	-0.009 [-0.076-0.057] P=0.769
		BMI	0.008 [-0.012-0.028] P=0.411
		Age	0.001 [-0.030-0.031] P=0.969
		Previous Cycles	0.013 [-0.071-0.096] P=0.753
		Starting FSH	0.002 [-0.004-0.008] P=0.411
		Total FSH	0.000 [-0.001-0.000] P=0.378
	D3 Grade 3	TET	-0.012 [-0.079-0.055] P=0.713
		BMI	0.013 [-0.007-0.033] P=0.181
		Age	0.001 [-0.030-0.033] P=0.928
		Previous Cycles	0.009 [-0.075-0.094] P=0.816
		Starting FSH	-0.001 [-0.007-0.005] P=0.692
		Total FSH	0.000 [-0.001-0.000] P=0.900
	D3 Grade 4	TET	0.003 [-0.029-0.035] P=0.854
		BMI	-0.008 [-0.018-0.002] P=0.100
		Age	0.004 [-0.011-0.019] P=0.626
		Previous Cycles	-0.013 [-0.054-0.027] P=0.498
		Starting FSH	0.002 [-0.001-0.005] P=0.102
		Total FSH	0.000 [0.000-0.000] P=0.143
	D3 Grade 1+Grade 2	TET	0.009 [-0.071-0.089] P=0.813
		BMI	-0.005 [-0.029-0.018] P=0.642
		Age	-0.005 [-0.042-0.032] P=0.783
		Previous Cycles	0.004 [-0.096-0.104] P=0.937
		Starting FSH	-0.001 [-0.008-0.006] P=0.724
		Total FSH	0.000 [-0.000-0.001] P=0.476
	D3 Grade 3+Grade 4	TET	-0.009 [-0.089-0.071] P=0.813
		BMI	0.005 [-0.018-0.029] P=0.642
		Age	0.005 [-0.032-0.042] P=0.783
		Previous Cycles	-0.004 [-0.104-0.096] P=0.937
		Starting FSH	0.001 [-0.006-0.008] P=0.724
		Total FSH	0.000 [-0.001-0.000] P=0.476

Table S5.5 Continued

Transcript	Outcome	Variable	Est [95% CI] P-value
TET3 Cumulus	D3 Grade 1	TET	0.028 [-0.010-0.066] P=0.145
		BMI	-0.012 [-0.033-0.009] P=0.241
		Age	-0.001 [-0.032-0.031] P=0.959
		Previous Cycles	0.004 [-0.089-0.097] P=0.931
		Starting FSH	-0.005 [-0.010-0.001] P=0.073
		Total FSH	**0.000 [0.000-0.001] P=0.031**
	D3 Grade 2	TET	-0.020 [-0.051-0.012] P=0.208
		BMI	0.007 [-0.011-0.024] P=0.441
		Age	-0.002 [-0.028-0.024] P=0.873
		Previous Cycles	0.007 [-0.069-0.082] P=0.853
		Starting FSH	0.003 [-0.001-0.008] P=0.170
		Total FSH	0.000 [-0.001-0.000] P=0.166
	D3 Grade 3	TET	-0.008 [-0.042-0.025] P=0.607
		BMI	0.011 [-0.008-0.030] P=0.235
		Age	0.002 [-0.026-0.029] P=0.893
		Previous Cycles	0.002 [-0.080-0.083] P=0.969
		Starting FSH	-0.001 [-0.005-0.004] P=0.818
		Total FSH	0.000 [0.000-0.000] P=0.778
	D3 Grade 4	TET	0.000 [-0.017-0.017] P=0.993
		BMI	-0.005 [-0.014-0.004] P=0.257
		Age	0.001 [-0.013-0.015] P=0.885
		Previous Cycles	-0.012 [-0.053-0.028] P=0.537
		Starting FSH	**0.002 [0.000-0.005] P=0.046**
		Total FSH	0.000 [0.000-0.000] P=0.053
	D3 Grade 1+Grade 2	TET	0.008 [-0.031-0.048] P=0.664
		BMI	-0.006 [-0.028-0.016] P=0.590
		Age	-0.003 [-0.035-0.030] P=0.860
		Previous Cycles	0.011 [-0.085-0.106] P=0.818
		Starting FSH	-0.002 [-0.008-0.004] P=0.488
		Total FSH	0.000 [0.000-0.001] P=0.277
	D3 Grade 3+Grade 4	TET	-0.008 [-0.048-0.031] P=0.664
		BMI	0.006 [-0.016-0.028] P=0.590
		Age	0.003 [-0.030-0.035] P=0.860
		Previous Cycles	-0.011 [-0.106-0.085] P=0.818
		Starting FSH	0.002 [-0.004-0.008] P=0.488
		Total FSH	0.000 [-0.001-0.000] P=0.277

Table S5.5 Continued

Transcript	Outcome	Variable	Est [95% CI] P-value
TET1 Granulosa	D3 Grade 1	TET	0.021 [-0.068-0.110] P=0.631
		BMI	-0.003 [-0.068-0.110] P=0.631
		Age	0.002 [-0.037-0.040] P=0.933
		Previous Cycles	0.049 [-0.039-0.138] P=0.259
		Starting FSH	**-0.008 [-0.015-0.000] P=0.039**
		Total FSH	0.000 [0.000-0.001] P=0.074
	D3 Grade 2	TET	-0.067 [-0.146-0.012] P=0.093
		BMI	-0.003 [-0.023-0.016] P=0.723
		Age	0.003 [-0.031-0.038] P=0.841
		Previous Cycles	-0.028 [-0.106-0.051] P=0.476
		Starting FSH	0.003 [-0.004-0.009] P=0.383
		Total FSH	0.000 [-0.001-0.000] P=0.336
	D3 Grade 3	TET	0.019 [-0.054-0.093] P=0.590
		BMI	0.005 [-0.013-0.024] P=0.554
		Age	-0.003 [-0.035-0.029] P=0.844
		Previous Cycles	-0.004 [-0.077-0.069] P=0.907
		Starting FSH	0.001 [-0.005-0.007] P=0.635
		Total FSH	0.000 [-0.000-0.000] P=0.812
	D3 Grade 4	TET	0.027 [-0.017-0.071] P=0.218
		BMI	0.001 [-0.010-0.012] P=0.820
		Age	-0.002 [-0.021-0.017] P=0.838
		Previous Cycles	-0.018 [-0.061-0.026] P=0.411
		Starting FSH	0.004 [0.000-0.007] P=0.053
		Total FSH	0.000 [0.000-0.000] P=0.119
	D3 Grade 1+Grade 2	TET	-0.046 [-0.128-0.036] P=0.254
		BMI	-0.009 [-0.027-0.014] P=0.513
		Age	0.005 [-0.031-0.041] P=0.774
		Previous Cycles	0.022 [-0.059-0.103] P=0.583
		Starting FSH	-0.005 [-0.012-0.002] P=0.140
		Total FSH	0.000 [0.000-0.001] P=0.289
	D3 Grade 3+Grade 4	TET	0.046 [-0.036-0.128] P=0.254
		BMI	0.007 [-0.014-0.027] P=0.513
		Age	-0.005 [-0.041-0.031] P=0.774
		Previous Cycles	-0.022 [-0.103-0.059] P=0.583
		Starting FSH	0.005 [-0.002-0.012] P=0.140
		Total FSH	0.000 [-0.001-0.000] P=0.289

Table S5.5 Continued

Transcript	Outcome	Variable	Est [95% CI] P-value
TET2 Granulosa	D3 Grade 1	TET	0.014 [-0.040-0.068] P=0.606
		BMI	-0.004 [-0.020-0.012] P=0.596
		Age	0.002 [-0.027-0.032] P=0.884
		Previous Cycles	**0.093 [0.020-0.167] P=0.014**
		Starting FSH	**-0.007 [-0.012--0.002] P=0.006**
		Total FSH	**0.000 [0.000-0.001] P=0.027**
	D3 Grade 2	TET	-0.038 [-0.081-0.006] P=0.089
		BMI	-0.009 [-0.021-0.004] P=0.187
		Age	0.001 [-0.023-0.024] P=0.962
		Previous Cycles	-0.048 [-0.107-0.012] P=0.114
		Starting FSH	0.003 [-0.002-0.007] P=0.207
		Total FSH	0.000 [0.000-0.000] P=0.247
	D3 Grade 3	TET	-0.015 [-0.063-0.034] P=0.545
		BMI	0.014 [-0.001-0.028] P=0.061
		Age	-0.005 [-0.032-0.021] P=0.693
		Previous Cycles	-0.024 [-0.091-0.042] P=0.458
		Starting FSH	0.002 [-0.003-0.006] P=0.475
		Total FSH	0.000 [0.000-0.00] P=0.584
	D3 Grade 4	TET	**0.038 [0.011-0.066] P=0.007**
		BMI	-0.001 [-0.009-0.007] P=0.818
		Age	0.003 [-0.012-0.017] P=0.734
		Previous Cycles	-0.021 [-0.059-0.016] P=0.249
		Starting FSH	**0.003 [0.000-0.006] P=0.022**
		Total FSH	0.000 [0.000-0.000] P=0.097
	D3 Grade 1+Grade 2	TET	-0.024 [-0.079-0.031] P=0.385
		BMI	-0.013 [-0.029-0.003] P=0.120
		Age	0.003 [-0.027-0.033] P=0.857
		Previous Cycles	0.046 [-0.029-0.121] P=0.223
		Starting FSH	-0.005 [-0.010-0.001] P=0.076
		Total FSH	0.000 [0.000-0.001] P=0.192
	D3 Grade 3+Grade 4	TET	0.024 [-0.031-0.079] P=0.385
		BMI	0.013 [-0.003-0.029] P=0.120
		Age	-0.003 [-0.033-0.027] P=0.857
		Previous Cycles	-0.046 [-0.121-0.029] P=0.223
		Starting FSH	0.005 [-0.001-0.010] P=0.076
		Total FSH	0.000 [-0.001-0.000] P=0.192

Table S5.5 Continued

Transcript	Outcome	Variable	Est [95% CI] P-value
TET3 Granulosa	D3 Grade 1	TET	0.021 [-0.029-0.070] P=0.402
		BMI	-0.007 [-0.023-0.009] P=0.397
		Age	0.008 [-0.024-0.040] P=0.627
		Previous Cycles	0.051 [-0.019-0.122] P=0.150
		Starting FSH	**-0.008 [-0.013--0.002] P=0.006**
		Total FSH	**0.000 [0.000-0.001] P=0.016**
	D3 Grade 2	TET	-0.020 [-0.062-0.022] P=0.332
		BMI	-0.005 [-0.019-0.009] P=0.495
		Age	0.000 [-0.027-0.027] P=0.981
		Previous Cycles	-0.005 [-0.065-0.055] P=0.868
		Starting FSH	0.003 [-0.001-0.008] P=0.161
		Total FSH	0.000 [-0.001-0.000] P=0.141
	D3 Grade 3	TET	-0.023 [-0.064-0.017] P=0.254
		BMI	*0.013 [0.000-0.027] P=0.056*
		Age	-0.009 [-0.035-0.018] P=0.512
		Previous Cycles	-0.018 [-0.076-0.041] P=0.526
		Starting FSH	0.002 [-0.003-0.006] P=0.488
		Total FSH	0.000 [0.000-0.000] P=0.603
	D3 Grade 4	TET	*0.023 [-0.001-0.046] P=0.056*
		BMI	-0.001 [-0.009-0.006] P=0.715
		Age	0.001 [-0.014-0.016] P=0.881
		Previous Cycles	-0.028 [-0.062-0.006] P=0.099
		Starting FSH	**0.003 [0.000-0.006] P=0.025**
		Total FSH	0.000 [0.000-0.000] P=0.094
	D3 Grade 1+Grade 2	TET	0.000 [-0.045-0.046] P=0.990
		BMI	-0.012 [-0.027-0.004] P=0.128
		Age	0.007 [-0.022-0.037] P=0.614
		Previous Cycles	0.046 [-0.019-0.112] P=0.159
		Starting FSH	-0.005 [-0.010-0.001] P=0.077
		Total FSH	0.000 [0.000-0.001] P=0.186
	D3 Grade 3+Grade 4	TET	0.000 [-0.046-0.045] P=0.990
		BMI	0.012 [-0.004-0.027] P=0.128
		Age	-0.007 [-0.037-0.022] P=0.614
		Previous Cycles	-0.046 [-0.112-0.019] P=0.159
		Starting FSH	0.005 [-0.001-0.010] P=0.077
		Total FSH	0.000 [-0.001-0.000] P=0.186

BMI = body mass index, FSH = follicle stimulating hormone CI = confidence interval

Table S5.6 Differences in cycle outcomes fertilisation rate, embryos transferred, pregnancy rates, live birth rates, gestation length and birth weight from changes to *TET1*, *TET2* and *TET3* expression in cumulus cells

	TET1 CC		*TET2 C*C		*TET3* CC	
	Unadjusted	Adjusted	Unadjusted	Adjusted	Unadjusted	Adjusted
Fertilisation rate Unstandardised β [CI] P=	3.72 [-1.099-8.544] P=0.124	2.814 [-2.269-7.898] P=0.259	**5.214 [0.785-9.643] P=0.023**	4.625 [-0.206-9.456] P=0.060	0.826 [-2.205-3.856] P=0.582	-0.165 [-2.621-2.291] P=0.891
Embryos transferred Unstandardised β [CI] P-value	0.062 [-0.023-0.153] P=0.172	0.072 [-0.036-0.179] P=0.179	0.066 [-0.025-0.157] P=0.151	0.074 [-0.025-0.173] P=0.134	-0.006 [-0.067-0.054] P=0.829	-0.011 [-0.077-0.054] P=0.724
Embryo utilisation (%) (per number of oocytes inseminated/injected) Unstandardised β [CI] P-value	2.697 [-1.383-6.777] P=0.184	1.700 [-2.858-6.258] P=0.442	3.734 [-0.053-7.521] P=0.053	2.736 [-1.285-6.757] P=0.173	1.798 [-0.814-4.410] P=0.170	0.992 [-1.434-3.418] P=0.407
Embryo utilisation (%) (per number of fertilised embryos) Unstandardised β [CI] P-value	2.020 [-3.745-7.786] P=0.472	2.180 [-5.200-9.559] P=0.537	1.178 [-4.245-6.601] P=0.659	1.424 [-5.737-8.584] P=0.683	1.797 [-1.246-4.840] P=0.236	1.845 [-1.599-5.289] P=0.278
Biochemical Pregnancy (from ET) Odds Ratio [CI] P-value	1.131 [0.748-1.711] P=0.560	1.711 [0.689-4.249] P=0.247	1.055 [0.704-1.579] P=0.796	1.197 [0.626-2.289] P=0.588	0.893 [0.704-1.133] P=0.352	0.706 [0.459-1.086] P=0.113
Foetal heart at scan Odds Ratio [CI] P-value	1.131 [0.748-1.711] P=0.560	1.711 [0.689-4.249] P=0.247	1.055 [0.704-1.579] P=0.796	1.197 [0.626-2.289] P=0.588	0.893 [0.704-1.133] P=0.352	0.706 [0.459-1.086] P=0.113
Live Birth Odds Ratio [CI] P-value	1.00 [0.669-1.495] P=1.000	1.703 [0.688-4.219] P=0.250	0.933 [0.615-1.417] P=0.746	1.104 [0.578-2.108] P=0.765	0.845 [0.655-1.090] P=0.195	0.714 [0.472-1.082] P=0.113

Adjusted for body mass index (BMI), age, previous cycles, starting follicle stimulating hormone (FSH) dose, and Total FSH Dose. CI = confidence interval. See Table S5.8 for statistics on adjustments

Table S5.7 Differences in cycle outcomes fertilisation rate, embryos transferred, embryo utilization, pregnancy rates, live birth rates, gestation length and birth weight from changes to *TET1*, *TET2* and *TET3* expression in granulosa cells

	TET1 GC		*TET2 GC*		*TET3 GC*	
	Unadjusted	Adjusted	Unadjusted	Adjusted	Unadjusted	Adjusted
Fertilisation rate Unstandardised β [CI] P=	4.965 [-0.383-10.314] P=0.068	**7.272 [1.610-12.933] P=0.014**	2.2389 [-1.338-6.116] P=0.203	2.811 [-1.233-6.854] P=0.168	0.205 [-2.727-3.133] P=0.889	0.522 [-2.838-3.881] P=0.756
Embryos transferred Unstandardised β [CI] P=	0.109 [-0.009-0.226] P=0.069	*0.128 [-0.006-0.262] P=0.061*	0.016 [-0.074-0.107] P=0.717	0.025 [-0.074-0.123] P=0.615	-0.001 [-0.071-0.070] P=0.987	-0.003 [-0.084-0.077] P=0.933
Embryo utilisation (%) (per number of oocytes inseminated/injected)	1.967 [-3.312-72.46] P=0.454	4.652 [-0.740-10.044] P=0.088	0.712 [-2.992-4.417] P=0.700	0.974 [-2.928-4.877] P=0.617	0.508 [-2.321-3.338] P=0.720	0.528 [-2.697-3.753] P=0.743
Embryo utilisation (%) (per number of fertilised embryos)	-3.577 [-9.065-1.910] P=0.193	-2.512 [-8.702-3.678] P=0.412	-0.612 [-4.974-3.749] P=0.778	-0.550 [-5.107-4.006] P=0.808	0.949 [-2.525-4.423] P=0.585	0.929 [-2.949-4.806] P=0.631
Biochemical Pregnancy (from ET) Odds Ratio [CI] P=	0.866 [0.570-1.317] P=0.503	0.913 [0.554-1.506] P=0.721	1.211 [0.846-1.735] P=0.296	1.179 [0.767-1.813] P=0.453	1.245 [0.902-1.719] P=0.182	1.223 [0.825-1.815] P=0.317
Foetal heart at scan Odds Ratio [CI] P=	0.745 [0.478-1.159] P=0.192	0.872 [0.522-1.456] P=0.600	1.129 [0.786-1.623] P=0.512	1.182 [0.753-1.854] P=0.467	1.163 [0.846-1.600] P=0.353	1.273 [0.841-1.928] P=0.254
Live Birth Odds Ratio [CI] P=	0.933 [0.595-1.464] P=0.764	1.251 [0.646-2.419] P=0.507	1.326 [0.866-2.030] P=0.194	1.386 [0.831-2.313] P=0.211	1.369 [0.908-2.064] P=0.134	1.540 [0.940-2.521] P=0.086
Gestation Length Unstandardised β [CI] P=	0.271 [-0.556-1.099] P=0.453	1.453 [-17.621-20.527] P=0.510	-0.407 [-1.310-0.495] P=0.321	0.683 [-2.375-3.741] P=0.438	-0.005 [-0.730-0.720] P=0.987	0.553 [-0.289-1.396] P=0.106
Birth weight Unstandardised β [CI] P=	-177.659 [-484.025-128.707] P=0.196	a	20.543 [-324.252-365.339] P=0.889	447.300 [-2575.609-3470.208] P=0.311	142.559 [-78.290-363.407] P=0.165	249.465 [-621.086-1120.017] P=0.171

Adjusted for body mass index (BMI), age, previous cycles, starting follicle stimulating hormone (FSH) dose, and total FSH dose. a=sample size for the test is below the degrees of freedom required to run the adjusted model. CI= confidence interval See Table S5.8 for statistics on adjustments

Table S5.8 Multiple imputed regression estimates for Table S5.6 and S5.7

Outcome	*TET1-3* Test	Variable	Est [95%CI] P-value
Total Fertilisation Rate (%) Odds ratio [95% CI] P value	*TET1* Cumulus	TET	2.814 [-2.269-7.898] P=0.259
		BMI	-1.236 [-3.320-0.847] P=0.227
		Age	-1.097 [-3.643-1.450] P=0.376
		Previous Cycles	-0.388 [-10.211-9.436] P=0.935
		Starting FSH	0.156 [-0.405-0.717] P=0.565
		Total FSH	-0.016 [-0.057-0.024] P=0.403
	TET2 Cumulus	TET	*4.625 [-0.206-9.456] P=0.060*
		BMI	-0.967 [-2.596-0.662] P=0.232
		Age	-0.870 [-30156-1.416] P=0.440
		Previous Cycles	2.295 [-4.629-9.220] P=0.500
		Starting FSH	-0.059 [-0.479-0.361] P=0.775
		Total FSH	0.004 [-0.027-0.035] P=0.789
	TET3 Cumulus	TET	-0.165 [-2.621-2.291] P=0.891
		BMI	-0.556 [-1.802-0.691] P=0.367
		Age	**-2.416 [-4.329--0.504] P=0.015**
		Previous Cycles	3.463 [-1.938-8.864] P=0.198
		Starting FSH	0.009 [-0.285-0.302] P=0.953
		Total FSH	-0.009 [-0.032-0.014] P=0.419
	TET1 Granulosa	TET	**7.272 [1.610-12.933] P=0.014**
		BMI	1.406 [-0.117-2.930] P=0.069
		Age	-1.588 [-4.018-0.842] P=0.192
		Previous Cycles	-1.942 [-6.774-2.890] P=0.418
		Starting FSH	0.130 [-0.331-0.591] P=0.568
		Total FSH	-0.013 [-0.047-0.022] P=0.456
	TET2 Granulosa	TET	2.811 [-1.233-6.854] P=0.168
		BMI	0.256 [-0.934-1.446] P=0.666
		Age	-0.741 [-2.738-1.255] P=0.458
		Previous Cycles	-2.333 [-6.547-1.880] P=0.270
		Starting FSH	0.063 [-0.292-0.417] P=0.722
		Total FSH	-0.003 [-0.029-0.024] P=0.829
	TET3 Granulosa	TET	0.522 [-2.838-3.881] P=0.756
		BMI	0.429 [-0.716-1.575] P=0.454
		Age	-0.933 [-2.922-1.055] P=0.349
		Previous Cycles	-1.752 [-5.920-2.417] P=0.401
		Starting FSH	0.011 [-0.350-0.371] P=0.952
		Total FSH	-0.003 [-0.030-0.023] P=0.797

Table S5.8 Continued

Outcome	*TET1-3* Test	Variable	Est [95%CI] P-value
Embryo utilization (%) (per number of oocytes inseminated/injected) Odds ratio [95% CI] P value	*TET1* Cumulus	TET	1.700 [-2.858-6.258] P=0.442
		BMI	-0.857 [-2.725-1.011] P=0.347
		Age	-1.717 [-4.001-0.566] P=0.131
		Previous Cycles	0.447 [-8.361-9.256] P=0.916
		Starting FSH	0.244 [-0.258-0.747] P=0.319
		Total FSH	-0.013 [-0.049-0.023] P=0.461
	TET2 Cumulus	TET	2.736 [-1.285-6.757] P=0.173
		BMI	-0.691 [-2.047-0.665] P=0.303
		Age	-1.496 [-3.3999-0.406] P=0.118
		Previous Cycles	2.650 [-3.114-8.414] P=0.352
		Starting FSH	0.068 [-0.281-0.418] P=0.690
		Total FSH	0.001 [-0.025-0.027] P=0.958
	TET3 Cumulus	TET	0.992 [-1.434-3.418] P=0.407
		BMI	-0.414 [-1.645-0.817] P=0.494
		Age	**-2.398 [-4.287--0.508] P=0.015**
		Previous Cycles	4.210 [-1.124-9.544] P=0.116
		Starting FSH	0.054 [-0.236-0.344] P=0.706
		Total FSH	-0.003 [-0.026-0.019] P=0.755
	TET1 Granulosa	TET	4.652 [-0.740-10.044] P=0.088
		BMI	1.344 [-0.107-2.795] P=0.068
		Age	**-2.753 [-5.067--0.439] P=0.021**
		Previous Cycles	-2.229 [-6.831-2.373] P=0.330
		Starting FSH	0.249 [-0.190-0.688] P=0.256
		Total FSH	-0.017 [-0.050-0.016] P=0.294
	TET2 Granulosa	TET	0.974 [-2.928-4.877] P=0.617
		BMI	0.357 [-0.792-1.505] P=0.534
		Age	-1.855 [-3.782-0.072] P=0.059
		Previous Cycles	-1.145 [-5.212-2.921] P=0.573
		Starting FSH	0.105 [-0.237-0.448] P=0.537
		Total FSH	0.000 [-0.025-0.026] P=0.982
	TET3 Granulosa	TET	0.528 [-2.697-3.753] P=0.743
		BMI	0.556 [-0.544-1.655] P=0.314
		Age	-1.773 [-3.682-0.136] P=0.068
		Previous Cycles	-1.012 [-5.014-2.990] P=0.613
		Starting FSH	0.082 [-0.265-0.428] P=0.637
		Total FSH	-0.001 [-0.026-0.025] P=0.962

Table S5.8 Continued

Outcome	*TET1-3* Test	Variable	Est [95%CI] P-value
Embryo utilization (%) (per number of fertilised embryos) Odds ratio [95% CI] P value	*TET1* Cumulus	TET	2.180 [-5.200-9.559] P=0.537
		BMI	0.806 [-2.121-3.733] P=0.564
		Age	-0.915 [-4.062-2.232] P=0.543
		Previous Cycles	-0.328 [-12.093-11.438] P=0.953
		Starting FSH	0.067 [-0.721-0.855] P=0.858
		Total FSH	0.010 [-0.051-0.072] P=0.728
	TET2 Cumulus	TET	1.424 [-5.737-8.584] P=0.683
		BMI	0.402 [-1.653-2.457] P=0.687
		Age	-0.833 [-3.712-2.047] P=0.553
		Previous Cycles	-0.130 [-8.583-8.322] P=0.975
		Starting FSH	0.022 [-0.582-0.626] P=0.939
		Total FSH	0.009 [-0.040-0.059] P=0.698
	TET3 Cumulus	TET	1.845 [-1.599-5.289] P=0.278
		BMI	0.508 [-1.340-2.356] P=0.574
		Age	-1.468 [-4.160-1.225] P=0.270
		Previous Cycles	2.061 [-5.933-10.055] P=0.597
		Starting FSH	0.023 [-0.446-0.492] P=0.918
		Total FSH	0.007 [-0.032-0.045] P=0.918
	TET1 Granulosa	TET	-2.512 [-8.702-3.678] P=0.412
		BMI	0.099 [-1.417-1.616] P=0.894
		Age	-1.460 [-3.834-0.915] P=0.218
		Previous Cycles	-1.971 [-7.169-3.227] P=0.443
		Starting FSH	0.132 [-0.321-0.585] P=0.554
		Total FSH	-0.004 [-0.038-0.031] P=0.832
	TET2 Granulosa	TET	-0.550 [-5.107-4.006] P=0.808
		BMI	0.383 [-0.981-1.746] P=0.573
		Age	-1.966 [-4.233-0.301] P=0.087
		Previous Cycles	0.629 [-4.750-6.007] P=0.814
		Starting FSH	0.108 [-0.300-0.516] P=0.597
		Total FSH	0.003 [-0.028-0.033] P=0.857
	TET3 Granulosa	TET	0.929 [-2.949-4.806] P=0.631
		BMI	0.477 [-0.856-1.810] P=0.473
		Age	-1.587 [-3.846-0.672] P=0.163
		Previous Cycles	-0.098 [-5.127-4.931] P=0.969
		Starting FSH	0.113 [-0.303-0.528] P=0.587
		Total FSH	0.003 [-0.028-0.034] P=0.826

Table S5.8 Continued

Outcome	*TET1-3* Test	Variable	Est [95%CI] P-value
Biochemical Pregnancy exp(B) [CI] P=value	*TET1* Cumulus	TET	1.711 [0.689-4.249] P=0.247
		BMI	0.105 [0.004-3.039] P=0.190
		Age	1.461 [0.768-2.779] P=0.248
		Previous Cycles	0.113 [0.004-2.940] P=0.190
		Starting FSH	0.959 [0.878-1.046] P=0.345
		Total FSH	1.007 [0.996-1.019] P=0.221
	TET2 Cumulus	TET	1.197 [0.626-2.289] P=0.588
		BMI	0.621 [0.303-1.273] P=193
		Age	0.988 [0.734-1.332] P=0.939
		Previous Cycles	0.455 [0.141-1.467] P=054
		Starting FSH	0.986 [0.938-1.036] P=0.569
		Total FSH	1.002 [0.998-1.007] P=0.328
	TET3 Cumulus	TET	0.706 [0.459-1.086] P=0.113
		BMI	0.799 [0.605-1.056] P=0.115
		Age	0.820 [0.634-1.062] P=0.133
		Previous Cycles	0.435 [0.135-1.397] P=0.162
		Starting FSH	1.019 [0.970-1.071] P=0.448
		Total FSH	0.999 [0.996-1.003] P=0.761
	TET1 Granulosa	TET	0.913 [0.554-1.506] P=0.721
		BMI	1.011 [0.893-1.144] P=0.864
		Age	0.879 [0.713-1.084] P=0.879
		Previous Cycles	1.030 [0.664-1.596] P=0.896
		Starting FSH	0.978 [0.939-1.018] P=0.978
		Total FSH	1.002 [0.999-1.005] P=0.216
	TET2 Granulosa	TET	1.179 [0.767-1.813] P=0.453
		BMI	0.979 [0.878-1.091] P=0.698
		Age	0.863 [0.715-1.042] P=0.125
		Previous Cycles	0.992 [0.652-1.509] P=0.970
		Starting FSH	0.986 [0.954-1.018] P=0.384
		Total FSH	1.001 [0.999-1.004] P=0.347
	TET3 Granulosa	TET	1.223 [0.825-1.815] P=0.317
		BMI	0.987 [0.884-1.101] P=0.812
		Age	0.852 [0.705-1.029] P=0.097
		Previous Cycles	0.869 [0.566-1.333] P=0.521
		Starting FSH	0.995 [0.962-1.028] P=0.745
		Total FSH	1.001 [0.998-1.003] P=0.520

Table S5.8 Continued

Outcome	*TET1-3* Test	Variable	Est [95%CI] P-value
Foetal Heart exp(B) [CI] P=value	*TET1* Cumulus	TET	1.711 [0.689-4.249] P=0.247
		BMI	0.105 [0.004-3.039] P=0.190
		Age	1.461 [0.768-2.779] P=0.248
		Previous Cycles	0.113 [0.004-2.940] P=0.190
		Starting FSH	0.959 [0.878-1.046] P=0.345
		Total FSH	1.007 [0.996-1.019] P=0.221
	TET2 Cumulus	TET	1.197 [0.626-2.289] P=0.588
		BMI	0.621 [0.303-1.273] P=193
		Age	0.988 [0.734-1.332] P=0.939
		Previous Cycles	0.455 [0.141-1.467] P=0.054
		Starting FSH	0.986 [0.938-1.036] P=0.569
		Total FSH	1.002 [0.998-1.007] P=0.328
	TET3 Cumulus	TET	0.706 [0.459-1.086] P=0.113
		BMI	0.799 [0.605-1.056] P=0.115
		Age	0.820 [0.634-1.062] P=0.133
		Previous Cycles	0.435 [0.135-1.397] P=0.162
		Starting FSH	1.019 [0.970-1.071] P=0.448
		Total FSH	0.999 [0.996-1.003] P=0.761
	TET1 Granulosa	TET	0.872 [0.522-1.456] P=0.600
		BMI	1.056 [0.909-1.226] P=0.478
		Age	0.852 [0.672-1.080] P=0.185
		Previous Cycles	0.642 [0.272-1.511] P=0.310
		Starting FSH	0.988 [0.946-1.031] P=0.571
		Total FSH	1.002 [0.998-1.005] P=0.364
	TET2 Granulosa	TET	1.182 [0.753-1.854] P=0.467
		BMI	1.009 [0.904-1.127] P=0.867
		Age	0.837 [0.681-1.028] P=0.090
		Previous Cycles	0.598 [0.267-1.341] P=0.212
		Starting FSH	0.995 [0.962-1.030] P=0.778
		Total FSH	1.001 [0.998-1.003] P=0.534
	TET3 Granulosa	TET	1.273 [0.841-1.928] P=0.254
		BMI	1.021 [0.911-1.144] P=0.717
		Age	*0.823 [0.669-1.012] P=0.065*
		Previous Cycles	0.485 [0.199-1.182] P=0.111
		Starting FSH	1.007 [0.971-1.044] P=0.726
		Total FSH	1.000 [0.998-1.003] P=0.806

Table S5.8 Continued

Outcome	*TET1-3* Test	Variable	Est [95%CI] P-value
Live Birth exp(B) [CI] P=value	*TET1* Cumulus	TET	1.703 [0.688-4.219] P=0.250
		BMI	0.098 [0.002-3.861] P=0.215
		Age	1.470 [0.750-2.881] P=0.262
		Previous Cycles	0.167 [0.005-5.556] P=0.317
		Starting FSH	0.931 [0.847-1.023] P=0.137
		Total FSH	0.010 [0.997-1.023] P=0.146
	TET2 Cumulus	TET	1.104 [0.578-2.108] P=0.765
		BMI	0.624 [0.277-1.410] P=0.257
		Age	1.030 [0.760-1.397] P=0.847
		Previous Cycles	0.603 [0.184-1.974] P=0.403
		Starting FSH	0.973 [0.926-1.023] P=0.288
		Total FSH	1.003 [0.998-1.008] P=0.205
	TET3 Cumulus	TET	0.714 [0.472-1.082] P=0.113
		BMI	0.831 [0.633-1.090] P=0.180
		Age	0.868 [0.686-1.099] P=0.239
		Previous Cycles	0.630 [0.211-1.879] P=0.407
		Starting FSH	0.997 [0.950-1.046] P=0.907
		Total FSH	1.001 [0.997-1.004] P=0.682
	TET1 Granulosa	TET	1.251 [0.646-2.419] P=0.507
		BMI	1.132 [0.952-1.345] P=0.161
		Age	0.800 [0.806-1.052] P=0.111
		Previous Cycles	0.652 [0.273-1.561] P=0.337
		Starting FSH	0.993 [0.952-1.036] P=0.744
		Total FSH	1.001 [0.998-1.004] P=0.558
	TET2 Granulosa	TET	1.386 [0.831-2.313] P=0.211
		BMI	1.040 [0.928-1.166] P=0.499
		Age	0.868 [0.702-1.074] P=0.193
		Previous Cycles	0.729 [0.351-1.516] P=0.398
		Starting FSH	0.987 [0.951-1.025] P=0.502
		Total FSH	1.001 [0.988-1.004] P=0.421
	TET3 Granulosa	TET	1.540 [0.940-2.521] P=0.086
		BMI	1.057 [0.936-1.195] P=0.369
		Age	0.846 [0.682-1.050] P=0.130
		Previous Cycles	0.567 [0.245-1.310] P=0.184
		Starting FSH	0.999 [0.960-1.040] P=0.980
		Total FSH	1.001 [0.998-1.004] P=0.658

Table S5.8 Continued

Outcome	*TET1-3* Test	Variable	Est [95%CI] P-value
Gestation (weeks) Odds ratio [95% CI] P value	*TET1* Granulosa	TET	**4.367 [2.344-6.390] P=0.006**
		BMI	**0.553 [0.116-0.990] P=0.029**
		Age	-0.658 [-1.427-0.112] P=0.073
		Previous Cycles	-0.245 [-5.849-5.359] P=0.898
		Starting FSH	0.008 [-0.116-0.131] P=0.858
		Total FSH	-0.003 [-0.014-0.008] P=0.460
	TET2 Granulosa	TET	**4.988 [0.992-8.984] P=0.026**
		BMI	-0.964 [-2.270-0.342] P=0.110
		Age	1.163 [-0.486-2.812] P=0.122
		Previous Cycles	6.280 [-1.709-14.269] P=0.094
		Starting FSH	-0.057 [-0.253-0.140] P=0.469
		Total FSH	-0.004 [-0.019-0.010] P=0.470
	TET3 Granulosa	TET	1.725 [-2.873-6.323] P=0.356
		BMI	-0.432 [-1.889-1.026] P=0.457
		Age	0.976 [-1.275-3.226] P=0.295
		Previous Cycles	10.964 [-9.265-31.193] P=0.207
		Starting FSH	-0.078 [-0.423-0.268] P=0.567
		Total FSH	-0.008 [-0.026-0.011] P=0.314
Birth weight Odds ratio [95% CI] P value	*TET1* Granulosa	TET	a
		BMI	a
		Age	a
		Previous Cycles	a
		Starting FSH	a
		Total FSH	a
	TET2 Granulosa	TET	447.300 [-2575.609-3470.208] P=0.311
		BMI	-90.424 [-783.438-602.591] P=0.346
		Age	145.610 [-660.497-951.718] P=0.262
		Previous Cycles	429.465 [-5128.410-5897.340] P=0.506
		Starting FSH	-14.765 [-99.999-70.469] P=0.271
		Total FSH	0.419 [-5.668-6.506] P=0.542
	TET3 Granulosa	TET	249.465 [-621.086-1120.017] P=0.171
		BMI	-54.478 [-337.891-228.935] P=0.247
		Age	61.858 [-509.678-633.394] P=0.400
		Previous Cycles	-438.728 [-8823.101-7945.645] P=0.626
		Starting FSH	-2.816 [-105.373-99.741] P=0.786
		Total FSH	0.127 [-3.842-4.096] P=0.754

a=sample size for the test is below the degrees of freedom required to run the adjusted model.

BMI = body mass index, FSH = follicle stimulating hormone, CI = confidence interval

5.11 References

ASA, E., TABATABAEE, R., FARROKHI, A. & NEJATBAKHSH, R. 2017. Relationship between meiotic spindles visualization and intracytoplasmic sperm injection outcomes in human oocytes. *Anatomy and Cell Biology,* 50**,** 26-32.

BARKER, D. J. P. & OSMOND, C. 1986. INFANT MORTALITY, CHILDHOOD NUTRITION, AND ISCHAEMIC HEART DISEASE IN ENGLAND AND WALES. *The Lancet,* 327**,** 1077-1081.

BARTOLACCI, A., BURATINI, J., MOUTIER, C., GUGLIELMO, M. C., NOVARA, P. V., BRAMBILLASCA, F., RENZINI, M. M. & DAL CANTO, M. 2019. Maternal body mass index affects embryo morphokinetics: a time-lapse study. *Journal of Assisted Reproduction and Genetics,* 36**,** 1109-1116.

BISHOP, C. V., REITER, T. E., ERIKSON, D. W., HANNA, C. B., DAUGHTRY, B. L., CHAVEZ, S. L., HENNEBOLD, J. D. & STOUFFER, R. L. 2019. Chronically elevated androgen and/or consumption of a Western-style diet impairs oocyte quality and granulosa cell function in the nonhuman primate periovulatory follicle. *Journal of Assisted Reproduction and Genetics,* 36**,** 1497-1511.

BRION, M.-J. A., NESS, A. R., ROGERS, I., EMMETT, P., CRIBB, V., DAVEY SMITH, G. & LAWLOR, D. A. 2010. Maternal macronutrient and energy intakes in pregnancy and offspring intake at 10 y: exploring parental comparisons and prenatal effects. *The American Journal of Clinical Nutrition,* 91**,** 748-756.

BRUNET, C., AOUINTI, S., HUGUET, F., MACIOCE, V., RANISAVLJEVIC, N., GALA, A., AVIGNON, A., MURA, T. & SULTAN, A. 2020. Impact of Women Obesity and Obesity Severity on Live Birth Rate after In Vitro Fertilization. *Journal of clinical medicine,* 9**,** 2414.

CARDOZO, E. R., KARMON, A. E., GOLD, J., PETROZZA, J. C. & STYER, A. K. 2016. Reproductive outcomes in oocyte donation cycles are associated with donor BMI. *Human Reproduction,* 31**,** 385-392.

CHAFFIN, C. L., LATHAM, K. E., MTANGO, N. R., MIDIC, U. & VANDEVOORT, C. A. 2014. Dietary Sugar in Healthy Female Primates Perturbs Oocyte Maturation and In Vitro Preimplantation Embryo Development. *Endocrinology,* 155**,** 2688-2695.

CHOMCZYNSKI, P. 1993. A reagent for the single-step simultaneous isolation of RNA, DNA and proteins from cell and tissue samples. *Biotechniques,* 15**,** 532-4, 536.

DESMET, K. L. J., MAREI, W. F. A., RICHARD, C., SPRANGERS, K., BEEMSTER, G. T. S., MEYSMAN, P., LAUKENS, K., DECLERCK, K., VANDEN BERGHE, W., BOLS, P. E. J., HUE, I. & LEROY, J. L. M. R. 2020. Oocyte maturation under lipotoxic conditions induces carryover transcriptomic and functional alterations during post-hatching development of good-quality blastocysts: novel insights from a bovine embryo-transfer model. *Human Reproduction,* 35**,** 293-307.

DESQUIRET-DUMAS, V., CLÉMENT, A., SEEGERS, V., BOUCRET, L., FERRÉ-L'HOTELLIER, V., BOUET, P. E., DESCAMPS, P., PROCACCIO, V., REYNIER, P. & MAY-PANLOUP, P. 2017. The mitochondrial DNA content of cumulus granulosa cells is linked to embryo quality. *Human Reproduction,* 32**,** 607-614.

DOWNS, S. M. 1995. The Influence of Glucose, Cumulus Cells, and Metabolic Coupling on ATP Levels and Meiotic Control in the Isolated Mouse Oocyte. *Developmental Biology,* 167**,** 502-512.

DOWNS, S. M., HUMPHERSON, P. G. & LEESE, H. J. 2002. Pyruvate utilization by mouse oocytes is influenced by meiotic status and the cumulus oophorus. *Molecular Reproduction and Development,* 62**,** 113-123.

DUNNING, K. R., AKISON, L. K., RUSSELL, D. L., NORMAN, R. J. & ROBKER, R. L. 2011. Increased Beta-Oxidation and Improved Oocyte Developmental Competence in Response to l-Carnitine During Ovarian In Vitro Follicle Development in Mice. *Biology of Reproduction,* 85**,** 548-555.

DUNNING, K. R., LANE, M., BROWN, H. M., YEO, C., ROBKER, R. L. & RUSSELL, D. L. 2007. Altered composition of the cumulus-oocyte complex matrix during in vitro maturation of oocytes. *Human Reproduction,* 22**,** 2842-2850.

EFIMOVA, O. A., PENDINA, A. A., TIKHONOV, A. V., FEDOROVA, I. D., KRAPIVIN, M. I., CHIRYAEVA, O. G., SHILNIKOVA, E. M., BOGDANOVA, M. A., KOGAN, I. Y., KUZNETZOVA, T. V., GZGZYAN, A. M., AILAMAZYAN, E. K. & BARANOV, V. S. 2015. Chromosome hydroxymethylation patterns in human zygotes and cleavage-stage embryos. *Reproduction,* 149**,** 223-233.

FEIL, D., HENSHAW, R. C. & LANE, M. 2008. Day 4 embryo selection is equal to Day 5 using a new embryo scoring system validated in single embryo transfers. *Human Reproduction,* 23**,** 1505-1510.

FORSÉN, T., ERIKSSON, J. G., TUOMILEHTO, J., TERAMO, K., OSMOND, C. & BARKER, D. J. P. 1997. Mother's weight in pregnancy and coronary heart disease in a cohort of finnish men: follow up study. *BMJ,* 315**,** 837.

FROTA, I. M. A., LEITÃO, C. C. F., COSTA, J. J. N., BRITO, I. R., VAN DEN HURK, R. & SILVA, J. R. V. 2011. Stability of housekeeping genes and expression of locally produced growth factors and hormone receptors in goat preantral follicles. *Zygote,* 19**,** 71-83.

GARDNER, D. K. & SCHOOLCRAFT, W. B. 1999. In-vitro culture of human blastocyst. *Towards reproductive certainty: Infertility and Genetics Beyond 1999***,** 378-388.

GEBHARDT, K. M., FEIL, D. K., DUNNING, K. R., LANE, M. & RUSSELL, D. L. 2011. Human cumulus cell gene expression as a biomarker of pregnancy outcome after single embryo transfer. *Fertility and Sterility,* 96**,** 47-52.e2.

GILCHRIST, R. B., LANE, M. & THOMPSON, J. G. 2008. Oocyte-secreted factors: regulators of cumulus cell function and oocyte quality. *Human Reproduction Update,* 14**,** 159-177.

GORSHINOVA, V. K., TSVIRKUN, D. V., SUKHANOVA, I. A., TARASOVA, N. V., VOLODINA, M. A., MAREY, M. V., SMOLNIKOVA, V. U., VYSOKIKH, M. Y. &

SUKHIKH, G. T. 2017. Cumulus cell mitochondrial activity in relation to body mass index in women undergoing assisted reproductive therapy. *BBA Clinical,* 7**,** 141-146.

GU, F., CHAUHAN, V., KAUR, K., BROWN, W., LAFAUCI, G., WEGIEL, J. & CHAUHAN, A. 2013. Alterations in mitochondrial DNA copy number and the activities of electron transport chain complexes and pyruvate dehydrogenase in the frontal cortex from subjects with autism. *Translational Psychiatry,* 3**,** e299-e299.

GU, T.-P., GUO, F., YANG, H., WU, H.-P., XU, G.-F., LIU, W., XIE, Z.-G., SHI, L., HE, X., JIN, S.-G., IQBAL, K., SHI, Y. G., DENG, Z., SZABO, P. E., PFEIFER, G. P., LI, J. & XU, G.-L. 2011. The role of Tet3 DNA dioxygenase in epigenetic reprogramming by oocytes. *Nature,* 477**,** 606-610.

GUO, H., ZHU, P., YAN, L., LI, R., HU, B., LIAN, Y., YAN, J., REN, X., LIN, S., LI, J., JIN, X., SHI, X., LIU, P., WANG, X., WANG, W., WEI, Y., LI, X., GUO, F., WU, X., FAN, X., YONG, J., WEN, L., XIE, S. X., TANG, F. & QIAO, J. 2014. The DNA methylation landscape of human early embryos. *Nature,* 511**,** 606-610.

HAMMOND, J. M., BARANAO, J. L. S., SKALERIS, D., KNIGHT, A. B., ROMANUS, J. A. & RECHLER, M. M. 1985. Production of insulin-like growth factors by ovarian granulosa cells. *Endocrinology,* 117**,** 2553-2555.

HAN, L., REN, C., LI, L., LI, X., GE, J., WANG, H., MIAO, Y.-L., GUO, X., MOLEY, K. H., SHU, W. & WANG, Q. 2018. Embryonic defects induced by maternal obesity in mice derive from Stella insufficiency in oocytes. *Nature Genetics,* 50**,** 432-442.

HUNZICKER-DUNN, M. & MAIZELS, E. T. 2006. FSH signaling pathways in immature granulosa cells that regulate target gene expression: Branching out from protein kinase A. *Cellular Signalling,* 18**,** 1351-1359.

INOUE, A. & ZHANG, Y. 2011. Replication-Dependent Loss of 5-Hydroxymethylcytosine in Mouse Preimplantation Embryos. *Science (New York, N.Y.),* 334**,** 194-194.

ITO, S., D'ALESSIO, A. C., TARANOVA, O. V., HONG, K., SOWERS, L. C. & ZHANG, Y. 2010. Role of Tet proteins in 5mC to 5hmC conversion, ES cell self-renewal, and ICM specification. *Nature,* 466**,** 1129-1133.

ITO, S., SHEN, L., DAI, Q., WU, S. C., COLLINS, L. B., SWENBERG, J. A., HE, C. & ZHANG, Y. 2011. Tet proteins can convert 5-methylcytosine to 5-formylcytosine and 5-carboxylcytosine. *Science,* 333**,** 1300-1303.

IWATA, H., GOTO, H., TANAKA, H., SAKAGUCHI, Y., KIMURA, K., KUWAYAMA, T. & MONJI, Y. 2011. Effect of maternal age on mitochondrial DNA copy number, ATP content and IVF outcome of bovine oocytes. *Reproduction, Fertility and Development,* 23**,** 424-432.

KAYE, L., SUELDO, C., ENGMANN, L., NULSEN, J. & BENADIVA, C. 2016. Survey assessing obesity policies for assisted reproductive technology in the United States. *Fertility and Sterility,* 105**,** 703-706.e2.

KOIVUNEN, P., LEE, S., DUNCAN, C. G., LOPEZ, G., LU, G., RAMKISSOON, S., LOSMAN, J. A., JOENSUU, P., BERGMANN, U., GROSS, S., TRAVINS, J., WEISS, S., LOOPER, R., LIGON, K. L., VERHAAK, R. G. W., YAN, H. & KAELIN, W. G., JR. 2012. Transformation by the (R)-enantiomer of 2-hydroxyglutarate linked to EGLN activation. *Nature,* 483**,** 484-488.

LEARY, C., LEESE, H. J. & STURMEY, R. G. 2015. Human embryos from overweight and obese women display phenotypic and metabolic abnormalities. *Human Reproduction,* 30**,** 122-132.

LEE, K., HAMM, J., WHITWORTH, K., SPATE, L., PARK, K.-W., MURPHY, C. N. & PRATHER, R. S. 2014. Dynamics of TET family expression in porcine preimplantation embryos is related to zygotic genome activation and required for the maintenance of NANOG. *Developmental Biology,* 386**,** 86-95.

LEESE, H. J. & BARTON, A. M. 1985. Production of pyruvate by isolated mouse cumulus cells. *Journal of Experimental Zoology,* 234**,** 231-236.

LUKE, B. 2017. Adverse effects of female obesity and interaction with race on reproductive potential. *Fertility and Sterility,* 107**,** 868-877.

LUKE, B., BROWN, M. B., STERN, J. E., MISSMER, S. A., FUJIMOTO, V. Y., LEACH, R. & GROUP, A. S. W. 2011. Female obesity adversely affects assisted reproductive technology (ART) pregnancy and live birth rates†. *Human Reproduction,* 26**,** 245-252.

MADOGWE, E., TANWAR, D. K., TAIBI, M., SCHUERMANN, Y., ST-YVES, A. & DUGGAVATHI, R. 2020. Global analysis of FSH-regulated gene expression and histone modification in mouse granulosa cells. *Molecular Reproduction and Development,* 87**,** 1082-1096.

MAHMADALIYEVA, M. R., KOGAN, I. Y., NIAURI, D. A., MEKINA, I. D. & GZGZYAN, A. M. 2018. The effect of excess body weight and obesity on the effectiveness of assisted reproductive technologies programs. *Journal of Obstetrics and Women's Diseases,* 67**,** 32-39.

MERHI, Z., POLOTSKY, A. J., BRADFORD, A. P., BUYUK, E., CHOSICH, J., PHANG, T., JINDAL, S. & SANTORO, N. 2015. Adiposity Alters Genes Important in Inflammation and Cell Cycle Division in Human Cumulus Granulosa Cell. *Reproductive Sciences,* 22**,** 1220-1228.

MONNIAUX, D. & PISSELET, C. 1992. Control of Proliferation and Differentiation of Ovine Granulosa Cells by Insulin-like Growth Factor-I and Follicle-Stimulating Hormone in Vitro. *Biology of Reproduction,* 46**,** 109-119.

NG, M., FLEMING, T., ROBINSON, M., THOMSON, B., GRAETZ, N., MARGONO, C., MULLANY, E. C., BIRYUKOV, S., ABBAFATI, C., ABERA, S. F., ABRAHAM, J. P., ABU-RMEILEH, N. M. E., ACHOKI, T., ALBUHAIRAN, F. S., ALEMU, Z. A., ALFONSO, R., ALI, M. K., ALI, R., GUZMAN, N. A., AMMAR, W., ANWARI, P., BANERJEE, A., BARQUERA, S., BASU, S., BENNETT, D. A., BHUTTA, Z., BLORE, J., CABRAL, N., NONATO, I. C., CHANG, J.-C., CHOWDHURY, R., COURVILLE, K. J., CRIQUI, M. H., CUNDIFF, D. K., DABHADKAR, K. C.,

DANDONA, L., DAVIS, A., DAYAMA, A., DHARMARATNE, S. D., DING, E. L., DURRANI, A. M., ESTEGHAMATI, A., FARZADFAR, F., FAY, D. F. J., FEIGIN, V. L., FLAXMAN, A., FOROUZANFAR, M. H., GOTO, A., GREEN, M. A., GUPTA, R., HAFEZI-NEJAD, N., HANKEY, G. J., HAREWOOD, H. C., HAVMOELLER, R., HAY, S., HERNANDEZ, L., HUSSEINI, A., IDRISOV, B. T., IKEDA, N., ISLAMI, F., JAHANGIR, E., JASSAL, S. K., JEE, S. H., JEFFREYS, M., JONAS, J. B., KABAGAMBE, E. K., KHALIFA, S. E. A. H., KENGNE, A. P., KHADER, Y. S., KHANG, Y.-H., KIM, D., KIMOKOTI, R. W., KINGE, J. M., KOKUBO, Y., KOSEN, S., KWAN, G., LAI, T., LEINSALU, M., LI, Y., LIANG, X., LIU, S., LOGROSCINO, G., LOTUFO, P. A., LU, Y., MA, J., MAINOO, N. K., MENSAH, G. A., MERRIMAN, T. R., MOKDAD, A. H., MOSCHANDREAS, J., NAGHAVI, M., NAHEED, A., NAND, D., NARAYAN, K. M. V., NELSON, E. L., NEUHOUSER, M. L., NISAR, M. I., OHKUBO, T., OTI, S. O., PEDROZA, A., et al. 2014. Global, regional, and national prevalence of overweight and obesity in children and adults during 1980–2013: a systematic analysis for the Global Burden of Disease Study 2013. *The Lancet,* 384**,** 766-781.

OGINO, M., TSUBAMOTO, H., SAKATA, K., OOHAMA, N., HAYAKAWA, H., KOJIMA, T., SHIGETA, M. & SHIBAHARA, H. 2016. Mitochondrial DNA copy number in cumulus cells is a strong predictor of obtaining good-quality embryos after IVF. *Journal of Assisted Reproduction and Genetics,* 33**,** 367-371.

OVESEN, P., RASMUSSEN, S. & KESMODEL, U. 2011. Effect of prepregnancy maternal overweight and obesity on pregnancy outcome. *Obstetrics & Gynecology,* 118**,** 305-312.

PACELLA-INCE, L., ZANDER-FOX, D. L. & LANE, M. 2014a. Mitochondrial SIRT3 and its target glutamate dehydrogenase are altered in follicular cells of women with reduced ovarian reserve or advanced maternal age. *Human Reproduction,* 29**,** 1490-1499.

PACELLA-INCE, L., ZANDER-FOX, D. L. & LANE, M. 2014b. Mitochondrial SIRT5 is present in follicular cells and is altered by reduced ovarian reserve and advanced maternal age. *Reproduction, Fertility and Development,* 26**,** 1072-1083.

PACELLA, L., ZANDER-FOX, D. L., ARMSTRONG, D. T. & LANE, M. 2012. Women with reduced ovarian reserve or advanced maternal age have an altered follicular environment. *Fertility and Sterility,* 98**,** 986-994.e2.

PELUFFO, M. C., TING, A. Y., ZAMAH, A. M., CONTI, M., STOUFFER, R. L., ZELINSKI, M. B. & HENNEBOLD, J. D. 2012. Amphiregulin promotes the maturation of oocytes isolated from the small antral follicles of the rhesus macaque. *Human Reproduction,* 27**,** 2430-2437.

PHILIBERT, R., PLUME, J., GIBBONS, F., BRODY, G. & BEACH, S. 2012. The Impact of Recent Alcohol Use on Genome Wide DNA Methylation Signatures. *Frontiers in Genetics,* 3, 1-8.

ROBKER, R. L., AKISON, L. K., BENNETT, B. D., THRUPP, P. N., CHURA, L. R., RUSSELL, D. L., LANE, M. & NORMAN, R. J. 2009. Obese Women Exhibit Differences in Ovarian Metabolites, Hormones, and Gene Expression Compared with Moderate-Weight Women. *The Journal of Clinical Endocrinology & Metabolism,* 94**,** 1533-1540.

SERMONDADE, N., HUBERLANT, S., BOURHIS-LEFEBVRE, V., ARBO, E., GALLOT, V., COLOMBANI, M. & FRÉOUR, T. 2019. Female obesity is negatively associated with live birth rate following IVF: a systematic review and meta-analysis. *Human Reproduction Update,* 25**,** 439-451.

SHEN, L., INOUE, A., HE, J., LIU, Y., LU, F. & ZHANG, Y. 2014. Tet3 and DNA Replication Mediate Demethylation of Both the Maternal and Paternal Genomes in Mouse Zygotes. *Cell Stem Cell,* 15**,** 459-470.

SIMMONS, J. M., MÜLLER, T. A. & HAUSINGER, R. P. 2008. Fe(II)/alpha-ketoglutarate hydroxylases involved in nucleobase, nucleoside, nucleotide, and chromatin metabolism. *Dalton transactions (Cambridge, England : 2003)***,** 5132-5142.

SIMMS, D., CIZDZIEL, P. E. & CHOMCZYNSKI, P. 1993. TRIzol: A new reagent for optimal single-step isolation of RNA. *Focus,* 15**,** 532-535.

STEVENSON, B. R., SILICIANO, J. D., MOOSEKER, M. S. & GOODENOUGH, D. A. 1986. Identification of ZO-1: a high molecular weight polypeptide associated with the tight junction (zonula occludens) in a variety of epithelia. *The Journal of Cell Biology,* 103**,** 755-766.

STYNE-GROSS, A., ELKIND-HIRSCH, K. & SCOTT, R. T. 2005. Obesity does not impact implantation rates or pregnancy outcome in women attempting conception through oocyte donation. *Fertility and Sterility,* 83**,** 1629-1634.

SU, Y.-Q., SUGIURA, K. & EPPIG, J. J. 2009. Mouse oocyte control of granulosa cell development and function: paracrine regulation of cumulus cell metabolism. *Seminars in Reproductive Medicine,* 27**,** 32-42.

SUPRAMANIAM, P. R., MITTAL, M., MCVEIGH, E. & LIM, L. N. 2018. The correlation between raised body mass index and assisted reproductive treatment outcomes: a systematic review and meta-analysis of the evidence. *Reproductive Health,* 15**,** 34.

SUTTON-MCDOWALL, M. L., GILCHRIST, R. B. & THOMPSON, J. G. 2004. Cumulus expansion and glucose utilisation by bovine cumulus–oocyte complexes during in vitro maturation: the influence of glucosamine and follicle-stimulating hormone. *Reproduction,* 128**,** 313-319.

TAHILIANI, M., KOH, K. P., SHEN, Y., PASTOR, W. A., BANDUKWALA, H., BRUDNO, Y., AGARWAL, S., IYER, L. M., LIU, D. R., ARAVIND, L. & RAO, A. 2009. Conversion of 5-Methylcytosine to 5-Hydroxymethylcytosine in Mammalian DNA by MLL Partner TET1. *Science (New York, N.Y.),* 324**,** 930-935.

TOMARI, H., HONJO, K., KUNITAKE, K., ARAMAKI, N., KUHARA, S., HIDAKA, N., NISHIMURA, K., NAGATA, Y. & HORIUCHI, T. 2018. Meiotic spindle size is a strong indicator of human oocyte quality. *Reproductive Medicine and Biology,* 17**,** 268-274.

UH, K., WAX, N., FARRELL, K. & LEE, K. 2020. 46 Presence of porcine TET3L isoform in oocytes: Potential involvement in the DNA demethylation process. *Reproduction, Fertility and Development,* 32**,** 148-148.

VAN HARMELEN, V., SKURK, T., RÖHRIG, K., LEE, Y. M., HALBLEIB, M., APRATH-HUSMANN, I. & HAUNER, H. 2003. Effect of BMI and age on adipose tissue cellularity and differentiation capacity in women. *International Journal of Obesity,* 27**,** 889-895.

VEECK, L. L. 1999. *An Atlas of Human Gametes and Conceptuses,* CRC Press

WALLACE, M., COTTELL, E., GIBNEY, M. J., MCAULIFFE, F. M., WINGFIELD, M. & BRENNAN, L. 2012. An investigation into the relationship between the metabolic profile of follicular fluid, oocyte developmental potential, and implantation outcome. *Fertility and Sterility,* 97**,** 1078-1084.e8.

WANG, H., LIU, L., GOU, M., HUANG, G., TIAN, C., YANG, J., WANG, H., XU, Q., XU, G. L. & LIU, L. 2020. Roles of Tet2 in meiosis, fertility and reproductive aging. *Protein & Cell*.

WILLIS, D., MASON, H., GILLING-SMITH, C. & FRANKS, S. 1996. Modulation by insulin of follicle-stimulating hormone and luteinizing hormone actions in human granulosa cells of normal and polycystic ovaries. *The Journal of Clinical Endocrinology & Metabolism,* 81**,** 302-309.

WU, S. C. & ZHANG, Y. 2010. Active DNA demethylation: many roads lead to Rome. *Nature Reviews Molecular Cell Biology,* 11**,** 607.

XU, P., HUANG, B.-Y., ZHAN, J.-H., LIU, M.-T., FU, Y., SU, Y.-Q., SUN, Q.-Y., WANG, W.-H., CHEN, D.-J. & LIU, J.-Q. 2019. Insulin Reduces Reaction of Follicular

Granulosa Cells to FSH Stimulation in Women With Obesity-Related Infertility During IVF. *The Journal of Clinical Endocrinology & Metabolism,* 104**,** 2547-2560.

YANG, X., WU, L. L., CHURA, L. R., LIANG, X., LANE, M., NORMAN, R. J. & ROBKER, R. L. 2012. Exposure to lipid-rich follicular fluid is associated with endoplasmic reticulum stress and impaired oocyte maturation in cumulus-oocyte complexes. *Fertility and Sterility,* 97**,** 1438-1443.

YEO, C. X., GILCHRIST, R. B. & LANE, M. 2009. Disruption of bidirectional oocyte-cumulus paracrine signaling during in vitro maturation reduces subsequent mouse oocyte developmental competence. *Biology of Reproduction,* 80**,** 1072-1080.

YEO, C. X., GILCHRIST, R. B., THOMPSON, J. G. & LANE, M. 2008. Exogenous growth differentiation factor 9 in oocyte maturation media enhances subsequent embryo development and fetal viability in mice. *Human Reproduction,* 23**,** 67-73.

ZANDER-FOX, D. L., HENSHAW, R., HAMILTON, H. & LANE, M. 2012. Does obesity really matter? The impact of BMI on embryo quality and pregnancy outcomes after IVF in women aged ≤38 years. *Australian and New Zealand Journal of Obstetrics and Gynaecology,* 52**,** 270-276.

ZEILINGER, S., KÜHNEL, B., KLOPP, N., BAURECHT, H., KLEINSCHMIDT, A., GIEGER, C., WEIDINGER, S., LATTKA, E., ADAMSKI, J., PETERS, A., STRAUCH, K., WALDENBERGER, M. & ILLIG, T. 2013. Tobacco Smoking Leads to Extensive Genome-Wide Changes in DNA Methylation. *PLOS ONE,* 8**,** e63812.

ZHANG, A., XU, B., SUN, Y., LU, X., GU, R., WU, L., FENG, Y. & XU, C. 2012. Dynamic changes of histone H3 trimethylated at positions K4 and K27 in human oocytes and preimplantation embryos. *Fertility and Sterility,* 98**,** 1009-1016.

ZHANG, Z., HE, C., ZHANG, L., ZHU, T., LV, D., LI, G., SONG, Y., WANG, J., WU, H., JI, P. & LIU, G. 2019. Alpha-ketoglutarate affects murine embryo development through metabolic and epigenetic modulations. *Reproduction,* 158**,** 125-135.

ZHU, H., KAVSAK, P., ABDOLLAH, S., WRANA, J. L. & THOMSEN, G. H. 1999. A SMAD ubiquitin ligase targets the BMP pathway and affects embryonic pattern formation. *Nature,* 400**,** 687-693.

ZHU, Y., YAN, H., TANG, M., FU, Y., HU, X., ZHANG, F., XING, L. & CHEN, D. 2019. Impact of maternal prepregnancy body mass index on cognitive and metabolic profiles of singletons born after in vitro fertilization/intracytoplasmic sperm injection. *Fertility and Sterility,* 112**,** 1094-1102.e2.

This page has intentionally been left blank

Chapter 6 Discussion

6.1 Introduction

It is clear that the maternal metabolic environment during the period of oocyte maturation, cleavage and blastocyst development can have a profound impact on the health of the resultant offspring including increasing risk of obesity and metabolic and hypertension syndrome (Ge et al., 2014, Grindler and Moley, 2013, Gu et al., 2015, Han et al., 2018, Jungheim et al., 2010, Luzzo et al., 2012, Sinclair et al., 2007). Given the increasing rates of overweight and obesity worldwide (currently 38% of all reproductive aged women are overweight or obese (Ng et al., 2014)), a thorough understanding of the mechanism behind the metabolic control of programming and how maternal health can modulate this within the developing oocyte and embryo is essential for ensuring the health of future generations.

Maternal obesity alters the nutrient composition of the mature oocyte (Dunning et al., 2007, Gu et al., 2015, Hardy et al., 1989, Harris et al., 2009, Igosheva et al., 2010, Wakefield et al., 2008, Wen et al., 2020), whereby optimal nutrient uptake by the oocyte is critical for the establishment of key molecules/enzymes required for embryonic genome activation post fertilisation. This thesis demonstrates that a maternal high fat diet (HFD) and obesity increases the oxidative metabolism of pyruvate in the mitochondria, and thus may increase TCA cycle intermediaries, such as α-ketoglutarate, a key co-factor in establishment of DNA and histone methylation.

The programming of offspring health can be transmitted through epigenetic mechanisms, such as DNA methylation through 5 methylcytosine (5mC) and histone methylation through histone 3 lysine 4 methylation (H3K4me3-1). As outlined throughout this thesis, α-ketoglutarate is required by both TET1-3 and KDM5A-C for these proteins to demethylate 5mC to 5hmC and 5fC, and H3K4me3-2 respectively. Any alterations to metabolic balance resulting in changes to α-ketoglutarate levels could directly alter the methylation patterns for both DNA and histones (Figure 6.1), modifying expression of genes at embryonic genome activation and further downstream pathways important in foetal development.

Previous evidence in the literature suggested that altering TET function through HFD (Han et al., 2018) or supplementation of α-ketoglutarate throughout preimplantation embryo

development (Zhenzhen et al., 2019) is able to illicit modifications to embryo methylation and quality, indicating that even the narrowest windows of exposure are sufficient to modify embryonic programming. While these studies show that chemically/nutritionally disrupting oocytes and early embryo metabolism was able alter DNA and histone methylation, they do not mechanistically show that these changes are directly due to dysregulation of key metabolites, such as α-ketoglutarate driving TET-mediated demethylation of 5mC. Therefore, the overarching hypothesis of this thesis was that disruptions in mitochondrial activity (due to environmental disruption in the form of maternal HFD or increased BMI or due to *in vitro* manipulations such as IVM) modifies the availability of metabolic cofactors required by TET and KDM5 protein families for methylation, thereby altering DNA and histone methylation marks in the oocyte and embryo.

6.2 Effects of altered metabolism on oocyte and embryo quality and development

6.2.1 Pre- and peri-conception metabolism and epigenetic regulation

Oocyte maturation is a critical period of epigenetic control which allows accumulation of the transcripts and nutrients that are essential for growth of the resulting embryo prior to the initiation of embryonic genome activation (Eppig, 1996, Eppig et al., 2009, Hardy et al., 1989, Harris et al., 2009).

This study has demonstrated that metabolic stress either by over-nutrition (maternal HFD/overweight and obesity) or nutritional undersupply during *in vitro* culture (IVM) where IVM oocytes produce less total ATP (del Collado et al., 2017) with increased ROS production (Zeng et al., 2014) impacts epigenetic regulators and histone methylation of oocytes. This then causes downstream changes to DNA methylation in the early embryo; however, the impact can be varied depending on the environmental conditions. For instance, maternal HFD feeding in mice increased ROS production and pyruvate oxidation (indicative of increased mitochondrial metabolism) in the MII oocyte. This resulted in no changes to blastocyst development, however reduced the number of foetuses per embryo transferred and foetal crown:rump length. While in

the IVM mouse model, a global (whole oocyte) increase in KDM5A concentration was observed with IVM compared to *in vivo* maturation, which further increased with the addition of the competitive inhibitor 2-hydroxyglutarate (2HG). This resulted in a reduced proportion of hatching blastocysts on day 5, with reduced total cell count and ICM count under IVM+20mM 2HG. This reduction in cell count in the ICM was observed with the addition of 2HG only and was not observed with just IVM, nor for HFD.

This thesis has examined the effects of both a maternal HFD model to determine the changes under metabolic stress as would occur in women, however also included an *in vitro* model of metabolic stress using IVM and the addition of 2HG to further interfere with metabolic regulation. An animal model with a Western style high fat diet was used in this thesis for determining effects on oocyte maturation through to the period of conception in adult mice (Figure 6.1). Notwithstanding the limitations of using the BMI scale (particularly fraught for patients at BMI 25-30), the animal model attempted to best mirror any preconception alterations to the environment surrounding the developing oocyte. For embryo development both the HFD mouse model and the human cohort showed no significant alterations to embryo development. Other animal models of high fat diet have previously shown differences in embryo development for more extended periods of HFD exposure (16 weeks HFD opposed to 6 weeks) (Han et al., 2018), and also present with comorbidities such as hyperinsulinemia which may contribute to the differences observed between this and their HFD models.

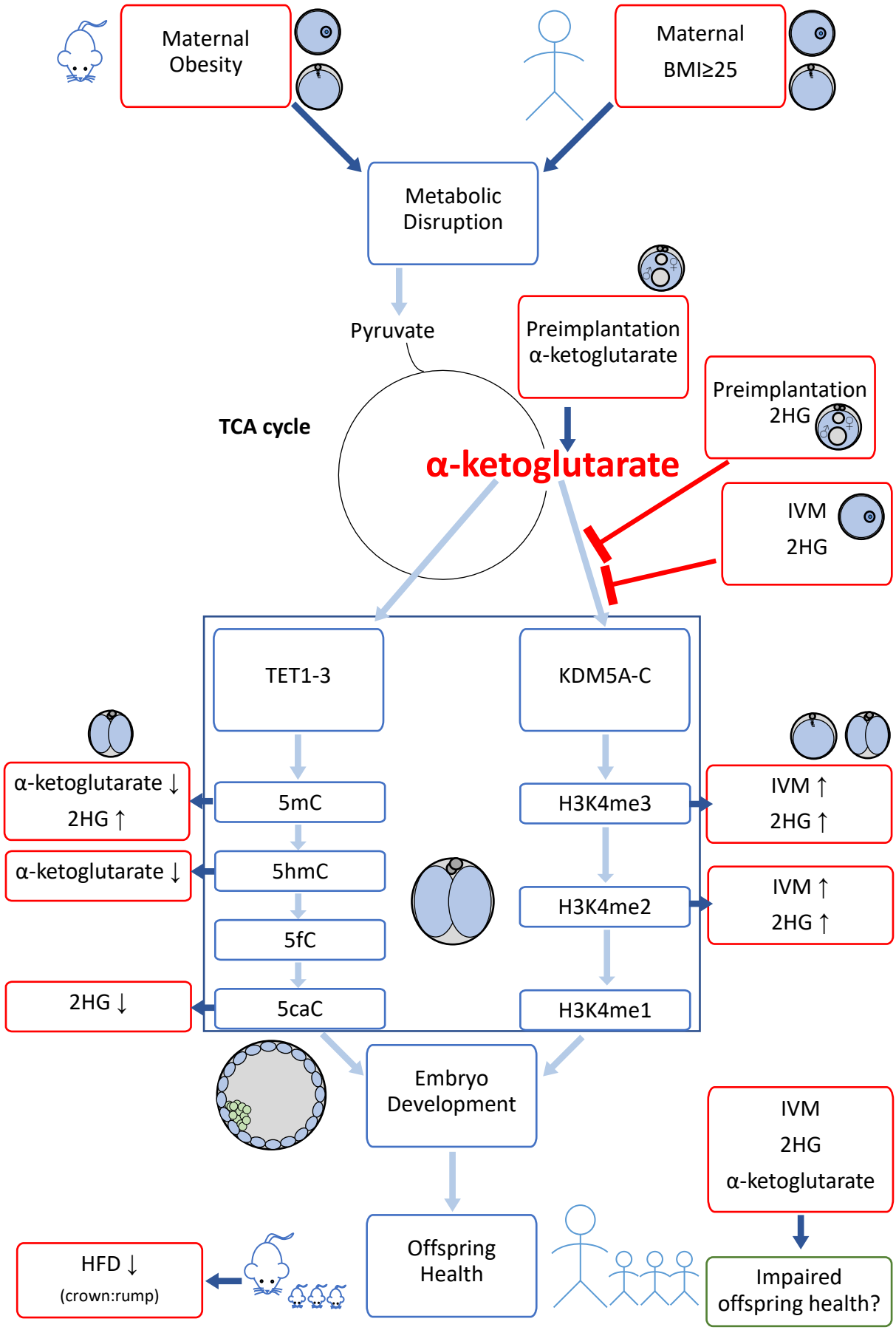
Maternal Obesity
Maternal BMI≥25
Metabolic Disruption
Pyruvate
TCA cycle
Preimplantation α-ketoglutarate
Preimplantation 2HG
α-ketoglutarate
IVM 2HG
TET1-3
KDM5A-C
α-ketoglutarate ↓ 2HG ↑
α-ketoglutarate ↓
2HG ↓
5mC
5hmC
5fC
5caC
H3K4me3
H3K4me2
H3K4me1
IVM ↑ 2HG ↑
IVM ↑ 2HG ↑
Embryo Development
IVM 2HG α-ketoglutarate
Offspring Health
Impaired offspring health?
HFD ↓ (crown:rump)

Figure 6.1 Mechanism of alterations to embryo development and offspring health due to alterations caused by maternal high fat diet (HFD), maternal overweight/obesity (body mass index (BMI) ≥ 25 kg/m^2) or supplementation of culture media with α-ketoglutarate or 2-hydroxyglturate (2HG)

In this study under maternal HFD, pyruvate uptake and pyruvate oxidation were measured using ultramicrofluorometric techniques in MII oocytes to determine the rate of use of pyruvate taken up through the TCA cycle. While this is a useful marker for pyruvate metabolism through the TCA cycle as opposed to through lactate in the cytoplasm, it does not accurately show α-ketoglutarate production and persistence for use by α-ketoglutarate dependent enzymes as opposed to as an intermediary for metabolism through the TCA cycle (Figure 6.1). Further studies using a similar enzyme-based assay for α-ketoglutarate at the MII stage would determine total levels of α-ketoglutarate available for TET-mediated demethylation. This was not performed in the present study due to the high oocyte number requirement for both technical and experimental replicates from diet fed mice (30 pools of 5 oocytes, n=150 oocytes per diet), as a performed pilot study with 7-8 pools of 5 oocytes was not statistically powered.

Embryo transfer experiments showed that a maternal HFD decreased crown:rump length in foetuses (Figure 6.1) which has been reproduced elsewhere (Han et al., 2018). However, to date no studies have focused on the supplementation of 2HG, nor any other inhibitor of H3K4me3 methylation removal, in oocyte maturation media nor embryo culture media. Further investigation of foetal development and offspring health in this setting would determine whether the alterations observed for DNA and H3K4 methylation and at the 2-cell stage translate to altered growth and health trajectories in offspring.

Overall, these changes posit that the developing oocyte, whether *in vivo* or *in vitro*, is highly sensitive to metabolic changes, which can cause changes to embryo development and foetal development. These effects are not only limited to the oocyte before fertilisation, as the early embryo is also highly susceptible to metabolic changes and is a critical period for establishment of epigenetic marks.

6.2.2 Embryo exposure to altered metabolism

Inhibition and activation of metabolic control was assessed during embryo development utilising 2HG and α-ketoglutarate respectively. These changes were assessed in *in vivo* fertilised embryos from the 1-cell stage, as there is significant TET activity during the active demethylation of the paternal genome post fertilisation (Santos et al., 2002), therefore this window of exposure was selected to determine methylation changes after embryonic genome activation. There is also a replication dependent loss of methylation marks throughout cleavage stage development (Inoue and Zhang, 2011), so addition of α-ketoglutarate and 2HG was continued throughout cleavage stages and through to blastocyst stage (for α-ketoglutarate only). This allowed to determine the effects of altered α-ketoglutarate as potentially seen with maternal obesity. 2HG supplementation was only performed until day 3 as beyond this point it completely inhibited embryo development.

Under α-ketoglutarate supplementation, embryos cultured in 14.0 mM α-ketoglutarate ceased development at the 2-cell stage, however all other concentrations did not impact on embryo development, nor blastocyst cell counts. Alterations with supplementation of α-ketoglutarate into embryo culture media have been examined previously (Zhang et al., 2019), however using concentrations of α-ketoglutarate ranging from 100 µM to 300 µM, an order of magnitude lower than our lowest concentration used in our studies (1.4 mM). The purpose of our study was to develop an *in vitro* model to show that increasing α-ketoglutarate could directly alter DNA demethylation in the embryo, rather than to improve poor embryo culture conditions, 2hich was mimicked by the study culturing in atmospheric oxygen (Zhang et al., 2019), which have proven metabolic implications (Houghton et al., 1996, Kelley and Gardner, 2019), and using KSOM culture media, which yields reduced embryo development relative to sequential human embryo media (Xu et al., 2004). The results from this thesis suggests that the embryo is particularly susceptible to altered α-ketoglutarate immediately post fertilisation, however metabolic stress during oocyte maturation also can change epigenetic marks. The implications of these changes through the oocyte maturation period could have effects on clinical outcomes through altered

metabolic profiles, including altered embryonic growth through altered gene expression as a result of epigenetic changes, leading to poorer health outcomes.

Under 2HG inhibition, embryos on day 3 were developmentally slower, however after transfer to media without 2HG there were no significant differences on embryo development, despite reductions in cell counts of inner cell mass, trophectoderm and total cells. 2HG acts as a competitive inhibitor for all α-ketoglutarate dependent enzymes (discussed in Section 3.7). This means that any alterations to the embryo phenotype cannot be proven to be due to only the inhibition of TETs or KDM5A-C, rather it shows a picture of inhibition of cellular α-ketoglutarate binding of multiple cellular enzymes.

At conception of this study, this was the first recorded use of 2HG as a competitive inhibitor of TET in embryos in order to examine changes in α-ketoglutarate availability, with previous studies using *in vitro* models (Sudhamalla et al., 2017), or its implications for hypermethylation in glioblastoma, where 2HG is produced by mutant isocitrate dehydrogenase (Dang et al., 2009, Pope et al., 2012, Xu et al., 2011a, Ye et al., 2013). Further, examination of metabolic models that see changes to α-ketoglutarate supply or inhibition is required in order to fully examine the changes due to α-ketoglutarate and other pathways affected by it. For example, the impact of α-ketoglutarate supply on KDM5A-C in the oocyte and measurement of TCA cycle activity through pyruvate oxidation, to determine further outcomes of direct metabolic changes.

6.3 Implications of altered metabolism in the oocyte on clinical outcomes

In the study assessing the effect of human increased body mass index (BMI ≥25 compared to BMI 18-25), cDNA from total cumulus and granulosa RNA extractions was used to examine expression of *TET1-3* gene expression. Cumulus cells contribute to oocyte health through transmission of nutrients including pyruvate (Dunning et al., 2011, Dunning et al., 2012), and granulosa cells for paracrine signalling (Hammond et al., 1985, Su et al., 2009), with both processes critical for providing nutrients and hormones required for embryo development and any changes to gene expression within these cells may impact on oocyte developmental competence.

TET1-3 expression was not significantly different with increased maternal BMI, which mirrored what was found in oocytes of maternal HFD in the mouse model. Where *TET1-3* was unchanged in mouse oocytes, despite reduced 5hmC and increased 5fC in the 2-cell embryo from HFD oocytes. This suggests that the phenotype observed with increased maternal BMI is more likely due to the changes in availability of pyruvate in the oocyte and resulting embryo as compared with altering TET content in the oocyte. Therefore, the increasing demethylation likely occurs via the present TET1-3 protein, whilst utilising the greater cellular α-ketoglutarate, rather than increasing expression of *TET1-3* in order to produce more TET1-3 enzyme to produce the observed changes in methylation. Without development of a non-invasive method of assessing the methylome, this is unlikely to be explored in human oocytes. However, establishment of methylation in 5mC, 5hmC, 5fC and 5caC in cumulus and granulosa cells may be possible, given future ethical clearance, to confirm the endpoint changes in the human are the same as those observed under HFD.

As explored under the IVM model with or without the addition of 2HG, altering the metabolic and epigenetic environment of the maturing oocyte only produces mild alterations to embryo development, and particularly no oocyte alterations to KDM5 protein content were seen. Previous studies have shown that embryos from women with a BMI >25 kg/m^2 display reduced blastocyst cell counts, with smaller blastocysts (Leary et al., 2015). This matches the phenotype

observed under 2HG supplementation in both IVM exposure and preimplantation culture, where ICM cell count was reduced and had fewer hatching blastocysts. IVM matured bovine oocytes have reduced ATP:ADP ratio compared to in-vivo matured oocytes, alongside dysregulation of the β-oxidation pathway to produce energy from lipids, suggesting total lower total energy production of IVM oocytes (del Collado et al., 2017). Together these show that alterations to the metabolic environment of the oocyte/embryo though IVM or maternal elevated body mass index can cause changes to embryo development, and therefore likely children's health outcomes. While our preliminary findings provide the initial evidence of the connection between metabolism and broad dysregulation of epigenetic marks (Figure 6.1), further experimentation using genomic techniques could provide a finer resolution/precision of these alterations.

In the cohort of women attending fertility treatment that were recruited for this study, observed reduced oocyte collection numbers from women with BMI >25 kg/m^2 were seen, with no changes to clinical pregnancy rates. This result is only calculated for a small number of fresh embryo transfer cycles performed from each collection and does not include data from subsequent frozen embryo transfers. It is possible that if the frozen embryo transfers outcomes were also followed up to increase power of clinical outcomes that the influence of *TET1-3* in cumulus and granulosa cells may demonstrate an association given these are measures taken from before fertilisation, and this will be the focus of continuing studies.

There are very few studies examining the effects that metabolic alterations have on human embryos given ethical considerations surrounding performing research on this material however one study has demonstrated embryos from women with BMI > 25 had reduced uptake of glucose, thus overall embryos had lower uptake of energy which may also contribute to embryo programming (Leary et al., 2015). Overall, this pilot study has established that whilst there were minimal effects of increased maternal BMI on *TET1-3* expression in cumulus and granulosa, this does not confirm that there is no effect on 5mC-5caC methylation in these cell type or the oocyte and resultant embryo. Further examinations of cumulus and granulosa cell

methylation to determine the mechanism for the observed adverse health outcome for children born from women with elevated maternal BMI are warranted.

6.4 Oocyte and early embryo DNA methylation

TET1-3 are the only currently known proteins capable of demethylating 5mC to 5hmC, and then to 5fC and 5caC for removal by thymine DNA glycosylase (Maiti and Drohat, 2011, Schomacher et al., 2016). As such, their presence is essential for the removal of methylation for enabling transcription in the early embryo, with knockout embryos resulting in high neonatal lethality (Tsukada et al., 2015).

In our HFD mouse model, TET3 was examined as it appears to be the most active and studied TET protein in the cleavage stage embryo (Dahl et al., 2016, Guo et al., 2014, Inoue et al., 2011). Under HFD, its relative concentration was not changed, however its distribution was altered, with changes to its presence associated with the chromatin. Despite TET being unchanged in its levels, 5hmC was reduced under HFD in the G1 2-cell, with a concomitant increase in 5fC (Figure 6.1). This indicates that the modifications to DNA methylation were not due to changes in TET3 concentrations, but may occur through a separate mechanism, such as increased α-ketoglutarate as an energy donor.

This time period of exposure to different environmental insults was investigated throughout this thesis. Under murine maternal HFD, the oocyte was grown under HFD conditions through to the pronuclear stage embryo, with IVM the environmental perturbation occurred only during oocyte maturation and did not continue past the point of insemination. Under human maternal obesity, this trend was similar to the murine HFD exposure save for clinical IVF/ICSI procedure rather than *in vivo* fertilisation and with α-ketoglutarate and 2HG, the metabolic disruption was inflicted throughout pre-implantation embryo development. As discussed previously, there are wide-ranging genome wide alterations to DNA methylation in the embryo occurring in the maturing oocyte and then immediately post fertilisation and up until genome activation and

beyond, all of which are susceptible to environmental influence. (Adenot et al., 1997, Santos et al., 2002, Shen et al., 2014).

As there is active demethylation of 5mC throughout pronuclear migration leading up to the first cleavage of the whole paternal genome, and in the maternal genome to a lesser extent (Santos et al., 2002), altering the supply of α-ketoglutarate through direct supplementation or inhibition via 2HG, would have a much greater effect to altering 5mC-5caC as opposed to throughout oocyte development where there are fewer genome wide changes. There have been reports that changes to 5hmC, 5fC and 5caC remain stable through preimplantation development, although, they are diluted through cleavage divisions (Inoue et al., 2011, Inoue and Zhang, 2011). However, through supplementation of 2HG, after removal to commercial media free of 2HG, embryos previously unable to progress past the 4-cell to 6-cell stage were able to develop to form blastocysts. This may suggest that 2HG in this given model may also be impacting other metabolic systems which may be halting embryo growth, such as through slowing of TCA cycle mediated energy production throughout the supplementation window. Overall, these results show changes during embryonic growth, as *in vivo* models such as HFD are not able to study this window in isolation of effects prior to fertilisation.

Conversely, the mouse model showed no alterations to embryo development under HFD despite the epigenetic alterations, and *in vitro* maturation showed differences with IVM compared to ovulated oocytes, with minimal extra changes observed with the addition of 2HG. This may suggest that embryo quality and on-time development may not be the best marker for epigenetic and metabolic health (discussed further in Section 4.4). *In vitro* maturation conditions lead to the most significant alterations to both embryo development and epigenetic alterations. However, as this oocyte maturation model focused on H3K4 methylation changes as opposed to alterations to TET and 5mC through 5caC the impact of IVM on DNA methylation remains to be investigated and is the focus of future studies. More recently, specific inhibitors for TETs and KDM5 protein families have been discovered, which allow for mechanistic studies based solely on TET inhibition, or KDM5 inhibition pathways to determine the exact mechanism of

such alterations. The use of these specific inhibitors would provide further insight into the role that TET/KDM5 inhibition has on embryo programming. For example a small molecule, called C35, has recently been discovered via molecular modelling as a competitive inhibitor for TET2, with no known off target effects (Singh et al., 2020). C35 has an inhibitory concentration (IC_{50}) (i.e., the concentration of inhibitor required to inhibit an enzyme's activity by 50%) of 1.2 μM against TET2 (Singh et al., 2020), which is much lower than both R-2HG and S-2HG (differences between R-2HG and S-2HG discussed in Section 3.7). The inhibitory effect of this concentration of C35 on embryo development or for effect on TET1 or TET3 is yet to be assessed. A logical extension to both our IVM and preimplantation embryo culture models would be to utilise C35 to confirm that alterations to blastocyst programming and offspring phenotype are due to TET and KDM5A-C alterations, rather than due to other more broadly derived metabolic changes. However, it has still been of value to examine the effects of maternal HFD, IVM with/without the addition of α-ketoglutarate and 2HG, as together these models have demonstrated that altered metabolism has the capacity to alter DNA and histone methylation linking metabolism with epigenetic readouts as a potential pathway involved in offspring programming and determination of adult health trajectories.

6.5 Oocyte and early embryo histone methylation

The lysine demethylase family KDM5A-C, similarly to TET1-3, use α-ketoglutarate as an energy source (Joberty et al., 2016), and is essential for the demethylation of H3K4me3 to H3K4me2 and H3K4me1 (Dahl et al., 2016). Demethylation of H3K4me3 is essential for correct embryonic genome activation in mice, where knockout of both KDM5A and KDM5B reduces expression of key genes for embryonic genome activation, including *Sox18* (Dahl et al., 2016), a transcription factor required for embryonic genome activation (Park et al., 2013). As such, this thesis also sought to examine the effects of 2HG, alongside the *in vitro* stress if IVM, on KDM5A-C in the oocyte for the same reasons at TET1-3.

Methylation of histone 3 lysine 4 was examined in our IVM model with and without 2HG as H3K4 methylation is modulated by KDM5A-D, which are also α-ketoglutarate dependent and function similarly to TET1-3 (See Section 1.10). This thesis has demonstrated that under IVM with or without the addition of 2HG, oocyte H3K4me3 and H3K4me2 were increased relative to ovulated MII, with no change to H3K4me1 (Figure 6.1). Further in G2 phase 2-cells, embryos derived from IVM increased H3K4me3 and H3K4me2, with similarly no change in H3K4me1. As KDM1A uses FAD as substrate as opposed to α-ketoglutarate (Burg et al., 2016), 2HG mediated would not alter its ability to remove H3K4me1, so this process may be functioning correctly to maintain consistent H3K4me1 in the genome.

Due to the limitation of using antibody-based densitometry and co-incubator of antibodies, the abundance of H3K4me3, H3K4me2 and H3K4me1 could not be directly compared with each other. However, the increase in both H3K4me3 and H3K4me2 indicates that with IVM, these residues are not being modified at the same rate as *in vivo*. This presents opportunities to now improve the metabolic suitability of IVM conditions to ameliorate the reduced development observed, such as potentially through the addition of additional α-ketoglutarate, to assist with normalising histone methylation to that observed from *in vivo* derived samples.

KDM5 proteins have also been discovered to have their own inhibitor, KDOAM-25 (Tumber et al., 2017). Similarly, to those experiments described above using C35 as a competitive

inhibitor for TETs, KDOAM-25 would highlight only the effects of inhibitingKDM5A-C without the broader metabolic inhibition to other α-ketoglutarate dependent pathways.

6.6 Potential improvements to methodology and techniques with modern technology

6.6.1 Detection of sequence specific DNA methylation in cells

During the evolution of this thesis, sequencing to single base accuracy has become achievable using bisulphite sequencing, without being highly specialised and cost prohibitive (Blaschke et al., 2013, Cortazar et al., 2011, Gu et al., 2011, Ito et al., 2010, Ito et al., 2011, Shen et al., 2013, Song et al., 2013, Xu et al., 2011b, Yamaguchi et al., 2012, Yang et al., 2014, Zhu et al., 2017). More recent reports have also highlighted the possibility of single cell sequencing for 5hmC (Mooijman et al., 2016), 5fC (Zhu et al., 2017) and 5caC (Ličytė et al., 2020). At the time of experimental design for this project, sequencing to separate the bases of 5fC and 5caC was not possible, with the only exception being mass spectrometry or measure of the total number of bases of each per cell (Guo et al., 2017, Zhang et al., 2016).

In addition, viable techniques available for further investigation of specific changes to methylation include methylated-DNA immunoprecipitation (meDIP) followed by microarray, or next generation sequencing (meDIP-seq) (Weber et al., 2005). However although these technologies do provide greater resolution to changes, they still rely on antibody based immunoprecipitation in order to identify 5mC residues within the genome (Weber et al., 2005). Furthermore, meDIP requires ~10 ng DNA input, which is approximately the equivalent of > 800 2-cell embryos per replicate. This amount of DNA would be ethically and financially nonviable to generate from oocytes or 2-cell embryos, due to the mouse numbers required (~640 mice), and noting the multiplication factor required to satisfy the numbers of replicates per group to allow for sufficient statistical power to detect differences. Given the relative strengths and weaknesses of bisulphite sequencing and methyl-DNA-immunoprecipitation, if sequencing was to be applied to this project, sequencing of 5mC, 5hmC, 5fC and 5caC using the bisulphite

sequencing would ideally be performed when single embryo sequencing methods become available. These would confirm our global findings of large-scale methylation changes, plus also allow examination of the differentially methylated regions between treatments, to establish the specific pathways that are altered by altered α-ketoglutarate.

6.6.2 Human oocyte and follicular cell measurements of DNA methylation marks and metabolites

Our examination of the effects of maternal BMI on *TET1-3* expression has provided limited observations. The most obvious limitation of this study was the small sample size, and hence the limited number of cumulus and granulosa cell collections made for this cohort. Increased sample size, particularly in the overweight group (BMI 25-30) and further examination of individual obesity sub-classifications (e.g. BMI 30-35, 35-40, 40 + etc.) would allow for more granular separation of obesity classifications.

Although in this pilot study there were no statistically significant alterations to *TET1-3* expression with increased maternal BMI, there was however an observed decrease in 5hmC and relative increase in 5fC in HFD 2-cells from mouse. This indicates that TET-mediated demethylation in the oocyte and early embryo may not be driven by alterations to TET transcript content, rather it is through other mechanisms, such as protein level or increasing/decreasing activity through substrate concentrations.

Under ideal conditions, examinations of *TET1-3*, and of 5mC, 5hmC, 5fC and 5caC would occur in the oocytes themselves. However, this would be difficult to perform in Australia on high quality oocytes from consenting patients. It may be possible to obtain ethical approval in order to examine other marks on discarded oocytes that were deemed unsuitable for insemination due to their maturation state or possibly on unfertilised MII oocytes however this would likely be of limited value, as determining the gene expression and epigenetic profile of immature oocytes or oocytes that failed to fertilise would in itself be a confounder.

Gene expression changes of *TET1*-3 in the cumulus or granulosa cells did not show any relationship to embryo quality, nor to implantation success in the resulting embryo. However, further work into sequencing alterations to 5mC or derivatives in cumulus or granulosa cells could provide insight into whether regardless of TET gene expression there are changes to DNA methylation. Additional allele specific understanding of methylation status could allow for examination of key regions of the genome, such as *OCT4*, where increased 5mC in the oocyte was observed in the *OCT4* promoter regions of embryos produced by ICSI (Al-Khtib et al., 2012).

While the above changes would extend the specificity of the results presented, the outcomes of the experiments presented within this thesis remain valid within the stated limitations. Moreover, as previous knowledge on the topic of metabolic induced epigenetic alterations in the early embryo was limited, these experiments have highlighted the exact areas of investigation to meaningfully expand the research.

6.7 Conclusion

This thesis has demonstrated that mouse maternal high fat diet feeding for 6 weeks increased the oxidation of pyruvate in the mitochondria, and in the 2-cell embryo reduced global 5hmC, and increased 5fC, suggesting an accelerated progression of methylation with maternal HFD. Increasing availability of the TET substrate α-ketoglutarate reduced 5mC, 5hmC and 5fC at the time of embryonic genome activation in a mouse model, whilst inhibition with the competitive inhibitor 2HG increased 5hmC and decreased 5caC. This indicates that increased α-ketoglutarate accelerates DNA demethylation, and inhibition increases 5mC via a reduction to demethylation, which also impaired embryo development beyond the 4-cell stage and decreased blastocyst cell count. Impairment of mouse oocyte maturation through IVM, which is presumed to be through metabolic stress, increased H3K3me3 and H3K4me2 in both the oocyte and 2-cell embryo, with reduced progression past the 4-6 cell on day 3. Elevated maternal body mass index (BMI > 25 kg/m^2) reduced the number of oocytes collected, with granulosa cell decreasing *TET1* was related with increased fertilisation, and decreased granulosa cell *TET2* was related to increased proportion of the lowest quality embryos on day 3 of embryo culture. Overall, these studies suggest that metabolic alterations to the oocyte and embryo milieu can directly alter DNA and H3K4 methylation through modulation of the TET/KDM5 substrate α-ketoglutarate, impairing embryo development that might compromise lifelong health. Future research is warranted to determine sequence specific methylomic changes, and any further alterations to *in vitro* culture systems to maintain closer to an *in vivo* metabolic environment in order to limit further changes from and "ideal" epigenetic status.

6.8 References

ADENOT, P. G., MERCIER, Y., RENARD, J.-P. & THOMPSON, E. M. 1997. Differential H4 acetylation of paternal and maternal chromatin precedes DNA replication and differential transcriptional activity in pronuclei of 1-cell mouse embryos. *Development,* 124**,** 4615-4625.

AL-KHTIB, M., BLACHÈRE, T., GUÉRIN, J. F. & LEFÈVRE, A. 2012. Methylation profile of the promoters of Nanog and Oct4 in ICSI human embryos. *Human Reproduction,* 27**,** 2948-2954.

BLASCHKE, K., EBATA, K. T., KARIMI, M. M., ZEPEDA-MARTÍNEZ, J. A., GOYAL, P., MAHAPATRA, S., TAM, A., LAIRD, D. J., HIRST, M., RAO, A., LORINCZ, M. C. & RAMALHO-SANTOS, M. 2013. Vitamin C induces Tet-dependent DNA demethylation in ESCs to promote a blastocyst-like state. *Nature,* 500**,** 222-226.

BURG, J. M., GONZALEZ, J. J., MAKSIMCHUK, K. R. & MCCAFFERTY, D. G. 2016. Lysine-Specific Demethylase 1A (KDM1A/LSD1): Product Recognition and Kinetic Analysis of Full-Length Histones. *Biochemistry,* 55**,** 1652-1662.

CORTAZAR, D., KUNZ, C., SELFRIDGE, J., LETTIERI, T., SAITO, Y., MACDOUGALL, E., WIRZ, A., SCHUERMANN, D., JACOBS, A. L., SIEGRIST, F., STEINACHER, R., JIRICNY, J., BIRD, A. & SCHAR, P. 2011. Embryonic lethal phenotype reveals a function of TDG in maintaining epigenetic stability. *Nature,* 470**,** 419-423.

DAHL, J. A., JUNG, I., AANES, H., GREGGAINS, G. D., MANAF, A., LERDRUP, M., LI, G., KUAN, S., LI, B., LEE, A. Y., PREISSL, S., JERMSTAD, I., HAUGEN, M. H., SUGANTHAN, R., BJØRÅS, M., HANSEN, K., DALEN, K. T., FEDORCSAK, P., REN, B. & KLUNGLAND, A. 2016. Broad histone H3K4me3 domains in mouse oocytes modulate maternal-to-zygotic transition. *Nature,* 537**,** 548.

DANG, L., WHITE, D. W., GROSS, S., BENNETT, B. D., BITTINGER, M. A., DRIGGERS, E. M., FANTIN, V. R., JANG, H. G., JIN, S., KEENAN, M. C., MARKS, K. M., PRINS, R. M., WARD, P. S., YEN, K. E., LIAU, L. M., RABINOWITZ, J. D.,

CANTLEY, L. C., THOMPSON, C. B., VANDER HEIDEN, M. G. & SU, S. M. 2009. Cancer-associated IDH1 mutations produce 2-hydroxyglutarate. *Nature,* 462**,** 739-744.

DEL COLLADO, M., DA SILVEIRA, J. C., OLIVEIRA, M. L. F., ALVES, B. M. S. M., SIMAS, R. C., GODOY, A. T., COELHO, M. B., MARQUES, L. A., CARRIERO, M. M., NOGUEIRA, M. F. G., EBERLIN, M. N., SILVA, L. A., MEIRELLES, F. V. & PERECIN, F. 2017. In vitro maturation impacts cumulus–oocyte complex metabolism and stress in cattle. *Reproduction,* 154**,** 881-893.

DUNNING, K. R., AKISON, L. K., RUSSELL, D. L., NORMAN, R. J. & ROBKER, R. L. 2011. Increased Beta-Oxidation and Improved Oocyte Developmental Competence in Response to l-Carnitine During Ovarian In Vitro Follicle Development in Mice. *Biology of Reproduction,* 85**,** 548-555.

DUNNING, K. R., LANE, M., BROWN, H. M., YEO, C., ROBKER, R. L. & RUSSELL, D. L. 2007. Altered composition of the cumulus-oocyte complex matrix during in vitro maturation of oocytes. *Human Reproduction,* 22**,** 2842-2850.

DUNNING, K. R., WATSON, L. N., SHARKEY, D. J., BROWN, H. M., NORMAN, R. J., THOMPSON, J. G., ROBKER, R. L. & RUSSELL, D. L. 2012. Molecular Filtration Properties of the Mouse Expanded Cumulus Matrix: Controlled Supply of Metabolites and Extracellular Signals to Cumulus Cells and the Oocyte1. *Biology of Reproduction,* 87.

EPPIG, J. J. 1996. Coordination of nuclear and cytoplasmic oocyte maturation in eutherian mammals. *Reproduction, Fertility and Development,* 8**,** 485-489.

EPPIG, J. J., O'BRIEN, M. J., WIGGLESWORTH, K., NICHOLSON, A., ZHANG, W. & KING, B. A. 2009. Effect of in vitro maturation of mouse oocytes on the health and lifespan of adult offspring. *Human Reproduction,* 24**,** 922-928.

GE, Z.-J., LUO, S.-M., LIN, F., LIANG, Q.-X., HUANG, L., WEI, Y.-C., HOU, Y., HAN, Z.-M., SCHATTEN, H. & SUN, Q.-Y. 2014. DNA Methylation in Oocytes and Liver of

Female Mice and Their Offspring: Effects of High-Fat-Diet–Induced Obesity. *Environmental Health Perspectives,* 122**,** 159-164.

GRINDLER, N. M. & MOLEY, K. H. 2013. Maternal obesity, infertility and mitochondrial dysfunction: potential mechanisms emerging from mouse model systems. *Molecular Human Reproduction,* 19**,** 486-494.

GU, L., LIU, H., GU, X., BOOTS, C., MOLEY, K. & WANG, Q. 2015. Metabolic control of oocyte development: linking maternal nutrition and reproductive outcomes. *Cellular and Molecular Life Sciences,* 72**,** 251-271.

GU, T.-P., GUO, F., YANG, H., WU, H.-P., XU, G.-F., LIU, W., XIE, Z.-G., SHI, L., HE, X., JIN, S.-G., IQBAL, K., SHI, Y. G., DENG, Z., SZABO, P. E., PFEIFER, G. P., LI, J. & XU, G.-L. 2011. The role of Tet3 DNA dioxygenase in epigenetic reprogramming by oocytes. *Nature,* 477**,** 606-610.

GUO, F., LI, X., LIANG, D., LI, T., ZHU, P., GUO, H., WU, X., WEN, L., GU, T.-P., HU, B., WALSH, COLUM P., LI, J., TANG, F. & XU, G.-L. 2014. Active and Passive Demethylation of Male and Female Pronuclear DNA in the Mammalian Zygote. *Cell Stem Cell,* 15**,** 447-458.

GUO, M., LI, X., ZHANG, L., LIU, D., DU, W., YIN, D., LYU, N., ZHAO, G., GUO, C. & TANG, D. 2017. Accurate quantification of 5-Methylcytosine, 5-Hydroxymethylcytosine, 5-Formylcytosine, and 5-Carboxylcytosine in genomic DNA from breast cancer by chemical derivatization coupled with ultra performance liquid chromatography- electrospray quadrupole time of flight mass spectrometry analysis. *Oncotarget,* 8**,** 91248-91257.

HAMMOND, J. M., BARANAO, J. L. S., SKALERIS, D., KNIGHT, A. B., ROMANUS, J. A. & RECHLER, M. M. 1985. Production of insulin-like growth factors by ovarian granulosa cells. *Endocrinology,* 117**,** 2553-2555.

HAN, L., REN, C., LI, L., LI, X., GE, J., WANG, H., MIAO, Y.-L., GUO, X., MOLEY, K. H., SHU, W. & WANG, Q. 2018. Embryonic defects induced by maternal obesity in mice derive from Stella insufficiency in oocytes. *Nature Genetics,* 50**,** 432-442.

HARDY, K., HOOPER, M. A. K., HANDYSIDE, A. H., RUTHERFORD, A. J., WINSTON, R. M. L. & LEESE, H. J. 1989. Non-invasive measurement of glucose and pyruvate uptake by individual human oocytes and preimplantation embryos. *Human Reproduction,* 4**,** 188-191.

HARRIS, S. E., LEESE, H. J., GOSDEN, R. G. & PICTON, H. M. 2009. Pyruvate and oxygen consumption throughout the growth and development of murine oocytes. *Molecular Reproduction and Development,* 76**,** 231-238.

HOUGHTON, F. D., THOMPSON, J. G., KENNEDY, C. J. & LEESE, H. J. 1996. Oxygen consumption and energy metabolism of the early mouse embryo. *Molecular Reproduction and Development,* 44**,** 476-485.

IGOSHEVA, N., ABRAMOV, A. Y., POSTON, L., ECKERT, J. J., FLEMING, T. P., DUCHEN, M. R. & MCCONNELL, J. 2010. Maternal Diet-Induced Obesity Alters Mitochondrial Activity and Redox Status in Mouse Oocytes and Zygotes. *PLoS ONE,* 5**,** e10074.

INOUE, A., SHEN, L., DAI, Q., HE, C. & ZHANG, Y. 2011. Generation and replication-dependent dilution of 5fC and 5caC during mouse preimplantation development. *Cell Research,* 21**,** 1670-1676.

INOUE, A. & ZHANG, Y. 2011. Replication-Dependent Loss of 5-Hydroxymethylcytosine in Mouse Preimplantation Embryos. *Science (New York, N.Y.),* 334**,** 194-194.

ITO, S., D'ALESSIO, A. C., TARANOVA, O. V., HONG, K., SOWERS, L. C. & ZHANG, Y. 2010. Role of Tet proteins in 5mC to 5hmC conversion, ES cell self-renewal, and ICM specification. *Nature,* 466**,** 1129-1133.

ITO, S., SHEN, L., DAI, Q., WU, S. C., COLLINS, L. B., SWENBERG, J. A., HE, C. & ZHANG, Y. 2011. Tet proteins can convert 5-methylcytosine to 5-formylcytosine and 5-carboxylcytosine. *Science,* 333**,** 1300-1303.

JOBERTY, G., BOESCHE, M., BROWN, J. A., EBERHARD, D., GARTON, N. S., HUMPHREYS, P. G., MATHIESON, T., MUELBAIER, M., RAMSDEN, N. G., READER, V., RUEGER, A., SHEPPARD, R. J., WESTAWAY, S. M., BANTSCHEFF, M., LEE, K., WILSON, D. M., PRINJHA, R. K. & DREWES, G. 2016. Interrogating the Druggability of the 2-Oxoglutarate-Dependent Dioxygenase Target Class by Chemical Proteomics. *ACS Chemical Biology,* 11**,** 2002-2010.

JUNGHEIM, E. S., SCHOELLER, E. L., MARQUARD, K. L., LOUDEN, E. D., SCHAFFER, J. E. & MOLEY, K. H. 2010. Diet-Induced Obesity Model: Abnormal Oocytes and Persistent Growth Abnormalities in the Offspring. *Endocrinology,* 151**,** 4039-4046.

KELLEY, R. L. & GARDNER, D. K. 2019. Individual culture and atmospheric oxygen during culture affect mouse preimplantation embryo metabolism and post-implantation development. *Reproductive BioMedicine Online,* 39**,** 3-18.

LEARY, C., LEESE, H. J. & STURMEY, R. G. 2015. Human embryos from overweight and obese women display phenotypic and metabolic abnormalities. *Human Reproduction,* 30**,** 122-132.

LIČYTĖ, J., GIBAS, P., SKARDŽIŪTĖ, K., STANKEVIČIUS, V., RUKŠĖNAITĖ, A. & KRIUKIENĖ, E. 2020. A Bisulfite-free Approach for Base-Resolution Analysis of Genomic 5-Carboxylcytosine. *Cell Reports,* 32**,** 108155.

LUZZO, K. M., WANG, Q., PURCELL, S. H., CHI, M., JIMENEZ, P. T., GRINDLER, N., SCHEDL, T. & MOLEY, K. H. 2012. High Fat Diet Induced Developmental Defects in the Mouse: Oocyte Meiotic Aneuploidy and Fetal Growth Retardation/Brain Defects. *PLoS One,* 7**,** e49217.

MAITI, A. & DROHAT, A. C. 2011. Thymine DNA Glycosylase Can Rapidly Excise 5-Formylcytosine and 5-Carboxylcytosine: POTENTIAL IMPLICATIONS FOR

ACTIVE DEMETHYLATION OF CpG SITES. *The Journal of Biological Chemistry,* 286**,** 35334-35338.

MOOIJMAN, D., DEY, S. S., BOISSET, J.-C., CROSETTO, N. & VAN OUDENAARDEN, A. 2016. Single-cell 5hmC sequencing reveals chromosome-wide cell-to-cell variability and enables lineage reconstruction. *Nature Biotechnology,* 34**,** 852-856.

NG, M., FLEMING, T., ROBINSON, M., THOMSON, B., GRAETZ, N., MARGONO, C., MULLANY, E. C., BIRYUKOV, S., ABBAFATI, C., ABERA, S. F., ABRAHAM, J. P., ABU-RMEILEH, N. M. E., ACHOKI, T., ALBUHAIRAN, F. S., ALEMU, Z. A., ALFONSO, R., ALI, M. K., ALI, R., GUZMAN, N. A., AMMAR, W., ANWARI, P., BANERJEE, A., BARQUERA, S., BASU, S., BENNETT, D. A., BHUTTA, Z., BLORE, J., CABRAL, N., NONATO, I. C., CHANG, J.-C., CHOWDHURY, R., COURVILLE, K. J., CRIQUI, M. H., CUNDIFF, D. K., DABHADKAR, K. C., DANDONA, L., DAVIS, A., DAYAMA, A., DHARMARATNE, S. D., DING, E. L., DURRANI, A. M., ESTEGHAMATI, A., FARZADFAR, F., FAY, D. F. J., FEIGIN, V. L., FLAXMAN, A., FOROUZANFAR, M. H., GOTO, A., GREEN, M. A., GUPTA, R., HAFEZI-NEJAD, N., HANKEY, G. J., HAREWOOD, H. C., HAVMOELLER, R., HAY, S., HERNANDEZ, L., HUSSEINI, A., IDRISOV, B. T., IKEDA, N., ISLAMI, F., JAHANGIR, E., JASSAL, S. K., JEE, S. H., JEFFREYS, M., JONAS, J. B., KABAGAMBE, E. K., KHALIFA, S. E. A. H., KENGNE, A. P., KHADER, Y. S., KHANG, Y.-H., KIM, D., KIMOKOTI, R. W., KINGE, J. M., KOKUBO, Y., KOSEN, S., KWAN, G., LAI, T., LEINSALU, M., LI, Y., LIANG, X., LIU, S., LOGROSCINO, G., LOTUFO, P. A., LU, Y., MA, J., MAINOO, N. K., MENSAH, G. A., MERRIMAN, T. R., MOKDAD, A. H., MOSCHANDREAS, J., NAGHAVI, M., NAHEED, A., NAND, D., NARAYAN, K. M. V., NELSON, E. L., NEUHOUSER, M. L., NISAR, M. I., OHKUBO, T., OTI, S. O., PEDROZA, A., et al. 2014. Global, regional, and national prevalence of overweight and obesity in children and adults during 1980–2013:

a systematic analysis for the Global Burden of Disease Study 2013. *The Lancet,* 384**,** 766-781.

PARK, S.-J., KOMATA, M., INOUE, F., YAMADA, K., NAKAI, K., OHSUGI, M. & SHIRAHIGE, K. 2013. Inferring the choreography of parental genomes during fertilization from ultralarge-scale whole-transcriptome analysis. *Genes & Development,* 27**,** 2736-2748.

POPE, W., PRINS, R., ALBERT THOMAS, M., NAGARAJAN, R., YEN, K., BITTINGER, M., SALAMON, N., CHOU, A., YONG, W., SOTO, H., WILSON, N., DRIGGERS, E., JANG, H., SU, S., SCHENKEIN, D., LAI, A., CLOUGHESY, T., KORNBLUM, H., WU, H., FANTIN, V. & LIAU, L. 2012. Non-invasive detection of 2-hydroxyglutarate and other metabolites in IDH1 mutant glioma patients using magnetic resonance spectroscopy. *Journal of Neuro-Oncology,* 107**,** 197-205.

SANTOS, F., HENDRICH, B., REIK, W. & DEAN, W. 2002. Dynamic Reprogramming of DNA Methylation in the Early Mouse Embryo. *Developmental Biology,* 241**,** 172-182.

SCHOMACHER, L., HAN, D., MUSHEEV, M. U., ARAB, K., KIENHOFER, S., VON SEGGERN, A. & NIEHRS, C. 2016. Neil DNA glycosylases promote substrate turnover by Tdg during DNA demethylation. *Nat Struct Mol Biol,* advance online publication.

SHEN, L., SONG, C.-X., HE, C. & ZHANG, Y. 2014. Mechanism and Function of Oxidative Reversal of DNA and RNA Methylation. *Annual Review of Biochemistry,* 83**,** 585-614.

SHEN, L., WU, H., DIEP, D., YAMAGUCHI, S., D'ALESSIO, ANA C., FUNG, H.-L., ZHANG, K. & ZHANG, Y. 2013. Genome-wide Analysis Reveals TET- and TDG-Dependent 5-Methylcytosine Oxidation Dynamics. *Cell,* 153**,** 692-706.

SINCLAIR, K. D., ALLEGRUCCI, C., SINGH, R., GARDNER, D. S., SEBASTIAN, S., BISPHAM, J., THURSTON, A., HUNTLEY, J. F., REES, W. D., MALONEY, C. A., LEA, R. G., CRAIGON, J., MCEVOY, T. G. & YOUNG, L. E. 2007. DNA methylation, insulin resistance, and blood pressure in offspring determined by maternal

periconceptional B vitamin and methionine status. *Proceedings of the National Academy of Sciences,* 104**,** 19351-19356.

SINGH, A. K., ZHAO, B., LIU, X., WANG, X., LI, H., QIN, H., WU, X., MA, Y., HORNE, D. & YU, X. 2020. Selective targeting of TET catalytic domain promotes somatic cell reprogramming. *Proceedings of the National Academy of Sciences,* 117**,** 3621.

SONG, C.-X., SZULWACH, KEITH E., DAI, Q., FU, Y., MAO, S.-Q., LIN, L., STREET, C., LI, Y., POIDEVIN, M., WU, H., GAO, J., LIU, P., LI, L., XU, G.-L., JIN, P. & HE, C. 2013. Genome-wide Profiling of 5-Formylcytosine Reveals Its Roles in Epigenetic Priming. *Cell,* 153**,** 678-691.

SU, Y.-Q., SUGIURA, K. & EPPIG, J. J. 2009. Mouse oocyte control of granulosa cell development and function: paracrine regulation of cumulus cell metabolism. *Seminars in reproductive medicine,* 27**,** 32-42.

SUDHAMALLA, B., DEY, D., BRESKI, M. & ISLAM, K. 2017. A rapid mass spectrometric method for the measurement of catalytic activity of ten-eleven translocation enzymes. *Analytical Biochemistry,* 534**,** 28-35.

TSUKADA, Y.-I., AKIYAMA, T. & NAKAYAMA, K. I. 2015. Maternal TET3 is dispensable for embryonic development but is required for neonatal growth. *Scientific Reports,* 5**,** 15876.

TUMBER, A., NUZZI, A., HOOKWAY, E. S., HATCH, S. B., VELUPILLAI, S., JOHANSSON, C., KAWAMURA, A., SAVITSKY, P., YAPP, C., SZYKOWSKA, A., WU, N., BOUNTRA, C., STRAIN-DAMERELL, C., BURGESS-BROWN, N. A., RUDA, G. F., FEDOROV, O., MUNRO, S., ENGLAND, K. S., NOWAK, R. P., SCHOFIELD, C. J., LA THANGUE, N. B., PAWLYN, C., DAVIES, F., MORGAN, G., ATHANASOU, N., MÜLLER, S., OPPERMANN, U. & BRENNAN, P. E. 2017. Potent and Selective KDM5 Inhibitor Stops Cellular Demethylation of H3K4me3 at Transcription Start Sites and Proliferation of MM1S Myeloma Cells. *Cell chemical biology,* 24**,** 371-380.

WAKEFIELD, S. L., LANE, M., SCHULZ, S. J., HEBART, M. L., THOMPSON, J. G. & MITCHELL, M. 2008. Maternal supply of omega-3 polyunsaturated fatty acids alter mechanisms involved in oocyte and early embryo development in the mouse. *American Journal of Physiology - Endocrinology And Metabolism,* 294**,** E425-E434.

WEBER, M., DAVIES, J. J., WITTIG, D., OAKELEY, E. J., HAASE, M., LAM, W. L. & SCHÜBELER, D. 2005. Chromosome-wide and promoter-specific analyses identify sites of differential DNA methylation in normal and transformed human cells. *Nature Genetics,* 37**,** 853-862.

WEN, J., WANG, G.-L., YUAN, H.-J., ZHANG, J., XIE, H.-L., GONG, S., HAN, X. & TAN, J.-H. 2020. Effects of glucose metabolism pathways on nuclear and cytoplasmic maturation of pig oocytes. *Scientific Reports,* 10**,** 2782.

XU, J.-S., CHAN, S. T.-H., LEE, W. W. M., LEE, K.-F. & YEUNG, W. S. B. 2004. Differential growth, cell proliferation, and apoptosis of mouse embryo in various culture media and in coculture. *Molecular Reproduction and Development,* 68**,** 72-80.

XU, W., YANG, H., LIU, Y., YANG, Y., WANG, P., KIM, S.-H., ITO, S., YANG, C., WANG, P., XIAO, M.-T., LIU, L.-X., JIANG, W.-Q., LIU, J., ZHANG, J.-Y., WANG, B., FRYE, S., ZHANG, Y., XU, Y.-H., LEI, Q.-Y., GUAN, K.-L., ZHAO, S.-M. & XIONG, Y. 2011a. Oncometabolite 2-Hydroxyglutarate Is a Competitive Inhibitor of α-Ketoglutarate-Dependent Dioxygenases. *Cancer Cell,* 19**,** 17-30.

XU, Y., WU, F., TAN, L., KONG, L., XIONG, L., DENG, J., BARBERA, A. J., ZHENG, L., ZHANG, H., HUANG, S., MIN, J., NICHOLSON, T., CHEN, T., XU, G., SHI, Y., ZHANG, K. & SHI, YUJIANG G. 2011b. Genome-wide Regulation of 5hmC, 5mC, and Gene Expression by Tet1 Hydroxylase in Mouse Embryonic Stem Cells. *Molecular Cell,* 42**,** 451-464.

YAMAGUCHI, S., HONG, K., LIU, R., SHEN, L., INOUE, A., DIEP, D., ZHANG, K. & ZHANG, Y. 2012. Tet1 controls meiosis by regulating meiotic gene expression. *Nature,* 492**,** 443-447.

YANG, H., LIN, H., XU, H., ZHANG, L., CHENG, L., WEN, B., SHOU, J., GUAN, K., XIONG, Y. & YE, D. 2014. TET-catalyzed 5-methylcytosine hydroxylation is dynamically regulated by metabolites. *Cell Research,* 24**,** 1017-1020.

YE, D., MA, S., XIONG, Y. & GUAN, K.-L. 2013. R-2-hydroxyglutarate as the key effector of IDH mutations promoting oncogenesis. *Cancer Cell,* 23**,** 274-276.

ZENG, H.-T., RICHANI, D., SUTTON-MCDOWALL, M. L., REN, Z., SMITZ, J. E. J., STOKES, Y., GILCHRIST, R. B. & THOMPSON, J. G. 2014. Prematuration with Cyclic Adenosine Monophosphate Modulators Alters Cumulus Cell and Oocyte Metabolism and Enhances Developmental Competence of In Vitro-Matured Mouse Oocytes1. *Biology of Reproduction,* 91.

ZHANG, L., LI, Z., CHEN, G., HUANG, Q., ZHANG, J., WEN, J., YE, X. & CAI, C. 2016. Validation and quantification of genomic 5-carboxylcytosine (5caC) in mouse brain tissue by liquid chromatography-tandem mass spectrometry. *Analytical Methods,* 8**,** 5812-5817.

ZHANG, Z., HE, C., ZHANG, L., ZHU, T., LV, D., LI, G., SONG, Y., WANG, J., WU, H., JI, P. & LIU, G. 2019. Alpha-ketoglutarate affects murine embryo development through metabolic and epigenetic modulations. *Reproduction,* 158**,** 125-135.

ZHENZHEN, Z., CHANGJIU, H., LU, Z., TIANQI, Z., DONGYING, L., GUANGDONG, L., YUKUN, S., JING, W., HAO, W., PENGYUN, J. & GUOSHI, L. 2019. Alpha-ketoglutarate affects murine embryo development through metabolic and epigenetic modulations. *Reproduction,* 158**,** 123-133.

ZHU, C., GAO, Y., GUO, H., XIA, B., SONG, J., WU, X., ZENG, H., KEE, K., TANG, F. & YI, C. 2017. Single-Cell 5-Formylcytosine Landscapes of Mammalian Early Embryos and ESCs at Single-Base Resolution. *Cell Stem Cell,* 20**,** 720-731.e5.

Appendices

Appendix A1 Additional Imputations for 5.6.5: Effect of *TET1-3* expression on embryo quality grading through preimplantation embryo development

Additional imputations on the adjusted model for *TET3* ΔCt in cumulus cells show increasing starting FSH dose increases grade 4 embryo proportion on day 3 (β=0.002, P<0.05).

Additional imputations on the adjusted model for *TET1* ΔCt in granulosa cells on embryo quality show increasing starting FSH decreases the proportion of grade 1 embryos on day 3 (β=-0.008, P<0.05).

Additional imputations on the adjusted model for *TET2* ΔCt in granulosa cells on embryo quality show increasing number of previous fresh cycles increases proportion of grade 1 embryos on day 3 (β=0.093, P<0.05), whilst increasing starting FSH dose decreased this proportion (β=-0.007, P<0.01).

Additional imputations on the adjusted model for *TET3* ΔCt in granulosa cells on embryo quality shows increasing starting FSH decreased the proportion of grade 1 embryos on day 3 (β=-0.008 P<0.05, Table S5.5)

Appendix A2 Additional imputations to 5.6.6: Effect of *TET1-3* expression on oocyte fertilisation, embryo transfer results and pregnancy and live birth

Additional imputations on the adjusted model for *TET1* ΔCt in cumulus cells showed increasing starting FSH decreased the number of oocytes collected (β=-0.121, P<0.01) (Table S5.8).

Additional imputations on the adjusted model for *TET2* ΔCt in cumulus cells showed increasing age increased the number of oocytes collected (β=0.40-, P<0.05) and increasing starting FSH decreased the number of oocytes collected (β=-0.100, P<0.01) (Table S5.8).

Additional imputations on the adjusted model for *TET3* ΔCt in cumulus cells showed increasing age decreased total fertilisation rate (β=-2.416, P<0.05), increasing number of previous cycles increased number of embryos transferred (β=0.146, P<0.05) (Table S5.8).

Additional imputations on the adjusted model for *TET1* ΔCt in granulosa cells showed increasing BMI increased gestation length (β=0.553, P<0.05) (Table S5.8).